INFORMATION TO USERS

This manuscript has been reproduced from the microfilm master. UMI films the text directly from the original or copy submitted. Thus, some thesis and dissertation copies are in typewriter face, while others may be from any type of computer printer.

The quality of this reproduction is dependent upon the quality of the copy submitted. Broken or indistinct print, colored or poor quality illustrations and photographs, print bleedthrough, substandard margins, and improper alignment can adversely affect reproduction.

In the unlikely event that the author did not send UMI a complete manuscript and there are missing pages, these will be noted. Also, if unauthorized copyright material had to be removed, a note will indicate the deletion.

Oversize materials (e.g., maps, drawings, charts) are reproduced by sectioning the original, beginning at the upper left-hand corner and continuing from left to right in equal sections with small overlaps.

ProQuest Information and Learning
300 North Zeeb Road, Ann Arbor, MI 48106-1346 USA
800-521-0600

Characterization of the $NADP^+$-dependent malic enzyme of *Sinorhizobium* (*Rhizobium*) *meliloti* and investigations into the requirements of malate uptake and malic enzyme activity in bacteroids

By

MICHAEL JAMES MITSCH, B. Sc., M. Sc.

A Thesis Submitted to the School of Graduate Studies in Partial Fulfillment of the Requirements for the Degree Doctor of Philosophy

McMaster University

DOCTOR OF PHILOSOPHY (2000) McMASTER UNIVERSITY

(Biology) Hamilton, Ontario

TITLE: Characterization of the $NADP^+$-dependent malic enzyme of *Sinorhizobium* (*Rhizobium*) *meliloti* and investigations into the requirements of malate uptake and malic enzyme activity in bacteroids

AUTHOR: Michael James Mitsch, B. Sc., M. Sc. (University of Calgary)

SUPERVISOR: Professor T. M. Finan

NUMBER OF PAGES: 278

Abstract

Malic enzymes are responsible for the conversion of malate to pyruvate with the concomitant reduction of a nicotinamide cofactor. Previous experiments revealed that *Sinorhizobium* (*Rhizobium*) *meliloti* has both a diphosphopyridine (NAD^+) dependent enzyme (DME), which is essential for nitrogen fixation, and a triphosphopyridine ($NADP^+$) dependent enzyme (TME), which is not required for symbiotic N_2 fixation. Sequence analysis of *tme* revealed that it encodes a protein of 761 amino acids, which is much larger than previously described prokaryotic malic enzymes. The elongated structure comprises an unusual chimeric organization with the N-terminal region of the protein showing similarity to other malic enzymes, including six conserved domains implicated in malic enzyme function. The C-terminal region shows similarity to phosphotransacetylase enzymes (PTA) and deletion of this PTA-like domain results in a decrease, but not an abolishment of malic enzyme activity, indicating that this region is not essential for the conversion of malate to pyruvate. Native TME is an octamer in structure while the truncated form lacking the PTA-like domain forms a dimer. The *tme* gene was overexpressed in a malic enzyme deficient *Escherichia coli* strain and the resulting protein was purified to homogeneity and biochemically characterized. TME showed typical Michaelis-Menten type kinetics for both malate and $NADP^+$ and K_m's of 2.6 mM and 33 μM were deduced respectively. TME activity was not affected by end products, tricarboxylic acid (TCA) cycle intermediates or glycolyitic intermediates such as glucose-6-phosphate. Purified TME was utilized to produce antibodies.

To investigate the requirements of the malic enzyme in symbiotic nitrogen fixation several metabolic engineering experiments were carried out. The NAD^+-dependent malic enzyme (SfcA) from *E. coli*, which lacks the PTA-like extension, was expressed in *S. meliloti dme* mutant strains. The *S. meliloti dme*$^-$, *sfcA* derivatives formed nodules that fixed N_2 at rates indistinguishable from those formed by wild type *S. meliloti*. Hence, the SfcA protein can functionally replace DME. In addition, *dme* was expressed from the *tme* promoter in *S. meliloti dme* mutant strains to determine levels of *tme* expression in bacteroids. The *S. meliloti* strains that expressed the *ptme-dme* construct produced plants that had 30% the dry weight and acetylene reduction activity relative to wild type inoculated and had approximately 30% DME activity relative to wild type bacteroids. To support these observations antibodies specific for each malic enzyme

were used to quantitate the amount of TME and DME in free-living cells and bacteroids and revealed that TME levels drop to 20% while DME levels double during the transition from free-living cells to bacteroids. Other metabolic engineering attempts were made by overexpressing *dme* in *S. meliloti* bacteroids. The resulting increase in DME levels in bacteroids did not result in increased symbiotic N_2 fixation or improved plant growth. In order to determine if cofactor specificity is responsible for the requirement of DME during symbiosis attempts were made to alter the cofactor requirement of TME. Regions of *dme* corresponding to the putative co-factor binding site were exchanged for the corresponding regions of *tme* to produce chimeric proteins. Also, point mutations were introduced into the putative co-factor binding site of TME. In all cases the proteins proved unstable in an *E. coli* background and no alteration in cofactor specificity was detected. The point mutants were stable in a *S. meliloti* background but no alteration in cofactor dependence was observed.

To investigate the carbon source utilized during symbiosis a malate specific permease from *S. bovis* was expressed in *S. meliloti* strains lacking the dicarboxylic acid transporter DctA. When expressed as a single copy construct on the chromosome using either the *dme* or *dctA* promoter no nitrogen fixation was detected. When the constructs were expressed from a high copy number plasmid the resulting plants showed 40% nitrogen fixation and 25% plant dry weights relative to wild type inoculated plants. When these constructs were expressed in *dctA* deficient *Rhizobium leguminosarum* strains partial symbiotic N_2 fixation was again noted with the *dme* promoter construct while the *dctA* promoter produced plants that were identical to wild type inoculated plants in terms of nitrogen fixation and plant dry weight. This would indicate that malate is present in nodules of leguminous plants and is capable of supporting nitrogen fixation but the extent of this support is *Rhizobiaceae* and host plant dependent.

Acknowledgements

I would like to thank Dr. Finan for the opportunity to complete this work in his laboratory, for the rigorous training, and for teaching me the valuable lessons of determination and self-reliance. I sincerely thank him for his efforts on my behalf. I would also like to thank the members of my committee for their time and comments on this work. I also thank the many members of the Finan lab for all of their help, support, and friendship over the years. To Sylvie Bardin and Kim Napper for helping me through the first awkward months, to Patrick Chain, Shelley O'Brien, Scott Clark, and Kim Wong for being such good friends and playmates and for making my middle years so much fun, to Alison Cowie who looked after us, taught us a great deal and kept us all out of trouble, to Yuan Ze-chun and Ismael Hernandez-Lucas who taught me patience and good humor are essential in all endeavors, and to the newest members of the Finan laboratory, Sean Reichheld, Shawn MacLlelan, and Punita Anjea for making my last year so interesting. I would also like to thank the members of the department who graced me with their friendship over the years and made my non-work hours so enjoyable. Thanks to Marta Boszko, Macarana Busto, Rob Kulathenow, John Audia, Lily Wong, Chantel Desouza, Deb Lorenzen, Amanda Hawley, Liisa Koski, the baseball team, and all the rest of the inmates at the life sciences building.

I cannot adequately express the debt of gratitude I owe my family for their love and support, without it I would never have made it. Thank you to my parents Julius and Geraldine and my sister Kathy for good-natured e-mails and phone calls. The distance may have been great but you were beside me the whole time. I also wish to thank Catherine Barber for listening to my whining and reminding me of better things ahead. I hope I do not disappoint you. Last but most certainly not least, I would like to extend my sincerest thanks and gratitude to Dr. Ralph Voegele who taught me so much about so many things and was a very good friend and golf partner. Thank you Ralph, I would never have made it without you.

Table of Contents

List of Tables

List of Figures

Abbreviations

ADP	adenosine diphosphate
AMP	adenosine monophosphate
ARA	acetylene reduction assay
ATP	adenosine triphosphate
BLAST	basic local alignment sequence tool
bp	base pair
BSA	bovine serum albumin
CoA	coenzyme A
cAMP	cyclic AMP
DEPC	diethyl pyrocarbonate
DME	diphosphopyridine dependent malic enzyme
ΔDME	truncated diphosphopyridine dependent malic enzyme
DNA	deoxyribonucleic acid
dNTP	deoxynucleotides
DPH	2,4-Dinitrophenylhydrazine
DTT	dithiothreital
ECL	enhanced chemiluminescence
EDTA	dethylene-diaminetetra-acetic acid disodium salt
Fix	nitrogen fixation phenotype
GDP	guanosine diphosphate
Gm	gentamicin
GTP	guanosine triphosphate
kbp	kilo base pair
kDa	kilo dalton
LB	Luria-Bertani media
LBmc	Luria-Bertani media with magnesium and calcium
ME	malic enzyme
MDH	malate dehydrogenase
MMS	mops media sucrose
MOPS	3-[N-morpholino] propane-sulfonic acid
mRNA	messenger ribonucleic acid
MTT	3-[4,5-Dimethylthiazol-2-yl]-2,5-diphenyltetrazolium bromide
M9	minimal media
NAD^+	nicotinamide adenine dinucleotide
$NADP^+$	nicotinamide adenine dinucleotide phosphate
$NAD(P)^+$	nicotinamide adenine dinucleotide/dinucleotide phosphate
Nm	neomycin
OD	optical density
PAGE	polyacrylamide gel electrophoresis
PCK	phosphoenolpyruvate carboxykinase

PCR	polymerase chain reaction
PEP	phosphoenol pyruvate
Pi	inorganic phosphate
PMS	phenazine methosulfate
PTA	phosphotransacetylase enzyme
PYC	pyruvate carboxylase
RNA	ribonucleic acid
rpm	revolutions per minute
SDS	sodium dodeo
TAE	tris-acetate-EDTA buffer
TEMED	N,N,N',N'-tetramethyl-ethylenediamine
TCA	tricarboxylic acid cycle
TME	triphopshopyridine dependent malic enzyme
ΔTME	truncated triphosphopyridine dependent malic enzyme
TY	tryptone yeast

Chapter 1

Literature review

Symbiotic nitrogen fixation

In the third century B.C. the first recorded observation of the benefits of symbiotic nitrogen fixation was made by Theophrastus who described the use of faba beans to enrich the arable lands of Greece (Raven *et al.*, 1996). Since these first simple observations a great deal of information has been obtained regarding the biology of symbiotic nitrogen fixation. Members of the family *Rhizobiaceae* are characterized by their ability to enter into a symbiotic relationship with a plant forming a structure, known as a nodule, within which they fix atmospheric nitrogen. This fixed nitrogen is then transferred to the plant host to enhance growth. This ability to convert atmospheric dinitrogen to ammonia is limited to prokaryotic organisms and the capability of several of these organisms to form nodules on important crops such as alfalfa or soybean has stimulated research in symbiotic nitrogen fixation. Symbiotic diazotrophs include *Rhizobium leguminosarum* which interacts with peas (*Pisium sp.*), lentils (*Lens sp.*), and clover (*Trifolium sp.*), *Bradyrhizobium japonicum* with soybeans (*Glycine sp.*), and *Azorhizobium caulinodans* which can fix nitrogen in both a free-living state and in conjunction with the tropical legume *Sesbania rostrata*. *Sinorhizobium* (formerly *Rhizobium*) *meliloti* forms root nodules on sweet clover (*Melilotus alba*) and alfalfa (*Medicago sativa*).

Bacterial genes involved in the formation of N_2 fixing nodules are referred to as the *nod*, *fix* and *nif* genes. The *nod* genes are expressed in response to flavinoids and isoflavinoids released from the plant (Denarie *et al.*, 1992, van Rhijn and Vanderleyden, 1995). These genes include the common *nod* genes *nodABC* which are found in every symbiotic nitrogen fixing organism. *nod* gene products are responsible for the synthesis of compounds known as Nod factors which are responsible for root hair curling and inducing mitotic activity in the host plant cells.. The bacteria enter the root in structures known as infection threads and as the bacteria are released from the infection threads into the cytoplasm of the plant cell they are enveloped by the host cell membrane. Once encased in this host derived "peribacteroid" membrane the cells cease replicating and produce the terminally differentiated bacteroid (Hirsh and Smith, 1987; Vasse *et al.*, 1990). Genes required for N_2 fixation that are induced specifically during association with the plant host and which are unique to the *Rhizobiaceae* are referred to as *fix* genes while the *nif* genes show homology to genes present in free-living nitrogen fixing organisms such as *Klebsiella pnuemonia* (Cannon *et al.*, 1985). The *fix* genes include *fixL* which encodes a protein which detects oxygen present in the host plant (David *et al.*, 1988, de Philip *et al.*, 1990) and regulatory proteins such as those encoded by *fixJ* and *fixK* (Batut *et al.*, 1989) which regulate expression of other *fix* and *nif* genes. These include the *fixGHIS* (Kahn *et al.*, 1989) and *fixNOQP* (David *et al.*, 1987) operons that encode a cation transport system and a respiratory pathway that has a high affinity for the terminal electron acceptor oxygen respectively. The latter system is required because of the low oxygen levels found within the nodule (Hennecke, 1993). In addition to the

production of a cytochrome system capable of operating under reduced oxygen concentrations an oxygen binding heme protein, known as leghemoglobin, is produced. Leghemoglobin transports oxygen from the outer to the inner regions of the nodule and allows the oxidative respiratory processes of the bacteroid to continue while at the same time maintaining a low oxygen concentration to protect the nitrogenase enzyme. *NifQBEVS* encode the proteins required for the formation FeMo cofactor utilized at the active site of the nitrogenase enzyme (Merrick,. 1993). Nitrogenase itself is encoded by the operon *nifHDK* (Roberts and Brill, 1981) and due to its presence in several organisms, not all able to fix atmospheric nitrogen, it has been hypothesized that the ancestral form of the enzyme was present as a detoxifying system for survival in the primeval atmosphere (Silver and Prostgate 1973). This would explain why such an energetically expensive process ($N_2 + 8H^+ + 8e^- + 16ATP \rightarrow 2NH_3 + H_2 + 16ADP + 16P_i$) would be developed and continue to be maintained. Upon the completion of the induction and expression of the *fix* and *nif* genes the bacteroids are capable of fixing atmospheric nitrogen and transferring it to the plant host. The fixed atmospheric nitrogen is believed to exit the bacteroid as ammonia and since the nitrogen acquisition pathways nitrate reductase, glutamine synthetase, and glutamate synthetase are reduced in bacteroids (Darrow, 1980, Howitt and Gresshoff, 1985, Howitt *et al.*, 1986, Carlson *et al.*, 1987, DeBruijin *et al.*, 1989, Shatters *et al.*, 1989) the ammonia is assimilated by the plant host through the action of glutamine synthetase and glutamate synthase (Atkins, 1991). Recent evidence with *B. japonicum* indicates that alanine may also act as an export product of nitrogen rather than ammonia (Waters *et al.*, 1998). This would require

the production of alanine from ammonia which would require pyruvate and the enzyme alanine dehydrogenase.

The morphological changes which occur as a result of the alteration from free-living cells to symbiotic bacteroids (Hirsch and Smith, 1987) are linked to different locations of the indeterminant, or still growing, nodule of the plant and Vasse *et al.*, (1990) have proposed a nomenclature to describe these areas. The nodule is dived into four regions in which different cellular processes are occurring within the bacterium. Distal to the root is Zone I made up of the meristimatic area containing dividing plant cells and no bacteria. The bacteria are deposited by the infection threads to the early symbiotic Zone II containing the newly divided plant cells from Zone I. A layer made up of amyoplast-rich cells separates Zone II from Zone III and is the site at which the *fix* and *nif* genes are activated (de Maagd *et al.*, 1994, Labes and Finan, 1993). Therefore Zone III, the microaerobic late symbiotic zone, contains mature fully developed bacteroids and is the site of nitrogen fixation. The final area, that proximal to the root itself is the senescent Zone IV and contains bacteroids in the process of being degraded.

Carbon sources available from the plant host for nitrogen fixation

Research into carbon sources, which are present and available for metabolism by bacteroids in the root nodules, has revealed that C_4-dicarboxylic acids succinate and malate are the dominant carbon compounds (Vance and Heichel, 1991). Photosynthate, namely sucrose, is translocated to the nodule and metabolized to the organic acid phosphoenolpyruvate (PEP) which is converted to malate by the high levels of PEP carboxylase and malate dehydrogenase activities present in the plant tissue. This results

in the accumulation of organic acids in the plant cytosol. In addition, the activities of TCA cycle enzymes in the plant cell cytosol are low which may limit catabolism through the TCA cycle resulting in an accumulation of C_4-dicarboxylic acids. Several $^{14}CO_2$ labeling studies with nodules have shown that malate is the dominant carbon source produced (Vance *et al.*, 1983; Kouchi and Nakaji, 1985; Snapp and Vance, 1986; Rosendahl *et al.*, 1990). In order to be utilized by the metabolic machinery of the bacteroid, the carbon sources must traverse both the host derived peribacteroid membrane, enter the peribacteroid space, and then be transported across the bacteroid membrane. The peribacteroid membrane is relatively impermeable to sugars but does contain a dicarboxylate transporter capable of rapidly transferring C_4-dicarboxylic acids to the bacteroid (Streeter, 1987, Day *et al.*, 1989). In addition to this, studies with bacteroids themselves show that they are capable of taking up C_4-dicarboxylates at rates significantly higher than that for sugars such as glucose (Salminen and Streeter, 1987, Udvardi *et al.*, 1988). Mutants of the *Rhizobiaceae* that are deficient for C_4-dicarboxylate transport are uniformly unable to fix atmospheric nitrogen in association with their respective plant hosts (Ronson *et al.*, 1981; Finan *et al.*, 1983). Taken together, this body of evidence suggests that C_4-dicarboxylates are the dominant carbon source made available to the bacteroid as a source of energy and reductant for nitrogen fixation.

C_4-dicarboxylate transport in the *Rhizobiaceae*

In order to utilize the carbon sources obtained from the plant host members of the *Rhizobiaceae* have specialized transport systems designed to take up C_4-dicarboxylates

from the peribacteroid space. This transporter, termed DctA has been extensively characterized in *S. meliloti*, *R. leguminosarum* and *B. japonicum*. The reported K_m for DctA ranges from 2 to 15 μM depending on the organism (Finan *et al.*, 1981, Finan *et al.*, 1983, McAllister and Lepo 1983, San Francisco and Jacobson, 1985, Engelke *et al.*, 1987, Udvardi *et al.*, 1988), requires an energized membrane in order to function (Finan *et al.*, 1981, McAllister and Lepo, 1983), and appears to catalyze co-transport of C_4-dicarboxylates and protons (Udvardi and Day, 1997). DctA is able to transport fumarate, malate, succinate, and aspartate (Glenn *et al.*, 1980, Finan *et al.*, 1981, Watson *et al.*, 1993) but the relative rate of transport and K_m for each compound may be variable (McRae *et al.*, 1989). This could indicate a preference for some compound over the others but at present this hypothesis has not been explored. The *dct* operon is made up of three genes; *dctA*, the transporter itself, and two regulatory elements *dctB* and *dctD* which form a two component regulatory system made up of a membrane bound receptor and a DNA binding transcriptional activator, respectively (Ronson *et al.*, 1984, Ronson *et al.*, 1987, Engelke, *et al.*, 1989, Watson, 1990). DctB is activated through interactions with C_4-dicarboxylates in the periplasmic space and is believed to undergo a conformational change which activates the cytoplasmically located DctD. Once induced DctD, in association with the sigma factor NtrA (σ^{54}), acts as a transcriptional activator for the *dctA* promoter (Ronson *et al.*, 1987, Yarosh *et al.*, 1989).

Bacteroid metabolism

The bacteroids are dependent upon the plant host for a carbon source and as previously stated most experimental evidence implicates C_4-dicarboxylic acids such as

malate and succinate as the likely candidates (For reviews see Day and Copeland, 1991: Streeter, 1991). Sugars such as glucose, sucrose and fructose are not readily taken up by isolated bacteroids (Glenn and Dilworth, 1981, Reibach and Streeter, 1983, Saliminen and Streeter, 1987, Copeland *et al.*, 1989). Although members of the *Rhizobiaceae* employ enzymes of the Entner-Doudoroff pathway in a free-living state (Keele *et al.*, 1969, Irigoyen *et al.*, 1990) it is unlikely that this system is essential in bacteroids as mutants defective for sugar transport or catabolism are still capable of fixing nitrogen in association with the plant host (Hornez *et al.*, 1994, Ronson and Primrose, 1979). In addition, enzymes required for gluconeogenesis have diminished activity in bacteroids and are not required for nitrogen fixation. Acetate acts as a poor substrate for members of the *Rhizobiaceae* under free-living conditions yet the acetate activating enzymes acetate kinase, phosphotransacetylase, and acetyl-CoA synthetase have been identified in *S. meliloti* (Summers *et al.*, 1999, Cai *et al.*, 2000) and *B. japonicum* (Preston *et al.*, 1989). Acetate is a potentially important carbon source as it can be readily converted to acetyl-CoA, a metabolite for the TCA cycle. The relative importance of this system for the bacteroid may be limited as acetate kinase and acetate kinase/phosphotransacetylase mutants are not impaired in terms of their symbiotic abilities (Summers *et al.*, 1999) nor will acetate support nitrogenase activity in isolated bacteroids (Miller *et al.*, 1988). Amino acids can also be utilized by the *Rhizobiaceae* and both glutamate and proline have been shown to sustain nitrogenase activity in isolated bacteroids (Bergersen and Turner, 1990, Zhu *et al.*, 1992). However, recent evidence shows that a proline dehydrogenase mutant of *S. meliloti* retains its ability to induce nitrogen fixing nodules

(Jimenez-Zurdo *et al.*, 1995) indicating that catabolism of this amino acid is not essential for symbiosis.

The TCA cycle (Figure 1.1) is believed to be the primary avenue to metabolize C_4 compounds to produce ATP and reducing power (Streeter, 1991). Evidence to support the importance of the TCA cycle in energy production rests with the symbiotic phenotype generated by strains deficient for enzymes of the TCA cycle. Mutants lacking isocitrate dehydrogenase (McDermott and Kahn, 1992), succinate dehydrogenase (Finan *et al.*, 1983, Gardiol *et al.*, 1987), citrate synthase (Mortimer *et al.*, 1999) and α-ketoglutarate dehydrogenase (Johnson *et al.*, 1966, Duncan and Fraenkel, 1979) activity all yield an inability to fix N_2 during symbiosis. Recent evidence with *B. japonicum* has shown that mutants lacking α-ketoglutarate dehydrogenase are able to use malate and succinate as a sole carbon source and therefore do not require an intact TCA cycle for metabolism of C_4-dicarboxylates (Green and Emerich, 1997a, Green and Emerich, 1997b). The glyoxylate shunt (Figure 1.1) is a potential alternate pathway for the TCA cycle, however isocitrate lyase activity is low in *B. japonicum* (Green *et al.*, 1998) and *S. meliloti* cells (Duncan and Fraenkel, 1979). Its activity can be induced with the fatty acid oleate (Johnson *et al.*, 1966) or acetate (Duncan and Fraenkel, 1979) as the sole carbon source. Interestingly malate synthase, the second component of the glyoxylate shunt, is constitutive in free- living cells and its activity is unaffected by carbon source availability (Johnson *et al.*, 1966, Duncan and Fraenkel, 1979). However there is no detectable isocitrate lyase activity in *S. meliloti*, or *R. leguminosarum* bacteroids and low levels of

Figure 1.1. Tricarboxylic acid (TCA) cycle. *PYK*; pyruvate kinase, *POD*; pyruvate orthophosphate dikinase, *PCK*; phosphoenolpyruvate carboxykinase, *PDH*; pyruvate dehydrogenase, *ACS*; acetate synthetase, *ACK*; acetate kinase, *PTA*; phosphotransacetylase, *PYC*; pyruvate carboxylase, *Cit*; citrate synthase, *Acon*; aconitase, *IDH*; Isocitrate dehydrogenase, *IL*; isocitrate lyase, *MS*; malate synthase, *αKDH*; α-ketoglutarate dehydrogenase, *SCoALIG*; succinyl CoA ligase, *SDH*; succinate dehydrogenase, *Fum*; fumarase, *MDH*; malate dehydrogenase, *ME*; malic enzyme.

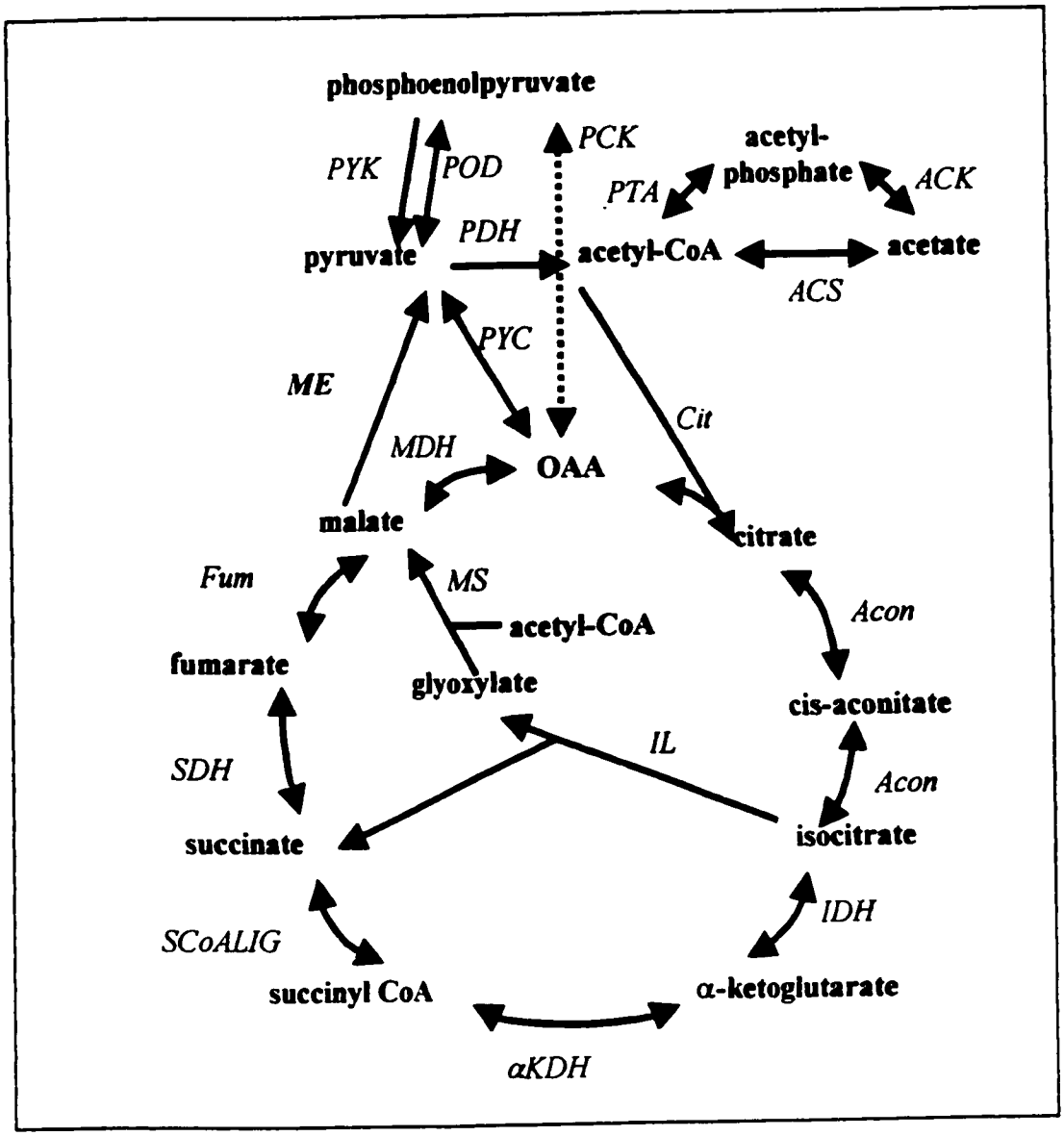
phosphoenolpyruvate
PYK
POD
PCK
acetyl-
phosphate
PTA
ACK
PDH
pyruvate
acetyl-CoA
acetate
ACS
PYC
ME
Cit
MDH
OAA
malate
citrate
Fum
MS
acetyl-CoA
Acon
fumarate
glyoxylate
cis-aconitate
IL
SDH
Acon
succinate
isocitrate
IDH
SCoALIG
succinyl CoA
α-ketoglutarate
αKDH

activity in *B. japonicum* (Johnson *et al.*, 1966) indicating that the glyoxylate shunt is absent or plays a limited role in bacteroids.

When C_4-dicarboxylates are metabolized via the TCA cycle, two moles of malate are utilized. One is oxidized to form oxaloacetate while the second is converted to acetyl-CoA and these two molecules finally combine to form citrate via citrate synthase. To maintain the TCA cycle using C_4-dicarboxylates as the sole carbon source, a pathway to generate acetyl-CoA is essential. Several such enzymatic pathways exist but their relative importance for nitrogen fixation is variable. Pyruvate can be produced from oxaloacetate by the action of pyruvate carboxylase (PYC) (Figure 1.1), however, mutants of several *Rhizobium* species lacking this activity are able to fix nitrogen (Arwas *et al.*, 1986; Ronson and Primrose, 1979; Dunn *et al.*, 1996) indicating its role in bacteroids is not essential. Oxaloacetate decarboxylase, which converts oxaloacetate to pyruvate, has not been detected in *S. meliloti* (Duncan and Fraenkel, 1979) and therefore is not likely to play a role in symbiosis. Phosphoenolpyruvate carboxykinase (PCK), in association with pyruvate kinase, could be used to produce pyruvate (Figure 1.1) and Pck mutants vary in terms of their effects on nitrogen fixation. In *R. leguminosarum* Pck mutants induce nodules capable of fixing N_2 during symbiosis (McKay *et al.*, 1985) while in *S. meliloti* Pck^- strains induce nodules that have 60% nitrogen fixation ability relative to wild type nodules (Osteras *et al.*, 1991). Interestingly the symbiotic phenotype of Pck mutants of the broad host range *Rhizobium sp.* NGR234 is host dependent (Osteras *et al.*, 1991). The latter result may reflect differences in the carbon sources available to the bacteria during the infection process. Malic enzymes are capable of oxidative decarboxylation of

malate to pyruvate with a concomitant reduction of a nicotinamide cofactor. Since no other pathway leading from TCA cycle intermediates to pyruvate appears to be functional at a level capable of sustaining nitrogen fixation in the *Rhizobiaceae*, it is conceivable that malic enzymes are the dominant means by which the TCA cycle is maintained in bacteroids.

Malic enzymes

Malic enzyme activity was originally identified by Ochoa *et al.* (1948) in pigeon liver extracts but since this initial discovery it has been isolated from a wide variety of plants, animals, and bacteria. In plants it is required for several metabolic processes including providing pyruvate, a source of CO_2 for carbon fixation, regulating cytosolic pH, and providing a source of reducing powers for anabolic processes (For reviews see Wedding, 1989; Edwards and Andreo, 1992). In animals malic enzymes are used to for several cellular processes including production of reduced cofactors for lipogenesis, formation of pyruvate for amino acid production and acetyl-CoA to maintain the TCA cycle (Magnuson *et al.*, 1986; Morioka *et al.*, 1989; Loeber *et al.*, 1991; Kulkarni *et al.*, 1993). In prokaryotes, malic enzymes have been identified and characterized from several organisms including *Esherichia coli* (Katsuki *et al.*, 1967, Spina *et al.*, 1970; Yamaguchi *et al.*, 1973), *Bacillus subtilis* (Diesterhaft and Freese, 1973), *Pseudomonas putida* (Garrido-Pertierra *et al.*, 1983), *Pseudomonas diminuta* (Suye *et al.*, 1992), *Clostridium thermocellum* (Lamed and Zeikus, 1981), *Sulfolobus solfataricus* (Bartolucci *et al.*, 1987; Guagliardi *et al.*, 1988), *Bacillus stearothermophilus* (Kobayashi *et al.*, 1989), and most recently from *Streptococcus bovis* (Kawai *et al.*, 1996). Malic enzyme

genes have been identified in *Haemophilus influenzae* (Fleischmann *et al.*, 1995), *Syenchocystis sp.* PC6803 (Kaneko *et al.*, 1996), and *Rickettsia prowazekii* (Andersson *et al.*, 1998) whose genomes have been sequenced, however the encoded enzymes have not been characterized. The prokaryotic enzymes are variable in their cofactor requirements (NAD^+ or $NADP^+$), subunit sizes (40 kDa to 68 kDa), and oligomerization states (dimers to decamers) indicating a high degree of variability in their structure.

The malic enzymes of *E. coli* have been extensively studied and provided the first opportunity to contrast two enzymes carrying out the same reaction in one organism. The NAD^+-dependent enzyme is inhibited by CoA, oxaloacetate, and ATP and activated by aspartate (Sanwal, 1970b, Yamaguchi *et al.*, 1973). In contrast, the $NADP^+$-dependent enzyme is inhibited by acetyl-CoA and cAMP (Sanwal *et al.*, 1968, Spina *et al.*, 1968, Sanwal and Smando, 1969a, Sanwal and Smando, 1969b). Since enzymes carrying out the same reaction are usually part of separate pathways directed to different cellular processes, it has been hypothesized that the NAD^+-dependent enzyme is responsible for catabolism of malate and controlling the levels of C_4-dicarboxylic acids within the cell (Murai *et al.*, 1971). In contrast, the $NADP^+$-dependent enzyme, due to its sensitivity to acetyl-CoA, is responsible for supplying the cell with acetyl-CoA and NADPH for anabolic processes including lipid biosynthesis (Murai *et al.*, 1971).

Malic enzymes in the *Rhizobiaceae*

Malic enzymes have been studied in the *Rhizobiaceae* because of their potential importance in maintaining metabolic flux through the TCA cycle. A malic enzyme has been detected in free-living *R. leguminosarum* cells but no further characterization has

been carried out as yet (McKay *et al.*, 1988). Malic enzymes have also been identified and isolated from *B. japonicum* by several research groups. Kimura and Tajima (1989) have purified a $NADP^+$-dependent malic enzyme and it was found to be inhibited by citrate, malonate, and glyoxylate and therefore seems to be regulated by products of the organic acid metabolic pathway. The same group has gone on to isolate a NAD^+-dependent malic enzyme which is activated by products of the glycolytic pathway such as D-glucose-6-phosphate, D-fructose-6-phosphate, and D-fructose-1,6-diphosphate, and is inhibited by fumarate and ATP (Chen *et al.*, 1998). They also purified the $NADP^+$-dependent enzyme and showed that it is inhibited by metabolic intermediates such as isocitrate, acetyl-CoA, and ATP (Chen *et al.*, 1997). Based upon these observations the authors concluded that the $NADP^+$-dependent malic enzyme is responsible for the eventual production of acetyl-CoA to maintain the TCA cycle for energy production while the NAD^+-dependent enzyme is necessary for the production of reducing power or the generation of pyruvate for anabolic processes such as amino acid synthesis (Chen *et al.*, 1997). In contrast to previous predictions Copeland *et al.* (1989) concluded that the NAD^+-dependent malic enzyme of *B. japonicum* is responsible for generating pyruvate or NADH for energy production via the TCA cycle while the $NADP^+$-dependent malic enzyme is used to generate pyruvate and reducing powers for anabolic processes. Tomaszewska and Werner (1995) have looked at the structural nature of the malic enzymes of *B. japonicum* and have found that the $NADP^+$-dependent malic enzyme is active as a 60 kDa monomer while the NAD^+-dependent variant is a heterodimer made up of a 60 kDa and an 80 kDa subunit. By comparison, the purified proteins generated by

Chen *et al.*, (1997, 1998) showed that the enzymes are made up of subunits approximately 85 kDa and 77.6 kDa in size for the NAD^+- and $NADP^+$-dependent enzymes respectively and they exist as a dimer or tetramer depending on pH (Chen *et al.*, 1997, Chen *et al.*, 1998). The kinetic data available for these enzymes is variable among the three research groups but the general trend is that the $NADP^+$-dependent malic enzyme has a higher affinity (0.1 mM-0.18 mM) for malate than the NAD^+-dependent malic enzyme (1.9 mM-5 mM). In addition to their role in maintaining the TCA cycle, the malic enzymes may be necessary for other bacteroid processes. Alanine has been suggested to act as the source of nitrogen donated to the plant host (Waters *et al.*, 1998) and this amino acid can be generated by the activity of alanine dehydrogenase which converts pyruvate and ammonia to alanine. Also, the source of reductant for the nitrogenase enzyme has not been determined and it is possible that the NAD(P)H generated by the activity of the malic enzymes may be utilized by nitrogenase to fix atmospheric nitrogen. To date neither of these hypothesis has been explored.

Previous work in this laboratory has identified two malic enzymes in *Sinorhizobium* (*Rhizobium*) *meliloti*, one NAD^+-dependent (DME) and the other $NADP^+$-dependent (TME) (Driscoll and Finan, 1993). Both genes have been identified, subcloned, and sequenced (Mitsch *et al.*, 1998). Based on mutational studies, *dme* appears to be essential for symbiotic nitrogen fixation since abolishment of this gene results in an inability to fix N_2 during symbiosis (Driscoll and Finan, 1993) while *tme* does not appear to be required for nitrogen fixation (Driscoll and Finan, 1996). Furthermore, *dme* expression levels appear to be constitutive and in free-living cells are

neither growth phase nor carbon source dependent (Driscoll and Finan, 1993, Driscoll and Finan, 1997). By comparison, transcription of *tme* in bacteroids is approximately 20% of that in free-living cells (Driscoll and Finan, 1997) indicating that *tme* expression is reduced in bacteroids. Studies employing partially purified DME revealed that acetyl-CoA inhibits enzyme activity while TME is insensitive to most compounds (Driscoll and Finan, 1997) indicating that the enzymes are part of separate biochemical pathways. Recent results with purified DME showed while acetyl-CoA and oxaloacetate inhibit enzyme activity DME is activated by the C_4-dicarboxylates succinate and fumarate. These observations, paired with the fact that DME is necessary for nitrogen fixation, gives strong evidence that DME is used to maintain the TCA cycle within the bacteroid. The function of TME is unknown but it may be responsible for anabolic processes either by producing pyruvate for amino acid production or the generation of reducing power for cellular functioning as is believed to be the case in *E. coli* (Sanwal, 1970a, Murai *et al.*, 1971). The fact that it is not required in bacteroids, which are no longer undergoing rigorous growth and biosynthetic processes would support this hypothesis. Recent experiments concerning the expression of *tme* within bacteroids has shown that there are no adverse effects to the bacteroid or plant host when elevated levels of TME are present in bacteroids. Furthermore, these results also show that when *tme* is overexpressed in a *dme* mutant *S. meliloti* strain it is incapable of supporting symbiotic nitrogen fixation (Cowie, 1998) indicating that TME cannot functionally replace DME in bacteroids despite the fact the enzymes carry out a nearly identically reaction.

This work

This work was undertaken initially to characterize the $NADP^+$-dependent malic enzyme of *S. meliloti* in order to compare it to the well characterized, symbiotically essential DME. It was hoped that by comparing the two proteins at the amino acid sequence level and their respective biochemical characteristics we could determine why TME is not required for nitrogen fixation. This characterization involved the completion of the sequence of *tme*, carrying out detailed sequence analysis of the gene and comparing it to *dme* and other prokaryotic malic enzymes. During the course of these investigations the identification and importance of the unique C-terminal extensions of both *S. meliloti* enzymes became a focal point for continued study and debate. Studies were undertaken to assess the requirement of the unique C-terminal extension of the *S. meliloti* malic enzymes for activity. The C-terminal extension of TME was removed and experiments carried out to determine the effects on TME activity. To further assess the importance of the C-terminal region of the *S. meliloti* malic enzymes in symbiosis and nitrogen fixation the NAD^+-dependent malic enzyme from *E. coli* was expressed in *S. meliloti* cells and bacteroids.

In order to compare TME to DME at a biochemical level *tme* was overexpressed in *E. coli* and the resulting protein purified to homogeneity. Biochemical analysis of TME revealed that it has similar kinetic properties to DME but is not affected by TCA cycle intermediates. This led to speculation that it is TME's insensitivity and lack of ability to respond to TCA cycle intermediates that inhibits its ability to functionally replace DME in bacteroids. Another possibility is that cofactor availability in the

bacteroid limits TME's function as there maybe an insufficient amounts of $NADP^+$ present in bacteroids. This issue was addressed by attempting to alter the cofactor specificity of TME from $NADP^+$ to NAD^+.

Our interest in the malic enzyme was extended to malate uptake when a malate specific transporter was found to be co-expressed with the malic enzyme of *S. bovis*. The transport gene, *maeP*, was expressed in *S. meliloti* and *R. leguminosarum dctA* mutants to ascertain if the C_4-dicarboxylate malate is present and if this carbon source alone can support nitrogen fixation in alfalfa or pea nodules. Therefore this work is eclectic in nature and ranges from carbon transport to metabolism covering the uptake of malate to its utilization by the malic enzymes.

Chapter 2

Materials and Methods

Bacterial strains

Bacterial strains and plasmids are listed in Table 2.1. *E. coli* strains were grown in Luria-Bertani media (LB) (Miller, 1972) with appropriate antibiotics and incubated at 37°C or 30°C for *E. coli* and *S. meliloti* respectively. *S. meliloti* strains were grown in LB supplemented with 2.5 mM $MgSO_4$ and 2.5 mM $CaCl_2$ to yield LBmc. Antibiotics used were streptomycin 200 μg/ml, neomycin 200 μg/ml, gentamycin 20 μg/ml, and spectinomycin 100 μg/ml. *R. leguminosarum* strains were cultured using TY media (5 g tryptone, 3 g yeast extract, and 0.5 g $CaCl_2$, per litre) (Bergmeyer *et al.*, 1967) with streptomycin 200 μg/ml, neomycin 200 μg/ml, gentamycin 20 μg/ml and incubated under identical conditions as for *S. meliloti*. For *E. coli* ampicillin was used at 100 μg/ml and gentamycin at 10 μg/ml. Minimal media (M9) was utilized for plates and growth curves. M9 (Miller, 1972) consists of 5.8 g Na_2HPO_4, 3 g KH_2PO_4, 0.5 g NaCl, 1g NH_4Cl, per 1 litre of distilled deionized water. For solid media 15 g of agar was added per litre. After autoclaving and cooling, 1 mM $MgSO_4$, 0.25 mM $CaCl_2$, and 0.5 mg/L biotin and one of 15 mM succinate, 15 mM malate, or 15 mM glucose were used as carbon sources and the appropriate antibiotic was added.

Table 2.1. Table of bacterial strains and plasmids used.

Strain	Genotype/Description	Reference
S. meliloti		
Rm 1021	SU47, str 21	Meade *et al.*, 1982
RmF642	Rm1021, *dctA*14::Tn5	Yarosh *et al.*, 1989
RmF647	Rm1021, *dctA*26::Tn5	Yarosh *et al.*, 1989
RmG454	Rm1021, *dme*-2::Tn5	Driscoll and Finan, 1993
RmG455	Rm1021, *dme*-3::Tn5	Driscoll and Finan, 1993
RmG456	Rm1021, *dme*-1::Tn5	Driscoll and Finan, 1993
RmG994	Rm1021, *dme*-3::Tn5, *tme*-4::ΩSp	Driscoll and Finan, 1996
RmG995	Rm1021, *tme*-4::ΩSp	Driscoll and Finan, 1996
RmH194	Rm1021, *pckA*1::Tn3HoHo, *pod*-1, *dme*-1::Tn5, *tme*-4::ΩSp	Driscoll and Finan, 1996
RmH215	Rm1021, *tme*-2::Tn5	Driscoll and Finan, 1996
RmH217	Rm1021, *tme*-3::Tn5	Driscoll and Finan, 1996
RmH897	Rm1021, *dme*-3::Tn5, *tme*-4::ΩSpΦpTH433	Cowie, 1998
RmH899	Rm1021, *dme*-3::Tn5, *tme*-4::ΩSpΦpTH433	Cowie, 1998
RmH900	Rm1021, *tme*-4::ΩSpΦpTH433	Cowie, 1998
RmH948	Rm1021, *dctA*14::Tn5ΦpTH461	Cowie, 1998
RmH949	Rm1021, *dctA*26::Tn5ΦpTH461	Cowie, 1998
RmH978	Rm1021, *tme*-2::Tn5ΦpTH597	This work
RmH979	Rm1021, *dme*-2::Tn5ΦpTH597	This work
RmH980	Rm1021, *dme*-3::Tn5, *tme*-4::ΩSpΦpTH597	This work
RmH981	Rm1021, *tme*-4::ΩSpΦpTH597	This work
RmH996	Rm1021, *dme*-2::Tn5ΦpTH458	Cowie, 1998
RmH1000	Rm1021, *dme*-1::Tn5ΦpTH458	Cowie, 1998
RmK211	Rm1021, *pckA*1::Tn3HoHo, *pod*-1, *dme*-1::Tn5, *tme*-4::ΩSpΦpTH513	This work
RmK212	Rm1021, *tme*-2::Tn5ΦpTH513	This work
RmK213	Rm1021, *tme*-3::Tn5ΦpTH513	This work

RmK214	Rm1021, *dme*-2::Tn5ΦpTH513	This work
RmK215	Rm1021, *dme*-3::Tn5ΦpTH513	This work
RmK216	Rm1021, *dme*-1::Tn5ΦpTH513	This work
RmK217	Rm1021, *dme*-3::Tn5, *tme*-4::ΩSpΦpTH513	This work
RmK218	Rm1021, *tme*-4::ΩSpΦpTH513	This work
RmK219	Rm1021ΦpTH513	This work
RmK296	Rm1021 (pTH598)	This work
RmK297	Rm1021 (pTH599)	This work
RmK298	Rm1021 (pBBR1MCS-5)	This work
RmK299	Rm1021, *dctA*14::Tn5 (pTH600)	This work
RmK300	Rm1021, *dctA*26::Tn5 (pTH600)	This work
RmK301	Rm1021, *dctA*14::Tn5 (pBBR1MCS-5)	This work
RmK302	Rm1021, *dctA*26::Tn5 (pBBR1MCS-5)	This work
RmK303	Rm1021, *pckA*1::Tn3HoHo, *pod*-1, *dme*-1::Tn5, *tme*-4::ΩSp (pTH604)	This work
RmK304	Rm1021, *pckA*1::Tn3HoHo, *pod*-1, *dme*-1::Tn5, *tme*-4::ΩSp (pTH605)	This work
RmK305	Rm1021, *pckA*1::Tn3HoHo, *pod*-1, *dme*-1::Tn5, *tme*-4::ΩSp (pTH606)	This work
RmK306	Rm1021, *pckA*1::Tn3HoHo, *pod*-1, *dme*-1::Tn5, *tme*-4::ΩSp (pBBR1MCS-5)	This work
RmK307	Rm1021, *pckA*1::Tn3HoHo, *pod*-1, *dme*-1::Tn5, *tme*-4::ΩSp (pTH598)	This work
RmK308	Rm1021, *pckA*1::Tn3HoHo, *pod*-1, *dme*-1::Tn5, *tme*-4::ΩSp (pTH599)	This work
RmK376	Rm1021, *dctA*14::Tn5 (pTH648)	This work
RmK377	Rm1021, *dctA*26::Tn5 (pTH648)	This work
RmK380	Rm1021, *dctA*14::Tn5ΦpTH647	This work
RmK381	Rm1021, *dctA*26::Tn5ΦpTH647	This work
RmK401	Rm1021 (pTH648)	This work

RmK402	Rm1021, *pckA*1::Tn3HoHo, *pod*-1, *dme*-1::Tn5, *tme*-4::ΩSp (pTH669)	This work
RmK403	Rm1021, *pckA*1::Tn3HoHo, *pod*-1, *dme*-1::Tn5, *tme*-4::ΩSp (pTH670)	This work
R. leguminosarum		
3841	*R. leguminosarum* biovar *viciae* strain 300, Sm^r	Jonston and Beringer, 1975
RU714	3841 Δ*dctABD*::ΩSp^r	Reid *et al.*, 1996
RU727	3841 *dctA*::ΩSp^r	Reid *et al.*, 1996
RlK367	3841 (pBBR1MCS-5)	This work
RlK368	3841 Δ*dctABD*::ΩSp^r (pBBR1MCS-5)	This work
RlK369	3841 *dctA*::ΩSp^r (pBBR1MCS-5)	This work
RlK370	3841 (pTH600)	This work
RlK371	3841 Δ*dctABD*::ΩSp^r (pTH600)	This work
RlK372	3841 *dctA*::ΩSp^r (pTH600)	This work
RlK378	3841 Δ*dctABD*::ΩSp^r (pTH648)	This work
RlK379	3841 *dctA*::ΩSp^r (pTH648)	This work
E. coli		
CJ236	*dut1, ung1, thi-1, relA1*/pCJ105 (cam^rF')	Kunkel *et al.*, 1987
MT616	MT607 (pRK600)	Finan *et al.*, 1986
EJ1321	*galK2, pck, dme, tme*, Sm^r	Hansen and Juni, 1975
DH5α	F^-, *end*A1, *hsd*R17 ($r^-_k m^-_k$), *sup*E44, *thi*-1, *rec*A1, λ^-,*gyr*A96, *rel*A1, Φ80d*lacZ*ΔM15	Hanahan, 1983
EcG456	EJ1321 (pTH139)	Driscoll and Finan, 1997
EcJ201	DH5α (pTH392)	This work
EcJ202	EJ1321 (pTH392)	Mitsch *et al.*, 1998
EcJ203	DH5α (pTH393)	This work
EcJ204	EJ1321 (pTH393)	Mitsch *et al.*, 1998
EcJ205	EJ1321 (pTH392Δ*Pst*I)	Mitsch *et al.*, 1998

EcJ337	DH5α (pMEE1)	Stohls and Donnely, 1997
EcJ376	DH5α (pTH507)	This work
EcJ385	DH5α (pTH512)	This work
EcJ386	EJ1321 (pTH512)	This work
EcJ387	DH5α (pTH513)	This work
EcJ390	DH5α (pTH516)	This work
EcJ391	DH5α (pTH517)	This work
EcJ466	DH5α (pTH607)	This work
EcJ467	CJ236 (pTH607)	This work
EcJ469	DH5α (pTH596)	This work
EcJ470	DH5α (pTH597)	This work
EcJ507	DH5α (pTH646)	This work
EcJ508	DH5α (pTH647)	This work
EcJ509	DH5α (pTH648)	This work
EcJ511	DH5α (pTH650)	This work
EcJ512	DH5α (pTH651)	This work
EcJ541	DH5α (pTH601)	This work
EcJ542	EJ1321 (pTH601)	This work
EcJ543	DH5α pTH602)	This work
EcJ544	EJ1321 (pTH602)	This work
EcJ545	DH5α (pTH603)	This work
EcJ546	EJ1321 (pTH603)	This work
EcJ547	DH5α (pTH650)	This work
EcJ548	EJ1321 (pTH650)	This work
EcJ549	DH5α (pTH651)	This work
EcJ550	EJ1321 (pTH651)	This work
EcJ551	DH5α (pTH604)	This work
EcJ552	DH5α (pTH605)	This work
EcJ553	DH5α (pTH606)	This work

EcJ554	DH5α (pTH669)	This work
EcJ555	DH5α (pTH670)	This work
Plasmids		
pUC119	Amp^r cloning vector, ColE1 *oriV*	Vieira and Messing, 1987
pUC118	Amp^r cloning vector, ColE1 *oriV*	Vieira and Messing, 1987
PBluescript KS	Amp^r cloning vector, ColE1 *oriV*	Alting-Mees and Short, 1989
pUCP30T	Gm^r transfer vector, *oriT, oriV*	Schweizer *et al.*, 1997
pMEE1	PTRC99a with 1.8kb *NcoI*/*PstI* fragment carrying *sfcA*	Stohls and Donnely, 1997
pBBR1MCS-5	Gm^r broad host range mobilizable cloning vector	Kovach *et al.*, 1995
pRK600	pRK2013 *npt*::Tn9, Cm^r Nm^s-Km^r	Finan *et al.*, 1986
pTH139	pUC119 with 3.1kb *HindIII* fragment carrying *dme*	Driscoll and Finan, 1997
pTH251	pUC118 with 7.1kb *BamHI* fragment carrying *tme*	Mitsch *et al.*, 1998
pTH392	pUC119 with 2.7kb *HindIII* fragment carrying *tme*	Mitsch *et al.*, 1998
pTH393	pUC119 with 2.7kb *HindIII* fragment carrying *tme* (opposite orientation to pTH392)	This work
pTH392Δ*PstI*	*PstI* deletion of pTH392 removing 1160 bp of 3' end of *tme*	Mitsch *et al.*, 1998
pTH398	*SalI* deletion of pTH139	Cowie, 1998
pTH400	pTH398 with *SphI* site at ATG of *dme*	Cowie, 1998
pTH407B	pUC119 with *SphI* site at ATG of *tme*	Cowie, 1998
pTH409	pUC119 with *dme*-promoter *tme* gene fusion (*pdme-tme*)	Cowie, 1998
pTH408	pUC119 with *SphI* site at ATG of *dme*	Cowie, 1998
PTH412	PTH409 with *HindIII* site at 3' end of *dme*	Cowie, 1998
pTH449	pUC119 with *pdme-maeP* fusion	Cowie, 1998
pTH461	pUCP30T with *dme* promoter upstream of complete *maeP*	Cowie, 1998
pTH481	pTH400 with 660 bp *SphI*/*SstI* PCR fragment of *dme* to give *pdme-dme*	This work
pTH507	pUC118 with 2 kb *HindIII*/*SstI* fragment of pTH412	This work
pTH512	pTH408 with 1.8 kb *SphI*/*PstI* PCR fragment of *sfcA* to give *pdme-sfcA*	This work

pTH513	pUCP30T with 2.2kb *Hind*III/*Pst*I fragment of pTH512 *(pdme-sfcA)*	This work
pTH516	pUC119 with *Eco*RI and *Sst*I sites removed by *Sst*I followed by S1 nuclease treatment and religation	This work
pTH517	pTH516 with 3 kb *Hind*III/*Kpn*I fragment of pTH409 (*pdme-tme*)	This work
pTH596	pKS with *Hind*III/*Kpn*I *tme* promoter-*dme* gene	This work
pTH597	pUCP30T with *Bam*HI/*Kpn*I fragment from pTH596 to give *ptme-dme*	This work
pTH598	pBBR1MCS-5 with *Hind*III/*Kpn*I fragment from pTH408 (*dme*)	This work
pTH599	pBBR1MCS-5 with *Hind*III/*Kpn*I fragment from pTH407B (*tme*)	This work
pTH600	pBBR1MCS-5 with *Hind*III/*Kpn*I fragment from pTH449 (*pdme-mael'*)	This work
pTH601	pUC119 containing *pdme Hind*III/*Sst*I (1124 bp) *tme* (1.8 kb) hybrid gene	This work
pTH602	pUC119 containing *pdme Hind*III/*Sal*I (856 bp) *tme* (2.1 kb) hybrid gene	This work
pTH603	pUC119 containing *pdme Hind*III/*Sph*I (1231 bp) *tme* (1.7 kb) hybrid gene	This work
pTH604	pBBR1MCS-5 containing *Hind*III/*Kpn*I fragment of pTH601 *pdme* (1124 bp) *tme* (1.8 kb) hybrid gene	This work
pTH605	pBBR1MCS-5 containing *Hind*III/*Kpn*I fragment of pTH602 *pdme* (856 bp) *tme* (2.1 kb) hybrid gene	This work
pTH606	pBBR1MCS-5 containing *Hind*III/*Kpn*I fragment of pTH603 *pdme* (1231 bp) *tme* (1.7 kb) hybrid gene	This work
pTH607	*Sst*I deletion of pTH517 (*pdme-tme*ΔSstI)	This work
pTH646	pUC119 with 250bp *Hind*III/*Sph*I PCR fragment of *dctA* promoter	This work
pTH647	pTH461 with insertion of *Hind*III/*Sph*I fragment of pTH646 (*pdctA-mael'*)	This work
pTH648	pBBR1MCS-5 containing *Hind*III/*Kpn*I fragment of pTH647 (*pdctA-mael'*)	This work
pTH650	point mutation of pTH607 (N131D), *Hind*III/*Sst*I fragment ligated into pTH517 to yield *pdme-tme*N131D	This work
pTH651	point mutation of pTH607 (D113G), *Hind*III/*Sst*I fragment ligated into	This work

	pTH517 to yield *pdme tme*D113G	
pTH669	3 kb *Hind*III/*Kpn*I (*pdme-tme*N131D) fragment from pTH650 inserted into pBBR1MCS-5	This work
pTH670	3 kb *Hind*III/*Kpn*I (*pdme tme*D113G) fragment from pTH651 inserted into pBBR1MCS-5	This work

Growth curves

5 ml LBmc test tubes inoculated with the *S. meliloti* strains of interest were incubated on a rotating wheel at 30°C overnight. The following day, aliquots were removed

and transferred to 5 ml test tubes containing M9 liquid media until the OD_{675} of each tube was brought up to 0.1 absorbance units as measured in a Baush and Lomb spectronic 20. 100 µl of this stock was then used as an inoculant for 3 identical test tubes containing 5 ml of an M9 solution with the carbon source of interest. The tubes were then incubated on a rotating wheel at 30°C over a period of several days with OD_{675} readings taken on a Baush and Lomb spectronic 20 at indicated timed intervals.

Transductions

Transductions were carried out using the bacteriophage ϕM12 (Finan *et al.*, 1984). 5ml of LBmc was inoculated with the *S. meliloti* strain of interest and grown overnight. The sample was then subcultured and allowed to grow to an OD_{600} of approximately 0.4-0.5 after which time 50-100 µl of the bacteriophage was added and the culture was incubated at 30°C overnight. Clearing of the culture overnight was indicative of cell lysis and the remaining intact cells were lysed by the addition of 200 µl of chloroform. Cell debris was removed by centrifugation at 4000 rpm for 5 minutes in a Beckman GPR bench top centrifuge and the supernatant containing the phage lysate was transferred to screw cap tubes and stored at 4°C. Prior to use, the phage lysate was diluted to 1/20 in LBmc and 0.5 ml was added to 0.5 ml of recipient *S. meliloti* culture followed by incubation at room temperature for 20 minutes to allow for adsorption. The

samples were centrifuged at 4000 rpm for 5 minutes and the infected cell pellets were washed with sterile saline. This process was repeated for a total of three times and after the final centrifugation the pellet was resuspended in 0.5 ml of sterile saline. 0.1 ml aliquots were plated on LBmc selective media and resulting colonies were streak purified three times prior to further experimentation.

Conjugation

Plasmids pUCP30T (Schweizer *et al.*, 1997) and pBBR1MCS-5 (Kovach *et. al.*, 1995) both contain *oriT* sites which allow for transfer of the plasmid between bacterial strains. A helper *E. coli* strain that carries the plasmid pRK600 provided the gene products necessary for conjugation and mobilization of *oriT* containing plasmids. Overnight cultures of the *E. coli* donor, *S. meliloti* recipient, and the MT616 *E. coli* helper strain were transferred to microcentrifuge tubes and spun at 13000 rpm in a table top centrifuge. The pellets were resuspended in sterile saline and 20 µl of each strain was added to a microcentrifuge tube and the resulting 60 µl mixture was spotted onto LB plates. The plates were incubated at 30°C overnight to allow for growth of all three cultures and plasmid transfer. The mating spots were collected with a sterile wooden applicator stick or loop and transferred to a microcentrifuge tube containing 500 µl of sterile saline. Serial dilutions were carried out ranging from 10^{-1} to 10^{-6} and 100 µl of each was plated on selective media containing gentamicin (20 µg/ml) to select for the chromosomal insertion or the plasmid and an antibiotic specific for the recipient strain, usually neomycin or streptomycin. Unless otherwise specified 10^{-5} and 10^{-6} dilutions were sufficient for plasmid transfers with pBBR1MCS-5 while 10^{-1} or 10^{-2} dilutions were

sufficient to obtain chromosomal cointegrate strains. Selected colonies were streak purified on selective media three times prior to further experimentation.

Cell extracts

Cell free extracts were prepared from 5 ml overnight cultures of *S. meliloti* or *E. coli* grown in LBmc and LB respectively. The overnight cultures were transferred to sterile 15 ml Falcon conical tubes and centrifuged at 4000 rpm for 10 minutes in a Beckman GPR bench top centrifuge to pellet the cells. Once initiated, the samples were kept on ice during the entire procedure to minimize enzyme degradation. The resulting pellets were washed with 5 ml of sterile rinse buffer (10 mM Tris HCl pH 7.8, 1 mM $MgCl_2$) and centrifuged as before. The resulting pellet was then resuspended in 200 µl of sterile sonication buffer (10 mM Tris HCl pH 8.0, 1 mM $MgCl_2$, 10 mM KCl, 20% glycerol, 10 mM β-mercaptoethanol) and transferred to the sonicator. Sonication was carried out in a Heat systems ultrasonic processor XL with the following settings for *S. meliloti* strains; 30 seconds on, 20 seconds off, total time 45 minutes at 4°C, power output setting 8. For *E. coli* samples and bacteroids the cells were washed as above and resuspended in sonication buffer but total sonication time was reduced to 30 minutes. The sonicated samples were transferred from the 15 ml tubes to microcentrifuge tubes and centrifuged at 13000 rpm for 10 minutes at 4°C. The supernatant was transferred to a second microcentrifuge tube and the centrifugation procedure was repeated for a total of three times. The resulting cell free extract was stored at –80°C.

DNA manipulations

Restriction endonucleases and DNA modifying enzymes were used according to the manufacturers specifications. Digestion of DNA was verified by electrophoresis using 1% agarose gels in TAE buffer (Sambrook *et al.*, 1989), stained with ethidium bromide, and visualized with a transilluminator (Fisher Biotech model FBTIV-816). Photographs of gels were obtained with a Mitsubishi video copy processor using K65HM high density type thermal paper, and a Panasonic video monitor (TR930CB). DNA fragments for cloning were isolated from agarose gels with a Geneclean kit from Bio 101. Ligations were carried out in 10 µl final volumes at room temperature. Transformations were carried out with $CaCl_2$ treated DH5α or EJ1321 competent *E. coli* cells (Ausubel *et al.*, 1989) plated onto appropriate selective media, and incubated at 37°C overnight. Alkaline lysis procedures (Sambrook *et al.*, 1989) were used to isolated plasmid DNA from transformants in order to verify construct integrity. When required, DNA of increased purity for cloning experiments was obtained by using spin columns obtained by Qiagen (Qiagen, QIAprep miniprep kit).

Polymerase chain reaction

Oligonucleotides were designed with the aide of the Gene Runner 3.04 program (Hastings software, 1994). Primers used in all PCR reactions were obtained from the MOBIX central facility at McMaster University and resuspended in sterile distilled deionized water to a final concentration of 100 pmoles/µl. For all PCR reactions a series of $MgCl_2$ concentrations ranging from 0 to 4 mM was used to maximize probability of obtaining product. Reactions were carried out in 100 µl final volumes and contained

100pmoles of each primer, 10-50 ng of template plasmid DNA, 0.8 mM dNTP's, 1x Taq buffer (supplied), and 1 µl of platinum Taq (Gibco BRL). All PCR reactions were carried out in a Perkin-Elmer thermocycler (Perkin Elmer gene amp PCR system 2400). All PCR reactions had a 5 minute 94°C denaturation period prior to the PCR reaction itself and after completion of the reaction an elongation step of 7 minutes at 72°C and storage at 4°C was carried out prior to the tubes being removed and stored at -20°C. After the reaction was complete 20 µl of each sample was run on an agarose gel to verify fragment production. Successful reactions were pooled and precipitated with ethanol or purified via a Qiagen spin column procedure (Qiagen, QIAquick PCR purification kit). Upon purification PCR fragments were restricted with appropriate enzymes and used for cloning.

Sequencing

The sequence of both strands of the *tme* gene region was determined through a combination of subclone production and primer walking. Primers specific for *tme* were obtained from the MOBIX central facility at McMaster University while the IS50 primer used to sequence out of Tn5 and Tn5B20 insertions (5'-TCA CAT GGA AGT CAG ATC CT-3') was kindly provided by Dr R.J. Watson. DNA sequencing was performed at the MOBIX central facility at McMaster University using an ABI 373 Stretch DNA automated sequencer using dye terminator chemistry and cycle sequencing. The completed *tme* sequence was deposited in Genebank under the accession number O30808.

RNA isolation

RNA was isolated from LBmc grown *S. meliloti* cells using a Qiagen total RNA isolation kit (Qiagen, RNeasy midi prep kit). 50 ml of LBmc was inoculated with an overnight 5 ml LBmc preculture of the *S. meliloti* culture of interest and incubated in a series 25 incubator shaker (New Brunswick Scientific) at 30°C overnight to yield the $5x10^9$ cells required. The culture was transferred to a 50 ml conical Falcon tube and centrifuged for 5 minutes at 4000 rpm on a Beckman GPR table top centrifuge (used in all subsequent centrifugations). The supernatant was removed and the pellet resuspended in 1 ml of TE buffer containing lysozyme and incubated at room temperature for 5 minutes. 3.8 ml of RLT buffer was added and the samples vortexed vigorously. The bacterial lysate was centrifuged for 5 minutes at 4000 rpm and the resulting supernatant was transferred to a second 15 ml conical Falcon tube. 2.8 ml of ethanol was added and the sample vortexed and a portion of the resulting solution transferred by pipetteman to a RNeasy midi spin column resting in a 15 ml conical Falcon tube. The samples were then centrifuged for 5 minutes at 4000 rpm and the effluent discarded. The remaining portion of the sample was added to the column and the centrifugation step repeated. The effluent in the conical tube was removed and the column washed with 3.8 ml of buffer RW1. The samples were centrifuged at 4000 rpm for 5 minutes and the effluent discarded. The column was washed a second time with 2.5 ml of buffer RPE and centrifuged at 4000 rpm for 5 minutes. The effluent was discarded and the wash step repeated with another 2.5 ml of RPE buffer. The spin column was then dried by centrifugation at 4000 rpm for 5 minutes and the conical tube removed and replaced with a new one. The RNA was

then eluted by the addition of 200 µl RNase free water to the column and allowed to incubate at room temperature for 5 minutes. The column was centrifuged at 4000 rpm for 5 minutes and the effluent collected and transferred to an RNase free microcentrifuge tube. To eliminate contaminating DNA, Tris HCl pH 7.5 and $MgCl_2$ were added to 10 mM final concentration and 5 µl of RNase-free DNase was used. After incubation at 37°C for 1 hour the RNA was precipitated with 2 volumes of 95% ethanol and centrifuged at 13000 rpm. The pellet was washed with 70% ethanol and resuspended in RNase free water. RNA concentration was estimated by measuring an aliquot in a Varian spectrophotometer at 260 nm and RNA isolation and DNA elimination was verified by running an aliquot on a 1.2% agarose gel, staining with ethidium bromide, and observing on a transilluminator. The RNA was stored at –80°C prior to use.

Primer extension

Primer extension assays were carried out as described in Ausubel *et al.*, (1989). The oligonucleotide 5'-GAC CTT GAG AAT GAA AAT CG-3' was produced at the MOBIX central facility at McMaster University. The oligonucleotide is 60-79 base pairs from the putative translational start site. 10 pmoles of the oligonucleotide was labeled using 50 µCi of [γ-^{33}P] ATP (3000 Ci/mmol) obtained from NEN Life Science Products Inc. and 10 units of T4 polynucleotide kinase (New England Biolabs) in a total volume of 20 µl and incubated at 37°C at 37°C for 1 hour. After the labeling reaction was complete the primer was precipitated with 10 µg of tRNA, 180 µl of 0.5 M ammonium acetate, 10 mM EDTA, and 500 µl of 95% ethanol. The sample was spun down at 13000 rpm for 15 minutes at 4°C. The pellet was resuspended in 200 µl of 0.5 M ammonium acetate, 10

mM EDTA, and 500 µl of 95% ethanol and centrifuged again. This procedure was repeated for a total of three times in order to remove all unincorporated radioactivity. The final pellet was resuspended in 50 µl DEPC treated water and 1 µl of the primer was transferred to a 2.4 cm whatman GF-C filter and counts carried out in a Beckman LS1801 scintillation counter to determine incorporation levels. Approximately 10^6 counts per minute were used in each primer extension assay along with 30 µg of total bacterial RNA or tRNA as a control. The nucleotide mixture was precipitated by the addition of ammonium acetate to 0.3 M and 2.5 volumes of 95% ethanol. The samples were centrifuged at 13000 rpm for 15 minutes at 4°C and the resulting pellet was rinsed with 70% ethanol. The pellets were then resuspended in 30 µl of 3x aqueous hybridization buffer which contained 3 M NaCl, 0.5 M Hepes pH 7.5, and 1 mM EDTA and incubated at 30°C overnight. The volume of the samples was increased to 200 µl with 0.3 M ammonium acetate and 500 µl 95% ethanol was added for precipitation of the nucleic acids. The samples were then centrifuged at 13000 rpm with a table top centrifuge for 15 minutes at 4°C and the resulting pellet was rinsed with 70% ethanol. The resulting pellet was dissolved in 14.5 µl DEPC treated water, 5 µl of 5x reverse transcriptase buffer (Gibco-BRL), 3.5 µl of 4 mM dNTP's, 1 µl RNA guard (Pharmacia), 1 µl 0.1 M DTT, and 1.5 µl reverse transcriptase (Gibco-BRL). The samples were incubated at 30°C for 2 hours. After the incubation time 1 µl of 0.5 M EDTA and 1 µl of DNase free RNase was added to stop the reaction and degrade the mRNA template. After 30 minutes incubation at room temperature, 175 µl 0.5 M ammonium acetate, and 200 µl of buffer saturated

phenol was added, mixed, and centrifuged briefly. The upper aqueous phase was transferred to a new microcentrifuge tube and precipitated with 200 µl 95% ethanol and centrifuged at 13000 rpm at 4°C. The resulting pellet was rinsed with 70% ethanol and dried at room temperature until all the ethanol was removed. The pellet was resuspended in 2 µl DEPC treated water and 3 µl formamide dye. Carrying out a sequencing reaction with the same labeled primer produced the DNA ladder used to identify the transcriptional start site. A dideoxy sequencing reaction was carried out according to the specifications of the Sequenase 2.0 sequencing kit (Amersham) using pTH251 as a template. The samples were heated to approximately 90°C for 10 minutes and then run on a preheated 7% poly acrylamide sequencing gel (Ausubel *et al.*, 1989). Upon the completion of the electrophoresis run the gel was transferred to a sheet of Whatman paper and dried on a model 583 gel dryer (Bio-Rad) for 2 hours and transferred to an autoradiogram cassette and exposed for several weeks with Kodak X-OMAT film (Kodak). After several weeks of exposure the film was developed in a Kodak M35A X-OMAT processor.

In addition to identifying the transcriptional start site, the translational start site was verified by sequencing the TME protein itself. Purified TME was sent to the Alberta Peptide Institute (Edmonton, Alta) where the N-terminal region of the protein was sequenced on a Hewlett Packard G1005A protein sequencer.

Oligonucleotide directed mutagenesis

A small region of *tme* was obtained by subcloning a *Hind*III/*Sst*I fragment into pUC118 to produce pTH507. This construct was then utilized for oligonucleotide

directed mutagenesis following the method of Kunkel *et al.*, (1987) as outlined in Sambrook *et al.*, (1989). pTH507 was transformed into CJ236, an ung- dut- *E. coli* strain and single stranded DNA was produced by infecting the cells with the bacteriophage M13K07 (Sambrook *et al.*, 1989). Oligonucleotides containing the codons targeted for substitution were obtained from the MOBIX central facility at McMaster University. For the alteration of D to G at amino acid position 113 of TME the primer 5'-CGA TCG AAT CGA CGC CGG CGA AGC-3' was produced. This sequence differs from the *tme* sequence at the highlighted base where a C has replaced a T. Thus the codon in this region has been altered from GAC to GGC; a conversion from an aspartic acid residue to a glycine residue. The amino acid substitution at position 131 of TME was obtained with the primer 5'-CGC AGT CGA CAA ATT CGT CGA CGT TTT C-3'. This sequence differs from the *tme* sequence at the highlighted bases where a C has replaced a T and an A has replaced a G. The first substitution alters the codon from AAC to GAC which alters an asparagines to an aspartic acid residue while the second substitution replaces the TTC codon to TTT which conserves the phenylalanine residue at that position. The second alteration was made to delete an *Eco*RI site for identifying the proper amino acid substitution. 100 pmoles of each of these oligonucleotides was phosphorylated with 0.5 mM ATP and polynucleotide kinase in a 20 µl final volume. Incubation was carried out at 37°C for 45 minutes and the enzyme was heat inactivated by treatment at 65°C for 10 minutes. The phosphorylated oligonucleotides were diluted to 2 pmoles/µl and 1 µl of this was added to 0.2 µg of single stranded template DNA, 20 mM Tris HCl pH 7.4, 2 mM $MgCl_2$, 50 mM NaCl, in a 10 µl final volume. The samples were heated to

approximately 80°C to denature the DNA and allowed to cool to room temperature to facilitate DNA annealing. 1 µl of T4 DNA polymerase, 0.5 µl of T4 DNA ligase and 1 µl of 10x synthesis buffer (5 mM dNTP's, 10 mM ATP, 100 mM Tris HCl pH 7.4, 50 mM $MgCl_2$, 20 mM DTT) was added. The reaction was incubated at 37°C for 90 minutes. To verify that elongation occurred, 5 µl of each reaction was removed and run on a 1% agarose gel. The remainder of each sample was transformed into competent DH5α cells and plated on LB ampicillin plates. Clones for each sample were selected, minipreped, and analyzed for the loss of an *Aat*II site (for the conversion at amino acid residue 113) or the loss of an *Eco*RI site (for the conversion at amino acid residue 131). Once clones had been identified that lacked the restriction sites, sequencing reactions were carried out to verify successful mutagenesis.

Protein determination

To determine protein concentrations of the various cell free extracts and purified enzyme samples a modified Bradford (1976) assay was utilized. Small volumes (5-10 µl) of sample or dilutions thereof were added to sterile distilled water to a final volume of 800 µl. 200 µl of undiluted Biurets agent (Bio Rad) was added, the samples were vortexed, and left at room temperature for approximately 15 minutes. The absorbance at 595 nm was measured on a Varian Cary 1E UV-visible spectrophotometer and protein content was estimated from a standard curve of bovine serum albumin (BSA) made up of 0.1-20 µg of protein.

To estimate the amount of protein present for whole cell samples used for transport assays an alternative method was utilized (Lowry *et al.*, 1951). Cell

suspensions were diluted 1:1 in 1 M NaOH and boiled for 15 minutes. Dilutions of this stock were carried out with 0.5 M NaOH (usually 1/5) and the sample volume was increased to 800 µl with distilled deionized water. 200 µl of undiluted Biurets agent (Bio Rad) was added, the sample vortexed and the absorbance at 595 nm was determined using a Varian Cary 1E UV-visible spectrophotometer within one hour. Protein concentrations were estimated by the creation of a standard curve made up of 2.5 µg-15 µg of BSA resuspended in 0.5 M NaOH.

Malic enzyme assay

Two separate malic enzyme assays were utilized for determining enzyme activity. One relied upon the change of absorbance at 340 nm due to the reduction of $NAD(P)^+$ while the second was a colorometric assay based upon pyruvate formation. For both assays all samples were done in triplicate. In both cases a 995 µl reaction mix made up of 100 mM Tris HCl pH 7.8, 30 mM K-L- malate, 3 mM $MnCl_2$, and 1.5 mM $NAD(P)^+$ was used. For the reduction assay the reaction mixture was placed in a 3 ml plastic half microcuvette, 5 µl of cell extract was placed on the wall of the cuvette and the reaction initiated by covering the cuvette with parafilm and inverting it several times. The cuvette was then inserted into a Varian Cary 1E UV-visible spectrophotometer and the change in absorbance at 340 nm was recorded for 3 to 5 minutes. The change in absorbance over time was translated into specific activity (nmoles/min/mg protein) by the following formula:

$$(\text{Slope}/0.00622)/\text{mg protein}$$

where slope equals the change in absorbance over time, 0.00622 is the extinction coefficient of $NAD(P)^+$, and mg protein is the amount of cell extract added to the reaction mix.

The pyruvate formation assay consisted of placing the 995 µl reaction mixture in a 10 mm x 75 mm glass tube and adding 5 µl of cell extract to the side of the tube. The reaction was initiated by vortexing the sample and incubating for 10 minutes at room temperature. Following this incubation period, 0.33 ml of 0.1% 2,4-Dinitrophenylhydrazine (made fresh for every experiment by solubilizing the DPH in 2 M HCl and incubating at 30°C for one hour prior to the experiment) was added to stop the reaction and the sample vortexed briefly and incubated for a further 10 minutes. 1.67 ml of 2.5 M NaOH was added and the samples vortexed briefly and incubated at room temperature for 10 minutes. The samples were then centrifuged at 4500 rpm for 10 minutes in a Beckman GPR table top centrifuge. The resulting supernatant was transferred by Pasteur pipette to a 1.5 ml glass half microcuvette and the absorbance at 445 nm was obtained with a Varian Cary 1E UV-visible spectrophotometer. A standard curve of pyruvate concentrations between 0 and 200 nmoles was prepared in the same manner and used to estimate the amount of pyruvate generated in each assay. Specific activity was determined as nmoles pyruvate produced/minute/mg protein.

Malate dehydrogenase assay

Malate dehydrogenase (MDH) activity was determined by observing the change in absorbance at 340 nm due to the reduction of NAD^+. A 2995 µl reaction mix made up of 100 mM glycine NaOH pH 10, 85 mM Na_2-malate pH 7.5, and 2.5 mM NAD^+ and

placed in a 5 ml plastic half microcuvette. 5 µl of cell extract was added to the wall of the cuvette and the reaction initiated by covering the cuvette with parafilm and inverting it several times. The cuvette was then placed in a Varian Cary 1E UV-visible spectrophotometer and the change in absorbance at 340 nm was recorded over 3 to 5 minutes. The change in absorbance over time of this reaction was translated into a specific activity (nmoles/min/mg protein) using the extinction coefficient of 0.00622 for NAD.

Transport assay

Transport assays were carried out according to the method outlined by Finan *et al.*, (1981). For transport assays utilizing *S. meliloti* cells, 50 ml of M9 minimal media with 15 mM glucose was grown overnight at 30°C in a New Brunswick Scientific controlled environmental incubator shaker. The culture was transferred to a sterile 50 ml conical Falcon tube and the cells were pelleted at 4500 rpm in a Beckman GPR table top centrifuge for 10 minutes at 4°C and the resulting pellet was resuspended in TAS solution (40 mM MOPS pH 7.0, 20 mM KOH, 4 mM $MgSO_4$, 20 mM NH_4Cl, 0.2 mM $CaCO_3$, 0.1 mM NaCl, 1.2 mM K_2HPO_4, and 0.4 mM KH_2PO_4). Pellets were washed with TAS buffer for a total of three times and the pellet was resuspended to approximately 20 mg/ml in TAS buffer and stored on ice. The assays were conducted with radiolabelled L-[1,4(2,3)-^{14}C] malic acid (Amersham), 55 mCi/mmol. A typical assay involved adding 100 µl of cell suspension to 280 µl MMS buffer in a 10mm x 75mm test tube and pre-incubating the assay solution at 30°C for 5 minutes. The assay was then initiated by adding 20 µl of the radioactive substrate (0.8 mM malate) followed by vortexing and

removing aliquots over a predetermined time course (1-6 minutes). The samples removed were filtered through a vacuum manifold containing 0.45 μm nitrocellulose membranes (Millipore) and rinsed with 5-10 ml of TAS buffer to remove any unincorporated radioactive substrate. Filters were then placed under a heat lamp to dry the membranes after which time they were placed into scintillation vials with 5 ml of biodegradable counting scintillant (BCS) scintillation cocktail (Amersham) and radioactive counts per minute were determined with a Beckman LS1801 scintillation counter. Each assay was carried out in triplicate and uptake rates were then determined for three time points ranging from 1 to 6 minutes. Transport assays for *S. meliloti* cells were carried out with 40 μM of malate and, when required, succinate was added to a final concentration of 800 μM 15 seconds before the addition of the radioactive substrate in order to test for inhibition effects.

R. leguminosarum bacteroids from pea plants were isolated, resuspended in cold MMS buffer (40 mM MOPS, 20 mM KOH, 2 mM $MgSO_4$, 0.3 M sucrose, pH 7), and ground to a slurry in a mortar and pestle and stored on ice during the remainder of the procedure. The slurry was filtered through 4 layers of cheese cloth into a 15 ml conical Falcon tube and the suspension was centrifuged at 4°C and 500 rpm in a Beckman GPR table top centrifuge for 10 minutes. The supernatant was transferred to a fresh 15 ml conical Falcon tube and recentrifuged under the same conditions. The supernatant was centrifuged at 4°C at 4000 rpm in order to pellet the bacteroids. The pellet was resuspended in 5 ml of MMS and recentifruged to pellet the bacteroids. This rinse step was repeated for a total of three times to eliminate any plant debris. The bacteroid pellet

was resuspended to approximately 30 mg/ml in MMS buffer and stored on ice. All transport assays were completed within three hours of isolating the bacteroids and the sample was kept on ice during that time. Transport assays were carried out with radiolabelled L-[1,4(2,3)-^{14}C] malic acid (Amersham), 55 mCi/mmol. A typical assay involved adding 100 µl of bacteroid suspension to 280 µl MMS buffer in a 10mm x 75mm test tube and pre-incubating the assay solution at 30°C for 5 minutes. The assay was then initiated by adding 20 µl of the radioactive substrate followed by vortexing and removing aliquots over a predetermined time course (1-6 minutes). The samples removed were filtered through a vacuum manifold containing 0.45 µm nitrocelliulose membranes (Millipore) and rinsed with 5-10 ml of MMS buffer to remove any unincorporated radioactive substrate. Filters were then placed under a heat lamp to dry the membranes after which time they were placed into scintillation vials with 5 ml of biodegradable counting scintillant (BCS) scintillation cocktail (Amersham) and counts per minute determined with a Beckman LS1801 scintillation counter. Each assay was carried out in triplicate and uptake rates were then determined for three time points ranging from 1 to 6 minutes. Transport assays for bacteroids were carried out with 40 µM of malate and, when required, succinate or aspartate was added to a final concentration of 800 µM 15 seconds before the addition of the radioactive substrate in order to test inhibition effects. To determine the kinetic parameters of the malate permease, bacteroids obtained from pea plants inoculated with RIK372, a *dctA*$^-$, *pdme-maeP R. leguminosarum* strain were utilized in malate transport assays as outlined above. Each assay was carried out in triplicate and uptake rates were then determined for two

time points ranging from 1 to 2 minutes. Transport assays for bacteroids were carried out with 40, 80, 100, 200, and 400 μM malate concentrations.

SDS PAGE

7% polyacrylamide gels were used for separating proteins for observation and transfer to membranes for western analysis. MiniProtean II gel assembly's (Bio-Rad) were used exclusively for casting and running PAGE gels. Separating gels were made up of 2.55 ml H_2O, 1.25 ml 1.5 M Tris HCl pH 8.8, 1.15 ml acrylamide (30/2.6), 50 μl 10% SDS, 2.5 μl TEMED, and 25 μl 10% ammonium per sulfate. The separating gel solution was added to the MiniProtean II assembly's by pipetting enough solution to reach a point immediately under the teeth of the comb (approximately 4ml). The gels were polymerized at room temperature or at 37°C depending on time constraints. After polymerization had been achieved the stacking gel made up of 1.5 ml H_2O, 1.25 ml of 0.5 M Tris HCl pH 6.8, 0.33 ml acrylamide (30/2.6), 25 μl 10% SDS, 2.5 μl TEMED, and 12.5 μl 10% ammonium persulfate was added. The comb was inserted into the gel and polymerization allowed to occur. After polymerization the combs were removed, the gel assembly's were placed in the MiniProtean II chamber and submerged in running buffer (14.4 g glycine, 3 g Tris base, and 1 g SDS per litre). The wells were cleared of any unpolymerized acrylamide by gentle injection of running buffer via a syringe. The protein samples (usually between 1-2 μg total protein) were prepared in a microcentrifuge tube with 4x loading buffer (Sambrook *et al.*, 1989) and heated to 100°C for 5 minutes and centrifuged at 13000 rpm to collect all material. Samples were placed

in the wells with a Hamilton syringe and run at 200 volts for approximately 30 minutes or until the bromophenol blue dye of the loading buffer reached the bottom of the gel.

The gel assembly's were removed from the MiniProtean II chamber, rinsed with water and the gels removed from the glass plates and transferred to weigh boats or to whatman paper if western blots were to be conducted (see below). The gels were stained with Coomassie brilliant blue stain for several hours and destained with repeated rinses of destain solution (Sambrook *et al.*, 1989) until protein bands were visible.

Native PAGE

Non-denaturing polyacrylamide gels were used to visualize the malic enzymes in the form of zymograms. The MiniProtean II gel assembly's (Bio Rad) were used to produce non-denaturing polyacrylamide gels. Separating gel solution contained 3 M Tris pH 8.9, 0.23 ml TEMED, and sterile distilled deionized water up to 100 ml. Separating gel acrylamide solution contained 28 g acrylamide, 0.74 g Bis-acrylamide and sterile distilled deionized water up to 100 ml. For the standard 6% gel, 1.5 ml of the separating gel buffer, 2.57 ml of the separating gel acrylamide solution, 0.75 ml of a 1% ammonium persulfate solution and the volume brought up to 12 ml by the addition of a 5% sucrose solution. Approximately 4 ml of this solution was injected between the glass slides of the MiniProtean II assembly and polymerized by incubation for 30 minutes at 37°C. Stacking gel solution contained 0.5 M Tris HCl pH 6.7, 0.46 ml TEMED, and sterile distilled deionized water up to 100ml. Stacking gel acrylamide solution contained 10 g acrylamide, 2.5 g Bis-acrylamide and sterile distilled deionized water up to 100 ml. For all non-denaturing gels, 1 ml of stacking gel buffer, 2 ml of stacking gel acrylamide

solution, 4 ml of 5% sucrose solution, 0.5 ml of a 0.2% riboflavin and 0.5 ml of 1% ammonium persulfate. Approximately 1 ml of the stacking gel solution was added to the surface of the separating gel, a comb was inserted and the stacking gel allowed to polymerize for 30 minutes at 37°C. After polymerization the comb was removed and the gel assemblies placed in the MiniProtean II electrophoresis chamber and running buffer was added. Non-denaturing gel running buffer consisted of 5.76 g glycine and 1.2 g Tris base and the volume brought up to 2 L with distilled deionized water. The wells of the gel were cleared of non polymerized acrylamide by injecting running buffer into the wells with a syringe. The electrophoresis tank was then transferred to a 4°C cold room and allowed to equilibrate for 30 minutes prior to sample addition. Protein extracts were prepared by transferring 30 μg-60 μg of protein solution to a microcentrifuge tube and adding 10 μl of 2x sample buffer (1 ml H_2O, 1 ml stacking gel solution, 1 ml 80% glycerol, and a small amount of bromophenol blue). The samples were mixed and stored on ice prior to transfer to the 4°C cold room. Samples were loaded on the gel using a Hamilton syringe an electrophoresis at a constant current of 4 mA until the dye had passed through the stacking gel (approximately 1 hour). Once the dye had entered the separating gel the current was increased to 7 mAmps and run until the dye had reached the end of the separating gel (approximately 3 hours). Once electrophoresis was complete the electrophoresis tanks were removed from the cold room, the assemblies disconnected and the gels gently removed from the glass plates by running sterile water between the gel and the glass plate. The gel was transferred to a weight boat and immersed in 100 ml of wash buffer prior to staining. Wash buffer contained 100 mM

Tris HCl pH 7.8, 30 mM K-L-malate pH 7.8, 3 mM $MnCl_2$, and 50 mM KCl. The wash buffer was removed after 15 minutes and replaced with 50 ml of staining solution. Staining solution was made up of 50 ml of wash buffer with 15 mg 3-[4,5-Dimethylthiazol-2-yl]-2,5-diphenyltetrazolium bromide (MTT), 15 mg $NAD(P)^+$ or NAD^+ and 2 mg phenazine methosulfate (PMS). The gels were covered with a second inverted weight boat and incubated at 30°C for up to 1 hour. After staining, the gels were rinsed repeatedly with water and photographed or dried down for storage.

For determination of the size of the native and truncated TME proteins the protocols outlined in the Sigma Non denaturing protein molecular weight marker kit were used (Technical bulletin No. MKR-137). Non-denaturing gels of 4.5%, 5%, 5.5%, 6%, 7%, 8%, 9%, and 10% were produced and loaded with approximately 30 μg of total protein. The gels were electrophoresed and stained as outlined above and the migration distance of the stained TME band through the separating gel was determined and recorded. In order to determine the size of the native TME protein a set of protein standards was utilized. Bovine milk α-lactalbumin (14.2 kDa), bovine erythrocyte carbonic anhydrase (29 kDa), chicken egg albumin (45 kDa), bovine serum albumin (both monomer, 66 kDa, and dimer,132 kDa, form), and Jack bean urease (both trimer, 272 kDa, and hexamer, 545 kDa) was used (Sigma non-denaturing protein molecular weight marker kit). All samples were resuspended in 1 ml of 50 mM NaCl, 1 mM sodium phosphate pH 7.0 except for the Jack bean urease which was resuspended in 1 ml sterile distilled deionized water. These standards were run on identical gels and identical conditions to those used for the TME samples. Once electrophoresis was complete, the

gels were stained with Coomassie brilliant blue and destained until protein bands were visible. The migration distance of the stained standards was determined and recorded for each gel concentration. The migration distances were plotted as 100[log(Rfx100)] vs. gel concentration for each of the standards and the samples from the gels stained for $NADP^+$-dependent activity. The slope values for the molecular weight standards were then plotted against their known molecular weights. The slopes of the native and truncated TME samples were then read from the standard curve and their molecular weights determined.

Western blots

SDS PAGE gels were produced as described previously (see above section) and transferred to Immobilon P membranes (Millipore) pretreated in methanol. Transfers were carried out using the western blot MiniProtean II system (Bio-Rad) with the gel being collected from the glass plate by overlaying it with a sheet of Whatman paper. The gel was then inserted next to the membrane and flanked by two sheets of Whatman paper and this sandwich was submerged in cold transfer blot buffer (2.84 g Tris base, 13.51 g glycine, 300 ml methanol and the volume brought up to 1.5 L with deionized, distilled H_2O) and rolled with a test tube to remove all air bubbles. This sandwich was then placed in the supports of the MiniProten II system and placed in the electrophoresis chamber. The chamber was filled with cold trans blot buffer, transferred to a 4°C cold room, and the proteins transferred to the membrane. Transfer was accomplished by electrophoresing the assembly at a constant voltage of 100 V for 1 hour at 4°C. The

assembly's were removed from the chamber and the membranes transferred to a weight boat while the gel was stained with Coomasie brilliant blue to verify protein transfer.

All subsequent reactions were carried out at room temperature with gentle agitation on a shaker. The membranes were left for several hours to overnight in 2.5 g milk powder (Carnation instant skim milk powder) and 50 ml post blot buffer (9 g NaCl, 10 ml 1 M Tris HCl pH 7.4, and H_2O up to a final volume of 1 L). The membranes were then treated with the primary antibody with a solution made up of 2.5 g milk powder, 50 ml post blot buffer, 25 µl NP40, and 5 µl of anti-TME or anti-DME antibody (a 1/10000 dilution) for 60 minutes. The membrane was rinsed with 50 ml of post blot buffer and 25 µl of NP40 for 10 minutes. This rinse procedure was repeated for a total of three times and the membranes were then exposed to the secondary antibody. 2.5 g milk powder, 50 ml post blot buffer, 25 µl NP40, and 50 µl of anti-rabbit antibody peroxidase (Sigma) were added to the membranes and incubated for 30 minutes. The membranes were then rinsed with 50 ml of post blot buffer with 25 µl NP40 for 10 minutes for a total of two times. The membranes were then rinsed with 10 mM Tris HCl pH 7.4 for a total of two times and then developed using enhanced chemiluminescence (ECL) reagent (Amersham). The membranes were immersed in a total of 16 ml of ECL solution, excess solution allowed to run off, membranes placed between two transparent plastic sheets, placed in an autoradiogram cassette, and exposed to Kodak X-OMAT AR film (Kodak) for between 15 seconds to 20 minutes depending on signal strength. The film was developed in a Kodak M35A X-OMAT processor.

Plant assays

Alfalfa seeds (*Medicago sativa* cultivar Iroquois obtained from Cayuga Ont. Co-Op) were surface sterilized by treatment with 95% ethanol for 20 minutes followed by 2.5% hypochlorite for 20 minutes. The seeds were then rinsed eight times with sterile deionized water for fifteen minutes each for a total time of 2 hours. The sterile seeds were then transferred to 1% water agar plates and left at room temperature in the dark for two days to allow for germination. Leonard assemblies were produced (Leonard, 1943) using a plastic cup suspended in a 250 ml beaker. The cup was filled close to the brim with a 1:1 (volume:volume) sand and vermiculite mixture and the assembly sealed together using aluminum foil and autoclave tape and covered with an aluminum foil cap. Jensens media was prepared and contained per litre: 1 g $CaHPO_4$, 0.2 g K_2HPO_4, 0.2 g $MgSO_4 \cdot 7H_2O$, 0.2 g NaCl, 0.1 g $FeCl_3$, 1 ml 1000x trace mineral solution and 1 ml 1000x biotin solution. The trace mineral solution was autoclaved prior to use and contained per litre; 1 g H_3BO_3, 1 g $ZnSO_4 \cdot 7H_2O$, 0.5 g $CuSO_4 \cdot 5H_2O$, 0.5 g $MnCl_2 \cdot 4H_2O$, 1 g $Na_2MoO_4 \cdot 2H_2O$, 10 g Na_2EDTA, 0.2 g NaFeEDTA. The trace biotin solution contained 0.4 g biotin per litre and was sterilized prior to addition to the Jensens solution. 250 ml of Jensens media was added to each Leonard assembly and autoclaved for 20 minutes on liquid cycle. The sterile Leonard assemblies were allowed to cool for several hours prior to planting. Ten seedlings 1-2 cm in length were planted approximately 2 cm deep in the Leonard assemblies and the pots were transferred to a Conviron growth chamber for 48 hours prior to inoculation. 100 µl of an overnight *S. meliloti* culture to be tested was transferred aseptically to a 15 ml sterile conical Falcon tube containing 10 ml of sterile

distilled deionized water. The contents were then added to a Leonard assembly and the caps were replaced for a further 24 hours. After this 24 hour period the caps were removed and the plants grown over a period of 4 weeks. Conditions for growth in the Conviron chamber were 16 hours of light at 23°C and 8 hours dark at 18°C. The plants were watered as required with sterile distilled deionized water and sacrificed for acetylene reduction assays and dry weight measurements. All plant assays were carried out in triplicate for statistical analysis and verification of reproducibility.

Experiments involving *R. leguminosarum* and pea plants were carried out as outlined above with the following exceptions. Pea seeds (*Pisium sativum* cultivar Lincoln obtained from William Dams seeds Ltd, Flamborough Ont.) were surface sterilized by placing the seeds in a sterile 50 ml conical Falcon tube and subjecting the seeds to a 30 minute treatment in 2.5% hypochlorite followed by a 30 minute treatment in 95% ethanol. The seeds were repeatedly rinsed with sterile distilled water for a period of two hours after which time the seeds were left overnight in sterile distilled water to imbibe the seeds. The following day the seeds were transferred to 1% water agar plates and left to germinate for 72 hours at room temperature in the dark. Five pea seedlings were transferred to previously prepared Leonard assemblies and placed in a Conviron growth chamber for 48 hours after which time they were inoculated with *R. leguminosarum* cultures prepared in the same manner as outlined for *S. meliloti* plant assays. After five weeks of growth at identical conditions as those for alfalfa plants the pea plants were sacrificed for acetylene reduction assays and plant dry weights.

Plants were dried in a chromatography oven (National Appliance Co., Portland Oregon) at 100°C over a period of two weeks after which time the plants were weighed and replaced in the oven for another two weeks and re-weighed to verify the plants were completely dried. All plants were weighed on a Mettler PE 60 balance.

Acetylene reduction assays

Three alfalfa plants (two for pea plants) from each strain tested were removed from each Leonards assembly, the sand:vermiculite removed by gentle agitation and treatment with distilled water, and the complete root systems removed while the plants themselves were collected for dry weight analysis. The root systems were placed in a 30 ml glass bottle and sealed with a serum stopper. 3 ml of air was removed from the bottle and replaced with 3 ml of purified acetylene (Liquid Air Ltd., Burlington Ont.). The samples were incubated for 20 minutes after which time 0.2 ml was removed with a syringe and injected into a Hewlett-Packard 5890A gas chromatograph. The following settings were used: air:25 psi, H_2:12 psi, N_2:60 psi (all gases obtained from Liquid Air Ltd., Burlington Ont.), column head pressure at 180 kpa, oven temperature 60°C, and detector temperature 250°C. At these settings the ethylene peak was released at 3 minutes post injection while the acetylene peak followed 30 seconds later. The ethylene peaks were integrated using the HP3365 Series II chemstation software and compared to a standard curve using purified ethylene (506 ppm, Union Carbide). Injecting 0.1 ml, 0.2 ml, 0.3 ml, 0.4 ml, and 0.5 ml of ethylene into the gas chromatogram and recording the area of each peak produced the standard curve. To determine the amount of ethylene produced by each sample the following formula was used:

$$V=nRT/Pr$$

where V is volume, T is standard temperature, R is 1 mole of gas with a volume of 22.4 L , Pr is standard pressure. Therefore, 1 ml of gas contains $1/2.24x10^{4}$ moles and 1 ml of ethylene (506 ppm) will have $5.06x10^{-4}/2.24x10^{4}$ or $2.26x10^{-8}$ moles. Therefore 0.2 ml of 506 ppm ethylene will have 4.52 nmoles of gas. This value was assigned to the area generated by 0.2 ml of ethylene from the standard curve and used to calculate the acetylene reduction activity for each sample using the formula:

area of the ethylene peak x std x 150/3plants x 0.33 hours

where std is number of moles of ethylene in 0.2 ml as determined from the standard curve, 150 represents the dilution factor (0.2 ml from 30 ml reaction volume), 3 root systems were inserted into each glass bottle and the incubation time was carried out for 20 minutes (0.33 hours).

Bacteroid isolation

Nodulated alfalfa plants were removed from Leonard assemblies approximately 4 weeks following inoculation. Bacteroids were isolated from 4 week old alfalfa plants by removing the plants from the Leonard assemblies and gentle agitation and treatment with distilled water to remove the sand:vermiculite. The roots were then stored in moist paper towels and kept on ice during the procedure. The root systems were cut from the 7-10 plants and the nodules were removed with a set of forceps. The nodules from each set of plants inoculated with one *S. meliloti* strain tested were pooled in a petri dish containing approximately 1 ml of ice cold MMS buffer (40 mM MOPS, 20 mM KOH, 2 mM $MgSO_4$, 0.3 M sucrose, pH 7) and kept on ice. Once all nodules had been collected they

were transferred to a cold mortar and ground with a pre-chilled pestle until no intact nodules were visible. The resulting slurry was filtered through eight layers of cheesecloth into a 15 ml sterile conical Falcon tube and the mortar was rinsed with 5 ml of MMS and this was passed through the cheesecloth. The tubes were centrifuged at 700 rpm in a Beckman GPR table top centrifuge for 5 minutes at 4°C to pellet the plant material. The supernatant was transferred to a second 15 ml Falcon tube and centrifuged at 4°C and 4000 rpm to pellet the bacteroids. The pellet was resuspended in 200 µl of MMS buffer and stored at–80°C or they could be sonicated to isolate the protein as outlined previously.

Antibody production

Polyclonal antibodies were obtained by following injection of 200 µg quantities of purified TME protein into commercially available antigen free female spf rabbits. The first intra muscular injection for immunization was performed with 1 ml of complete of Freund's adjuvant (Sigma), whereas biweekly boosts were carried out with 200µg of purified TME protein in 1 ml of incomplete Freund's adjuvant (Sigma) for a total of 8 weeks. Samples were removed prior to inoculation and at 7 and 21 days after initial inoculation in order to verify antibody production. SDS PAGE was carried out on EJ1321 cell extracts from *tme* overexpressing strains (EcJ202) and western blots conducted using each the blood sample from 0, 7, and 21 days post inoculation. Total blood (approximately 100 ml) was collected after 8 weeks and serum was obtained by centrifugation at 5000 rpm at 4°C for 10 minutes using a GSA rotor in a Sorval RC-5B refrigerated cetrifuge. The resulting supernatant was transferred to a conical 50 ml

Falcon tube and cetrifuged at 4000rpm at 4°C for 5minutes in a Beckman GPR table top centrifuge. The resulting antibodies were stored at –20°C.

Protein purification

The *tme* gene was subcloned into pUC 119 in an orientation such that the *lacZ* promoter was driving the expression of *tme*. This plasmid (pTH392) was transformed into the malic enzyme deficient *E. coli* strain EJ1321 (Hansen and Juni, 1975) and propagated in LB media and the cells harvested by centrifugation at 5000 rpm for 10 minutes at 4°C in a Sorval RC-5B centrifuge using a GSA rotor. During all subsequent steps the samples were kept on ice. The bacterial pellet was washed three times with sterile saline solution (0.85% NaCl) and resuspended in a buffer containing 20 mM Tris HCL pH 8.5, 1 mM $MgCl_2$, 10 mM KCl, 20% glycerol 1 mM DTT. The cell suspension was then subjected to lysis by passage through a French pressure cell three times at a cell pressure of 1200 bar. The sample was then centrifuged at 10000 rpm for 10 minutes at 4°C in a Sorval RC-5B centrifuge to pellet cell debris. The supernatant was further purified by centrifugation in a Beckman L8-70 ultra centrifuge using a Ti65 rotor at 100000 x g for 1 hour at 4°C to remove membrane bound proteins. The soluble protein fraction was then subjected to anion exchange chromatography using a MonoQ HR5/5 column (Pharmacia Biotech) and a Waters 625 HPLC system (Millipore Waters chromatography). Proteins were eluted with a linear gradient (8 ml) of buffer A (20 mM Tris HCL pH 8.5, 1 mM $MgCl_2$, 10 mM KCl, 20%glycerol 1 mM DTT) to 50% buffer B (20 mM Tris HCL pH 8.5, 1 mM $MgCl_2$, 1 M KCl, 20% glycerol, 1 mM DTT) and a subsequent isocratic elution (2 ml) with 50% buffer B. Fractions collected were analyzed

for TME activity via the reduction of $NADP^+$ (see previous enzyme assay conditions) and all peak samples pooled. These samples were dialyzed against buffer C (20 mM Tris HCl pH 7.3, 1 mM $MgCl_2$, 10 mM KCl, 20%glycerol, 1 mM DTT) and concentrated using a Centricon-100 micro concentrators (Amicon). These concentrated samples were further purified via size exclusion chromatography using a Protein Pak 300SW column (Waters), buffer C as the running buffer and the Waters 625 HPLC system used previously. Fractions were assayed via the reduction of $NADP^+$ and peak fractions were pooled and stored at –20°C.

Effectors

Molecules tested for their effects on TME activity were tested at various concentrations with a malate concentration of 10 mM and a $NADP^+$ concentration of 1.5 mM in an $NADP^+$ reduction assay. Substrate analogs were tested for their effects on TME activity at 10 mM concentrations with a malate concentration of 10 mM. Classification of inhibition of TME by malonate, D-tartrate, tartronate and glyoxylate were carried out at with substrate concentrations of 5 mM, 10 mM, 15 mM, and 25 mM malate.

Kinetics

Traditional Michaelis-Menten plots were generated for TME with varying substrate and co-factor concentrations. Secondary linear graphs were obtained by Lineweaver-Burk, Eadie-Hofstee, and Hanes-Woolf analysis. Hanes-Woolf plots provided the best fit for the data in all cases and were used to determine kinetic parameters (K_m, V_{max}) for both the substrate and cofactor.

In order to determine the K_m and V_{max} for the malate permease, initial velocities were measured at various malate concentrations (40 μM- 400 μM). Data was fitted to the Michaelis-Menten equation:

$$v_o=V_{max}*[S_o]/([S_o]+K_m)$$

where v_o is the rate of reaction, $[S_o]$ is the substrate concentration, V_{max} is the maximal rate of reaction, and K_m is the Michaelis-Menten constant. Values for K_m and V_{max} were estimated using SigmaPlot (Jandel San Rafael, CA) curve-fitting program that fits data to non-linear functions directly by non-linear regression (Kuo, 1992)

DNA/amino acid analysis

Sequence analysis was carried out with a variety of programs. The *tme* gene was assembled with PC gene (Intelligenetics), restriction and primers designed with the Gene Runner 3.04 program (Hastings software, 1994). A comparison to the gene bank data bases at the National Center for Biotechnology Information (NCBI) was carried out with the BLAST search engine (Altschul *et al.*, 1997). Alignments were carried out using the evol network at McMaster University and utilized the Clustal V and Clustal W (Thompson *et al.*, 1994) software packages. Phylogenetic analysis was carried out using the PHYLIP package and the protein sequence parsimony (protpars) and distance (protdist) programs (Felsenstein, 1993). These programs were run on the Sun work station of Dr. Brian Golding in the department of Biology at McMaster University.

Chapter 3

Sequence of *tme* and sequence analysis of the malic enzymes of *S. meliloti*

Abstract

Malic enzymes catalyze the oxidative decarboxylation of malate to pyruvate in conjunction with the reduction of a nicotinamide cofactor. The DNA sequence and transcriptional start sites of the gene encoding the triphosphopyridine nucleotide dependent malic enzyme (TME, [EC 1.1.1.40]) of *S. meliloti* have been determined. The predicted TME proteins contains 761 amino acids and, like the diphosphopyridine nucleotide dependent malic enzyme (DME, [EC 1.1.1.39]), is approximately 320 amino acids larger than previously characterized prokaryotic malic enzymes. The TME C-terminal extension was similar in sequence to phosphotransacetylase enzymes [EC 2.3.1.8]. Truncated TME proteins that lacked this C-terminal region retained some malic enzyme activity but were unable to oligomerize into the native state. Database searches revealed that similar chimeric malic enzymes were uniquely present in gram negative bacteria. TME is therefore a member of a new class of malic enzyme characterized by the presence of a phosphotransacetylase-like domain at the C-terminus of the protein. These results were published in Mitsch *et al.*, 1998 in the Journal of Biological Chemistry volume 273 pp 9330-9336 and represent the authors contribution to that research article.

Methods and Materials

See Chapter 2 for all materials and methods. Bacterial strains and plasmids utilized are listed in Table 2.1.

Results

Nucleotide sequence of the *S. meliloti tme* gene.

The *S. meliloti tme* gene was subcloned as a 2.7kb *BspH*I fragment in plasmid pTH392 (Figure 3.1) which was sufficient to allow *E. coli* EJ1321 (*dme tme pck*) (Hansen and Juni, 1975) to grow on minimal media with succinate as sole carbon source. The nucleotide sequence of this fragment revealed an open reading frame (*tme*) of 2283 nucleotides encoding a protein of 761 amino acids. This deduced sequence differs from that previously reported from our laboratory (Mitsch *et al.*, 1998) due to two errors in annotation revealed by comparison to the recent sequence results from the *S. meliloti* genomic sequencing effort. A deletion of several base pairs at nucleotide 1851 relative to the translational start site resulted in a gap in the original sequence and a single base pair alteration at nucleotide 2284 relative to the translational start site resulted in misidentification of the stop codon. The differences in the deduced proteins did not adversely effect the deduced percent similarity or identity when compared to other malic enzymes. A potential ribosome binding site (5'-GGAA-3') was located 2 base pairs upstream of the ATG start codon. In addition, the deduced molecular weight of the protein was 82 kDa and this estimate is supported by the molecular weight estimates of the *S. meliloti* TME protein which was purified from *E. coli* strains carrying plasmid

Figure 3.1. Restriction map of the *tme* gene region. The extent of the *tme* gene region and direction of transcription are indicated. Restriction enzyme sites shown are: *BspH*I, Bp; *Cla*I, C; *Eco*RI, E; *Hind*III, H; *Pst*I, P; *Sal*I, Sa; *Sma*I, Sm; *Sph*I, Sp; *Sst*I, S. (P) Denotes *Pst*I of multiple cloning site used for gene truncation.

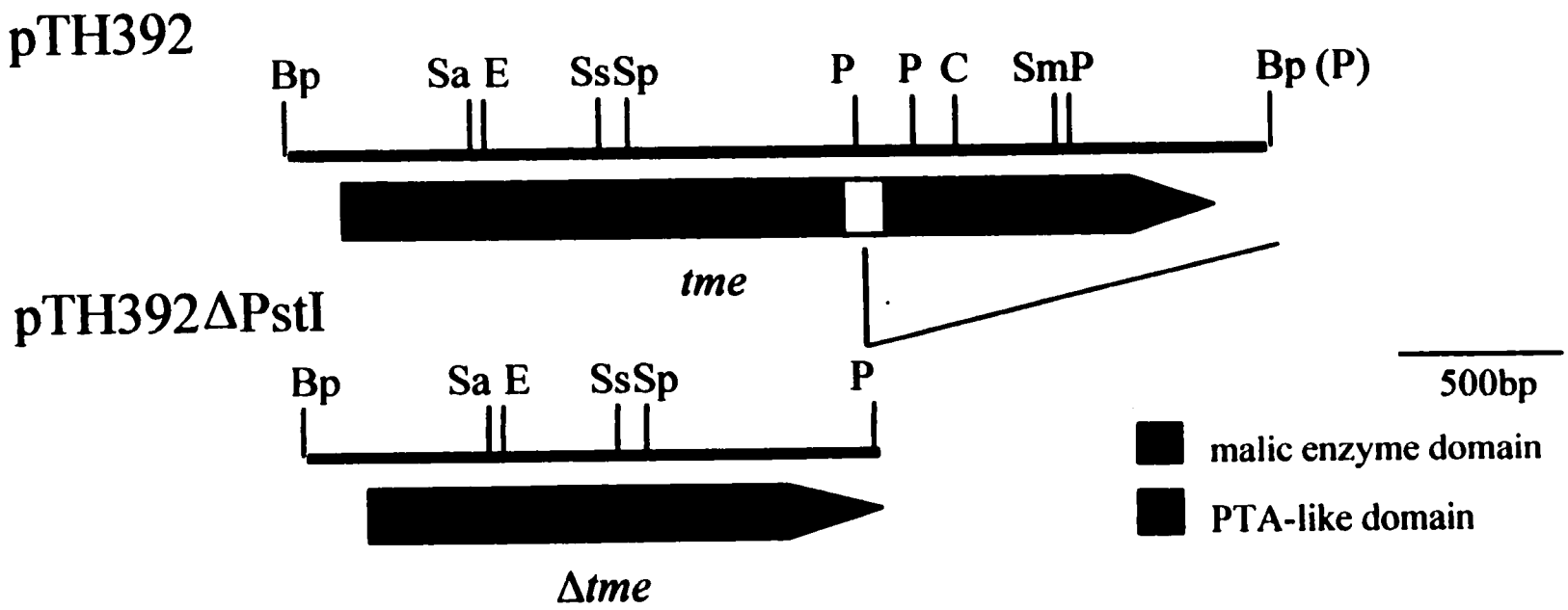
pTH392
Bp
Sa E
SsSp
P
P C
SmP
Bp (P)
tme
pTH392ΔPstI
Bp
Sa E
SsSp
P
500bp
malic enzyme domain
PTA-like domain
Δtme

Figure 3.2. Primer extension of *tme* and comparison to other *S. meliloti* promoters. **A.** Primer extension of *tme* with associated nucleotide sequence. Arrow shows transcriptional start site. Lane 1; mRNA isolated from free-living Rm1021, lane 2; tRNA control. **B.** Sequence comparison using ClustalW of various *S. meliloti* promoters previously mapped through primer extensions. Underlined regions represent putative –10 and –35 regions.

A

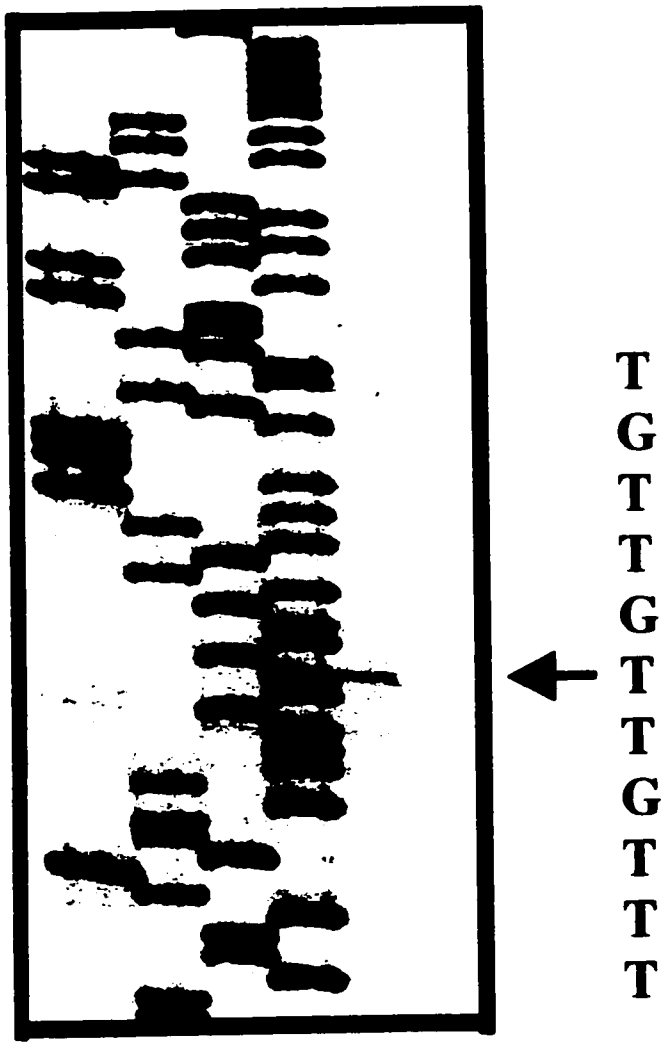

B

tme	-AGATGTCACACTATCCGC-----AAGCATTTATAGACGACAAC**A**	39
dme	-ACTGTACGTGCCGGGCGATTC--ATGCCAAAAGGCACG**ACA**---	39
hemA1	GGGTTGAC-CACTGATCGCTTTG-AAGGAAGAAAGG-CG**ACA**---	39
ntrA	CGCTTGAC-CAAATTCCAGTAAT-AAGCAATTTTTG-GGCC**A**---	39
orfA-pit	AACTTTCC---CCGAGCGCG--C-AAGTACAATATGACAACTGC**G**	39
trpE	-GCTTGCGCGCCAGCGCAAG-CC-GCGCTAACACTTCCGCC**A**---	39
nodD1	-CCTTGAT--TCCATTAACTTCA-GGGTTCTCTAATAGGACTC--	39
pck	ATCTTGTCTTGGGTCAGCCTTGC-CGGTATGTTCCGAC**GA**-----	39
hemA	TGCTTGACTTCGATCGATGTTCGGGAGAATGAAGTTTT**TG**------	39

pTH392, (Voegele *et al.*, 1999, Chapter 4). The *tme* gene showed a clear G+C bias of 84% at the third nucleotide position of the codons compared to the total G+C content of 65%.

Identification of the *tme* promoter regions.

The transcriptional start site was determined from primer extension experiments using a 20 bp oligonucleotide from within the *tme* structural gene. Employing RNA from wild type cells, the major transcriptional start site for *tme* was located 47 base pairs upstream from the ATG start codon (Figure 3.2A). A second minor extension product was located 65 base pairs upstream from the ATG but the significance of this product is currently unclear. Comparison of the *tme* promoter with other *S. meliloti* promoters including *dme* revealed that they were quite different (Figure 3.2B). No regions of similarity were detected in the –10 regions of any of the genes while a TTG motif was conserved at the –35 region however this conservation did not extend to the *tme* gene. The promoter region of *tme* instead resembled the *E. coli* consensus sequence for σ^{70} promoters.

Comparative analysis of the *S. meliloti* malic enzyme gene sequences.

Comparison of the *dme* and *tme* structural genes revealed they were 59% identical whereas the predicted proteins were 44% identical and 57% similar in amino acid sequence (Table 3.1). The identity of the two enzymes was high at the N-terminal domain (58% identity over 420 amino acids)but was reduced in the PTA region (27% identity over 350 amino acids) (Figure 3.3). Searches of the DNA and protein databases with the *tme*/TME and *dme*/DME sequences revealed disparate similarities to other

Table 3.1. Comparison of different prokaryotic malic enzymes to TME.

Source	EC designation[a]	% identity[b]	Length[c]	Accession number[d]	Reference
B. stearothermophilus	1.1.1.38	39	478	DEBSXS	Kobyashi *et al.*, 1989
E. coli	ND	45	759	P76558	Blattner *et al*, 1987
H. influenzae	ND	46	756	P43837	Fleishman *et al.*, 1995
R. prowazekii	ND	55	767	F71694	Andersson *et al.*, 1998
S. bovis	1.1.1.39	45	389	AAB07709	Kawai *et al.*, 1996
S. sp. PCC6803	ND	41	463	S74511	Kaneko *et al.*, 1996
S. meliloti DME	1.1.1.39	44	770	O30807	Mitsch *et al.*, 1998

[a] Classified according to cofactor specificity and oxaloacetate decarboxylation activity.
[b] Based upon comparison of overlapping amino acid residues of alignment.
[c] Number of amino acids residues of protein
[d] Swissprot accession code.
ND; not determined, information based upon sequence data alone with no biochemical data available

Figure 3.3. Multiple alignments using ClustalW of the prokaryotic malic enzymes and phosphotransacetylase enzyme demonstrating the chimeric structure of *S. meliloti* TME (Sm TME), DME (Sm DME), malic enzyme from *S. bovis* (Sb ME), and *M. thermophila* PTA (Mt PTA). The N-terminal region of both DME and TME show similarity to the malic enzyme while the C-termini have a high degree of similarity to the PTA enzyme. * Denotes identical amino acid residues while. Denotes similar amino acid residues. Numbers to the right are amino acid residues of the respective proteins.

prokaryotic malic enzymes (Table 3.1). Among these enzymes, two have been cloned and biochemically characterized, and these are from the gram-positive bacteria *Streptococcus bovis* (Kawai *et. al.*, 1996) and *Bacillus stearothermophilus* (Kobyashi *et al.*, 1989). These two enzymes together with the putative malic enzyme from the blue green algae *Synechocystis sp.* PCC6803 are considerably shorter than the *S. meliloti* malic enzymes. A multiple alignment of these shorter enzymes with DME and TME showed that the similarity between all the enzymes extended across the entire 415 amino acid N-terminal portion of the DME and TME proteins (Figure 3.3). On the other hand the predicted malic enzymes of *Haemophilus influenzae* (Fleishman *et al.*, 1995), *E. coli* (Blattner *et al.*, 1997) and *Rickettsia prowazekii* (Anderson *et al*, 1998), all of which were sequenced as part of genome sequencing projects, were similar in size to the *S. meliloti* malic enzymes and all these proteins showed similarity over their entire length (alignments not shown).

Phosphotransacetylase (PTA)-like domain at the C-terminus of the *S. meliloti* malic enzymes.

BLAST searches employing the C-terminal 320 amino acids from the DME and TME proteins revealed that these regions were similar to phosphotransacetylase (PTA) enzymes [EC 2.3.1.8] from several bacterial species. Alignment of the C-terminal 340 amino acids from both DME and TME with the 333 amino acid phosphotransacetylase enzyme from *Methanosarcina thermophila*, which has been sequenced and characterized biochemically (Latimer and Ferry, 1993), revealed 26% identity (46% similarity) between DME and the PTA enzyme while TME shared 24% amino acid identity and 37%

Figure 3.4. Alignment using ClustalW of the prokaryotic malic enzymes from *S. meliloti* TME (Sm TME), DME (Sm DME), *H. influenzae* (Hi ME), *E. coli* (Ec ME), *R. prowazekii* (Rp ME), *B. stearothermophilus* (Bs ME), *S. bovis* (Sb ME), *Synechocystis sp.* PCC6803 (Sp ME) showing eight highly conserved regions maintained in all sequences. Amino acid residues in bold type have been implicated in malic enzyme function (see results). * denotes identical amino acid residues while . denotes similar amino acid residues. Numbers to the left and right of the sequences refer to amino acid residue of the respective sequences.

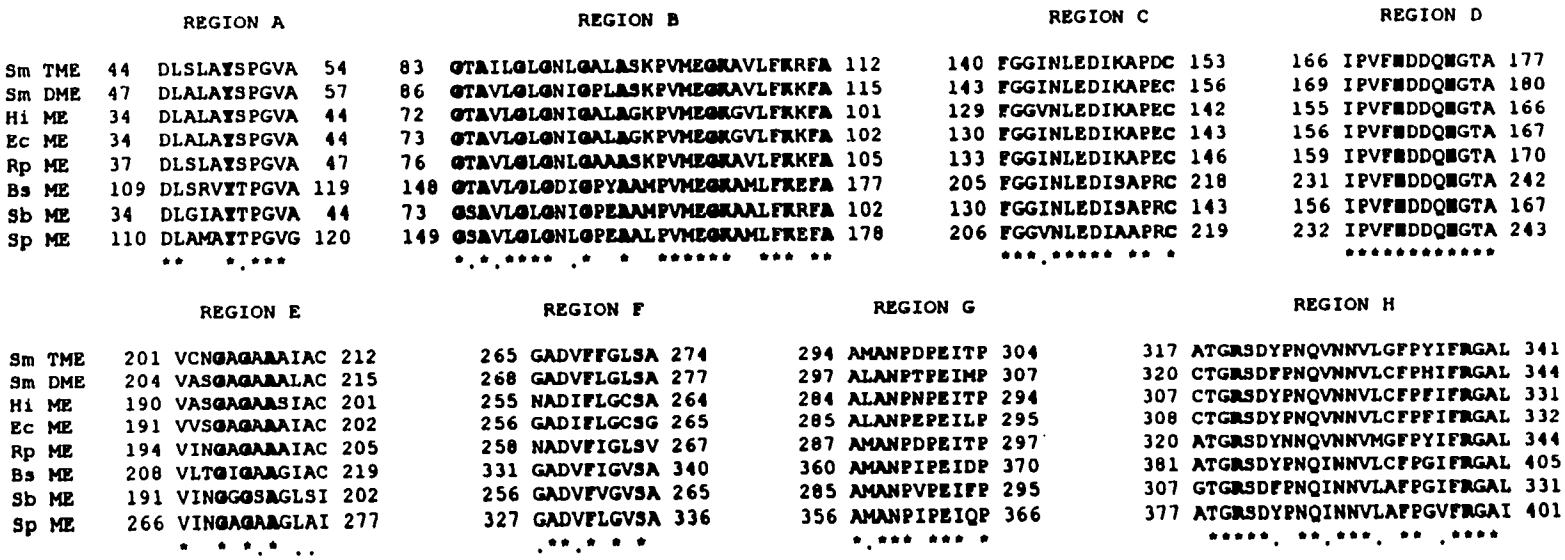
REGION A
REGION B
REGION C
REGION D
Sm TME 44 DLSLAYSPGVA 54 83 GTAILGLGNLGALASKPVMEGRAVLFKRFA 112 140 FGGINLEDIKAPDC 153 166 IPVFMDDQMGTA 177
Sm DME 47 DLALAYSPGVA 57 86 GTAVLGLGNIGPLASKPVMEGRAVLFKKFA 115 143 FGGINLEDIKAPEC 156 169 IPVFMDDQMGTA 180
Hi ME 34 DLALAYSPGVA 44 72 GTAVLGLGNIGALAGKPVMEGRGVLFKKFA 101 129 FGGVNLEDIKAPEC 142 155 IPVFMDDQMGTA 166
Ec ME 34 DLALAYSPGVA 44 73 GTAVLGLGNIGALAGKPVMEGRGVLFKKFA 102 130 FGGINLEDIKAPEC 143 156 IPVFMDDQMGTA 167
Rp ME 37 DLSLAYSPGVA 47 76 GTAVLGLGNLGAAASKPVMEGRAVLFKKFA 105 133 FGGINLEDIKAPEC 146 159 IPVFMDDQMGTA 170
Bs ME 109 DLSRVYTPGVA 119 148 GTAVLGLGDIGPYAAMPVMEGRAMLFKEFA 177 205 FGGINLEDISAPRC 218 231 IPVFMDDQMGTA 242
Sb ME 34 DLGIAYTPGVA 44 73 GSAVLGLGNIGPEAAMPVMEGRAALFKRFA 102 130 FGGINLEDISAPRC 143 156 IPVFMDDQMGTA 167
Sp ME 110 DLAMAYTPGVG 120 149 GSAVLGLGNLGPEAALPVMEGRAMLFKEFA 178 206 FGGVNLEDIAAPRC 219 232 IPVFMDDQMGTA 243
REGION E
REGION F
REGION G
REGION H
Sm TME 201 VCNGAGAAAIAC 212 265 GADVFFGLSA 274 294 AMANPDPEITP 304 317 ATGRSDYPNQVNNVLGFPYIFRGAL 341
Sm DME 204 VASGAGAAALAC 215 268 GADVFLGLSA 277 297 ALANPTPEIMP 307 320 CTGRSDFPNQVNNVLCFPHIFRGAL 344
Hi ME 190 VASGAGAASIAC 201 255 NADIFLGCSA 264 284 ALANPNPEITP 294 307 CTGRSDYPNQVNNVLCFPFIFRGAL 331
Ec ME 191 VVSGAGAAAIAC 202 256 GADIFLGCSG 265 285 ALANPEPEILP 295 308 CTGRSDYPNQVNNVLCFPFIFRGAL 332
Rp ME 194 VINGAGAAAIAC 205 258 NADVFIGLSV 267 287 AMANPDPEITP 297 320 ATGRSDYNNQVNNVMGFPYIFRGAL 344
Bs ME 208 VLTGIGAAGIAC 219 331 GADVFIGVSA 340 360 AMANPIPEIDP 370 381 ATGRSDYPNQINNVLCFPGIFRGAL 405
Sb ME 191 VINGGGSAGLSI 202 256 GADVFVGVSA 265 285 AMANPVPEIFP 295 307 GTGRSDFPNQINNVLAFPGIFRGAL 331
Sp ME 266 VINGAGAAGLAI 277 327 GADVFLGVSA 336 356 AMANPIPEIQP 366 377 ATGRSDYPNQINNVLAFPGVFRGAI 401

similarity with the *M. thermophila* PTA (Figure 3.3). Also of interest was the fact that the similarity between the DME, TME and PTA sequences was scattered along the entire length of the PTA enzyme sequence (Figure 3.3) with no large clusters of similarity.

Conserved regions within the malic enzyme proteins.

Eukaryotic malic enzymes, unlike their prokaryotic counterparts, have been reasonably well characterized with respect to conserved motifs and amino acids essential for activity (Hsu *et al.*, 1992; Walter *et al.*, 1994; Viljoen *et al.*, 1994). Motifs containing the putative cofactor and Mn^{2+} binding sites have been identified within the malic enzymes from *B. stearothermophilus* and *S. bovis* (Kobayashi *et al.*, 1989; Kawai *et al.*, 1996). An alignment of eight prokaryotic malic enzymes allowed us to identify eight regions that are highly conserved within these proteins (Figure 3.4, regions A to H). Some of these regions correspond to those implicated in the functioning of the eukaryotic malic enzymes.

Region A contains a tyrosine residue conserved in all of the prokaryotic malic enzymes examined. Chemical modification experiments with eukaryotic malic enzymes have implicated a corresponding tyrosine residue in L-malate binding (Hsu, 1982; Vilijoen *et al.*, 1994). Regions B and E have the required glycine, alanine, and lysine residues indicative of cofactor binding sites (Hanukoglu and Gutfinger, 1989; Wierenga *et al.*, 1986; Scrutton *et al.*, 1990). In addition the two lysine residues in region B are believed to be required for $NAD(P)^+$ binding (Hsu, 1982). Region C contains a conserved cysteine residue thought to be located at or near the active site of the eukaryotic enzymes (Tang and Hsu, 1974; Drincovich *et al.*, 1992) and may be

responsible for coordinating the binding of the L-malate substrate or the divalent metal ion (Hsu *et al.*, 1992). Region D represents a large block of thirteen amino acid residues that are absolutely conserved in the prokaryotic malic enzymes. This domain contains two histidine residues which, through chemical disruption studies of eukaryotic malic enzymes, were found to be required for cofactor binding (Chang and Hsu, 1977; Jawali and Bhagwat, 1987). The two conserved arginine residues within region H are believed to be required for interacting with the C-1 carboxyl group of the substrate (Rao *et al.*, 1991; Vernon and Hsu, 1983). The functions of conserved regions F and G remain unknown.

Deletion of the C-terminal PTA-like regions from TME.

In view of the apparent hybrid structure of TME we wished to determine whether proteins lacking the C-terminal PTA-like regions still retain malic enzyme activity. As *PstI* sites were conveniently located close to the end of the malic enzyme-like region of *tme*, a plasmid deletion derivative was constructed in which the DNA 3' to the *PstI* sites of *tme* was removed (Figure 3.1). The TME truncation removed the C-terminal 323 amino acids of the protein resulting in the loss of the PTA like region. The resulting plasmid, pTH392Δ*PstI* allowed the malic enzyme deficient *E. coli* strain EJ1321 (*dme tme pck*) to grow with succinate as sole carbon source which suggested that the truncated malic enzyme was active *in vivo*. $NADP^+$-dependent malic enzyme activity was readily detected in crude extracts of EJ1321 carrying the truncated *tme* construct however, the activity detected was about 10% of the activity detected in extracts of EJ1321 carrying the corresponding intact genes. Since extracts of EJ1321 alone lacked malic enzyme

Figure 3.5. Non-denaturing polyacrylamide gel of crude cell extract stained for $NADP^+$-dependent malic enzyme activity in *S. meliloti* and *E. coli* strains. Lane A, Rm1021 (wild type), lane B, RmG456 (*dme*-1), lane C, RmH215 (*tme*-2), lane D, EcJ202 (*dme*-, *tme*-, pTH392 (*tme*)), lane E, EcJ203 (*dme*-, *tme*-, pTH392Δ*Pst*I (Δ*tme*)), lane F, EJ1321 (*dme*-, *tme*-). 30 μg of protein was loaded for each sample. Positions of TME and truncated TME (ΔTME) lacking the C-terminal region are indicated by arrows.

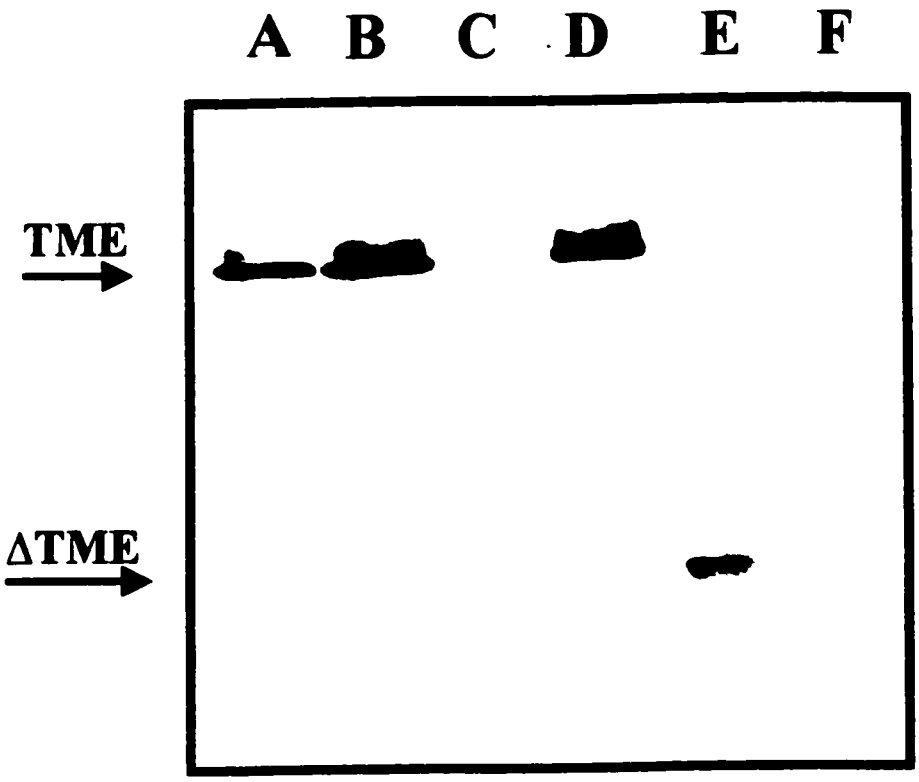
A
B
C
D
E
F
TME
ΔTME

Figure 3.6. Plot of retardation coefficients derived from Ferguson plots versus molecular weights of standard proteins. Positions of TME and ΔTME are indicated based upon their migration in non-denaturing polyacrylamide gels.

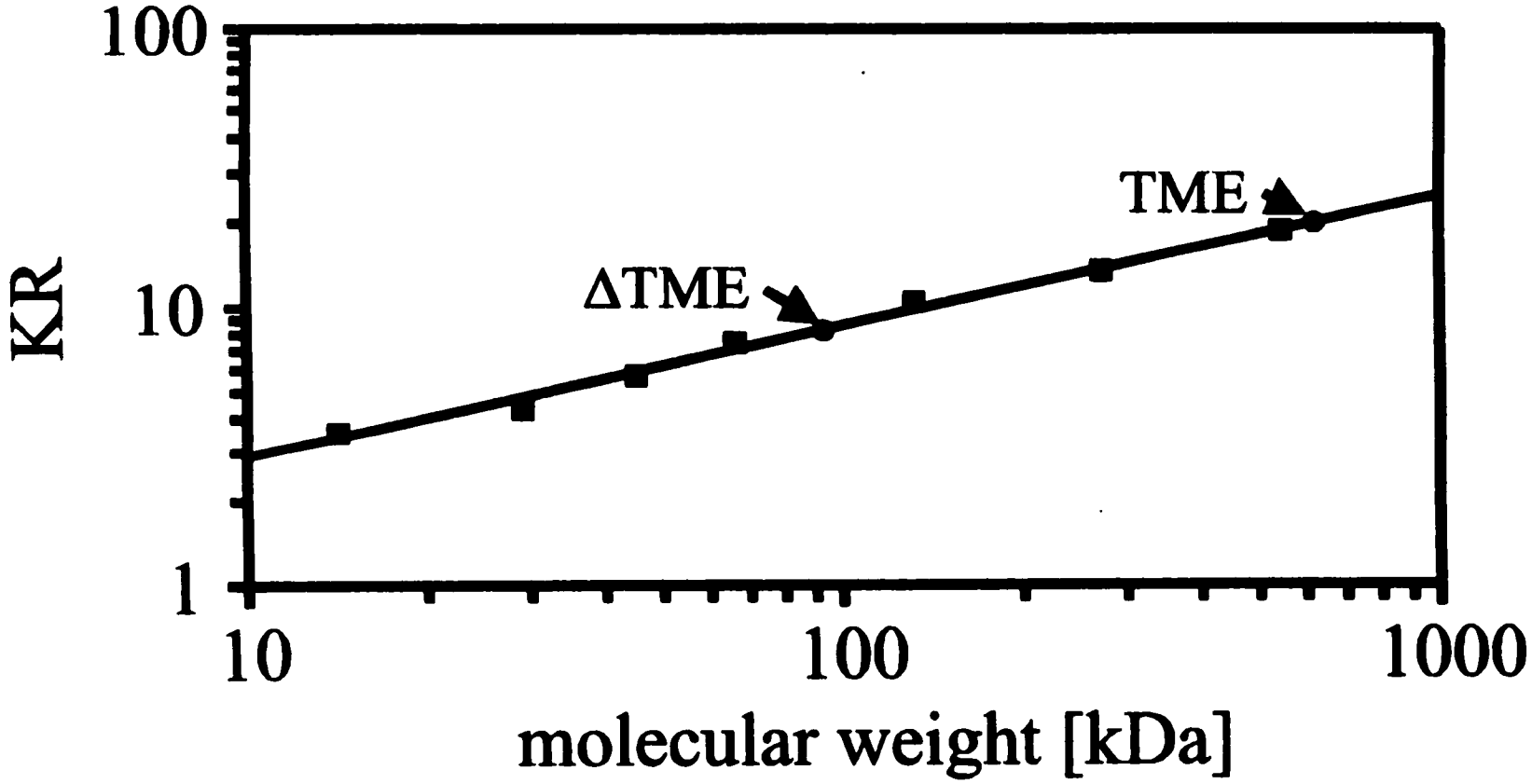
100
10
1
KR
ΔTME
TME
10
100
1000
molecular weight [kDa]

activity, this data clearly showed that the phosphotransacetylase-like C-terminal domain was not essential for malic enzyme activity.

Malic enzyme native molecular weight determination.

Malic enzyme activity was readily visualized as bands in non-denaturing polyacryalamide gels following a staining procedure based on the $NAD(P)^+$ and malate dependent reduction of MTT (Chapter 2). No activity band was detected in extracts of plasmid-free EJ1321 *E. coli* strains, while *E. coli* strains carrying the complete malic enzyme gene on plasmid pTH392 showed activity bands which co-migrated with the native TME proteins of wild type *S. meliloti* (Figure 3.5). Non-denaturing gels were used to determine the size of the native and truncated forms of TME (Figure 3.6). Through the method of Hedrick and Smith (1968) TME was found to have a molecular weight of approximately 620 kDa. Based upon the subunit molecular weight of TME, 82 kDa in SDS-PAGE gels (Voegele *et al.*, 1999) and the deduced molecular weight based upon the *tme* sequence, TME appears to form a homo-octamer.

The truncated *tme* gene produced a malic enzyme activity band that migrated much faster than the native enzymes indicating a smaller protein size (Figure 3.5). The native molecular weight of the truncated ΔTME proteins was estimated to be 93 kDa, (Figure 3.6), which is larger than a single subunit and would suggest a homo-dimer. This indicates that removal of the C-terminus of the proteins impedes oligomerization but that the enzyme is still capable of functioning at a reduced level. We note that in preliminary purification experiments involving gel filtration of truncated DME and TME proteins, ΔTME eluted as a 121 kDa protein, consistent with a dimeric state (data not shown).

Discussion

With the completion of the *tme* sequence it was possible to analyze the two malic enzyme genes of *S. meliloti*. Our data suggest that the two malic enzymes from *S. meliloti*, DME and TME, are representatives of a new class of malic enzymes which are primarily characterized by their large subunit size. The increased size of the malic enzymes results from a C-terminal extension of approximately 320 amino acids. While the C-terminal extension shows homology to phosphotransacetylase (PTA) enzymes [EC 2.3.1.8], all attempts to detect PTA activity using purified DME and TME proteins have been unsuccessful (Voegele *et al.*, 1999 and Chapter 4). The function of the C-terminal PTA-like domain is therefore currently unclear. In view of the unusual structure of the *S. meliloti* malic enzymes as discussed above, it is important to summarize the evidence that TME is in fact a malic enzyme. In previous studies, *tme S. meliloti* mutants were shown to lack $NADP^+$-dependent malic enzyme activitiy. In appropriate genetic backgrounds, these mutations resulted in growth phenotypes which were entirely consistent with an *in vivo* role for this enzyme in the conversion of malate to pyruvate (Driscoll and Finan, 1996, and Driscoll and Finan, 1997). Furthermore, expression of the *tme* gene in an *E. coli* EJ1321 strain lacking malic enzyme activity restored its ability to grow on succinate as the sole carbon source (Mitsch *et al.*, 1998). The purified protein has been shown to catalyze the oxidative decarboxylation of malate and the simultaneous reduction of $NADP^+$ (Voegele *et al.*, 1999, Chapter 4). Moreover, the N-terminal sequence of the purified protein is the same as that predicted by the nucleic acid sequence of the *tme* gene (Voegele *et al.*, 1999, Chapter 4). Therefore this evidence proves that TME is a malic enzyme.

The presence of the PTA-like domain in both DME and TME, which have different cofactor specificities and effectors (Voegele *et al.*, 1999, Chapter 4) suggests that it is neither related to cofactor specificity nor to effector binding. The observation that both DME (Mitsch *et al.*, 1998) and TME deletion derivatives lacking the C-terminal region retain (albeit reduced) malic enzyme activity clearly suggests that these two proteins have at least two major domains. With respect to structure, we found that while TME derivatives lacking the PTA-like domain retained malic enzyme activity, these proteins now appeared to be dimers. While this result suggests that the PTA-like domain may be involved in octamerization, it is also possible that the C-terminal deletion indirectly interfers with formation of the native oligomeric state. On the other hand, the formation of dimers by these deletion derivatives suggests that this may be the first step in the formation of the native octamer. DME, like TME is a holo-octamer and when the C-terminal region is deleted it to forms a dimer (Mitsch *et al.*, 1998). Therefore, the two malic enzymes have a very similar structure and subunit organization.

Recent genome sequencing projects have revealed putative malic enzyme genes in *E. coli*, *H. influenzae*, and *R. prowazekii* that are predicted to encode proteins similar in length and sequence to the *S. meliloti* malic enzymes. It is of interest to note that the malic enzymes from *B. japonicum* are approximately the same molecular weight (Chen *et al.*, 1997, Chen *et al*, 1998) as the malic enzymes of *S. meliloti* and although no sequence data is currently available, it is reasonable to assume that they too have a chimeric structure. The conservation of the PTA-like region in all these proteins represents strong evidence that this region plays some functional role be it structural or catalytic. These

results prompted us to further examine the phylogenetic relationships of all available prokaryotic malic enzymes. A maximum parsimony analysis using the eukaryotic malic enzymes (*Zea maize* and *Schizosaccharomyces pombe*) as an outgroup was carried out. The resulting tree (Figure 3.7) showed that the elongated enzymes cluster as a distinct group, one of which contained enzymes from *B. stearothermophilus* and *Synechocystis sp.* PCC6803 while the other contained *E. coli* SfcA and *B. subtilus* Mao2.bs. This indicates that there are at least three prokaryotic malic enzyme subgroups; the elongated group, the "traditional" shorter malic enzymes, and a group that resembles eukaryotic malic enzymes. The same phylogenetic tree was obtained when the analysis was carried out with proteins in which the PTA-like C-terminal domain was removed. Thus the apparent phylogenetic relationship between the enzymes is not solely as a result of the PTA-like C-terminal extension. The different placements of the reiterated malic enzymes from *E. coli* (SfcA and f759) and *B. subtilus* (Mao1.bs and Mao2.bs) indicates that these are paralogous proteins (proteins arising via gene duplication), and the linkage of SfcA with the Mao2 suggests that an ancestral malic enzyme gene duplication occurred prior to the divergence generating the gram positive and gram negative bacteria. These observations concerning the relationships between the different prokaryotic malic enzymes have been supported by recent analysis of eukaryotic malic enzymes (Boles *et al.*, 1998).

In light of the chimeric nature of some prokaryotic malic enzymes it is of interest to note that not all of the PTA enzymes share the same compact structure. The *S. meliloti* PTA gene has been recently identified and characterized (Summers *et al.*, 1999). It

Figure 3.7. Unrooted tree of the various prokaryotic malic enzymes using fitch analysis with the PHYLIP software package. Mao1.bs and Mao2.bs are putative malic enzymes from *B. subtilis* while SfcA is the NAD^+-dependent malic enzyme of *E. coli*. The lengths of the branches represent the distances of divergence and the highlighted box shows the elongated malic enzyme subdivision.

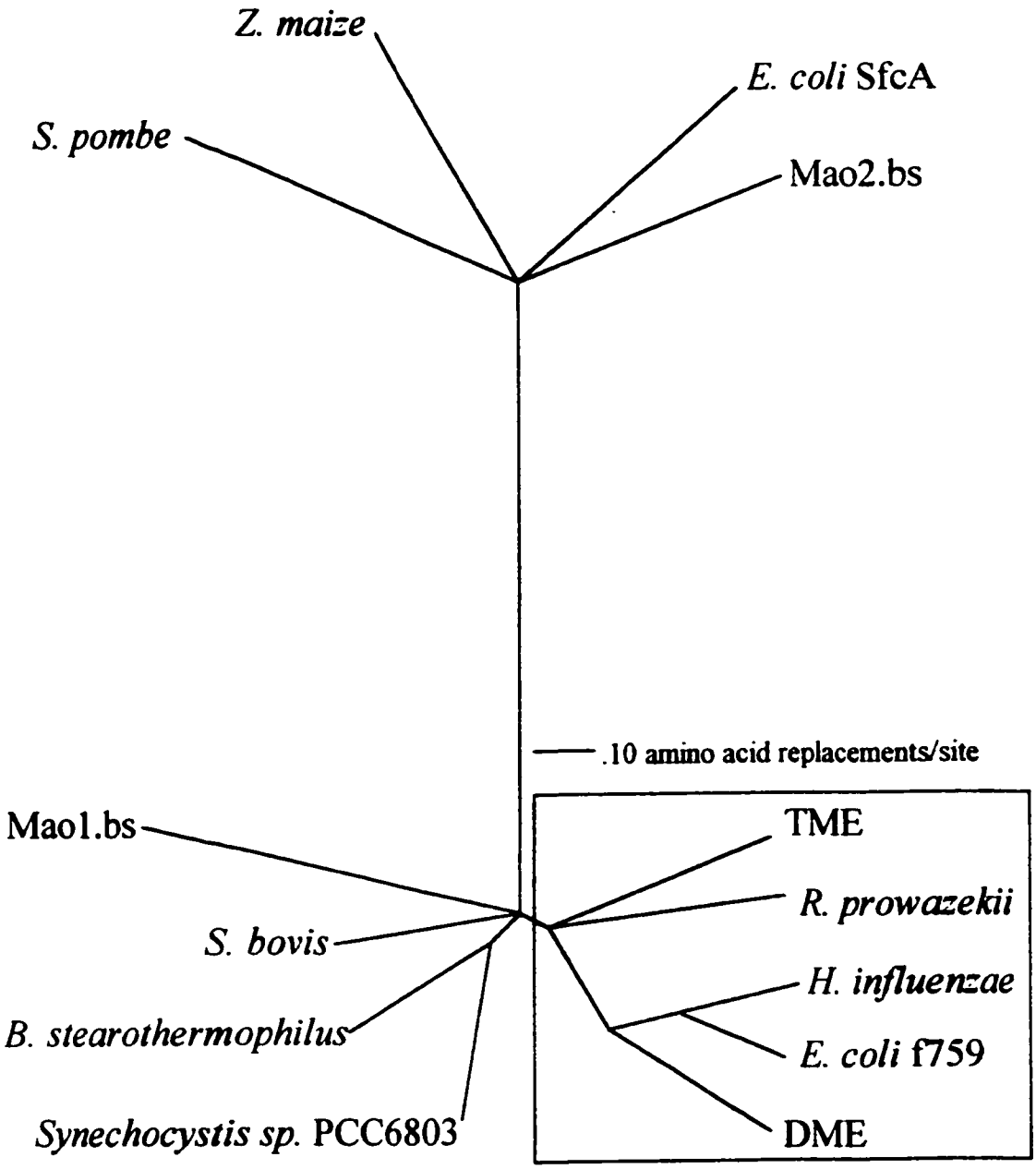
Z. maize
E. coli SfcA
S. pombe
Mao2.bs
.10 amino acid replacements/site
Mao1.bs
TME
R. prowazekii
S. bovis
H. influenzae
B. stearothermophilus
E. coli f759
Synechocystis sp. PCC6803
DME

It encodes a protein 270 amino acids in length and shows homology to the PTA's of *Clostridium acetobutylicum* (333 amino acids, accession number P71103) and *M. thermophila* (333 amino acids, accession number P38503). By comparison, the PTA enzymes of *E. coli* (accession number JX0357), *H. influenzae* (accession number P45107), and *Synecochystis* sp. PCC6803 (accession number BAA17707), are made up of 713, 711, and 697 amino acids, respectively. Like our malic enzymes, the C-terminal portion of these proteins shows similarity to other smaller PTA enzymes while the N-terminal region of the *E. coli* PTA protein has similarity to cobyric acid synthase. The *E. coli* PTA gene has been used to complement a PTA deficient phenotype *in vivo* and biochemical characterization has shown that this enzyme does indeed have PTA activity (Matasuyama *et al.*, 1994) but it is not known if the elongated PTA proteins have any other enzymatic functions. It is interesting to speculate that the C-terminal portion of the PTA enzymes of *E. coli*, *H. influenzae*, and *Synecochystis* sp. PCC6803 and that of our malic enzymes may represent a common structure within proteins required for regulation of their activity via phosphate or acetyl-phosphate. As yet, there is no evidence to support this hypothesis.

Two malic enzymes have previously been purified from *E. coli*, however, neither of their reported molecular weights corresponds to that of the larger enzyme (f759) as predicted from the sequence of the *E. coli* genome (Blattner *et al.*, 1997). The amino acid composition of the *E. coli* NAD^+-dependent malic enzyme [EC 1.1.1.38] does match that predicted for the *sfcA* gene product (Blattner *et al.*, 1997, Mahjan *et al.*, 1990, Yamaguchi *et al.*, 1973). The *sfcA* gene was recently overexpressed and was proven to indeed

produce a NAD^+-dependent malic enzyme (Stols and Donnelly, 1997). Therefore we assume that the other malic enzyme gene (f759) encodes the previously characterized $NADP^+$-dependent malic enzyme [EC 1.1.1.40] (Sanwal and Smando, 1969a; Sanwal *et al.*, 1969b). However, this inference should be verified as the subunit molecular weight and the amino acid composition of the $NADP^+$-malic enzyme as reported by Spina *et al* (1968) fails to match the sizes and amino acid composition of the either malic enzymes deduced from the *E. coli* genome sequence.

Although DME and TME share a high degree of similarity at the protein sequence level, their functions *in vivo* seem to be quite different. Results from enzyme assays and *dme/tme* gene expression studies on *S. meliloti* bacteroid extracts had suggested that *dme* was expressed in bacteroids to levels comparible to free-living cells, while *tme* expression in bacteroids appeared to be 20% or less, the level in free-living cells (Driscoll and Finan, 1996, Driscoll and Finan, 1997). The determination and comparison of the transcriptional start sites of the *dme* and *tme* genes was therefore of particular interest. Comparison of the *dme* and *tme* promoters shows that they are quite different. The *tme* promoter has sequences resembling the -10/-35 motifs of *E. coli* σ^{70} type promoters wheras the *dme* promoter lacked sequences resembling either the -10/-35 σ^{70} type promoters or the -24/-12 σ^{54} dependent promoters employed by many genes involved in N_2-fixation. The differences between the two promoters may yield insight into their differential regulation in bacteroids.

Chapter 4

Purification and biochemical characterization of TME

Abstract

To characterize TME at a biochemical level, *tme* was overexpressed in an *E. coli* malic enzyme deficient background, purified to homogeneity, and its kinetic parameters and responses to effector molecules and substrate analogs assessed. In comparison to the previously purified DME, TME had similar K_m's for substrate and cofactor but lacked DME's sensitivity to TCA cycle intermediates. Therefore despite their similarity in terms of structure, the two proteins differ in their biochemical characteristics. These results were previously published in Voegele *et al.*, 1999 in Biochimica and Biophysica Acta volume 1432 pp 275-285 and represent the author's contribution to that research article.

Materials and Methods

See Chapter 2 for all materials and methods. Bacterial strains and plasmids utilized are listed in Table 2.1. After examination of the *tme* sequence and surrounding nucleotides two *Bsp*HI sites were located 116 bp upstream and 182 bp downstream from the predicted translational start and stop sites, respectively. The 2.7 kb *Bsp*HI fragment was removed from pTH251 and inserted into the compatible *Nco*I site of the vector pAB2001 (Becker *et al.*, 1995). This vector was chosen for its unique *Nco*I site that is

flanked by several common restriction sites including *Hind*III. The resulting construct was digested with *Hind*III and the resulting 2.7 kb fragment was then inserted into pUC119 in both orientations relative to the *lac* promoter to yield pTH392 and pTH393 (Mitsch *et al.*, 1998). This allowed the *tme* gene of pTH392 to be driven by the plasmid-based promoter resulting in overproduction of the TME protein in the *E. coli* host. This was verified by complementation of the malic enzyme deficient *E. coli* strain EJ1321 with pTH392 that enabled growth on minimal media with succinate as the sole carbon source. PTH393 which has *tme* in the opposite orientation did not complement EJ1321 under the same conditions.

During the purification process, TME activity was monitored by the formation of NADPH at 340nm using an assay mixture containing 30 mM malate and 0.25 mM $NADP^+$. The K_m for $NADP^+$ was measured at 30 mM malate while the K_m for malate was determined at 1.5mM $NADP^+$. All effector studies were carried out at a malate concentration of 10 mM and a cofactor concentration of 1.5 mM in order to identify compounds that effect either K_m and/or V_{max}. Competitive inhibition assays were carried out with inhibitor concentrations of 5 mM and 15 mM for malonate, D-tartrate, and glyoxylate while the more potent inhibitor tartronate was tested at 0.1 mM and 1 mM. L-malate concentrations used were 5 mM, 10 mM, 15 mM, and 25 mM for all competitive inhibition assays.

Results

Purification results

After protein purification involving anion exchange, concentration via dialysis, and size exclusion chromatography (Table 4.1), TME was purified to approximately 92% as determined by coomassie brilliant blue staining of SDS PAGE and laser densitometry (Figure 4.1). Amino terminal sequencing of the purified protein verified the predicted amino acid sequence from the *tme* gene with the exception that the methionine was cleaved.

Kinetic parameters

TME showed typical Michaelis-Menten type behavior with varying substrate and cofactor concentrations (Figure 4.2A, Figure 4.2B). No activity was observed with NAD^+ replacing $NADP^+$ as cofactor indicating that TME is strictly $NADP^+$-dependent (Figure 4.2A). Secondary plots using the Hanes-Woolf equation gave K_m values of 33 μM for $NADP^+$ and a V_{max} of 53.6 μmol/min/mg protein. For L-malate, a Lineweaver-Burke plot yielded the best fit and a K_m of 2.6 mM and a V_{max} of 53 μmol/min/mg protein were determined. Since TME has been shown to exist as a octamer in its native state the catalytic constant k_{cat} was estimated at $582s^{-1}$, and the specific constant (k_{cat}/K_m) was calculated to be $2.2x10^5\ s^{-1}M^{-1}$. A Hill plot generated for TME was linear up to 12.5mM malate and gave a Hill coefficient of 0.95 (Figure 4.2C) indicating a lack of cooperativity of the enzyme indicating that substrate binding at one active site does not facilitate biding at other active sites of the octamer.

Table 4.1. Purification of TME from *E. coli* EJ1321 overexpressing the *tme* gene. Data represents values determined for a single purification experiment.

Step	Amount of protein (mg)	Total activity (μmol/min)	Yield (%)	Specific activity (μmol/min/mg)	Fold purification
Crude extract	17.3	61.8	100	3.6	1
MonoQ pool	1.6	23.3	38	9.4	2.6
Centricon pool	0.7	18.7	30	26.2	7.3
PP300SW pool	0.07	3.2	5	49	13.7

Figure 4.1. Coomasie stained SDS PAGE showing results of TME purification. Lane A; Protein standards, Lane B; 15μg *E. coli* EJ1321 (*dme-, tme-*) crude cell extract, Lane C; 15μg *E. coli* EcJ202 (EJ1321 (*dme-, tme-*) expressing pTH392 (*tme*)) crude cell extract overexpressing TME, Lane D; 5μg of purified TME. Numbers to the left indicate the molecular weights of the standard proteins in kDa while arrow to the right indicates the location of 82 kDa TME subunit.

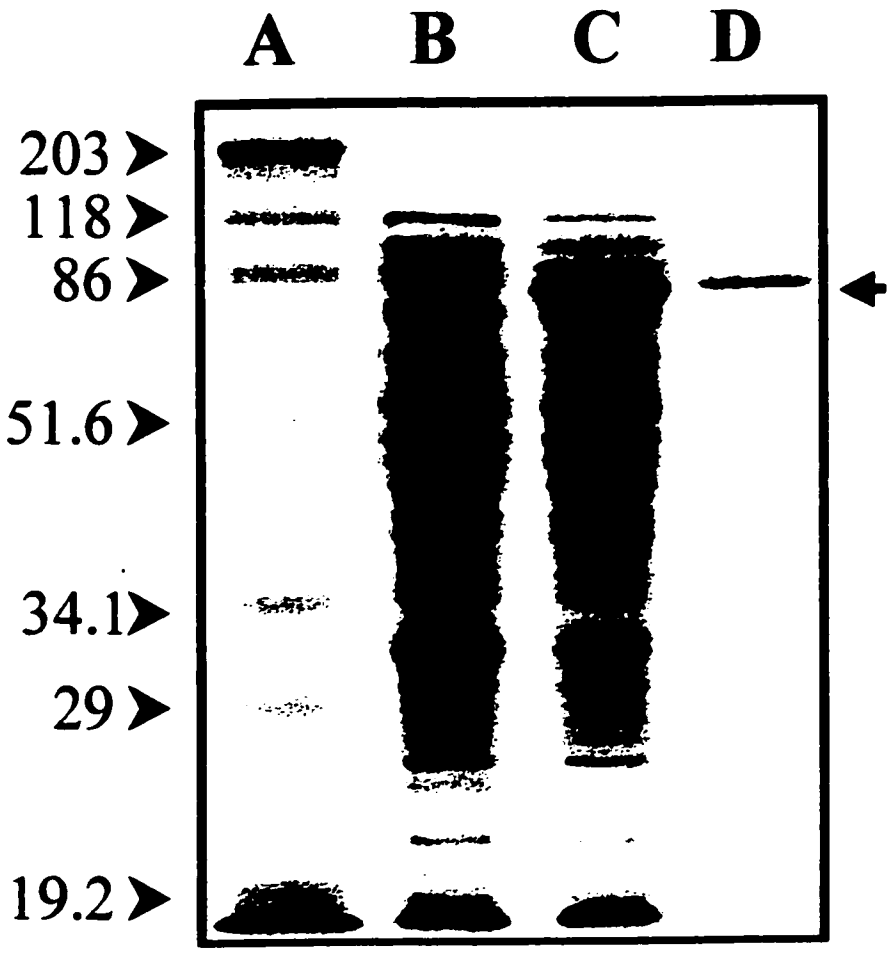
A
B
C
D
203
118
86
51.6
34.1
29
19.2

Figure 4.2. Differential response of TME to cofactor (**A**) and substrate (**B**), and (**C**) Hill plot indicating lack of positive co-operativity for TME. Michaelis-Menten plots depicting the response of TME to cofactors and substrate. **A**. Plot of rate versus cofactor concentration at a fixed substrate concentration of 30 mM malate. ♦ TME-NAD^+, ♦ TME-$NADP^+$. **B**. Plot of rate versus substrate concentration at a fixed $NADP^+$ concentration of 1.5 mM using TME. Data points are the means of triplicate experiments, error bars represent the standard error. **C**. Hill plot (log (v/V_{max}-v) vs log [S]) for data from Figure 4.B.

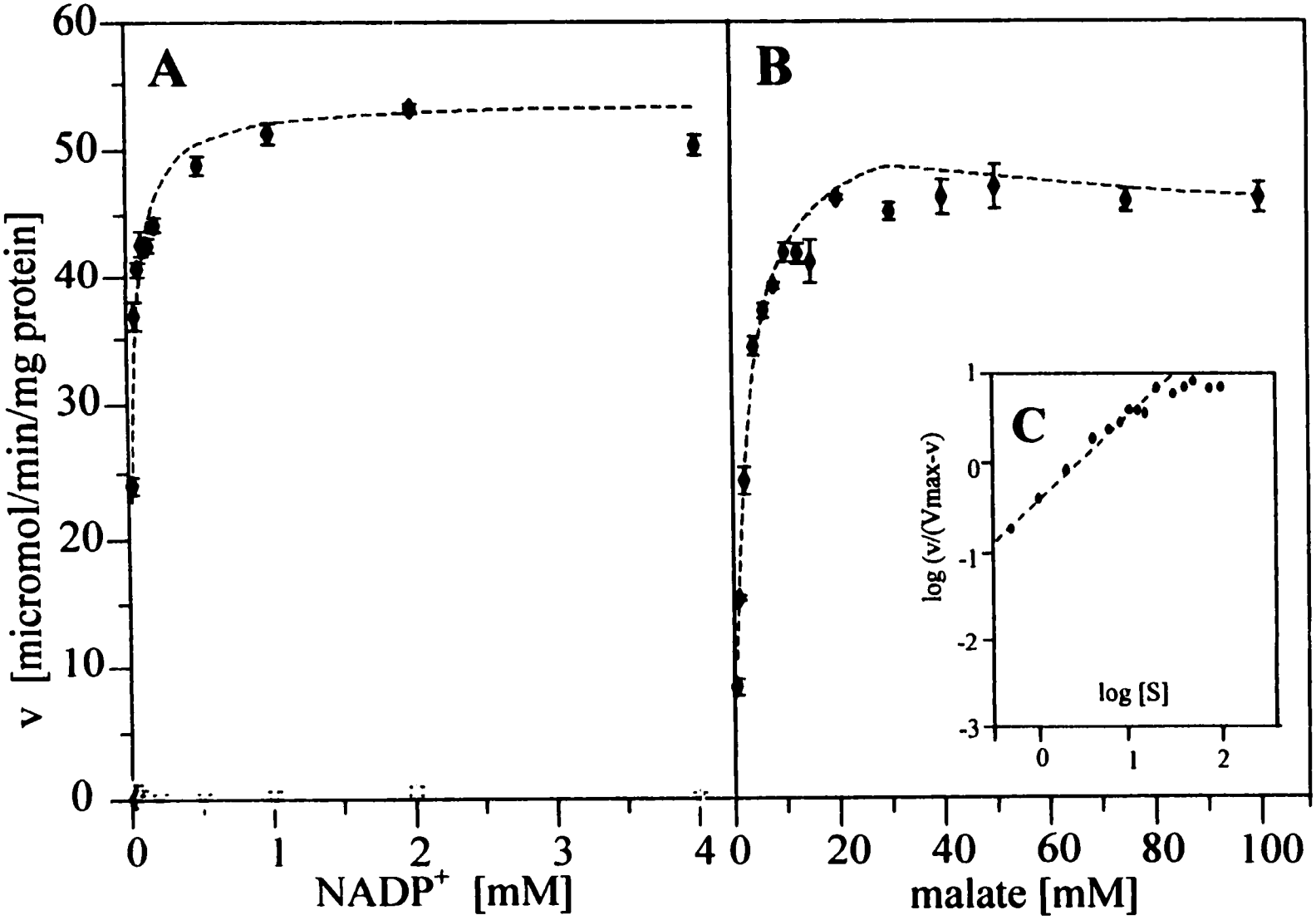
A
B
C
v [micromol/min/mg protein]
NADP+ [mM]
malate [mM]
log (v/(Vmax-v))
log [S]
0
10
20
30
40
50
60
0
1
2
3
4
0
20
40
60
80
100
-3
-2
-1
0
1
2

Table 4.2. Effects of various compounds on TME activity.

Compound	Concentration tested (mM)	% Relative activity[a]
Endproducts		
NADPH	0.25	80+/-5
$NaHC0_3$	50	53+/-2.3
pyruvate	10	81+/-3.8
Cellular metabolites		
CoA	0.2	95+/-5
ATP	1	90+/-1.7
ADP	1	95+/-5
AMP	1	89+/-4
cAMP	1	93+/-2.7
NADH	0.25	88.2+/-3.7
ammonia	1	110+/-1.8
ammonia	10	116+/-1.4
TCA cycle intermediates		
succinate	10	82+/-2.4
fumarate	10	91+/-3.4
acetyl-CoA	0.1	93+/-2.2
succinyl-CoA	0.1	92.1+/-4.9
isocitrate	10	90+/-4.2
α-ketoglutarate	10	90+/-2
Metabolic intermediates		
acetyl phosphate	1	88+/-2.8
fructose-1,6-bisphosphate	10	84+/-5
glucose	10	69+/-2.4
glucose-6-phosphate	10	106+/-1.6
glycerol-2-phosphate	10	91+/-3.7
glycerol	10	110+/-4.9
glutaric acid	10	104+/-5.2
phosphoenol pyruvate	10	87+/-4.6
hydroxybutyrate	10	92+/-1.3
hydroxybutyrate	1	92+/-3.6
acetate	10	93+/-2.4
lactate	10	87+/-1.3
butryl-CoA	0.1	104.9+/-3.7
malonyl-CoA	0.1	103.9+/-1.3
proprionyl-CoA	0.1	99+/-2.7
Amino acids		
aspartate	1	92+/-0.3
valine	10	98+/-2
alanine	10	96+/-8
leucine	10	95+/-6.7

[a] Activities are expressed as percent relative to a control assay with no effector present.

Inhibitor studies

To determine if TME activity was subjected to regulation by effectors, several compounds were tested for their effect on enzyme activity (Table 4.2). TME activity was unaffected by most compounds with only slight reductions in activity in the presence of end products pyruvate, bicarbonate, and NADPH, and the metabolites oxaloacetate, and glucose. This indicates that TME is not regulated by intermediates of the TCA cycle, glycolysis, or amino acids derived from pyruvate and is relatively insensitive to effector regulation.

Substrate analogs

The substrate analogs malonate, D-tartrate, and tartronate had adverse effects on TME activity (Table 4.3) presumably due to their competition with L-malate for binding at the active site. Lineweaver-Burke plots (Figure 4.3) revealed that all three compounds were indeed acting as competitive inhibitors and the observed effects were indeed due to competition for the substrate binding site. Secondary plots ($K_M/V_{max}(1+[I]/K_i)$ vs [I]) gave K_i values of 1.04 mM, 0.57 mM, and 0.04 mM for malonate, tartronate, and D-tartrate, respectively. The two carbon compound glyoxylate was also tested as an inhibitor of TME and was found to reduce its activity by 56% at 10 mM (Table 4.3). Observations with other substrate analogs yielded comparable drops in activity and since this was the only compound that may have physiological significance, its mode of inhibition on TME was investigated. The resulting Lineweaver-Burke plot (Figure 4.3) showed a mixed type of inhibition and secondary plots gave K_i (inhibitor constant with

Table 4.3. Inhibition of TME by substrate analogs.

Analog	R1[a]	R2[a]	% TME activity relative to no inhibitor present[b]
Acetate	-H	-H	103+/-3
Glyoxylate	=O		56+/-2
DL-lactate	-OH	$-CH_3$	86+/-5
Malonate	-H	-COOH	34+/-1
Tartronate	-OH	-COOH	0+/-0
D-malate	-OH	$-CH_2COOH$	66+/-3
L-tartrate	-OH	-CHOHCOOH	69+/-1
D-tartrate	-OH	-CHOHCOOH	27+/-0

[a] R1 and R2 represent substituents on the basic structure: For L-malate, R1 is –OH and R2 is $-CH_2COOH$.

[b] Activities are expressed as percent relative to a control assay with no substrate analog present.

Figure 4.3 . Determination of the type of inhibition on TME for malate analogs and glyoxylate. Malonate, D-tartrate, and glyoxylate were tested at 5 mM and 15 mM while tartronate was tested at 0.1mM and 1mM. Malate concentrations used were 5 mM, 10 mM, and 25 mM. Lineweaver-Burke plots for A; TME/tartronate, B; TME/D- tartrate, C; TME/malonate, D; TME/glyoxylate. ♦, no inhibitor, □ 5 mM malonate, D-tartrate, glyoxylate, or 0.1 mM tartronate, Δ 15 mM malonate, D-tartrate, glyoxylate, or 1 mM tartronate

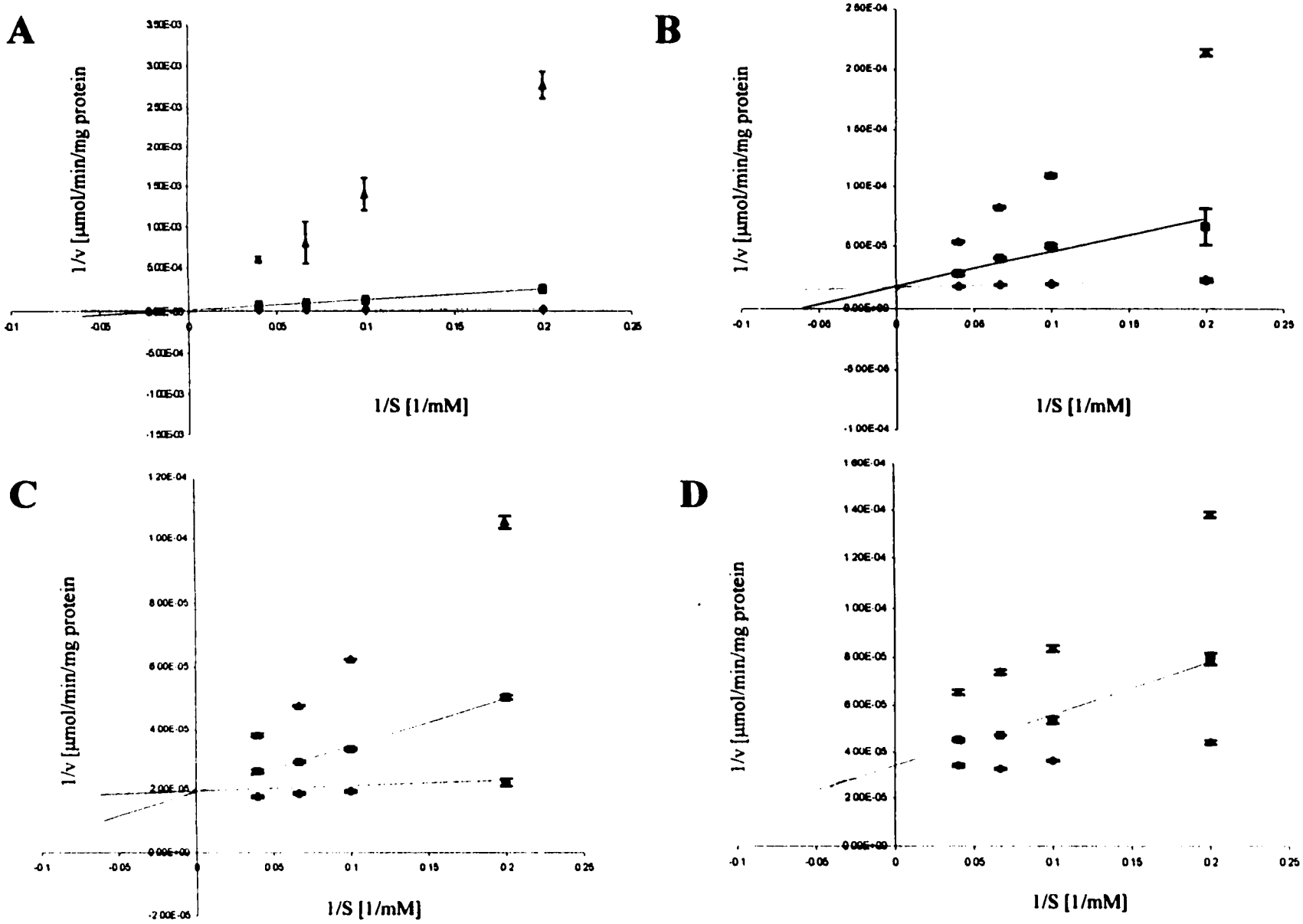
A
1/v [µmol/min/mg protein
1/S [1/mM]
B
1/v [µmol/min/mg protein
1/S [1/mM]
C
1/v [µmol/min/mg protein
1/S [1/mM]
D
1/v [µmol/min/mg protein
1/S [1/mM]

inhibitor binding to the enzyme) and K_I (inhibitor constant with inhibitor binding to the enzyme-substrate complex) values of 40.9 mM and 4.05 mM respectively. Since $K_I<K_i$ this would indicate inhibition of the non-competitive-uncompetitive type. This suggests that glyoxylate is not competing with L-malate at the substrate binding site and is instead regulating enzymatic activity at another location.

Discussion

The characterization of TME at the biochemical level allows us to compare it to several malic enzymes previously characterized. TME is strictly dependent upon $NADP^+$ for activity thus allowing us to give it the enzyme designation of EC 1.1.1.40. TME shows typical Michaelis–Menten behavior and has somewhat comparable K_m's for both substrate and cofactor (2.6 mM and 33 μM respectively) as DME (9.4 mM and 89 μM respectively (Voegele *et al.*, 1999)). Despite their similarity in terms of structure (Mitsch *et al.*, 1998, Chapter 3) the responses of the two malic enzymes to TCA cycle intermediates differed considerably with DME being allosterically regulated by acetyl-CoA, fumarate, and succinate and showing reduced activity with oxaloacetate (Voegele *et al.*, 1999). TME, by comparison was unaffected by these compounds. In the bacteroid, it is hypothesized that DME is required for maintaining the TCA cycle by providing a source of pyruvate for the eventual production of acetyl-CoA. Consistant with this, DME activity was stimulated by the presence of the C_4-dicarboxylic acids succinate and malate resulting in an increase in the production of pyruvate and presumably a greater level of acetyl-CoA for the production of citrate. When levels of pyruvate and acetyl-CoA are elevated, DME activity is repressed to reduce the drain of

C_4-dicarboxylates from the TCA cycle. Since TME cannot respond to TCA cycle intermediates in such a sensitive manner, it is unable to regulate its activity to maintain the TCA cycle and this may be a partial explanation why TME cannot functionally replace DME in bacteroids (Driscoll and Finan, 1993).

By comparison the $NADP^+$ malic enzyme of *B. japonicum* has been shown to be adversely effected by citrate (Kimura and Tajima, 1989), oxaloacetate, and acetyl-CoA and its activity induced by isocitrate (Chen *et al.*, 1997). In addition the $NADP^+$-dependent malic enzyme of *Pseudomonas putida* is stimulated by fumarate and succinate and is unaffected by acetyl-CoA (Garrido-Pertierra *et al.*, 1983) while the $NADP^+$-dependent enzyme of *E. coli* is unaffected by C_4-dicarboxylates, ATP, or fructose-1,6-diphosphate (Sanwal *et al.*, 1968) but is inhibited by end products, oxaloacetate, (Sanwal and Smando, 1969a, Sanwal and Smando, 1969b), acetyl-CoA (Spina *et al.*, 1968, Sanwal *et al.*, 1968), and glucose (Murai *et al.*, 1971). Therefore $NADP^+$-dependent malic enzymes vary in terms of their response to metabolic compounds. It is of interest to note that the NAD^+-dependent malic enzyme of *B. japonicum* is not sensitive to TCA cycle intermediates but is activated by D-glucose-6-phosphate, D-fructose-6-phosphate, and D-fructose-1,6-diphosphate (Chen *et al.*, 1998). In these respects it resembles TME with its insensitivity to TCA cycle intermediates. It is interesting to speculate on a possible role reversal for the malic enzymes of *S. meliloti* and *B. japonicum*: the NAD^+-dependent enzyme being necessary for maintaining the TCA cycle and the $NADP^+$-dependent enzyme not required in the former case but a reverse situation existing in the

latter. Until more genetic evidence is available for *B. japonicum* regarding the necessity of the malic enzymes this scenario is speculative.

E. coli, like *S. meliloti* and *B. japonicum* has two malic enzymes that differ in cofactor specificity (Katsuki *et al.*, 1967). In contrast, to the $NADP^+$-dependent enzyme, the NAD^+-dependent enzyme is activated by aspartate and inhibited by ATP and CoA (Sanwal, 1970b, Yamaguchi *et al.*, 1973). This differential regulation by metabolic compounds indicates that the two enzymes are likely fulfilling different cellular functions and has led to the hypothesis that the NAD^+-dependent enzyme is required for the catabolism of malate and regulating the pool of C_4-dicarboxylic acids and amino acids in the cell while the $NADP^+$-dependent enzyme is essential for generating acetyl-CoA and NADPH for lipid biosynthesis and anabolic metabolism in the cell (Muria *et al.*, 1973). If this hypothesis were extended to *S. meliloti*, DME would be required for catabolism of malate while TME would be required for anabolic processes. Bacteroid results (Driscoll and Finan, 1993, Driscoll and Finan, 1996) would support these suppositions as the senescent bacteroids would have reduced requirements for anabolic processes but would still require DME to maintain the TCA cycle for energy production, therefore *tme* expression would not be required.

Results with the substrate analogs show that the carboxyl group on the C1 atom is essential for substrate recognition. In addition, the effects of D-malonate and tartrate show that the position of the hydroxyl group at the C2 atom is critical for proper binding of the substrate at the active site. Also important is the presence of a second carboxyl group in proper orientation to the rest of the molecule as indicated by the total inhibition

by tartronate. The $NADP^+$-dependent malic enzymes from *B. japonicum* (Kimura and Tajima, 1989) and from the phototrophic bacterium *Chromatium vinosum* (Sahl and Truper, 1980) have been shown to be adversely effected by glyoxylate. A 58% drop in activity was found for partially purified $NADP^+$ malic enzyme from *B. japonicum* nodules while the malic enzyme of *C. vinosum* shows mixed inhibition in the presence of glyoxylate. *C. vinosum* has an incomplete TCA cycle that is used to fill a biosynthetic role and lacks the enzyme malate dehydrogenase. The $NADP^+$-dependent malic enzyme is therefore its only means to utilize malate or when acetate is assimilated via its functioning glyoxylate cycle. Recent evidence from *B. japonicum* mutants indicates that an insertion in the *sucA* gene results in the abolishment of the enzyme α-ketoglutarate dehydrogenase yet the mutants are able to grow on TCA cycle intermediates (Green and Emerich, 1997a). This suggests that a bypass of the TCA cycle such as the glyoxylate shunt (Figure 1.1) may be in place during free living and nitrogen fixing situations. If a similar situation in *S. meliloti* is occurring, the presence of large amounts of glyoxylate would inhibit what little TME there is in the bacteroid and complete its elimination from symbiosis while having little effect on the symbiotically essential DME. The only problem with this hypothesis is that the enzyme isocitrate lyase has not been detected at significant levels in either *S. meliloti* (Duncan and Fraenkel, 1979) or *B. japonicum* (Green *et al.*, 1998).

Recent evidence from our laboratory has shown that expression of *tme* to levels comparable to *dme* in bacteroids does not result in the ability to fix N_2 during symbiosis (Cowie, 1998) therefore eliminating the argument that TME could offset the loss of DME

if it were present in the bacteroids in sufficient quantities. It is possible that TME's insensitivity to TCA cycle intermediates would inhibit its ability to functionally replace DME. However a C-terminal truncated DME protein that is not inhibited by acetyl-CoA or C_4-dicarboxylates is capable of fixing atmospheric nitrogen during symbiosis in the absence of *dme* (Cowie, 1998). It would thus appear that the simplest explanation for the inability of TME to replace DME for N_2 fixation in bacteroids is that there is insufficient NADP+ to allow TME activity. If this were true it would indicate that $NADP^+$-dependent enzymes would face difficult challenges in the bacteroid. The $NADP^+$-dependent isocitrate dehydrogenase has been identified in *S. meliloti* (Chandrasekharan Nambiar and Shethna, 1976) and has a K_m for the cofactor of 15 μM or twice the affinity of TME and mutants deficient for isocitrate dehydrogenase form nodules that are incapable of fixing nitrogen (McDermott and Kahn, 1992) indicating that it is essential for symbiosis. The necessity of the $NADP^+$-dependent isocitrate dehydrogenase for symbiosis also weakens the argument for the glyoxylate shunt being functional in *S. meliloti*. Therefore it would appear that there is $NADP^+$ present in *S. meliloti* bacteroids but enzymes must have high affinities for the cofactor in order to be functional. Measurements of cofactor levels have been conducted in *B. japonicum* bacteroids and shown that that there is approximately 3 times and 2 times the level of NADPH relative to $NADP^+$ and NAD^+ to NADH respectively (Tajima and Kouzai, 1989). This could indicate that NAD^+ is the dominant currency of the bacteroid for enzyme activity or that the turnover rate for $NADP^+$/NADPH is extremely high. In any case the data is inconclusive regarding cofactor availability for enzymatic processes.

Chapter 5

Manipulations of malic enzyme production in *S. meliloti*; expression of *dme* from the *tme* promoter, quantification of the malic enzymes in *S. meliloti*, and overexpression of DME in *S. meliloti* bacteroids

Abstract

Experimental results from previous experiments employing plasmid born *tme::lacZ* gene fusions together with TME assay results suggest that *tme* expression and TME activity is reduced in N_2 fixing bacteroids. In order to determine if TME is actually produced in bacteroids and to determine if this level of expression is sufficient for producing proteins that have an impact on nitrogen fixation, the *dme* gene was placed under control of the *tme* promoter (*ptme-dme*), and recombined in the chromosome of *S. meliloti* strains deficient for the malic enzymes. Enzyme assays of free-living cells revealed that the strains were producing DME at rates comparable to wild type strains indicating the construct was functional. In contrast, alfalfa plants inoculated with strains expressing *dme* from the *tme* promoter had reduced nitrogen fixation activity and plant dry weights relative to plants inoculated with wild type *S. meliloti* strains. The results show that *tme* is indeed transcribed in *S. meliloti* bacteroids and this level of activity is approximately 30% that of the *dme* promoter. In addition, the relative amounts of both malic enzymes was estimated in both free-living cells and bacteroids by carrying out western blots with antibodies specific for TME and DME. These estimates showed that

the relative DME levels double while relative TME levels drop during the alteration from free-living cells to bacteroids. This supports the observations that *tme* is expressed at reduced rates in bacteroids relative to free-living cells.

Symbiotic nitrogen fixation is a carefully regulated process, however the rate limiting step for nitrogen fixation has yet to be determined. Oxidation of a reduced carbon source is required to generate ATP and reducing power for nitrogen fixation. Since the formation of pyruvate is essential to maintain the flux through the TCA cycle, the malic enzyme catalyzed oxidation of malate to pyruvate may represent the bottleneck for symbiotic nitrogen fixation. To address this issue, DME was over produced in *S. meliloti* bacteroids to assess if this would result in increased nitrogen fixation and plant growth. Increased NAD^+-dependent activity, 5 fold above the wild type strain Rm1021 was obtained, however no increase in plant dry weight or N_2 fixation was observed in alfalfa plants inoculated with this strain.

Methods and Materials

See Chapter 2 for all materials and methods. Bacterial strains and plasmids utilized are listed in Table 2.1. The strategy for constructing a *tme* promoter driven *dme* gene is shown in Figure 5.1. The *dme* gene was inserted down stream of the *tme* promoter by three separate ligations. Digesting pTH407b with *Hind*III and *Eco*RI released a 487 bp *tme* fragment that was inserted into pKS. The 2.98 kb *dme* fragment from pTH408 was isolated following digestion with *Hind*III and inserted into *Hind*III digested pKS vector. This resulted in the *dme* structural gene inserted in the vector such

Figure 5.1. Schematic diagram illustrating cloning strategy to produce *S. meliloti* strains expressing *dme* from the *tme* promoter. *dme*, *dme* gene region indicated by grey box, *tme*, *tme* gene region indicated by white box. Arrows within box indicate direction of transcription. Amp, ampicilian resistance, Gm, gentamycin resistance, oriT, origin of transfer. Dotted lines indicate region of homologous recombination, hatched box indicates *dme* gene region within the *S. meliloti* chromosome while triangle indicates transposon insertion within the *dme* gene of the *S. meliloti* chromosome. Relevant restriction sites are indicated; B, *Bam*HI, C, *Cla*I, E, *Eco*RI, H, *Hind*III, K, *Kpn*I, P, *Pst*I, Sa, *Sal*I, Sm, *Sma*I, Sp, *Sph*I, X, *Xba*I.

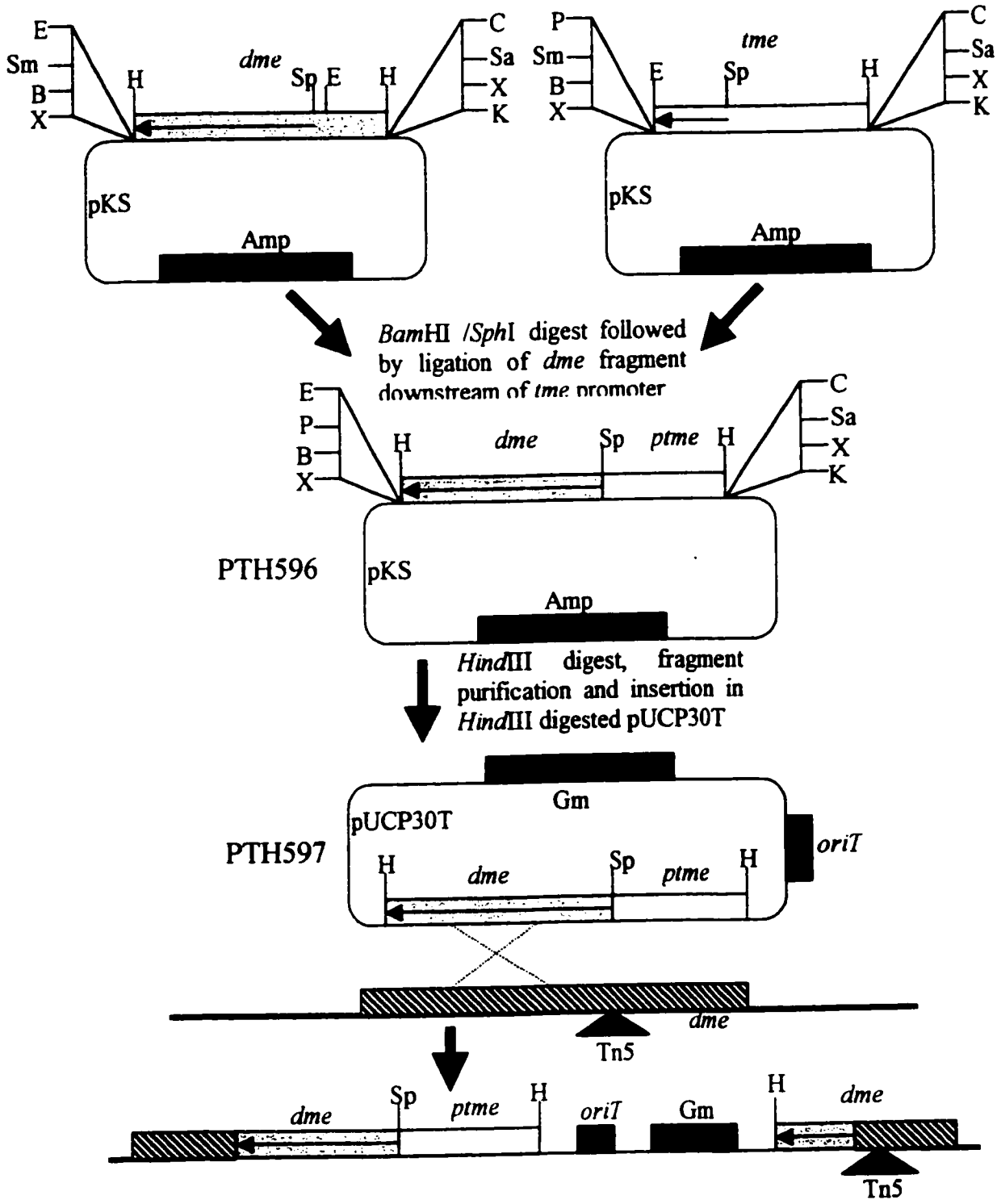
E
Sm
B
X
H
dme
Sp
E
H
C
Sa
X
K
pKS
Amp
P
Sm
B
X
tme
E
Sp
H
C
Sa
X
K
pKS
Amp
BamHI /SphI digest followed by ligation of dme fragment downstream of tme promoter
E
P
B
X
H
dme
Sp
ptme
H
C
Sa
X
K
PTH596
pKS
Amp
HindIII digest, fragment purification and insertion in HindIII digested pUCP30T
Gm
pUCP30T
PTH597
oriT
H
dme
Sp
ptme
H
dme
Tn5
dme
Sp
ptme
H
oriT
Gm
H
dme
Tn5

that the *Bam*HI site was at the 3' region of the gene. These two constructs allowed for the use of the *Sph*I site located in both fragments that was previously inserted into the translational start site of both genes (Cowie, 1998). The final construct was produced by removing the *dme* 2.8 kb fragment via a *SphI/Bam*HI digest followed by insertion downstream of the *tme* promoter in pKS resulting in pTH596. This construct resulted in 471 bp of *tme* being located upstream of the *dme* open reading frame with the translational start site of *dme* being fused to the translational start site of *tme* via the *Sph*I sites previously inserted into the two genes (Cowie, 1998). The 3.3 kb hybrid construct was then digested with *Bam*HI and *Kpn*I and inserted into pUCP30T to create plasmid pTH597. To produce strains expressing *dme* from the *tme* promoter, triparental matings were carried out with *dme*, *tme*, and *dme tme* mutant *S. meliloti* strains. The transconjugants were isolated by plating on LBGm (20 μg/ml) Nm (100 μg/ml) plates. Upon isolation of colonies bearing putative insertions of the pUCP30T vector within the chromosome of the *S. meliloti* strains, transductions were carried out to verify the site of cointegrate formation. Phage lysates prepared on the cointegrate strain were used to transduce Gm^r into Rm1021. In all cases the the Gm^r marker from pUCP30T was 100% linked to Nm^r from the *dme*::Tn*5* insertion. No linkage was detected between the markers for *tme* and the gentamicin marker of the pUCP30T construct pTH597.

In order to quantitate the amounts of DME and TME present in free-living cells and bacteroids a total of two western blots for DME and TME were produced. Cell free extracts were obtained from an overnight LBmc grown culture that was subjected to sonication (Chapter 2). Bacteroids were obtained from alfalfa plants inoculated with wild

type Rm1021 and the bacteroids isolated as previously reported (Chapter 2). Each SDS PAGE had a constant amount of total free-living protein with one gel containing varying amounts of purified protein (Chapter 3) while the second had varying amounts of total bacteroid protein. These blots were developed with anti-DME or anti-TME antibodies and exposed using an enhanced chemi-luminescesnce stain. Several exposures of varying times were carried out and the resulting X-ray films were then analyzed using a laser densitometer and relative intensities of each band was measured. Two time exposures (30 seconds and 1 minute) were used for each western blot to produce two separate standard curves for the purified protein and these were used to estimate the amount of DME or TME per 2 μgs of free-living cell extract. The values obtained for TME and DME were then used to estimate the amount of each protein in bacteroid total protein extracts. The intensity of the 2 μg total protein of free-living extract was then compared to the standard curves of total bacteroid protein obtained from the two exposures (30 seconds and 1 minute) of each western blot. Therefore, knowing the amount of malic enzyme protein present in the free-living extract allowed us to obtain an estimate of the amount of DME or TME present in the bacteroid sample. In all cases an average was determined for the values obtained for each standard curve and these values are reported.

The *dme* gene was subcloned into pBBR1MCS-5 as a 3kb *Hind*III/*Kpn*I fragment from pTH408 resulting in the creation of pTH598. *tme* was subcloned onto pBBR1MCS-5 as a 3kb *Hind*III/*Kpn*I fragment from pTH407B resulting in the creation of pTH599. The plasmids were transferred to wild type *S. meliloti* cells via a triparental mating and the strains were then tested for malic enzyme over expression and symbiotic N_2 fixation.

Results

Expression of the *ptme-dme* construct in *S. meliloti*

Enzyme assays carried out on strains expressing *dme* from the *tme* promoter revealed that free-living cells had reduced levels of DME activity relative to wild type *S. meliloti* cells (approximately 72-77%) (Table 5.1) indicating that the *tme* promoter is less active than the *dme* promoter in *S. meliloti* cells grown on LBmc. This corresponds well with estimates of protein content in free-living *S. meliloti* cells where TME is present at 69% the level of DME (Figure 5.6 and results presented below) which suggests that strains RmH979 and RmH980 are indeed expressing *dme* from the *tme* promoter as anticipated. We also note that RmH981 expresses *dme* from both the *dme* promoter and the *tme* promoter and this results in DME levels that are elevated relative to wild type indicating that the two promoters act in an additive nature to overproduce DME relative to wild type cells (Table 5.1). The $NADP^+$-dependent enzyme assays are more difficult to interpret since, under our assay conditions, both DME and TME would be active and contribute to the formation of pyruvate. What is clear is that RmH979 and RmH981 show higher levels of $NADP^+$-dependent activity relative to their parental controls RmG454 and RmG995 presumably due to the elevated levels of DME due to the expression of the *ptme-dme* construct.

Expression of the *ptme-dme* construct in *S. meliloti* bacteroids

Plant assays carried out with strains expressing *dme* from the *tme* promoter revealed a partial symbiotic N_2 fixation phenotype. The plants inoculated with *S. meliloti* strains lacking a functional *dme* gene but expressing the *ptme-dme* construct were much

Table 5.1. Enzyme assays on extracts obtained from various *S. meliloti* strains expressing *dme* from the *tme* promoter.

Strains	Genotypes	NAD^+-dependent activity (nmoles/min/mg)[a]	% NAD^+-dependent activity relative to wild type	$NADP^+$-dependent activity (nmoles/min/mg)[a]	% $NADP^+$-dependent activity relative to wild type	MDH (nmoles/min/mg)[b]
Rm1021	wild type	107+/-3.5	100	46.9+/-2.0	100	313.3+/-3.9
RmG454	*dme2*	52.1+/-2.0	49	59.4+/-0.7	127	543.1+/-25.5
RmG994	*dme3, tme4*	53.6+/-1.2	50	5.0+/-1.3	11	439.3+/-40.6
RmG995	*tme4*	113.9+/-1.1	107	24.8+/-1.9	53	381+/-21.5
RmH979	*dme2*, Φ*ptme-dme*	76.5+/-2.1	72	64.7+/-2.9	138	375+/-26.2
RmH980	*dme3, tme4*, Φ*ptme-dme*	82.2+/-2.6	77	4.3+/-1.2	9	352.5+/-15.0
RmH981	*tme4*, Φ*ptme-dme*	123.5+/-0.2	115	28.8+/-4.7	61	387.9+/-24.4

[a] Specific activity is expressed as nmoles of pyruvate formed/minute/mg protein with the mean +/- standard error of triplicate samples.

[b] Specific activity is expressed as nmoles NADH formed/minute/mg protein with the mean +/- standard error of triplicate samples

Figure 5.2. Photograph of alfalfa plants inoculated with *S. meliloti* strains expressing *dme* under control of the *tme* promoter.

Rm1021 **RmG454** **RmH979** **uninoculated**
wild type ***dme2*** ***dme2,***
Φptme-dme

Rm1021 **RmG994** **RmH980** **uninoculated**
wild type ***dme3, tme4*** ***dme3, tme4,***
Φptme-dme

Table 5.2. Acetylene reduction assays and plant dry weights of plants inoculated with various *S. meliloti* strains expressing *dme* from the *tme* promoter.

Strain	Genotype	ARA (nmoles/min/plant)[a]	% ARA relative to wild type	Plant dry weight (mgs)[b]	% Plant dry weight relative to wild type
Rm1021	wild type	1004 +/- 2	100	46.8 +/- 4.8	100
RmG454	*dme2*	13 +/- 2	1	10.1 +/- 0.8	22
RmG994	*dme2, tme4*	ND	0	9.5+/-0.5	20
RmG995	*tme4*	1039+/-69	104	54.6+/-8.3	117
RmH979	*dme2, Φptme-dme*	341+/-73	34	16.6+/-1.0	36
RmH980	*dme3, tme4, Φptme-dme*	214+/-34	21	16.5+/-1.6	35
RmH981	*tme4, Φptme-dme*	400 +/- 106	40	46.4+/-6.8	99
uninoculated	-	-	-	8.5 +/- 1.5	18

[a] Acetylene reduction activity is expressed as mean of nmoles of ethylene produced/minute +/- standard error of triplicate samples containing three root systems each.

[b] Plant dry weight is expressed as mean of +/- standard error of triplicate pots containing 7-10 plants each.

ND none detected

smaller than plants inoculated with wild type *S. meliloti* strain Rm1021 but were larger and less chlorotic than the plants inoculated with the *dme* deficient *S. meliloti* strains inoculated plants (Figure 5.5). The acetylene reduction assays revealed that expression of the *ptme-dme* construct in bacteroids resulted in acetylene reduction activities that are 21-34% that plants inoculated with wild type *S. meliloti* (Table 5.2). This trend of reduced activity was mirrored in the dry weights of the plants inoculated with *S. meliloti dme*$^-$ strains expressing the *ptme-dme* construct. RmH979 and RmH980 both showed plant dry weights that are approximately 35% that of wild type inoculated plants. If DME activity can be correlated with plant growth due to the requirement of DME for a symbiotic N_2 fixation, we can assume that the *tme* promoter expressing *dme* is capable of producing only 21% the protein of the *dme* promoter. Thus *tme* promoter activity within bacteroids is approximately 20% that of the *dme* promoter under similar conditions.

Enzyme assays carried out upon bacteroid extracts obtained from alfalfa plants inoculated with *S. meliloti* strains expressing *dme* from the *tme* promoter showed a different trend from that obtained from free-living cells. *S. meliloti dme* deficient strains expressing the *ptme-dme* construct had 27-34% the NAD^+-dependent activity of wild type bacteroid extracts (Table 5.3). Once again the $NADP^+$-dependent assay results are more difficult to rationalize due to the variability in DME and TME activity with $NADP^+$ and also the variability in gene expression within bacteroids. What is demonstrated is the rise in $NADP^+$-dependent activity in strains expressing the *ptme-dme* construct (RmH979 and RmH980) as opposed to their parental strains (RmG454 and RmG994). This is most

Table 5.3. Enzyme assays of bacteroid extracts from various *S. meliloti* strains expressing *dme* from the *tme* promoter.

Strains	Genotypes	NAD^+-dependent activity (nmoles/min/mg)[a]	% NAD^+-dependent activity relative to wild type	$NADP^+$-dependent activity (nmoles/min/mg)[a]	% $NADP^+$-dependent activity relative to wild type	MDH (nmoles/min/mg)[b]
Rm1021	wild type	115.3+/-1.6	100	33.6+/-3.3	100	1135+/-13
RmG454	*dme2*	14.4+/-0.1	13	0.9+/-0.1	3	62+/-1
RmG994	*dme3, tme4*	ND	0	ND	0	461+/-1
RmG995	*tme4*	140.7+/-2.0	122	60.9+/-1.3	181	672+/-23
RmH979	*dme2*, Φ*ptme-dme*	31+/-0.6	27	6.8+/-1.0	20	317+/-2
RmH980	*dme3, tme4*, Φ*ptme-dme*	39.6+/-0.9	34	0.2+/-0.1	1	235+/-7
RmH981	*tme4*, Φ*ptme-dme*	115.5+/-2.4	100	42.1+/-1.4	125	155+/-3

[a] Specific activity is expressed as nmoles of pyruvate formed/minute/mg protein with the mean +/- standard error of triplicate samples.

[b] Specific activity is expressed as nmoles NADH formed/minute/mg protein with the mean +/- standard error of triplicate samples

ND none detected

Figure 5.3. Western blot of bacteroid extracts obtained from alfalfa plants inoculated with *S. meliloti* strains expressing *dme* from the *tme* promoter. 2 μg of each extract was loaded. Arrows to the left indicate location of markers, numbers are molecular weights. Position of DME subunit is indicated. 2 μg of free-living extract of Rm1021 (Rm1021FL) is presented as a control.

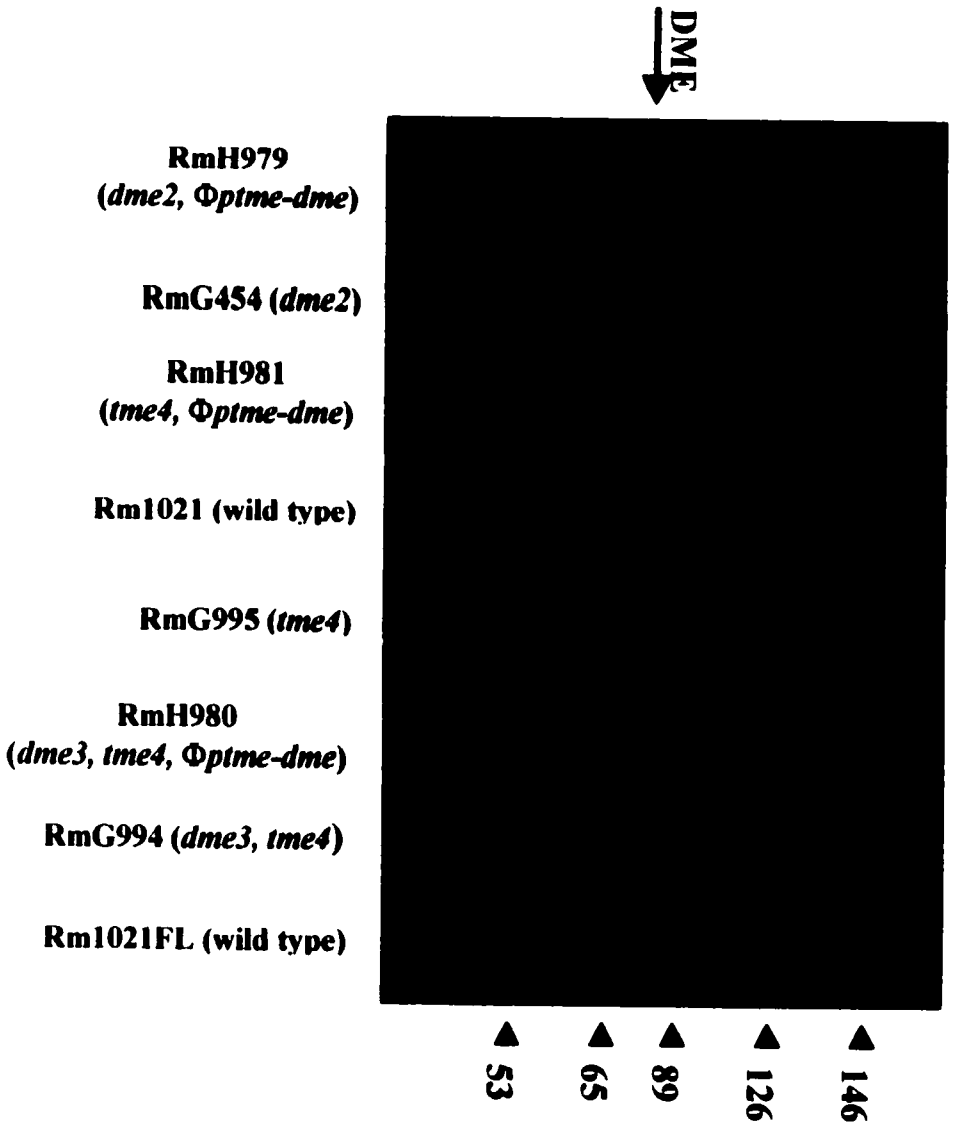
DME
RmH979
(dme2, Φptme-dme)
RmG454 (dme2)
RmH981
(tme4, Φptme-dme)
Rm1021 (wild type)
RmG995 (tme4)
RmH980
(dme3, tme4, Φptme-dme)
RmG994 (dme3, tme4)
Rm1021FL (wild type)
53
65
89
126
146

likely due to the elevated levels of DME present in these bacteroid extracts due to the activity of the *ptme-dme* construct. Western blots of bacteroid extracts clearly show that the relative amounts of DME are variable among the different strains with low levels of DME being observed for bacteroids obtained for strains RmH979 and RmH980 while RmG995 and RmH981 have DME levels approximat-approximating wild type in intensity (Figure 5.3).

Quantification of TME and DME

The results obtained from the western blots (Figure 5.4-5.7) indicate that there is 6.8+/-0.6 ng of DME/μg of free-living protein (Figure 5.4) and 4.7+/-0.6 ng of TME/μg of free-living protein (Figure 5.6). In contrast the situation in the bacteroid is vastly different with 14.2+/-0.6 ng of DME/μg of bacteroid protein (Figure 5.5) and 0.9+/-0.003 ng of TME/μg of bacteroid protein (Figure 5.7) being present. This indicates that the relative amounts of each protein are very different during the transition from free-living cell to nitrogen fixing bacteroid with relative DME levels doubling while TME levels are reduced by one fifth. In addition the results obtained show that TME levels in free-living cells are reduced to approximately 69% that of DME.

Overexpression of *dme* and *tme* in *S. meliloti* cells and bacteroids

Enzyme assays on free-living cells over expressing the malic enzymes verified that the two constructs pTH598 and pTH599 were producing excessive amounts of DME and TME respectively (Table 5.4). The elevated $NADP^+$-dependent activity of RmK297 can be attributed to the fact that DME is capable of utilizing $NADP^+$ as a cofactor (K_m of 1.56 mM for $NADP^+$, Km of 89 μM for NAD^+) to a limited extent (Chapter 4, Voegele *et*

Figure 5.4. SDS PAGE subjected to western blot using antibody specific for DME. **A.** Western blot to quantify DME amounts in free-living cells. Lane 1. 100 ng of purified DME, lane 2, 2 μg of protein from crude cell extract of free-living cells, lane 3, 50 ng purified DME, lane 4, 25 ng purified DME, lane 5, 2 μg of protein from crude cell extract of free-living cells lane 6, 10 ng purified DME, lane 7, 5 ng purified DME, lane 8, 2 μg of protein from crude cell extract of free-living cells lane 9, 1 ng purified DME. Arrow indicates the position of the 82 kDa subunit of DME. Secondary bands seen are breakdown products of DME seen at elevated protein amounts. **B.** Graph of laser densitometry areas versus amount of purified DME for two exposure times for the autoradiogram in **A.** Linear regression data and formula for each exposure is included in the graph.

A

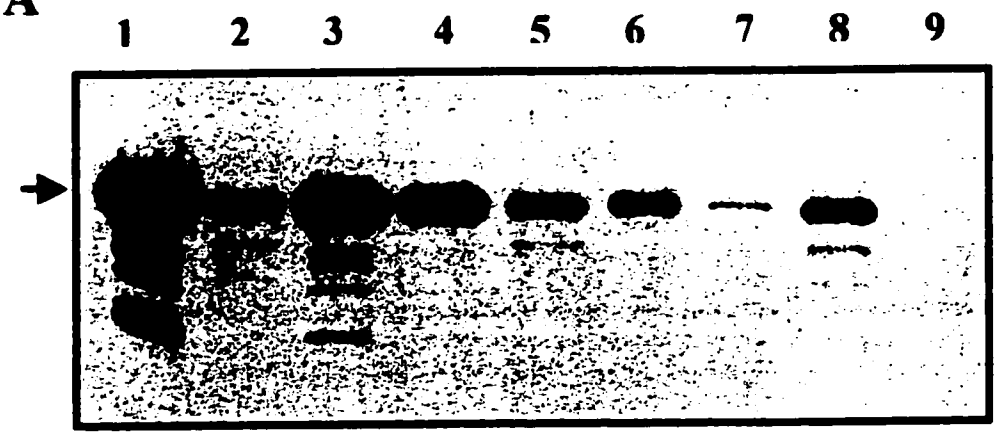
1
2
3
4
5
6
7
8
9

B

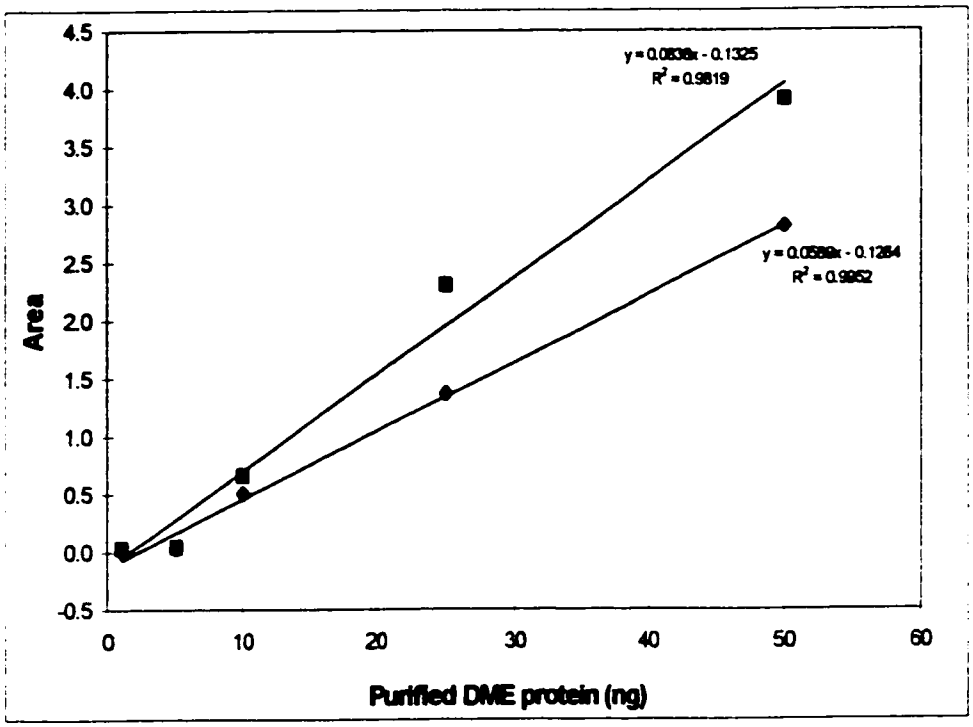
y = 0.0838x - 0.1325
R² = 0.9819
y = 0.0588x - 0.1264
R² = 0.9952
Area
Purified DME protein (ng)
4.5
4.0
3.5
3.0
2.5
2.0
1.5
1.0
0.5
0.0
-0.5
0
10
20
30
40
50
60

Figure 5.5. SDS PAGE subjected to western blot using antibody specific for DME. **A.** Western blot to quantify DME amounts in bacteroids. Lane 1. 0.5 μg of protein from sonicated bacteroids, lane 2, 2 μg of protein from crude cell extract of free-living cells, lane 3, 1 μg of protein from sonicated bacteroids, lane 4, 1.5 μg of protein from sonicated bacteroids, lane 5, 2 μg of protein from crude cell extract of free-living cells, lane 6, 2 μg of protein from sonicated bacteroids, lane 7, 2.5 μg of protein from sonicated bacteroids, lane 8, 2 μg of protein from crude cell extract of free-living cells, lane 9, 3 μg of protein from sonicated bacteroids. Arrow indicates the position of the 82 kDa subunit of DME. **B.** Graph of laser densitometry areas versus amount of total bacteroid protein for two exposure times for the autoradiogram in **A**. Linear regression data and formula for each exposure is included in the graph.

A

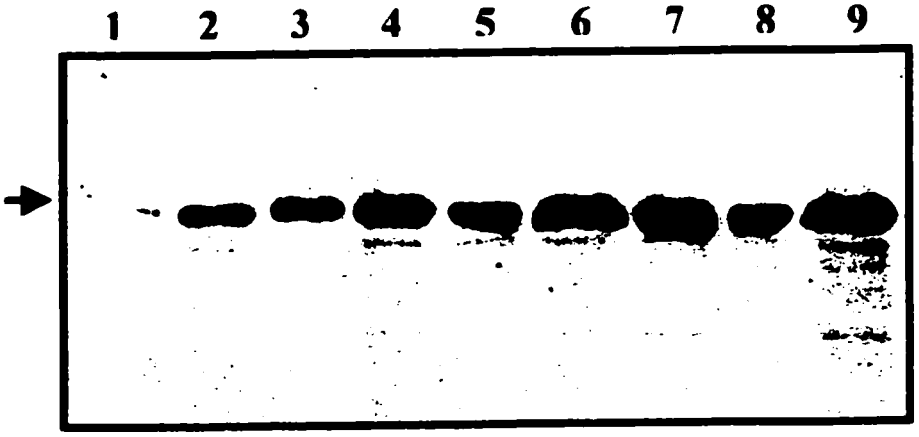
1
2
3
4
5
6
7
8
9

B

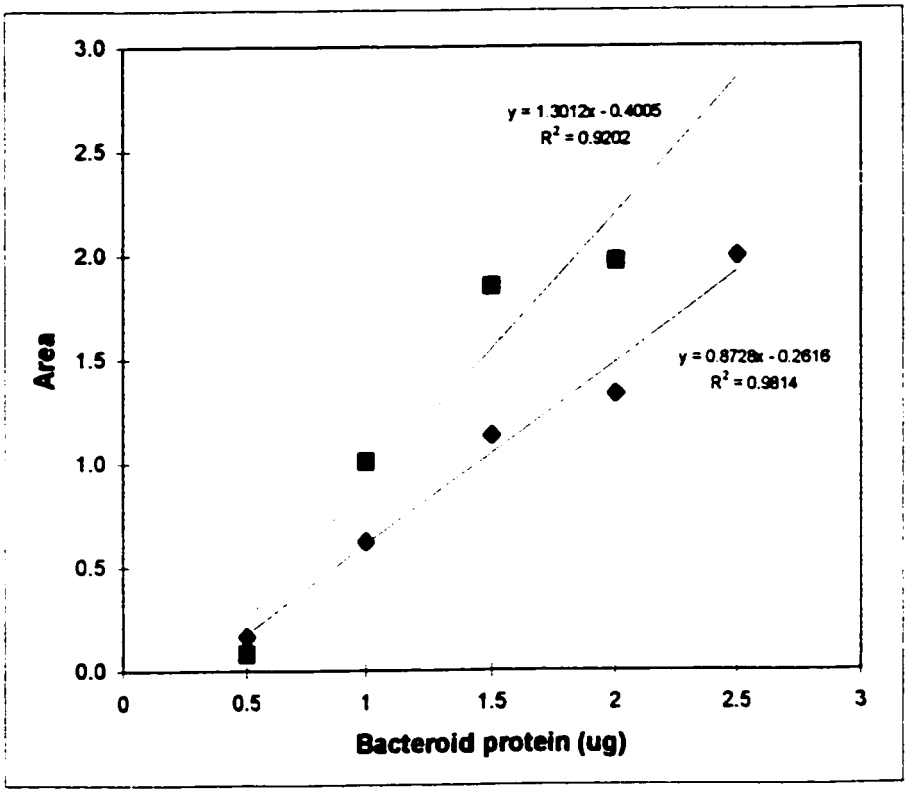
3.0
2.5
2.0
1.5
1.0
0.5
0.0
Area
0
0.5
1
1.5
2
2.5
3
Bacteroid protein (ug)
y = 1.3012x - 0.4005
R² = 0.9202
y = 0.8728x - 0.2616
R² = 0.9814

Figure 5.6. SDS PAGE subjected to western blot using antibody specific for TME. **A.** Western blot to quantify TME amounts in free-living cells. Lane 1. 1 ng of purified TME, lane 2, 2 μg of protein from crude cell extract of free-living cells, lane 3, 5 ng purified TME, lane 4, 10 ng purified TME, lane 5, 2 μg of protein from crude cell extract of free-living cells, lane 6, 25 ng purified TME, lane 7, 50 ng purified TME, lane 8, 2 μg of protein from crude cell extract of free-living cells, lane 9, 100 ng purified TME. Arrow indicates position of 82 kDa subunit of TME. Second band seen at approximately 60 kDa is a breakdown product of TME seen at elevated protein amounts. **B.** Graph of laser densitometry areas versus amount of purified TME for two exposure times for the autoradiogram in **A.** Linear regression data and formula for each exposure is included in the graph.

A

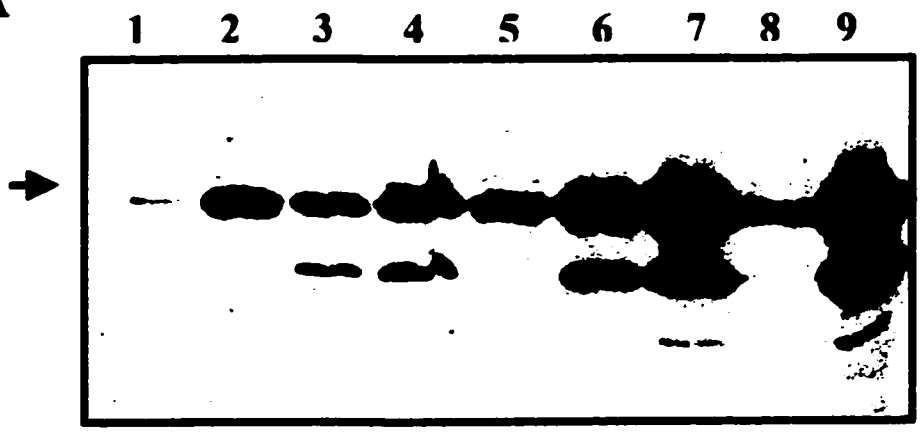
1
2
3
4
5
6
7
8
9

B

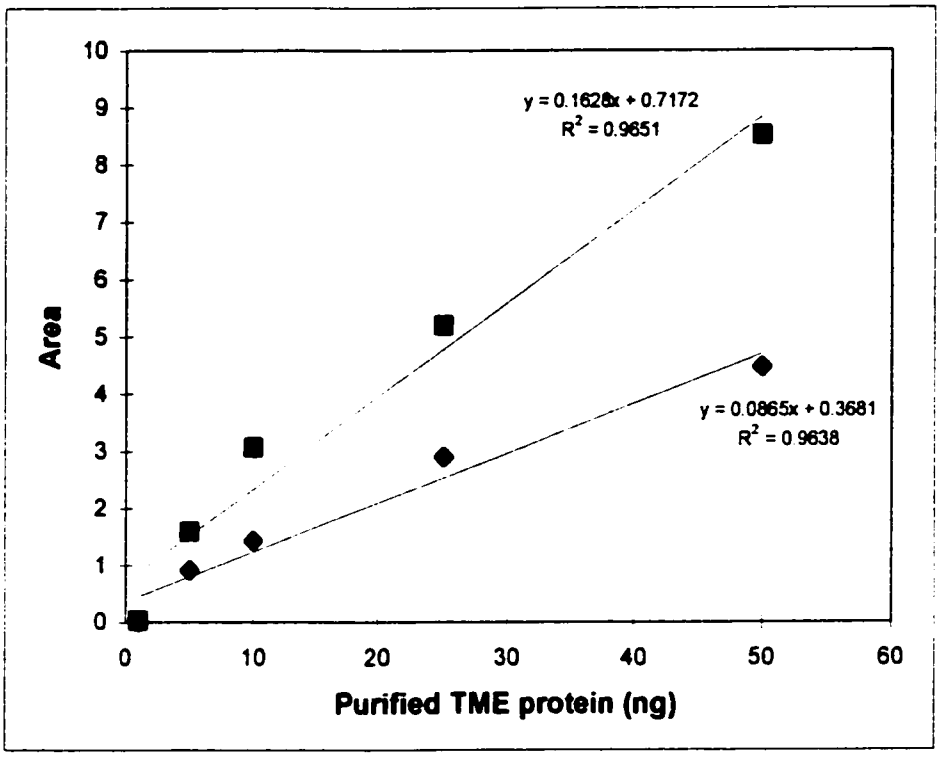
y = 0.1626x + 0.7172
R² = 0.9651
y = 0.0865x + 0.3681
R² = 0.9638
Area
Purified TME protein (ng)
0
1
2
3
4
5
6
7
8
9
10
0
10
20
30
40
50
60

Figure 5.7. SDS PAGE subjected to western blot using antibody specific for TME. **A.** Western blot to quantify TME amounts in bacteroids. Lane 1. 2 μg of protein from sonicated bacteroids, lane 2, 2 μg of protein from crude cell extract of free-living cells, lane 3, 4 μg of protein from sonicated bacteroids, lane 4, 6 μg of protein from sonicated bacteroids, lane 5, 2 μg of protein from crude cell extract of free-living cells, lane 6, 8 μg of protein from sonicated bacteroids, lane 7, 10 μg of protein from sonicated bacteroids, lane 8, 2 μg of protein from crude cell extract of free-living cells, lane 9, 12 μg of protein from sonicated bacteroids. Arrow indicates position of 82 kDa subunit of TME. **B.** Graph of laser densitometry areas versus amount of total bacteroid protein for two exposure times for the autoradiogram in **A**. Linear regression data and formula for each exposure is included in the graph.

A

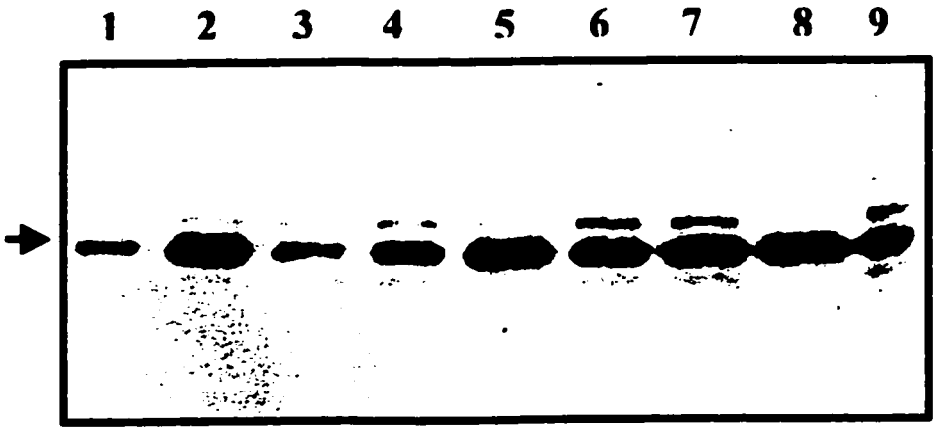
1
2
3
4
5
6
7
8
9

B

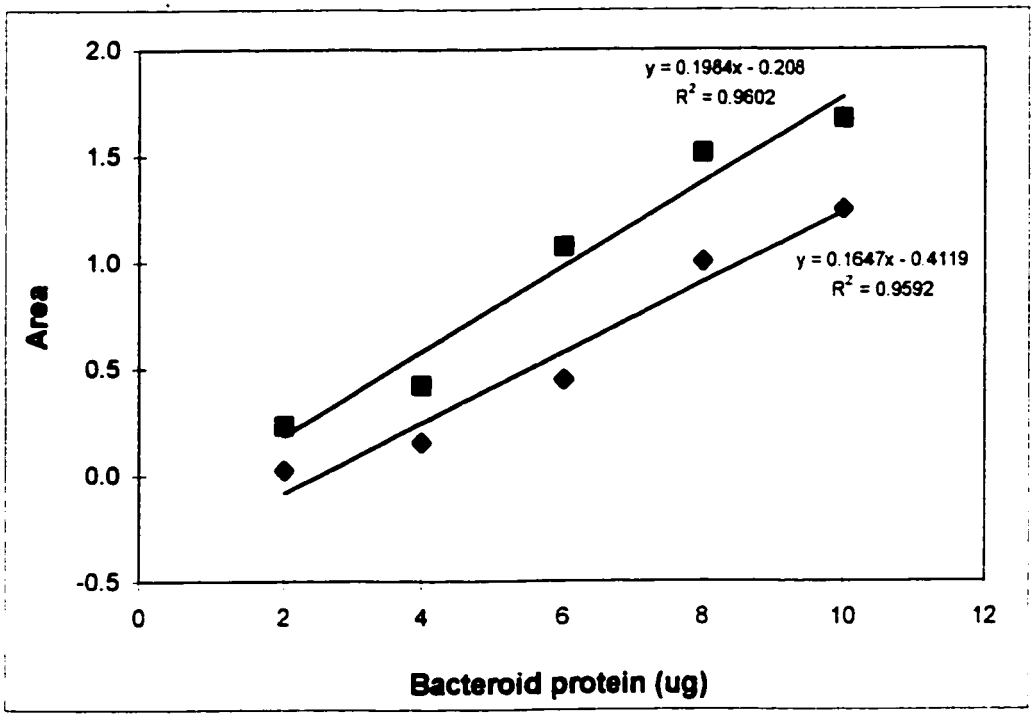
y = 0.1984x - 0.208
R² = 0.9602
y = 0.1647x - 0.4119
R² = 0.9592
Area
Bacteroid protein (ug)
2.0
1.5
1.0
0.5
0.0
-0.5
0
2
4
6
8
10
12

Table 5.4. Enzyme assays on free-living *S. meliloti* cells overexpressing the malic enzymes

Strain	Genotype	NAD^+-dependent activity (nmoles/min/mg)[a]	% activity relative to wild type	$NADP^+$-dependent activity (nmoles/min/mg)[a]	% activity relative to wild type	MDH activity (nmoles/min/mg)[b]
Rm1021	wild type	119.8 +/- 13.2	100	22.7 +/- 5	100	202 +/- 15
RmK296	Rm1021, *dme*	621.5 +/- 31.2	519	138.6 +/- 13.5	608	176 +/- 1
RmK297	Rm1021, *tme*	118.7 +/- 2.3	99	671.8 +/- 26.3	2959	183 +/- 14
RmK298	Rm1021 pBBR1MCS-5	122 +/-8.4	102	25.3 +/-5.4	114	213 +/- 4

[a] specific activity is expressed as nmoles of pyruvate formed /minute/mg protein with the mean +/- standard error of triplicate samples.

[b] specific activity is expressed as nmoles NADH formed /minute/mg protein with the mean +/- standard error of triplicate samples

al., 1999). Once over production of the malic enzymes had been verified plant tests were initiated.

Plant tests with *S. meliloti* strains overexpressing *dme* and *tme*

Alfalfa plants inoculated with the *dme* over expressing strain RmK296 did not differ in appearance from plants inoculated with wild type strains of *S. meliloti* (Figure 5.8). In addition there was no obvious difference between the plants inoculated with the *tme* over expressing strain RmK297 and plants inoculated with wild type *S. meliloti* strains (Figure 5.8). These visual assessments were followed by acetylene reduction assays and isolation of the plants for dry weight analysis (Table 5.5). Relative to strain RmK298, wild type Rm1021 strain carrying the plasmid pBBR1MCS-5, RmK296 has elevated acetylene reduction activity while RmK297 shows reduced acetylene reduction activity. In addition, the wild type strain Rm1021 has reduced activity relative to the same strain carrying pBBR1MCS-5. T-test analysis showed that the variation in acetylene reduction activity was statistically significant for only RmK296 relative to wild type inoculated plants. These trends are not carried over in the assessment of plant dry weight. There is no significant alteration between plant dry weights despite the over expression of the malic enzymes and this observation was supported by t-test statistical analysis which showed that the variation in plant dry weight was not significant.

Enzyme assays were conducted on bacteroid extracts isolated from these plants in order to determine if the over expression of the malic enzymes observed in free living cells was maintained during symbiosis. NAD^+-dependent malic enzyme assays revealed that strain RmK296 over expressing *dme* had increased levels of DME activity as

Figure 5.8. Photograph of alfalfa plants inoculated with *S. meliloti* strains overexpressing the malic enzymes *tme* or *dme*.

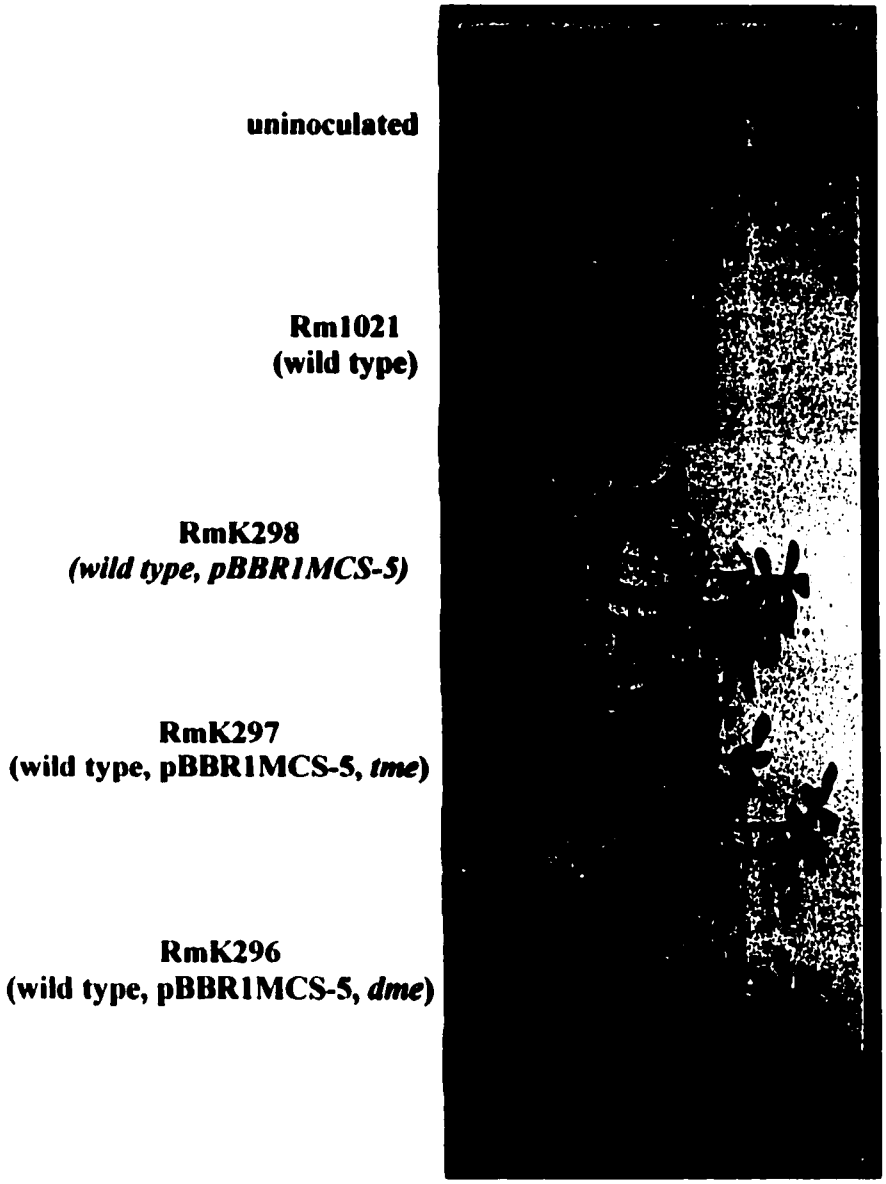
uninoculated
Rm1021
(wild type)
RmK298
(wild type, pBBR1MCS-5)
RmK297
(wild type, pBBR1MCS-5, tme)
RmK296
(wild type, pBBR1MCS-5, dme)

Table 5.5. Acetylene reduction assay results and plant dry weights of alfalfa plants inoculated with *S. meliloti* strains overexpressing the malic enzymes

Strain	Genotype	ARA activity (nmoles/min /plant)[a]	% ARA activity relative to wild type	% Plasmid retention[b]	Plant dry weight (mgs)[c]	% Plant dry weight relative to wild type
Rm1021	wild type	797 +/- 95	78	-	72.1 +/- 4.4	117
RmK296	Rm1021, *dme*	1417 +/- 263	139	66	77.2 +/- 7.9	109
RmK297	Rm1021, *tme*	695 +/- 117	68	78	71.3 +/- 7.7	108
RmK298	wild type, pBBR1MCS-5	1022 +/- 227	100	62	66.2 +/- 7.2	100
uninoculated	-	-	-	-	6.2 +/- 0.2	9

[a] Acetylene reduction activity is expressed as mean of nmoles of ethylene produced/minute +/- standard error of triplicate samples containing three root systems each.

[b] Plasmid retention determined as percent number of gentamycin cells in streptomycin resistant cells obtained from nodules.

[c] Plant dry weight is expressed as mean of +/- standard error of triplicate pots containing 7-10 plants each.

Table 5.6. Enzymes assays of bacteroid extracts obtained from alfalfa plants inoculated with *S. meliloti* strains overexpressing the malic enzymes.

Strain	Genotype	NAD^+-dependent activity (nmoles/min/mg)[a]	% activity relative to wild type	$NADP^+$-dependent activity (nmoles/min/mg)[a]	% activity relative to wild type	MDH activity (nmoles/min /mg)[b]
Rm1021	wild type	114.3 +/- 2.0	65	ND	-	1520 +/- 28
RmK296	Rm1021, *dme*	657.6 +/- 3.2	375	27.3 +/- 2.4	569	1534 +/- 14
RmK297	Rm1021, *tme*	133.2 +/- 1.7	76	20.2 +/- 5.4	421	1376 +/- 7
RmK298	Rm1021 pBBR1MCS-5	175.2 +/- 4.0	100	4.8 +/-0	100	1831 +/- 15

[a] Specific activity is expressed as nmoles of pyruvate formed /minute/mg protein with the mean +/- standard error of triplicate samples.

[b] Specific activity is expressed as nmoles NADH formed /minute/mg protein with the mean +/- standard error of triplicate samples

ND none detected

compared to wild type Rm1021 bacteroids and strain RmK298 carrying pBBR1MCS-5 (Table 5.6). Both RmK296 and RmK297 bacteroid samples show elevated levels of TME approximately 4-5 fold higher than wild type bacteroids. In RmK297 this is due to the over expression of *tme* from the pTH599 plasmid. In RmK296, the producing elevated levels of DME (which can then utilize $NADP^+$) account for the apparent increased TME activity. Malate dehydrogenase levels among the different bacteroid extracts remained relatively constant (Table 5.6) despite the increase in DME or TME.

Discussion

Previous data from our laboratory indicated that *tme* is not required for symbiotic nitrogen fixation (Driscoll and Finan, 1996). This is based upon the fact that *tme* deficient *S. meliloti* strains are capable of inducing nodules and producing alfalfa plants that are indistinguishable from wild type inoculated plants. In free-living cells *tme* expression is not dependent on carbon source availability as *tme::lacZ* gene fusion studies reveal that *tme* is active in the presence of complex media LBmc as well as glucose, malate, and succinate (Driscoll and Finan, 1996). Previous attempts to determine *tme* expression levels and TME amounts in bacteroids have met with limited success. Assays carried out with bacteroid extracts showed approximately 25 nmoles/min/mg $NADP^+$-dependent malic enzyme activity which when compared to TME activity levels in free-living cells indicated that TME levels were 20% in bacteroids relative to free-living cells (Driscoll and Finan, 1996). This estimate is highly suspect since DME is known to utilize $NADP^+$ as a cofactor and in light of the fact that the *tme* deficient strain RmG927 gave an $NADP^+$-dependent activity of 22 nmoles/min/mg in the

same experiment it seems clear that the activity detected was not due to TME but rather DME. Therefore relying upon enzyme assay data with $NADP^+$ as a cofactor has limited sensitivity as both DME and TME will contribute to the formation of pyruvate. A second attempt to measure *tme* activity in bacteroids centered around β-galactosidase fusions to *tme*. These experiments showed that *tme* was expressed at 20% relative to free-living cells (Driscoll and Finan, 1997). The reporter system employed utilized the plasmid pRMT100 that carried a *tme*-β-galactosidase fusion. Therefore loss of plasmid during bacteroid formation and copy number problems are easily envisioned and both would lead to inaccuracies in the calculations and estimates for *tme* activity in bacteroids. Therefore a new approach was adopted in order to gain a more accurate estimate of *tme* activity in bacteroids and amounts of TME present.

Quantification of the malic enzymes in free-living cells and bacteroids confirm previous observations that TME levels in the bacteroid are approximately 20% that of free-living cells (Driscoll and Finan, 1996) and that *tme* expression is reduced in bacteroids (Driscoll and Finan, 1997). By estimating the amounts of TME in bacteroids we have observed that TME levels go from approximately 5 ng/μg total protein in free-living cells to approximately 1 ng/μg total protein in bacteroids which represent a drop of 80%. In addition the quantification of TME supports the observations obtained with NAD^+-dependent pyruvate formation assays with the *ptme-dme* construct that TME levels are lower in free-living cells as compared to DME levels (approximately 70%). Western blots show that DME is present at 6.8 ng/μg total protein while TME is present at 4.7 ng/μg total protein, or approximately 69% that of DME. In contrast to TME, the

relative levels of DME double when *S. meliloti* free-living cells become bacteroids. Since *dme* appears to be constitutively expressed (Driscoll and Finan, 1993, Driscoll and Finan, 1997) it is unlikely that *dme* expression levels increase in bacteroids relative to free-living cells but rather it is do to a decrease in protein production in the bacteroid.

Plant tests with strains expressing the *ptme-dme* construct showed that levels of acetylene reduction activity and associated plant dry weights were reduced to approximately 20% of the levels measured for plants inoculated with the wild type strain Rm1021. NAD^+-dependent pyruvate formation assays and western blot analysis revealed that the *ptme-dme* strains had reduced DME activity (17-25%) relative to wild type bacteroids. The values obtained correlate well with the previous observation that *tme* expression is reduced during symbiotic conditions (Driscoll and Finan, 1996, Driscoll and Finan, 1997). These results would indicate that a certain DME concentration in bacteroids is crucial for symbiotic N_2 fixation phenotype and that altering levels of DME directly affects nitrogen fixation ability. These results also delineate the region of the *tme* promoter responsible for the repression phenomena seen in bacteroids. The *ptme-dme* construct employed in these experiments was made up of 106 bp upstream of the *tme* gene relative to the translational start site. This region includes 59 bp upstream from the previously identified *tme* transcriptional start site (Mitsch *et al.*, 1998, Chapter 3). An examination of this region did not reveal any conserved residue motifs associated with down regulation of the actual genes during symbiosis such as FixK (Waelkens *et al.*, 1992) suggesting that the regulation of the *tme* gene is under the control of a as yet

undescribed system and may involve an activator or sigma factor only present in free-living cells.

The differential activity of two genes encoding similar proteins with identical activity has been noted previously for members of the *Rhizobiacea*. *B. japonicum* maintains two genes for glutamine synthesis, *glnA* and *glnII*. *glnA* is not affected by nitrogen limitation while *glnII* is regulated in response to nitrogen availability, this differential response assists in gene expression and bacterial response to environmental conditions (Carlson *et al.*, 1987). A similar system may be present with TME and DME with the former repressed during symbiosis while the latter gene expression is maintained. It may be that TME activity is not required within the senescent bacteroid. The $NADP^+$-dependent enzyme of *E. coli* is believed to be involved in anabolic processes within the cell such as producing pyruvate for amino acid synthesis or the generation of reduced cofactor for fatty acid synthesis (Sanwal, 1970a). If this supposition is extended to *S. meliloti* it is clear that this function would not be required in the senescent bacteroid and may even impede the action of the symbiotically essential DME. This would explain the down regulation of *tme* during the conversion from a free-living to a bacteroid condition.

One of the major goals of research in symbiotic nitrogen fixation is to increase nitrogen fixation in order to increase plant growth. Towards that end several avenues of research have been pursued in order to identify the rate limiting step in symbiotic nitrogen fixation. This step could include the import of carbon for energy production, metabolism of this carbon source to yield the energy required for nitrogen fixation, and

the amount of reductant available for nitrogen fixation. Alternatively, and more realistically, it may be a combination of all of these events. The malic enzyme represents an unusual lynch pin for carbon metabolism and TCA cycle activity as it utilizes a C_4-dicarboxylic acid donated by the plant host and diverts it from general metabolism in order to produce pyruvate to maintain the TCA cycle. Thus, the malic enzyme is a crucial step in controlling carbon uptake, TCA cycle activity, and since it generates a reduced cofactor it may also control levels of reductant in the bacteroid. It is therefore an excellent candidate for controlling the levels of nitrogen fixation in symbiosis.

We wished to ascertain if over-production of DME would lead to elevated levels of nitrogen fixation or increased plant growth. To create strains capable of over producing DME, we employed the gentamycin resistant broad host range high copy number plasmid pBRR1MCS-5, capable of replicating in both *E. coli* and *S. meliloti* (Kovach *et al.*, 1995), was used to increase the copy number of *dme* and *tme*. Enzyme assays on extracts from free-living *S. meliloti* cells and bacteroids revealed elevated levels of DME and TME enzyme activity (5 and 29 fold respectively compared to wild type cells). Plant assays revealed that these strains neither increased nitrogenase activity nor plant dry weights were appreciably increased, indicating that an increase in DME activity was insufficient to dramatically increase nitrogen fixation. It is conceivable that with a K_m for malate of 9.4mM, the activity of DME is not governed by the amount of protein present but rather the amount of substrate available however previous results with the truncated form of DME lacking the C-terminal region revealed that this protein was capable of inducing plants indistinguishable from alfalfa plants inoculated with wild type

S. meliloti cells (Cowie, 1998, Appendix 1). The kinetic characteristics of this truncated DME protein revealed that it had a K_m of 36 mM for malate that is 4 times higher than the intact DME (Voegele, unpublished results. Therefore, since this truncated protein is able to induce wild type levels of nitrogenase activity it is plausible that the concentration of malate within the bacteroid is at least 36 mM. One other observation we can make is regarding the levels of TME activity in RmK297. These levels are elevated due to the increase in gene copy number but the increase is not as substantial as that seen with free-living cells relative to wild type S. *meliloti* cells. This would indicate that the repression of *tme* is still occurring in bacteroids and that the increase in gene copy number and the concomitant increase of the *tme* promoter did not result in a titration of a factor responsible for inhibiting *tme* activity. This could mean that the factor responsible for repressing *tme* activity is in excess in the bacteroid, it is a physical constant present during symbiosis such as depressed oxygen levels, or that *tme* is activated by a factor in free living which is absent in bacteroids.

There have been several attempts to increase nitrogenase activity of bacteria. The *dctA* gene itself was overexpressed in *S. meliloti* by placing it downstream from a *Salmonella typhimurium* promoter that resulted in constitutive expression of the gene. This construct did not induce an increase in plant dry weight but did elevate the acetylene reduction activity 31-60% relative to positive controls (Rastogi *et al.*, 1991). Other studies have focused upon overproducing the *rnf* operon that is believed to be responsible for producing the source of reductant for the nitrogenase enzyme in *Rhodobacter capsulatus*. By increasing the copy number of this operon and observing a concomitant

increase in the membrane associated iron containing proteins RnfB and RnfC an increase in nitrogen fixation of 50 to 100% relative to wild type cells was obtained (Jeong and Jouanneau, 2000). Expression of an *ntrC* mutant of *Rhizobium etli* resulted in the production of symbiotic specific cbb_3 terminal oxidases in free-living cells indicating a derepression in the free living state. When the *fixNOQP* operon of *B. japonicum* was expressed in conjunction with this *ntrC* mutant in *R. etli* the rates of nitrogen fixation *in planta* increased two fold relative to wild type inoculated plants (Soberon *et al.*, 1999). In addition to these laboratory results field tests have shown that overexpression of both *nifA*, the positive regulator of the nitrogenase regulon, and the *dctA* operon result in increases in alfalfa yields under certain field conditions (Bosworth *et al.*, 1994).

Chapter 6

Expression of the *sfcA* malic enzyme gene of *E. coli* in *S. meliloti*

Abstract

The NAD(P)$^+$-dependent malic enzyme (DME) activity is required for symbiotic N_2-fixation by *S. meliloti* in alfalfa root nodules. We have previously shown that the C-terminal PTA like region can be removed from the protein without loss of malic enzyme activity indicating that this region is not essential for the conversion of malate to pyruvate. This observation did not reveal if the C-terminal domain is required for symbiotic nitrogen fixation. In order to determine if the PTA like domain is required for symbiotic nitrogen fixation an analogous malic enzyme lacking the C-terminal domain was expressed in bacteroids. The *sfcA* gene codes for the NAD$^+$-dependent malic enzyme from *E. coli* yet it lacks the PTA like domain associated with other alpha α-proteobacterial malic enzymes previously identified. The *dme* structural gene was replaced by the *sfcA* structural gene such that *sfcA* expression was driven from the *dme* promoter (designated *pdme-sfcA*). The resulting construct was recombined into the chromosome of *S. meliloti dme* mutant strains. Analysis of these recombinants revealed that the *pdme-sfcA* chimer expressed *E. coli* NAD(P)$^+$-dependent malic enzyme activity in *S. meliloti* and that the resulting enzyme activity restored almost complete symbiotic N_2-fixation activity in the *S. meliloti dme* mutant strains. Thus the C-terminal PTA-like domain of DME is not required for N_2-fixation.

Materials and Methods

See Chapter 2 for all materials and methods. Bacterial strains and plasmids utilized are listed in Table 2.1. The primers 5'-GAA ACA GAG CAT GCA ACC AAA AAC AAA AAA AC-3' and 5'-CTC TCA TCC GCC AAA ACA GCC-3' were used to amplify *sfcA* from the plasmid pMEE1 generously donated by Dr. Mark Donnely from the Environmental research division, Argonne National Laboratory, Argonne Illinois. Bold type indicates the *Sph*I restriction site introduced in the PCR fragment. The PCR reaction was carried out according to the procedure outlined in Chapter 2 using pMEE1 as template with thirty five cycles consisting of 1 minute at 94°C, 1 minute annealing at 55°C, and 3 minutes extension at 72°C. The resulting 1.8kb fragment was digested with *Sph*I and *Pst*I and ligated to the vector pTH408. This ligation replaced the *dme* structural gene of pTH408 with the *sfcA* gene down stream of the *dme* promoter (Figure 6.1). The resulting plasmids were transformed into competent EJ1321 *E. coli* cells. Clones such as pTH512 expressing functional malic enzymes were selected for by plating on minimal media with succinate as the sole carbon source.

To introduce the *pdme-sfcA* construct into the chromosome of *S. meliloti*, the plasmid pUCP30T was utilized. pTH512 was digested with *Hind*III and *Pst*I and the resulting 2.1 kb fragment was inserted into pUCP30T DNA also digested with *Hind*III and *Pst*I (Figure 6.1). The resulting construct, pTH513, was introduced into several *dme*, *tme*, and *dme tme*, mutants through tri-parental matings (Figure 6.1). Strain RmH194 (*pckA*1::Tn3HoHo, *pod*-1, *dme*-1::Tn5, *tme*-4::ΩSp) is a *S. meliloti* derivative that is unable to utilize C_4-dicarboxylic acids as a sole carbon source as it is malic enzyme

Figure 6.1. Schematic showing PCR and cloning strategy employed in the generation of *S. meliloti* strains expressing the *sfcA* gene. Dotted arrows indicate primers utilized to generate *sfcA* gene. Open arrow represents *sfcA* gene region indicating direction of transcription. Hatched box represents the *dme* promoter region. Black box indicates gentamycin resistance gene while grey box represents origin of transfer. Black triangle represents transposon insertion in the *dme* gene of the *S. meliloti* chromosome. Dotted lines indicate region of homologous recombination. Restriction enzymes relevant to the constructions are indicated.

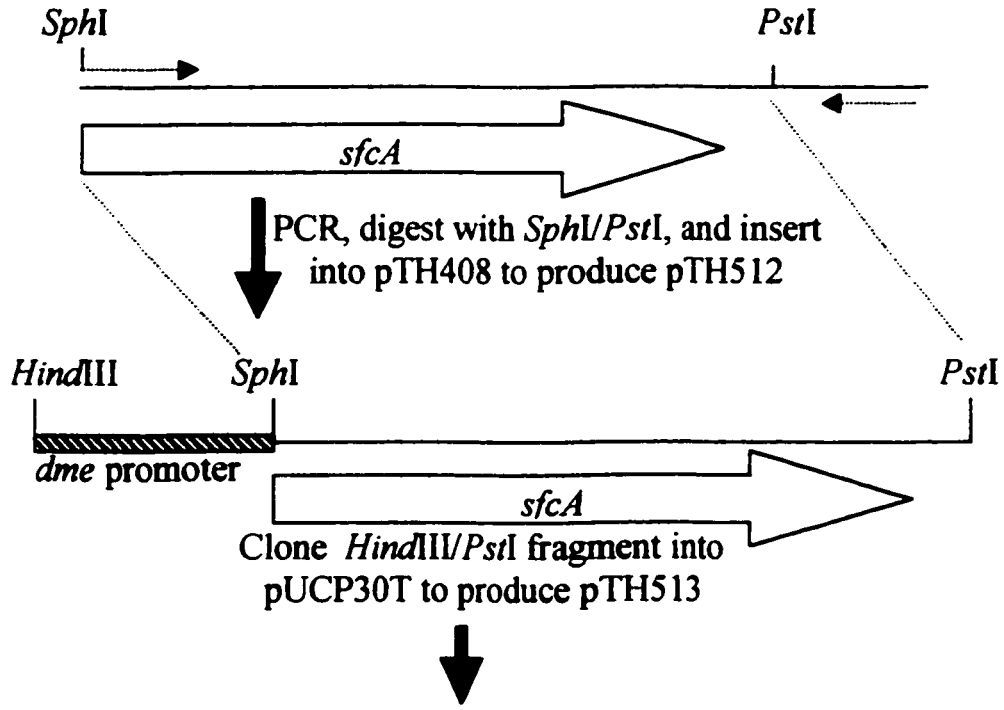

Recombination of pTH513 into the chromosome of *S. meliloti* *dme*::Tn5 via single crossover at the *dme* promoter region

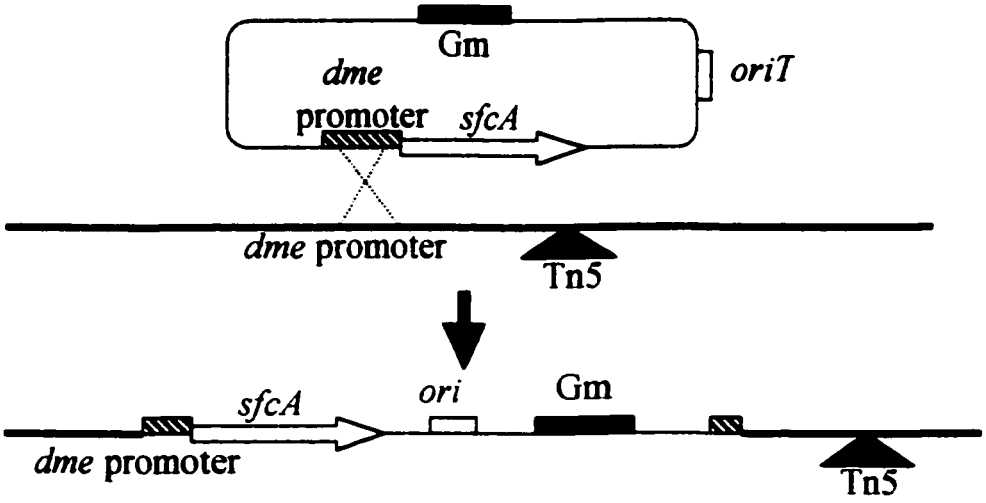

deficient and carries an insertion in the *pckA* gene rendering it unable to produce pyruvate from glucose. Therefore this strain can only utilize the TCA cycle for metabolism with a sugar as the primary metabolite to generate pyruvate. Plasmid pTH513 was introduced into strain RmH194 resulting in the generation of RmK211 and this strain was able to utilize succinate as the sole carbon source indicating that the SfcA protein is indeed functional in *S. meliloti* cells. To verify that insertion occurred at the *dme* promoter region transductions were carried out with *dme*::Tn*5* donor strains carrying *sfcA* (pTH513) recombined into the genome of *S. meliloti*. Lysates were prepared and used in association with wild type Rm1021. Of the resulting colonies isolated on LBGm plates replica plating of 30 colonies onto LBNm plates showed co-transduction between the neomycin resistance marker of the *dme* mutation and the gentamycin resistance marker of the pUCP30T insertion in all 30 colonies. This showed that the pUCP30T insertions occurred at the *dme* gene locus. No linkage was found between the spectinomycin and gentamycin resistance markers indicating that there is no linkage with the *tme* gene for strains RmK217 and RmK218.

Results

Sequence analysis and comparison of *sfcA* with the *dme* gene of *S. meliloti*

The malic enzymes of *S. meliloti* have an unusual chimeric structure with the N-terminal region bearing homology to other prokaryotic malic enzymes while the C-terminal region shows similarity to phosphotransacetylase enzymes. This chimeric nature as well as the shear size of these polypeptides makes structural comparisons

difficult and misleading. For these reasons only the N-terminal malic enzyme region of DME was compared to SfcA (Figure 6.2) and revealed 25% identity and 35% similarity between the two proteins. This low level of homology is offset by the fact that the two proteins share some of the conserved regions indicative of malic enzymes (Chapter 3, regions A to H). Region A is believed to be implicated in substrate binding as chemical modification experiments showed that the conserved tyrosine residue is required to bind L-malate (Viljoen *et al.*, 1994, Hsu, 1982). Region B and E contain the characteristic glycine and alanine rich regions indicative of the Rossman fold motif as well as the lysine residues required to bind the nicotinamide cofactor (Hanukoglu and Gutfinger, 1989, Wierenga *et al.*, 1986, Scrutton *et al.*, 1990). Region D has a characteristic motif, VFHDDQ that is characteristic of all prokaryotic malic enzymes and has reduced similarity in SfcA. The remaining regions F, G, and H have reduced similarity and lack the conserved amino acids found among prokaryotic malic enzymes (Chapter 3, Kobayashi *et al.*, 1989, Kawai *et al.*, 1996, Mitsch *et al.*, 1998).

PCR production of *sfcA* and complementation of EJ1321 cells

Enzyme assays and non-denaturing gels were utilized to verify that the *E. coli* malic enzyme was being produced in strain EcJ386, an EJ1321 derivative capable of growing on M9 with succinate as the sole carbon source. The non-denaturing gel showed that a protein significantly smaller than DME was being produced (Figure 6.3) which is consistent with the fact that DME is approximately 680 kDa (Mitsch *et al.*, 1998) while SfcA is approximately 203 kDa (Yamaguchi *et al.*, 1973). Furthermore the product present in EcJ386 was the same size as the protein product generated from EcJ337 that is

Figure 6.2. Alignment of the SfcA malic enzyme of *E. coli* and the N-terminal region of DME from *S. meliloti*. * and . denote identical and similar amino acid residues respectively. Underlined regions are eight highly conserved domains of prokaryotic malic enzymes and amino acid residues in bold type have been implicated in enzyme function (Chapter 3). Numbers to the right are amino acid residues of the respective proteins.

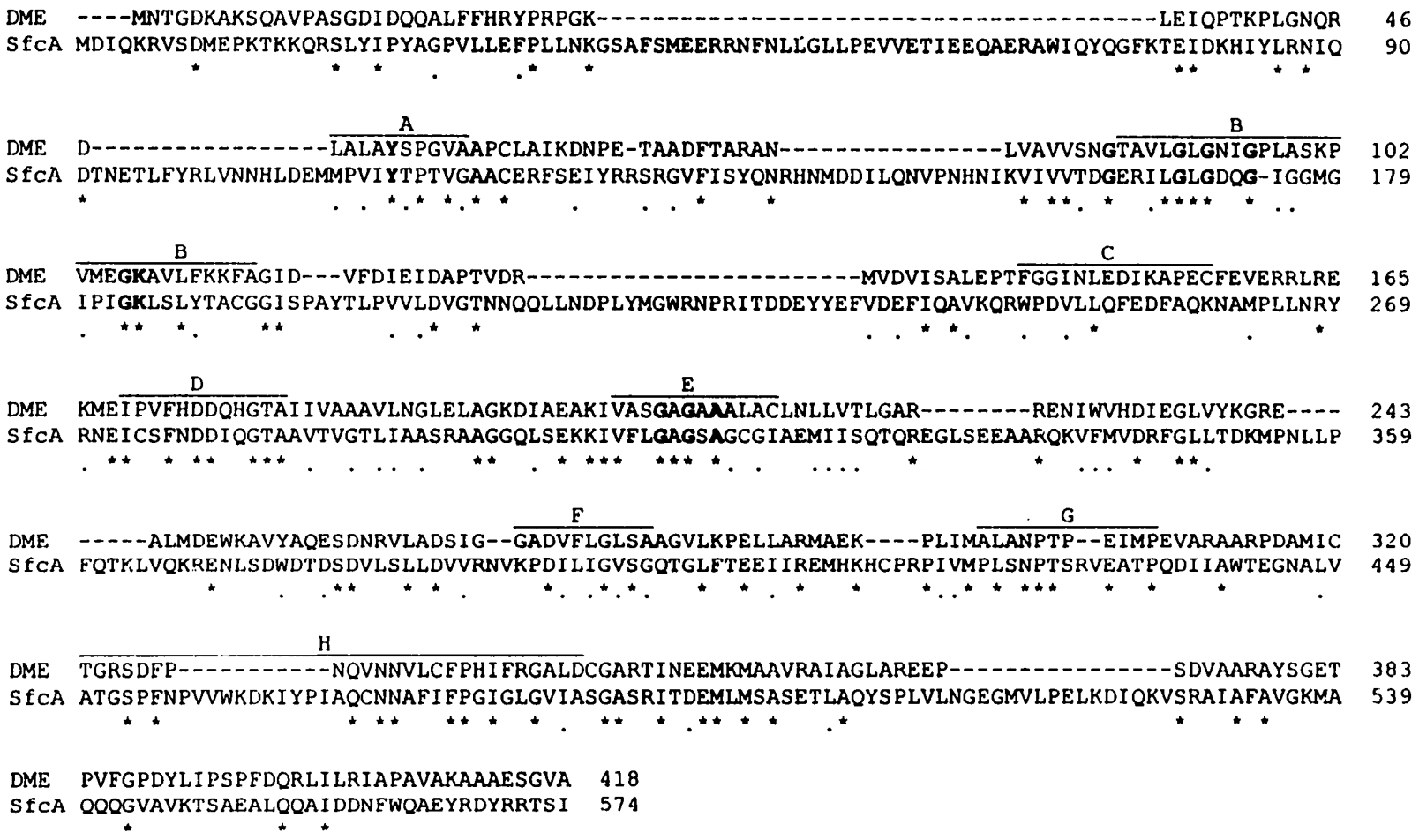
DME ----MNTGDKAKSQAVPASGDIDQQALFFHRYPRPGK----------LEIQPTKPLGNQR 46
SfcA MDIQKRVSDMEPKTKKQRSLYIPYAGPVLLEFPLLNKGSAFSMEERRNFNLLGLLPEVVETIEEQAERAWIQYQGFKTEIDKHIYLRNIQ 90
A
B
DME D----------LALAYSPGVAAPCLAIKDNPE-TAADFTARAN----------LVAVVSNGTAVLGLGNIGPLASKP 102
SfcA DTNETLFYRLVNNHLDEMMPVIYTPTVGAACERFSEIYRRSRGVFISYQNRHNMDDILQNVPNHNIKVIVVTDGERILGLGDQG-IGGMG 179
B
C
DME VMEGKAVLFKKFAGID---VFDIEIDAPTVDR----------MVDVISALEPTFGGINLEDIKAPECFEVERRLRE 165
SfcA IPIGKLSLYTACGGISPAYTLPVVLDVGTNNQQLLNDPLYMGWRNPRITDDEYYEFVDEFIQAVKQRWPDVLLQFEDFAQKNAMPLLNRY 269
D
E
DME KMEIPVFHDDQHGTAIIVAAAVLNGLELAGKDIAEAKIVASGAGAAALACLNLLVTLGAR--------RENIWVHDIEGLVYKGRE---- 243
SfcA RNEICSFNDDIQGTAAVTVGTLIAASRAAGGQLSEKKIVFLGAGSAGCGIAEMIISQTQREGLSEEAARQKVFMVDRFGLLTDKMPNLLP 359
F
G
DME -----ALMDEWKAVYAQESDNRVLADSIG--GADVFLGLSAAGVLKPELLARMAEK----PLIMALANPTP--EIMPEVARAARPDAMIC 320
SfcA FQTKLVQKRENLSDWDTDSDVLSLLDVVRNVKPDILIGVSGQTGLFTEEIIREMHKHCPRPIVMPLSNPTSRVEATPQDIIAWTEGNALV 449
H
DME TGRSDFP----------NQVNNVLCFPHIFRGALDCGARTINEEMKMAAVRAIAGLAREEP----------SDVAARAYSGET 383
SfcA ATGSPFNPVVWKDKIYPIAQCNNAFIFPGIGLGVIASGASRITDEMLMSASETLAQYSPLVLNGEGMVLPELKDIQKVSRAIAFAVGKMA 539
DME PVFGPDYLIPSPFDQRLILRIAPAVAKAAAESGVA 418
SfcA QQQGVAVKTSAEALQQAIDDNFWQAEYRDYRRTSI 574

Table 6.1. Enzyme assays on *E. coli* EJ1321 extracts overexpressing the *E. coli sfcA* gene and the malic enzymes of *S. meliloti*.

Strain	Genotype	NAD^+-dependent activity (nmoles/min/mg)[a]	$NADP^+$-dependent activity (nmoles/min/mg)[a]	MDH activity (nmoles/min/mg)[b]
EcG456	EJ1321 (pTH139; *dme*)	386.6+/-11.6	131.4+/-1.7	1042+/-5
EcJ202	EJ1321 (pTH392; *tme*)	48.3+/-0.9	485.2+/-6.3	1056+/-13
EcJ386	EJ1321 (pTH512; *sfcA*)	760.2+/-10.4	64.2+/-1.6	862+/-18
EJ1321	*dme-tme-*	53.6+/-2.3	1.3+/-0.1	969+/-30

[a] Specific activity is expressed as nmoles of pyruvate formed /minute/mg protein with the mean +/- standard error of triplicate samples.

[b] Specific activity is expressed as nmoles NADH formed /minute/mg protein with the mean +/- standard error of triplicate samples

Figure 6.3. Non-denaturing 7% polyacrylamide gel showing expression of *sfcA* in EJ1321 *E. coli* extracts. 30 μgs of protein was loaded per sample and the gel was stained to detect presence of NAD^+-dependent malic enzyme activity. Positions of DME and SfcA are indicated. Strains utilized are EcG456 (EJ1321, pTH139 (*dme*)), EJ1321, EcJ386 (EJ1321, pTH512 (*pdme-sfcA*)), EcJ337 (EJ1321, pMEE1 (*sfcA*))

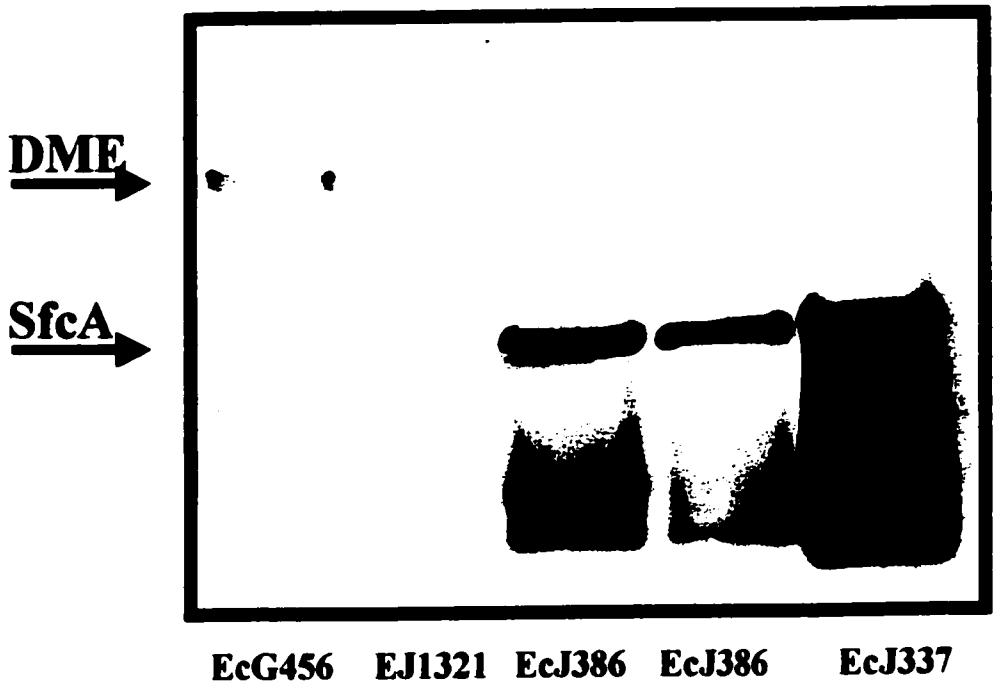
DME
SfcA
EcG456
EJ1321
EcJ386
EcJ386
EcJ337

a EJ1321 derivative expressing pMEE1 (Figure 6.3). Enzyme assays revealed that the complementing plasmid was producing an enzyme that had approximately double the activity as compared to EJ1321 cells expressing the DME protein (Table 6.1). Some activity was also detected with $NADP^+$ as cofactor, approximately 8% relative to activity with NAD^+ (Table 6.1), which is consistent with previous observations (Yamaguchi *et al.*, 1973) and its enzyme designation [EC 1.1.1.38].

Expression of the *sfcA* gene in *S. meliloti* cells

Enzyme assays on extracts from LBmc grown cells supported the observations with RmK211 that the SfcA protein was functional in *S. meliloti* (Table 6.2). In strains lacking *dme*, expressing *sfcA* under control of the *dme* promoter results in NAD dependent pyruvate formation activity from 1.5-2 fold relative to wild type. When *sfcA* was expressed in strains carrying the wild type *dme* gene (strains RmK219 and RmK218) there was an additive effect resulting in increased enzyme activity as detected by NAD^+ dependent pyruvate formation assays (Table 6.2). This trend was maintained in the TME deficient strain RmG995 where the introduction of *sfcA* under control of the *dme* promoter results in levels of NAD^+-dependent pyruvate formation 2 fold higher than wild type cells (Table 6.2). Thus the presence of SfcA results in increased NAD^+-dependent pyruvate formation activity, which is consistent with our expectation that *sfcA* would be expressed from the *dme* promoter. Native PAGE gels stained for NAD^+-dependent malic enzyme activity revealed that the SfcA protein was present in the free-living cell extracts as identified as a smaller band of activity relative to the large DME band (Figure 6.4). In addition a breakdown product corresponding to a dimer of DME was also detected in

Table 6.2. Enzyme assays on extracts obtained from *S. meliloti* strains expressing the *sfcA* gene.

Strain	Genotype	NAD^+-dependent activity (nmoles/min/mg)[a]	% activity relative to wild type	MDH activity (nmoles/min/mg)[b]
Rm1021	wild type	64.1 +/- 1.3	100	543+/-11
RmK219	wild type, Φ*pdme-sfcA*	113.6 +/- 10.6	177	612+/-17
RmG455	*dme3*	25.7 +/- 14.9	40	713+/-20
RmK215	RmG455, Φ*pdme-sfcA*	122.1 +/- 19.7	191	713+/-44
RmG456	*dme1*	29.0 +/- 8.5	45	717+/-16
RmK216	RmG456, Φ*pdme-sfcA*	98.6 +/- 9.8	154	598+/-4
RmG994	*dme3, tme4*	30.2 +/- 3.7	47	722+/-37
RmK217	RmG994, Φ*pdme-sfcA*	84.7 +/- 13.1	175	590+/-22
RmG995	*tme4*	67.1 +/- 3.2	105	583+/-14
RmK218	RmG995, Φ*pdme-sfcA*	135.2 +/- 11.5	211	722+/-37

[a] Specific activity is expressed as nmoles of pyruvate formed /minute/mg protein with the mean +/- standard error of triplicate samples.

[b] Specific activity is expressed as nmoles NADH formed /minute/mg protein with the mean +/- standard error of triplicate samples

Figure 6.4. Non-denaturing 7% polyacrylamide gel showing expression of *sfcA* in *S. meliloti* extracts. 30 μgs of protein was loaded per sample and the gel was stained to detect presence of NAD^+-dependent malic enzyme activity. Positions of DME and SfcA are indicated. Chevron arrow indicates position of dimers of DME.

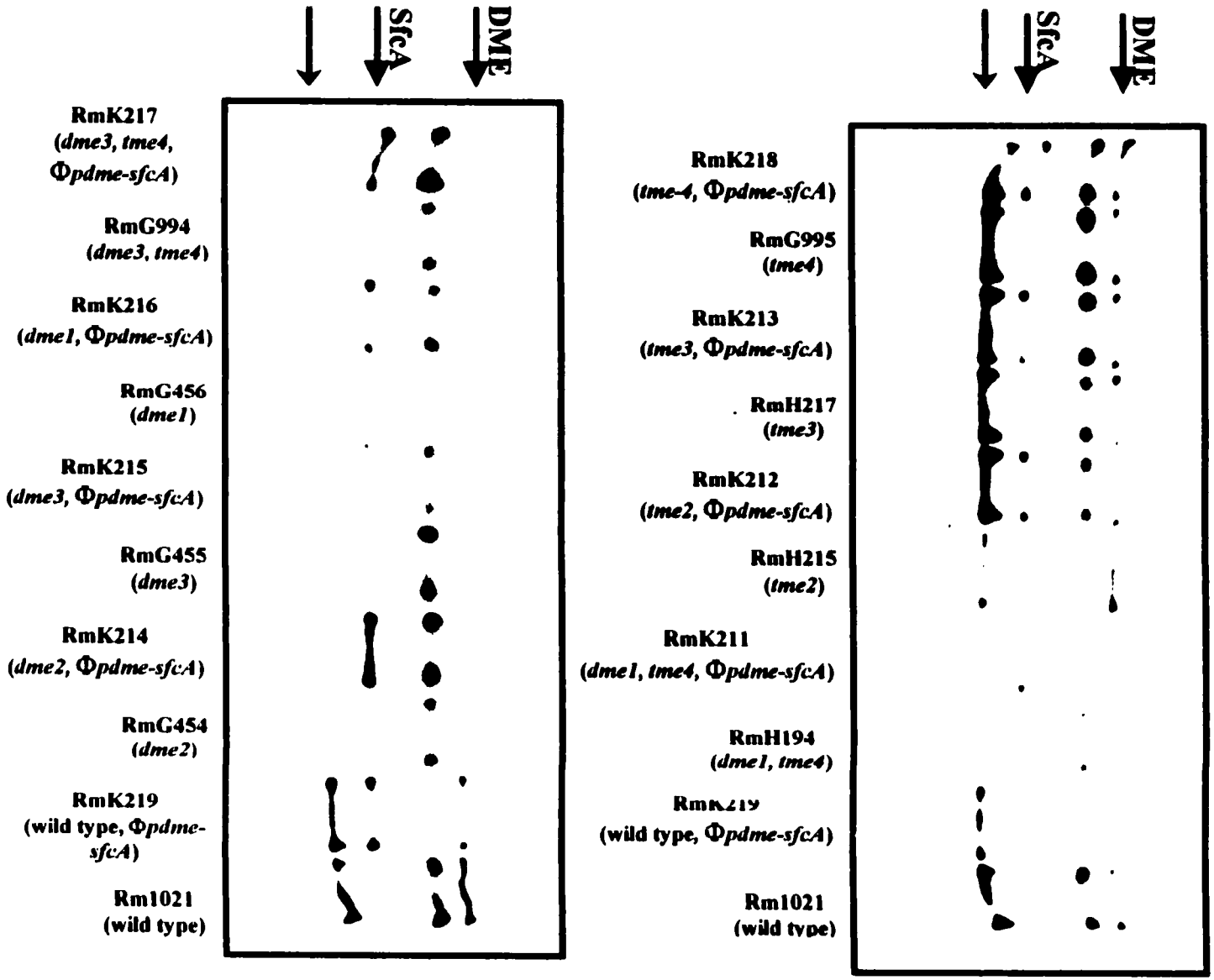
SfcA
DME
RmK217 (dme3, tme4, Φpdme-sfcA)
RmG994 (dme3, tme4)
RmK216 (dme1, Φpdme-sfcA)
RmG456 (dme1)
RmK215 (dme3, Φpdme-sfcA)
RmG455 (dme3)
RmK214 (dme2, Φpdme-sfcA)
RmG454 (dme2)
RmK219 (wild type, Φpdme-sfcA)
Rm1021 (wild type)
SfcA
DME
RmK218 (tme4, Φpdme-sfcA)
RmG995 (tme4)
RmK213 (tme3, Φpdme-sfcA)
RmH217 (tme3)
RmK212 (tme2, Φpdme-sfcA)
RmH215 (tme2)
RmK211 (dme1, tme4, Φpdme-sfcA)
RmH194 (dme1, tme4)
(wild type, Φpdme-sfcA)
Rm1021 (wild type)

samples expressing *dme*. Non-specific activity was detected in native PAGE gels and this may be due to a nonspecific dehydrogenase previously described in *S. meliloti* (Charles *et al.*, 1990).

Expression of the *sfcA* gene in *S. meliloti* bacteroids

Strains expressing the *sfcA* gene from the *dme* promoter were utilized in plant tests to assess the ability of the SfcA protein to compensate for the loss of DME in *S. meliloti* mutant strains. After 4 weeks the plants inoculated with *S. meliloti dme* deficient strains expressing *sfcA* were larger and greener than plants inoculated with the *dme* mutant strains or the uninoculated negative control plants (Figure 6.5). Acetylene reduction assays carried out on plants inoculated with *S. meliloti dme*$^-$ strains expressing *sfcA* revealed that these plants had nitrogenase activity that approached and in some cases exceeded wild type levels (Table 6.3). Despite the apparent rise in acetylene reduction activity, the plant dry weights show that strains expressing *sfcA* (RmK215-RmK217) are comparable to wild type inoculated plants with 65%-84% the mass of the positive control (Table 6.3) and t-tests show that there is no statistical significance in the variation. When *dme* and *sfcA* are co-expressed there appears to be an additive effect with plant dry weights and acetylene reduction activity of these strains (RmK218 and RmK219) exceeding the wild type inoculated controls (Table 6.3) however only for RmK218 does t-test results show that the difference in plant dry weight and acetylene reduction assay results between RmK218 and wild type inoculated plants is statistically significant however the importance of this is not clear. T-test analysis for RmK219 shows that the difference in plant dry weight and acetylene reduction assay are not statistically

Figure 6.5. Photograph of alfalfa plants inoculated with various *S. meliloti* strains expressing the *sfcA* gene under control of the *dme* promoter.

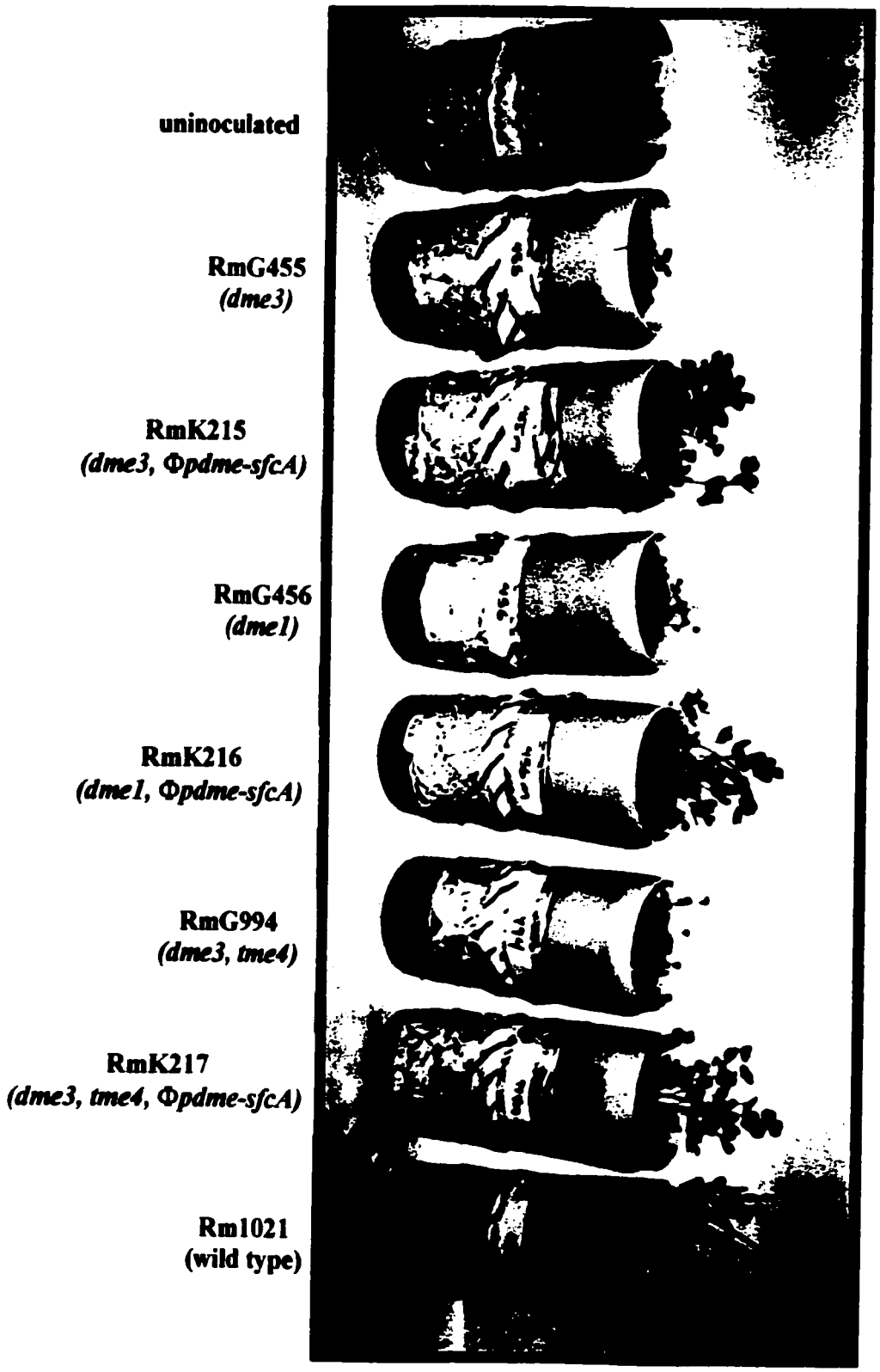
uninoculated
RmG455
(dme3)
RmK215
(dme3, Φpdme-sfcA)
RmG456
(dme1)
RmK216
(dme1, Φpdme-sfcA)
RmG994
(dme3, tme4)
RmK217
(dme3, tme4, Φpdme-sfcA)
Rm1021
(wild type)

Table 6.3. Plant results from alfalfa plants inoculated with various *S. meliloti* strains expressing the *sfcA* gene under control of the *dme* promoter.

Strain	Genotype	ARA (nmoles/min/plant)[a]	% ARA relative to wild type	Plant dry weight (mg)[b]	% Plant dry weight relative to wild type
Rm1021	wild type	342 +/- 59	100	40.6 +/- 3.7	100
RmK219	wild type, Φ*pdme-sfcA*	614 +/- 213	179	59.4 +/- 11.2	146
RmG455	*dme3*	5 +/- 1	2	7.4 +/- 0.6	18
RmK215	RmG455, Φ*pdme-sfcA*	447 +/- 23	131	34.3 +/- 3.2	84
RmG456	*dme1*	6 +/- 1	2	7.1 +/- 1.0	18
RmK216	RmG456, Φ*pdme-sfcA*	691 +/- 82	202	33.9 +/- 6.6	83
RmG994	*dme3, tme4*	ND	ND	8.8 +/- 0.6	22
RmK217	RmG994, Φ*pdme-sfcA*	621 +/- 163	182	26.3 +/- 1.4	65
RmG995	*tme4*	445 +/- 55	130	45.9 +/- 4.1	113
RmK218	RmG995, Φ*pdme-sfcA*	850 +/- 112	248	50.6 +/- 3.5	125
uninoculated	-	-	-	6.3 +/- .4	16

[a] Acetylene reduction activity is expressed as nmoles of ethylene produced and is presented as mean of triplicate samples containing three root systems each +/- standard error.

[b] Plant dry weight is expressed as mean of triplicate pots containing 7-10 plants each +/- standard error.

ND none detected.

significant relative to wild type inoculated plants. Enzyme assays conducted on bacteroids isolated from these strains revealed that bacteroids expressing *sfcA* had approximately half the NAD^+-dependent malic enzyme activity relative to wild type cells (Table 6.4). When *dme* and *sfcA* were co-expressed the bacteroids had 72 % NAD^+-dependent malic enzyme activity relative to wild type bacteroids (Table 6.4). This would indicate that the SfcA is less active or more unstable in bacteroids than it is in free-living cells but the amount of protein present is sufficient to maintain the TCA cycle and results in wild type levels of nitrogen fixation and plant dry weight. Native PAGE gels stained for NAD^+-dependent malic enzyme activity revealed that the SfcA protein was present in the bacteroid extracts and that no DME was present in these strains (Figure 6.6), thus the symbiotic N_2 fixation phenotype observed was due to expression of *sfcA* and not due to cross contamination with *dme* expressing *S. meliloti* strains. In addition a breakdown product corresponding to a dimer of DME was also detected in samples expressing *dme*. Non-specific activity was detected in native PAGE gels and this may be due to a nonspecific dehydrogenase previously described in *S. meliloti* (Charles *et al.*, 1990).

Discussion

The malic enzymes of *E. coli* have been studied for several decades with the NAD^+-dependent enzyme first identified by Katsuki and colleagues in 1967. The amino acid composition of the NAD^+-dependent malic enzyme was first obtained by Yamaguchi *et al.* in 1973 and the first record of any DNA sequence was in 1990 when Mahajan and colleagues reported a partial sequence associated with the *recE* gene that showed homology to eukaryotic malic enzymes and showed 83% similarity to rat and mouse

Table 6.4. Enzyme assays carried out on bacteroid extracts obtained from nodules produced by alfalfa plants inoculated with various *S. meliloti* strains expressing the *sfcA* gene from the *dme* promoter.

Strain	Genotype	NAD^+-dependent activity (nmoles/min/mg)[a]	% activity relative to wild type	MDH activity (nmoles/min/mg)[b]
Rm1021	wild type	102.8+/-2.4	100	3172+/-68
RmK219	wild type, Φ*pdme-sfcA*	73.8+-0.4	72	2894+/-28
RmG455	*dme3*	8.0/-1.1	8	3401+/-94
RmK215	RmG455, Φ*pdme-sfcA*	50.1+/-0.5	49	2908+/-47
RmG456	*dme1*	7.6+/-1.9	7	3103+/-60
RmK216	RmG456, Φ*pdme-sfcA*	45.5+/-1.1	44	4073+/-214
RmG994	*dme3, tme4*	ND	ND	2251+/-73
RmK217	RmG994, Φ*pdme-sfcA*	60.7+/-1.0	59	2739+/-300
RmG995	*tme4*	94.3+/-2.7	92	3199+/-139
RmK218	RmG995, Φ*pdme-sfcA*	76.5+/-10.9	74	2925+/-55

[a] Specific activity is expressed as nmoles of pyruvate formed /minute/mg protein with the mean of triplicate samples +/- standard error.

[b] Specific activity is expressed as nmoles NADH formed /minute/mg protein with the mean of triplicate samples +/- standard error.

ND none detected

Figure 6.6. Non-denaturing 7% polyacrylamide gel showing expression of *sfcA* in *S. meliloti* bacteroid extracts. 30 μgs of protein was loaded per sample and the gel was stained to detect presence of NAD^+-dependent malic enzyme activity. Positions of DME and SfcA are indicated. Cheveron arrow represents position of DME dimers.

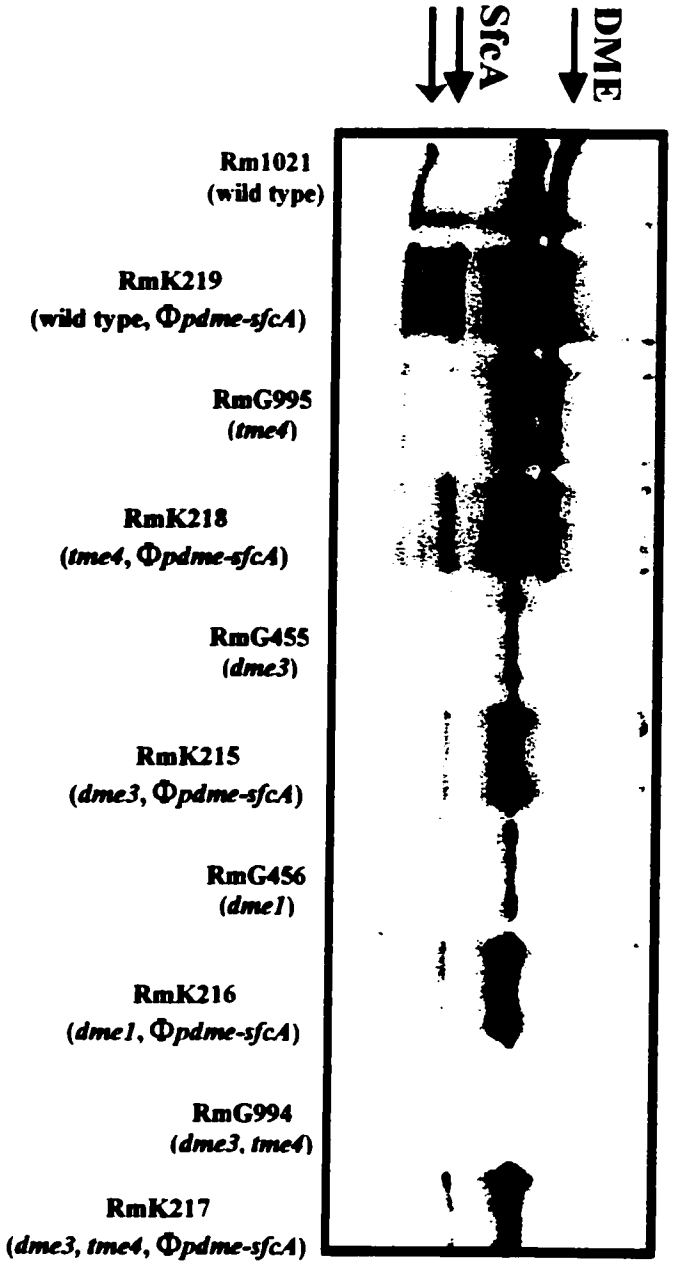
SfcA
DME
Rm1021
(wild type)
RmK219
(wild type, Φpdme-sfcA)
RmG995
(tme4)
RmK218
(tme4, Φpdme-sfcA)
RmG455
(dme3)
RmK215
(dme3, Φpdme-sfcA)
RmG456
(dme1)
RmK216
(dme1, Φpdme-sfcA)
RmG994
(dme3, tme4)
RmK217
(dme3, tme4, Φpdme-sfcA)

$NADP^+$-dependent malic enzymes and was designated *sfcA* (Mahajan *et al.*, 1990). It was not until the completion of the *E. coli* chromosome in 1997 by Blattner and colleagues that the complete open reading frame of *sfcA* was obtained and a deduced size of 574 amino acids with a predicted molecular weight of 64.3 kDa was determined. The SfcA protein of *E. coli* is a unique member of the prokaryotic malic enzyme group. It bears limited homology to other prokaryotic malic enzymes and instead appears more closely related to eukaryotic malic enzymes and the *Bacillus subtilis* malic enzyme Mao2.bs (Mitsch *et al.*, 1998, Boles *et al.*, 1998, Chapter 3)

The subunit molecular weight of SfcA was deduced by Yamaguchi and associates (1973) based upon density gradient centrifugation. The native protein was found to have a molecular weight of 198-203 kDa while the subunit was estimated to be 52.5-57.5 kDa (Yamaguchi *et al.*, 1973) which would indicate that the protein is a holo-tetramer. These estimates were supported by recent results from Stols and Donelly (1997) that estimated the size of the native protein as 260 kDa as determined by column chromatography. Thus, the SfcA protein is much smaller than the malic enzymes of *S. meliloti* in terms of both subunit (82 kDa) and native molecular weight (680 kDa) (Driscol and Finan, 1996, Mitsch *et al.*, 1998, Voegele *et al.*, 1999).

The NAD^+-dependent malic enzyme of *E. coli* has been biochemically characterized by several groups (Katsuki *et al.*, 1967, Sanwal, 1970b, Murai *et al.*, 1971, Yamaguchi *et al.*, 1973, Stols and Donnely, 1997) and its kinetic parameters have been established albeit with some discrepancies. The K_m for the substrate L-malate has been reported as 0.1 mM (Sanwal, 1970b), 0.26 mM (Stols and Donnely, 1997), and 0.4 mM

(Yamaguchi *et al.*, 1973) while The K_m for the NAD^+ cofactor has been estimated to be 23 μM (Sanwal, 1970b) and 55 μM (Yamaguchi *et al.*, 1973). SfcA has also been reported to utilize $NADP^+$ to some extent with 2% activity being detected with the purified enzyme in assays relative to activity with NAD^+ (Yamaguchi *et al.*, 1973) and an estimated K_m of 2.3 mM with $NADP^+$ as cofactor (Yamaguchi *et al.*, 1973). SfcA therefore compares well with DME as the *S. meliloti* malic enzyme has a K_m of 9.4 mM and 89 μM for the substrate and cofactor respectively (Voegele *et al.*, 1999).

SfcA is inhibited by acetyl-CoA and its derivatives such as CoA and malonyl CoA (Sanwal, 1970a). Oxaloacetate (Katsuki *et al.*, 1967), ATP and its derivatives ADP, AMP, as well as GTP, and GDP (Sanwal 1970a) also inhibit it. The enzyme is activated by aspartate (Sanwal, 1970b) as well as the C_4-dicarboxylate malate (Murai *et al.*, 1971). SfcA is therefore similar to the symbiotically essential DME as it is also activated by succinate and fumarate and is negatively affected by acetyl-CoA and oxaloacetate (Driscoll and Finan, 1997, Voegele *et al.*, 1999). This regulation by TCA cycle intermediates may be essential for proper functioning of the TCA cycle during symbiotic nitrogen fixation in order to maintain a pyruvate pool without disrupting the production of oxaloacetate by malate dehydrogenase.

When expressed in *S. meliloti* cells, SfcA is fully functional and is able to compensate for the loss of the native malic enzymes as determined by growth on minimal media with succinate as the sole carbon source and enzyme assays on cell free extracts. When produced in bacteroids, SfcA is capable of offsetting the loss of DME. Acetylene reduction activity is not adversely affected by the replacement of *dme* with *sfcA*

indicating that despite the alteration from a free-living to a bacteroid state the malic enzyme is still functional. Plant dry weights are also not appreciably different with the expression of *sfcA* instead of *dme* as compared to plants inoculated with wild type *S. meliloti* cells.

One hypothesis was that the PTA like region of DME was capable of a second enzymatic function, perhaps even the production of acetyl-CoA since PTA enzymes are responsible for the interconversion of acetyl-CoA and acetyl phosphate [EC 2.3.1.8]. This theoretical activity could be essential for symbiotic nitrogen fixation by allowing for maintenance of the TCA cycle by the production of acetyl-CoA without the production of pyruvate. Experiments with other organisms have shown that enzymes of the TCA cycle form multi enzyme complexes made up of fumarase, malate dehydrogenase, citrate synthase, aconitase and isocitrate dehydrogenase (Barnes and Weitzman, 1986). We hypothesized that the C-terminal region of DME may be required for the malic enzymes participation in this multi enzyme complex and may explain how it is able to function despite the presence of malate dehydrogenase and its high level of activity in *S. meliloti*. By producing SfcA in *S. meliloti* cells and bacteroids we were able to evaluate the necessity of the C-terminal extension. Since the malic enzyme of *E. coli* lacks the PTA like region found in DME it proved to be an effective tool to test several hypothesis concerning the nature or requirements of the C-terminal extension of the *S. meliloti* enzymes. Since the protein is fully functional and able to elicit wild type levels of nitrogenase activity and plant dry weights we must conclude that the C-terminal region is not essential for malic enzyme activity and function in *S. meliloti*. If the PTA like region

has some enzymatic function neither it, nor its product are required for symbiotic nitrogen fixation. Also, if the C-terminal region of the *S. meliloti* malic enzymes is utilized for interaction or formation of a multienzyme complex with the TCA cycle enzymes (Mitchell, 1996) this function is also not essential for function and nitrogen fixation.

Chapter 7

Expression of the malate specific permease, *maeP (malP)*, of *Streptococcus bovis* in *S. meliloti*

Abstract

Oxidation of carbon sources supplied to the bacteroids within nodules is essential for generating reducing power and ATP to maintain nitrogen fixation. Research into the importance of the malic enzymes of *S. meliloti* for maintaining the TCA cycle stimulated interest into the exact carbon source(s) provided to the bacteroid by the plant host. To establish if the dicarboxylate malate is present in the nodule, the malate specific permease, *maeP* (recently redesignated *malP*), from *Streptococcus bovis* was introduced into *S. meliloti* and *R. leguminosarum* mutants defective for the C_4-dicarboxylate transport protein DctA. To express the malate permease in *S. meliloti* and provide a target for recombination in the chromosome, the constitutive *dme* promoter or the *dctA* promoter from the native *S. meliloti* C_4-dicarboxylate transport system were utilized. *dct*$^-$ stains were then tested for expression of the malate permease under free-living conditions and for expression in bacteroids. When the *maeP* gene was under control of either promoter and was introduced into the chromosome of a dctA mutant *S. meliloti*, the symbiotic phenotype was indistinguishable from alfalfa plants inoculated with the *dctA*$^-$ *S. meliloti* strains. However, when the copy number of both constructs was increased by inserting the constructs on the plasmid pBBR1MCS-5, partial symbiotic N_2 fixation was

obtained. When these two promoter-*maeP* plasmid constructs were introduced into *dctA* mutants of *R. leguminosarum*, the *dme* promoter construct yielded partial symbiotic N_2 fixation while the *dctA* promoter construct yielded plants and nitrogenase activity that were indistinguishable from wild type inoculated plants. These results indicate that malate is present in nodules and its import is capable of supporting nitrogen fixation to varying extent in different leguminous plants.

Methods and Materials

See Chapter 2 for all methods and materials. Bacterial strains and plasmids are listed in Table 2.1. In previous experiments the *maeP* gene had been cloned downstream of the *dme* promoter (Cowie, 1998) and this construct had been recombined into the chromosome of the *dctA* mutant strains RmF642 (Rm1021 *dctA*14::Tn5) and RmF647 (Rm1021 *dctA*26::Tn5) by using the pUCP30T vector (Schweizer *et. al.*, 1997) to create strains RmH948 and RmH949 (Figure 7.1). The *Pdme-maeP* construct of pTH600 was constructed by ligating the 1.5 kb *Hind*III/*Kpn*I fragment (*Pdme-maeP*) of pTH449 into pBBR1MCS-5 (Figure 7.1). pTH600 was then transferred into the *dctA* mutants RmF642 and RmF647 via a triparental mating and transconjugants were selected for on LBGm (20 μg/ml) Nm (20 μg/ml) and the resulting strains were designated RmK299 and RmK300 (Figure 7.1) respectively. In all cases the *maeP* gene driven by the *dme* promoter complemented the inability of RmF642 and RmF647 to grow on malate but did not confer growth with succinate as the sole carbon source and confirmed the malate specificity of the MaeP permease (data not shown).

Figure 7.1. Schematic showing PCR and cloning strategy employed in the generation of *S. meliloti* strains expressing the *maeP* gene downstream of the *dme* promoter. Dotted arrows indicate primers utilized to generate *maeP* gene. Open arrow represents *maeP* gene region indicating direction of transcription. Hatched box represents the *dme* promoter region. Black box indicates gentamicin resistance gene while grey box represents origin of transfer. Black triangle represents transposon insertion in the *dctA* gene of the *S. meliloti* chromosome. Dotted lines indicate region of homologous recombination. Restriction enzymes relevant to the constructions are indicated.

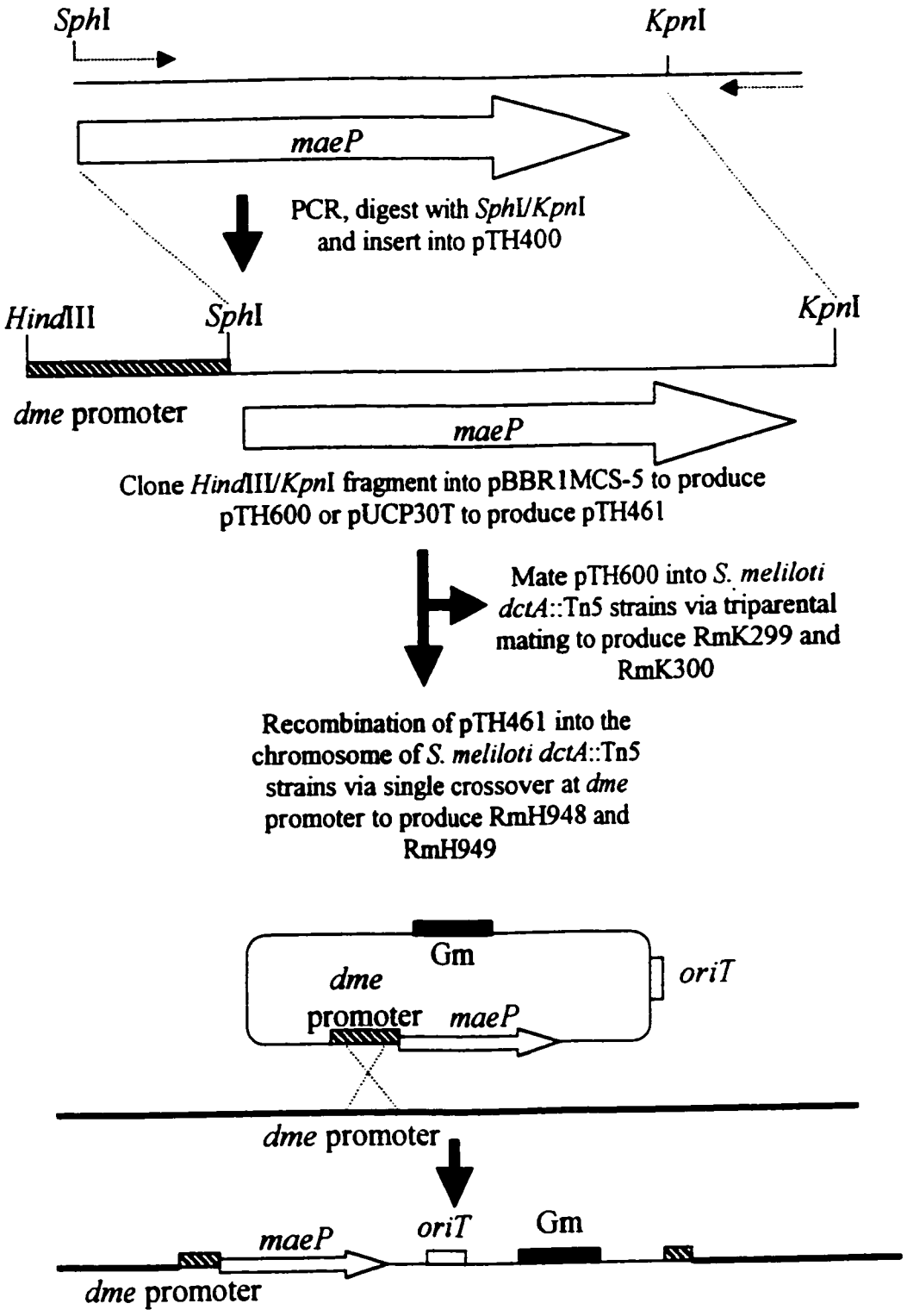
SphI
KpnI
maeP
PCR, digest with SphI/KpnI
and insert into pTH400
HindIII
SphI
KpnI
dme promoter
maeP
Clone HindIII/KpnI fragment into pBBR1MCS-5 to produce
pTH600 or pUCP30T to produce pTH461
Mate pTH600 into S. meliloti
dctA::Tn5 strains via triparental
mating to produce RmK299 and
RmK300
Recombination of pTH461 into the
chromosome of S. meliloti dctA::Tn5
strains via single crossover at dme
promoter to produce RmH948 and
RmH949
Gm
dme
promoter
maeP
oriT
dme promoter
maeP
oriT
Gm
dme promoter

The *dctA* promoter of *S. meliloti* was amplified by PCR using the primers 5'-ATG AGC ATG CTA TCC TCC AC-3' and 5'-GGA AGC TTG ACC ATG CG-3', bases in bold represent alterations from the original sequence in order to introduce *Sph*I and *Hind*III sites respectively. The primers were designed based upon the conserved sequence of *R. meliloti* strain JJ1c10 published by Dr. Robert Watson (1990), Agriculture Canada, Ottawa, Ontario (Accession #92199261). PCR procedures were carried out as outlined in Chapter 2 with the following conditions; denaturing at 94°C for 30 seconds, annealing at 55°C for 30 seconds, extension at 72°C for 30 seconds using approximately 100 ng of the template pTH31, a plasmid containing the *dctA-dctB* intergenic region (Yarosh *et al.*, 1989). The resulting 250 bp product was digested with *Hind*III and *Sph*I and inserted into pUC119 to yield plasmid pTH646. The integrity of the PCR fragment was verified by sequencing the 250 bp fragment using the M13 forward and reverse primers and comparing the results to Genbank. Comparisons of the sequence of the *dctA* promoter of *S. meliloti* strain Rm1021 obtained through the PCR of the *dctA/dctB* intergenic region (Figure 7.2) with *S. meliloti* strain Rm1021 published by Wang *et al.* (1989) revealed a single base pair alteration two base pairs upstream from the translational start site of *dctA* (G in our sequence, T in previously published sequence). Comparison with the *S. meliloti* strain Rm1021 published by Jiang *et al.* (1989) revealed a single base pair deletion 28 base pairs upstream from the translational start site of *dctB* (G in previously published sequence lacking in ours) and a single base pair alteration two base pairs upstream from the translational start site of *dctA* (G in our sequence, T in previously published sequence). When the *dctA* promoter sequence was compared to the

Figure 7.2. Schematic showing PCR and cloning strategy employed in the generation of *S. meliloti* strains expressing the *maeP* gene downstream of the *dctA* promoter. Dotted arrows indicate primers utilized to generate the *dctA* promoter region. Open arrow represents *maeP* gene region indicating direction of transcription. Hatched box represents the *dctA* promoter region. Black box indicates gentamicin resistance gene while grey box represents origin of transfer. Black triangle represents transposon insertion in the *dctA* gene of the *S. meliloti* chromosome. Dotted lines indicate region of homologous recombination. Restriction enzymes relevant to the constructions are indicated.

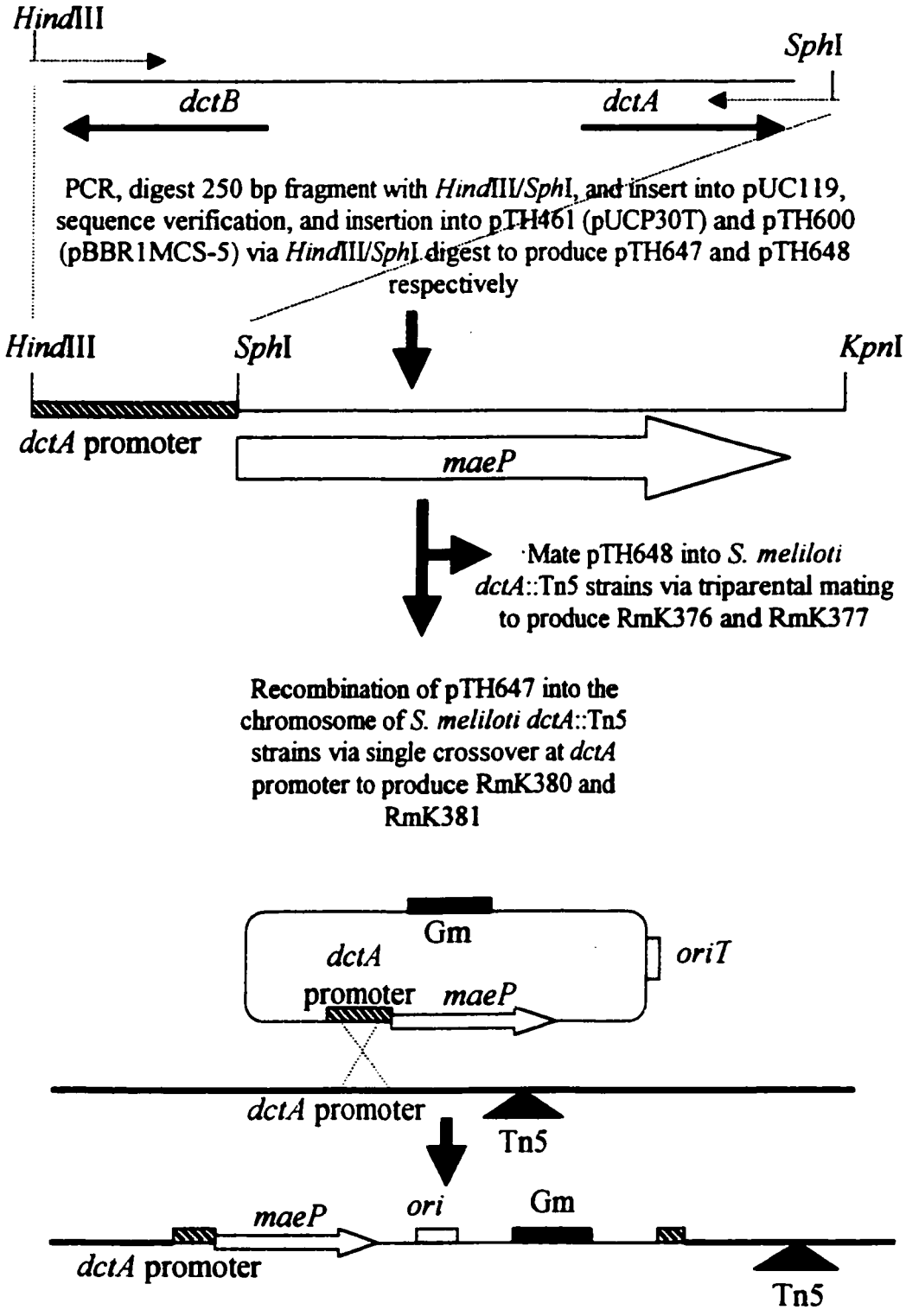
HindIII
SphI
dctB
dctA
PCR, digest 250 bp fragment with HindIII/SphI, and insert into pUC119, sequence verification, and insertion into pTH461 (pUCP30T) and pTH600 (pBBR1MCS-5) via HindIII/SphI digest to produce pTH647 and pTH648 respectively
HindIII
SphI
KpnI
dctA promoter
maeP
Mate pTH648 into S. meliloti dctA::Tn5 strains via triparental mating to produce RmK376 and RmK377
Recombination of pTH647 into the chromosome of S. meliloti dctA::Tn5 strains via single crossover at dctA promoter to produce RmK380 and RmK381
Gm
dctA
promoter
maeP
oriT
dctA promoter
Tn5
maeP
ori
Gm
dctA promoter
Tn5

sequence obtained from the *S. meliloti* genomic sequencing effort currently underway, the sequences were found to be identical with the exception of a single base pair alteration two base pairs upstream from the translational start site of *dctA* (G in our sequence, T in genomic sequencing effort). By comparison there are 7 base pair between the Rm1021 *dctA* promoter region and the sequence obtained from strain JJ1c10 (Watson, 1990). pTH646 was then digested by *Hind*III and *Sph*I and the 250 bp fragment inserted into similarly digested pTH461 to insert the *dctA* promoter upstream of the *maeP* gene to produce pTH647 (Figure 7.2). This construct was then used in a triparental mating with the *dctA* mutants RmF642 and RmF647 and transconjugants resulting form single recombinational events at the *dctA* promoter were selected for on LBGm (20 μg/ml) Nm (200 μg/ml) resulting in strains RmK380 and RmK381 (Figure 7.2). To produce a pBBR1MCS-5 derivative carrying the *PdctA-maeP* construct, pTH647, was digested with *Hind*III and *Kpn*I to produce a 1.2 kb fragment that was then ligated into pBBR1MCS-5 treated with *Hind*III and *Kpn*I (Figure 7.2). The resulting plasmid pTH648 was then transferred to the *dctA* mutants RmF642 and RmF647 via a triparental mating and transconjugants were selected for on LBGm (20 μg/ml) Nm (200 μg/ml) resulting in strains RmK376 and RmK377 respectively. In all cases, complementation of the *dctA*$^-$ phenotype was observed on minimal media with malate as the sole carbon source but not with succinate as the sole carbon source and confirmed the specificity of the malate permease (data not shown). To express the *maeP* gene in *R. leguminosarum* the plasmids pTH600 and pTH648 were transferred into two *dctA* mutants of *R. leguminosarum*, Ru714 (3841Δ*dctABD*::ΩSp) and Ru727 (3841Δ*dctA*::ΩSp) obtained

from Dr. Phillipe Poole of the University of Redding (Reid *et al.*, 1996). Transconjugants from triparental matings were selected for on TYGm (20 μg/ml) Sp (200 μg/ml).

Results

Expression of *maeP* in *S. meliloti*

The malate specific permease gene was introduced into *S. meliloti* strains as both a single chromosomal insertion and in the form of a multicopy plasmid pBBR1MCS-5. In these constructs *maeP* was expressed from either the malic enzyme promoter *Pdme*, or the *dctA* promoter *PdctA*. Hence, strain RmH948 (*dctA14*, Φ*Pdme-maeP*) is a *dctA* mutant carrying a chromosomal insertion of *maeP* under the control of the *dme* promoter while strain RmK299 (*dctA14*, *Pdme-maeP*) is a *dctA* mutant carrying a multicopy plasmid with *maeP* under the control of the *dme* promoter. The ability of various $dctA^-$ /$maeP^+$ strains to grow in minimal media with glucose or malate as the sole carbon source was determined. Growth curves with glucose as the sole carbon source are similar for all strains indicating that the strains were inoculated with comparable numbers of cells and are capable of utilizing glucose to the same extent (Figure 7.3 and Figure 7.4). With malate as the sole carbon source RmK299 and RmK300 (*Pdme-maeP* carried on pBBR1MCS-5) grew as well as strain RmK298 (wild type Rm1021 carrying the plasmid pBBR1MCS-5) while RmH948 and RmH949 (*Pdme-maeP* chromosomal insertions) reached the same terminal optical density but in approximately twice the time (Figure 7.3). When the *dctA* promoter was used to control *maeP* expression the reverse situation

Figure 7.3. Growth curves of *S. meliloti dctA* mutant strains and *dctA* mutant strains expressing the malate permease from the *S. meliloti dme* promoter with A; glucose and B; malate as the sole carbon source. RmK298 ◆ (wild type), RmK301 □ (*dctA14*), RmK302 ▲ (*dctA26*), RmH948 × (*dctA14*, Φ*Pdme-maeP*), RmH949 ○ (*dctA26*, Φ*Pdme-maeP*), RmK299 △ (*dctA14*, *Pdme-maeP*), RmK300 ◇ (*dctA26*, *Pdme-maeP*).

A

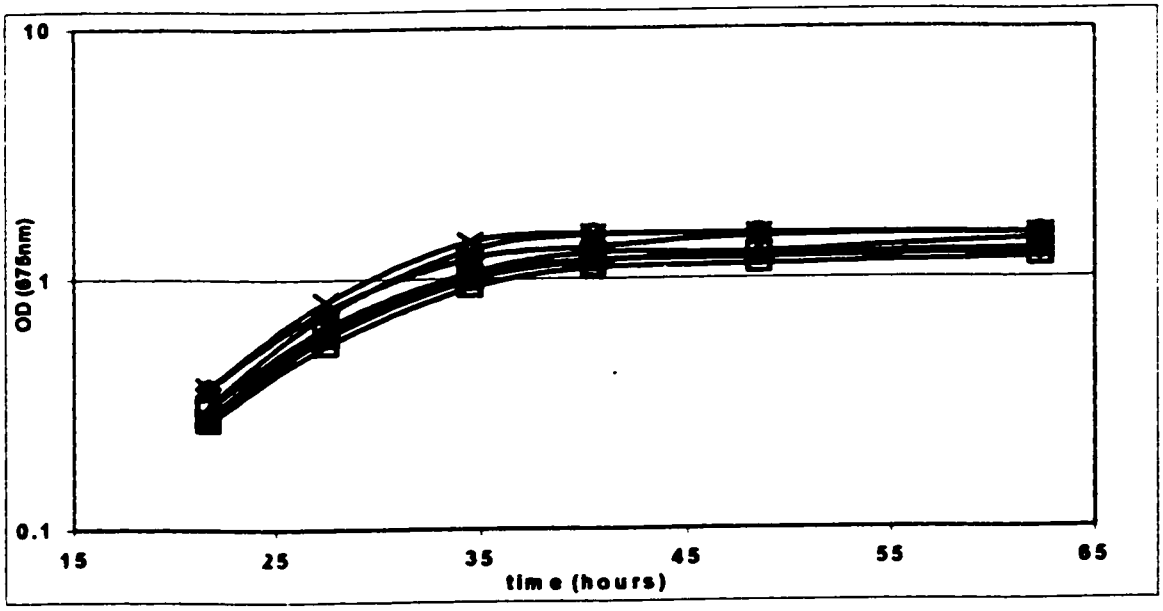
10
1
0.1
OD (675nm)
15
25
35
45
55
65
time (hours)

B

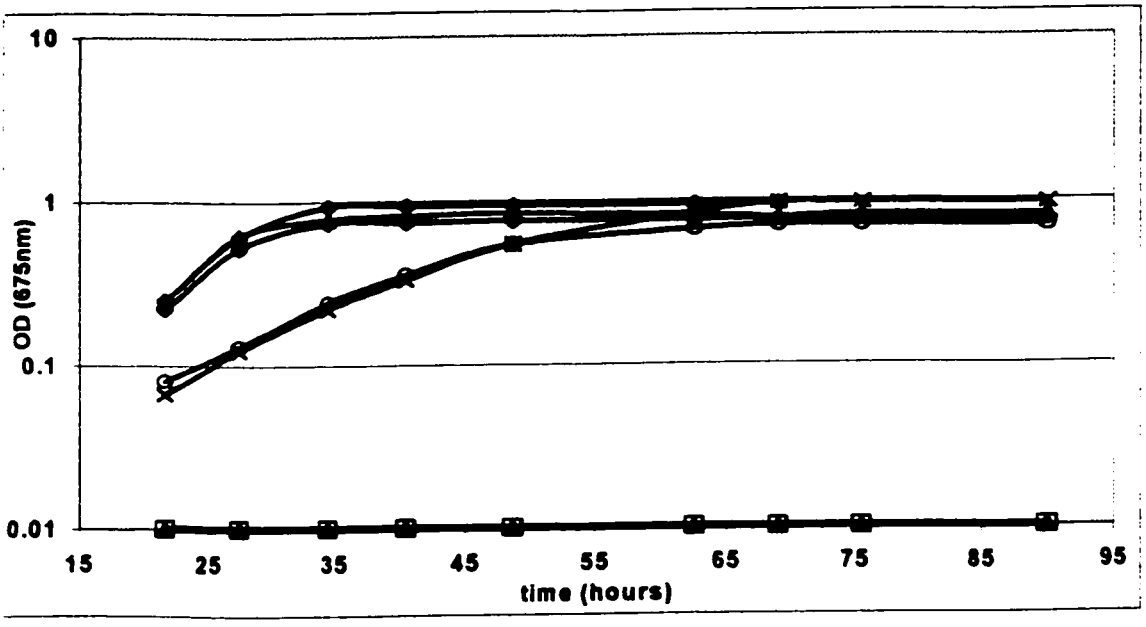
10
1
0.1
0.01
OD (675nm)
15
25
35
45
55
65
75
85
95
time (hours)

Figure 7.4. Growth curves of *S. meliloti dctA* mutant strains and *dctA* mutant strains expressing the malate permease from the *S. meliloti dctA* promoter with A; glucose and B; malate as the sole carbon source. RmK298 ◆ (wild type), RmK301 □ (*dctA14*), RmK302 ▲ (*dctA26*), RmK376 ✖ (*dctA14, PdctA-maeP*), RmK377 ◇ (*dctA26, PdctA-maeP*), RmK380 △ (*dctA14, ΦPdctA-maeP*), RmK381 ○ (*dctA26, ΦPdctA-maeP*).

A

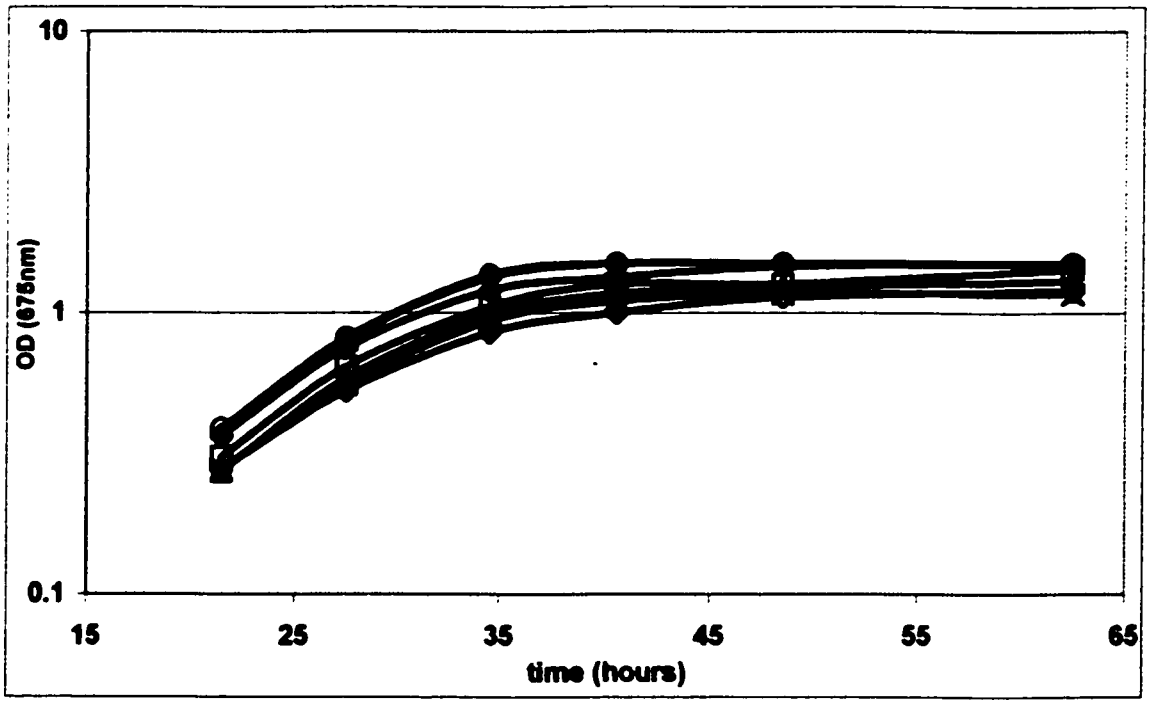
10
1
0.1
OD (675nm)
15
25
35
45
55
65
time (hours)

B

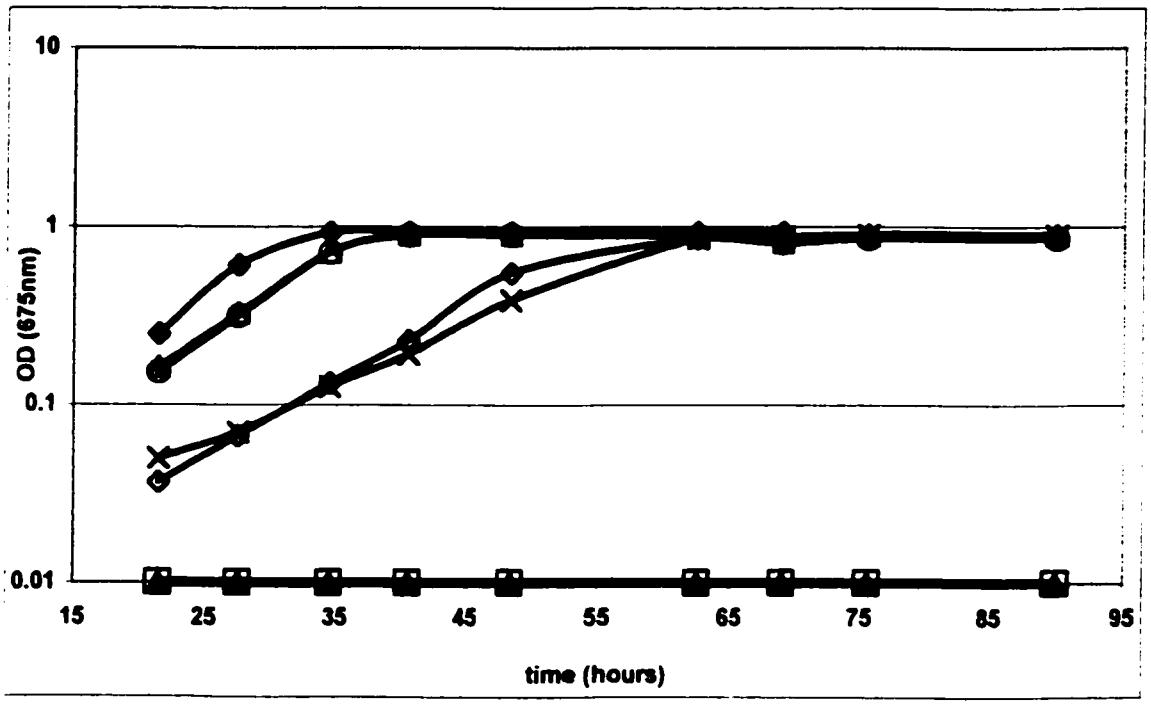
10
1
0.1
0.01
OD (675nm)
15
25
35
45
55
65
75
85
95
time (hours)

Figure 7.5. Transport assays for free-living *S. meliloti* cells with 40 μM malate (**A**) and 40 μM malate and 800 μM succinate (**B**). RmK298 ◆ (wild type), RmK301 ▲ (*dctA14*), RmH948 ✖ (*dctA14*, *ΦPdme-maeP*), RmK299 ○ (*dctA14*, *Pdme-maeP*), RmK380 ◇ (*dctA14*, *ΦPdctA-maeP*), RmK376 □ (*dctA14*, *PdctA-maeP*).

A.

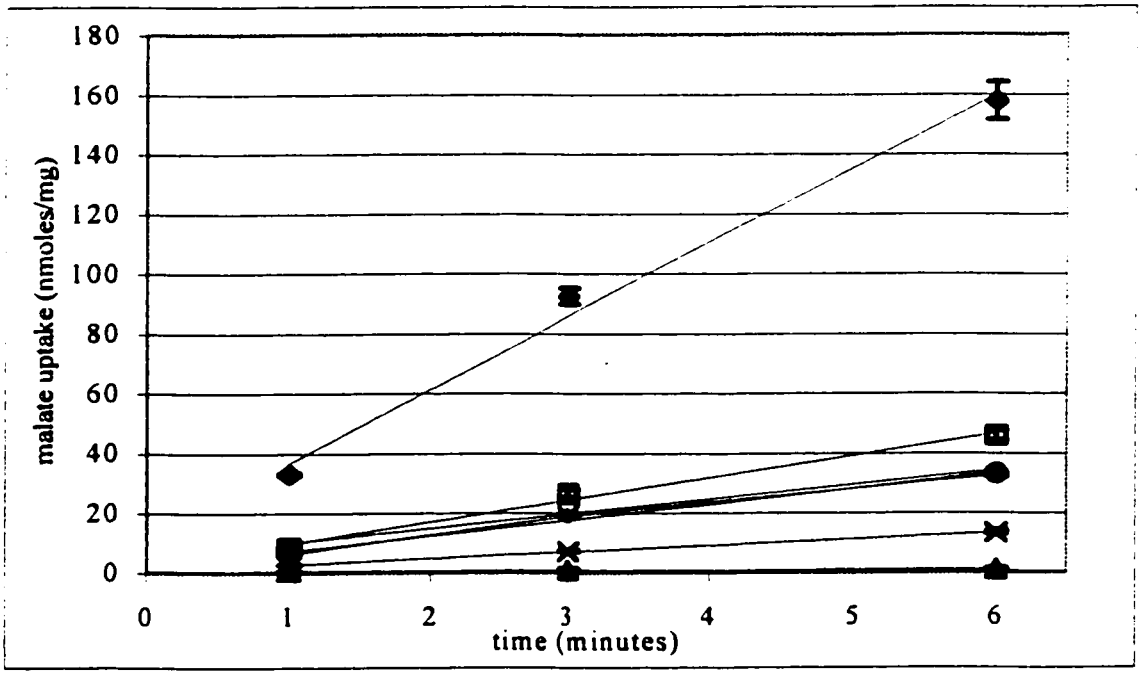
malate uptake (nmoles/mg)
180
160
140
120
100
80
60
40
20
0
0
1
2
3
4
5
6
time (minutes)

B.

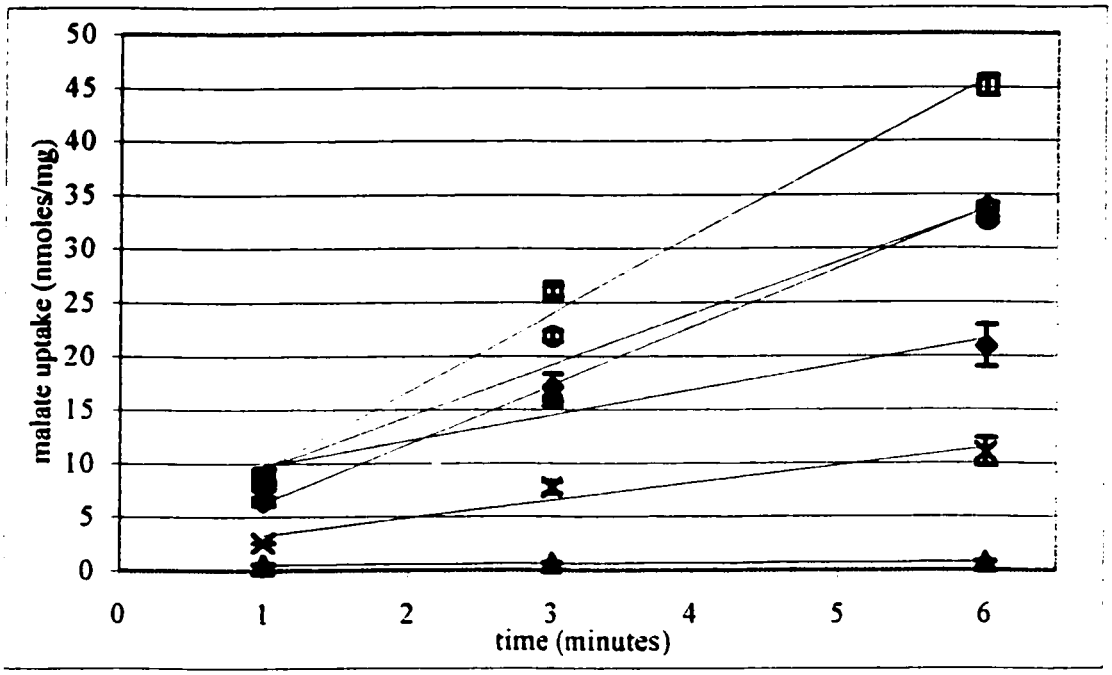
malate uptake (nmoles/mg)
50
45
40
35
30
25
20
15
10
5
0
0
1
2
3
4
5
6
time (minutes)

was obtained (Figure 7.4). The single copy of *maeP* introduced into the chromosome and under the control of the *dctA* promoter (RmK380 and RmK381) resulted in growth patterns similar to wild type cells while over expression of the *PdctA-maeP* construct (strains PmK376 and RmK377 with *PdctA-maeP* carried on pBBR1MCS-5) results in slower growth (Figure 7.4).

Malate uptake in *S. meliloti* cells

Malate uptake assays with free-living *S. meliloti dctA*⁻ strains expressing the *maeP* gene with the two promoters revealed a linear relationship in terms of malate uptake over the 6 minute time course utilized (Figure 7.5). When the *maeP* gene is expressed on the plasmid as opposed to the chromosomal insertion the malate uptake rate is 1.6 and 2.3 times higher with the *dctA* promoter or the *dme* promoter respectively (Table 7.1). These results support the observations made with the growth curves with malate as the sole carbon source as it shows that strains expressing the *maeP* transporter from the *dme* promoter inserted into the chromosome (RmH948) has a lower rate of uptake than the same construct expressed on the plasmid (RmK299). In addition, the *PdctA-maeP* construct inserted into the chromosome (RmK380) has comparable rates of malate uptake as the strain expressing the *Pdme-maeP* construct from a plasmid (RmK299). The malate uptake rates with the constructs expressed from the plasmid are very low when compared to wild type *S. meliloti* strains with only 19% and 31% the rate of uptake for the *Pdme-maeP* and *dctA-maeP* constructs respectively. When 800 μM succinate was added to the assay, wild type *S. meliloti* cells showed only limited malate uptake, approximately 10%, relative to an assay with malate alone (Table 7.1). By comparison the *dctA*⁻ strains

expressing the malate permease from either the *dme* or *dctA* promoter showed no inhibtion of malate uptake when succinate was present in the assay (Table 7.1).

Expression of *maeP* in *S. meliloti* bacteroids

To determine if any of the constructs were capable of restoring N_2-fixation ability to *dctA*⁻ mutants two experiments were carried out. In the first experiment, alfalfa plants were inoculated with strains in which the *maeP* gene was expressed from the *dme* promoter. After 5 weeks of growth the plants were harvested and an examination of the root systems revealed RmK299 (*dctA14 Pdme-maeP*) and RmK300 (*dctA26 Pdme-maeP*)strains produced nodules that were comparable to wild type nodules in terms of size but had a lower degree of red pigmentation (Figure 7.6). These plants were also larger and greener than their *dctA*⁻ parental strains but not as large or as lush as plants inoculated with the wild type *S. meliloti* strain (Figure 7.7). Acetylene reduction assays revealed that the strains carrying a single copy of the *maeP* gene expressed from the *dme* promoter had less than 1% the activity of nodules produced from the wild type *S. meliloti* strain (Table 7.2). However when the copy number of the *Pdme-maeP* construct was increased via the plasmid pBBR1MCS-5, the acetylene reduction activity also increased (Table 7.2). Both RmK299 and RmK300 showed acetylene reduction activities of 38% and 46% activity respectively relative to wild type inoculated plants (Table 7.2). Plant dry weights obtained from these strains support the hypothesis that the multi copy situation induces higher levels of nitrogen fixation. Both RmK299 and RmK300 inoculated plants had elevated dry weights relative to the negative controls and the single copy *Pdme-maeP* strains (Table 7.2). Nodule content and strain verification was carried

Table 7.1. Transport assay results of free-living *S. meliloti dctA14* strains expressing the malate permease from the *S. meliloti dme* or *dctA* promoter.

Sample	Genotype	Malate uptake rate (nmoles/ min/mg)[a]	% activity relative to wild type	Calculated theoretical V_{max}[b]	Malate uptake rate (nmoles/ min/mg)[c]	% activity relative to wild type	Malate uptake rate with succinate (nmoles/ min/mg)[d]	% activity relative to uptake rate without succinate
RmK298	wild type	24.7+/-1.4	100	-	25.5+/-2.1	100	2.4+/-0.5	10
RmH948	*dctA14*, *ΦPdme-maeP*	2.1+/-0.08	9	4.3+/-0.2	3.3+/-0.1	13	1.6+/-0.3	76
RmK299	*dctA14*, *Pdme-maeP*	4.8+/-0.1	19	9.9+/-0.1	8.8+/-0.1	35	4.8+/-0.02	100
RmK376	*dctA14*, *PdctA-maeP*	7.7+/-0.2	31	15.0+/-0.4	11.0+/-0.1	43	7.3+/-0.2	95
RmK380	*dctA14*, *ΦPdctA-maeP*	5.2+/-0.1	21	10.6+/-0.2	8.4+/-0.2	33	5.5+/-0.1	106
RmK301	*dctA*14	0.1+/-0.05	0.4	-	0.16+/-0.01	0.6	0.05+/-0.01	50

[a] Malate uptake rates are expressed as mean +/- standard error of triplicate samples measured over 6 minutes with 40 μM malate

[b] Theoretical V_{max} was determined using the malate uptake rate determined with 40 μM malate, a K_m of 41.4, and the Briggs-Haldane equation ($V_o=V_{max}[S_o]/[S_o]K_m$)

[c] Malate uptake rates are expressed as mean +/- standard error of triplicate samples measured over 6 minutes with 80 μM malate

[d] Malate uptake rates are expressed as mean +/- standard error of triplicate samples measured over 6 minutes with 40 μM malate in the presence of 800 μM succinate

ND none detected

Figure 7.6. Photograph of nodules isolated from alfalfa plants 38 days after inoculation with *S. meliloti dctA* mutant strains expressing the malate permease from the *S. meliloti dme* promoter.

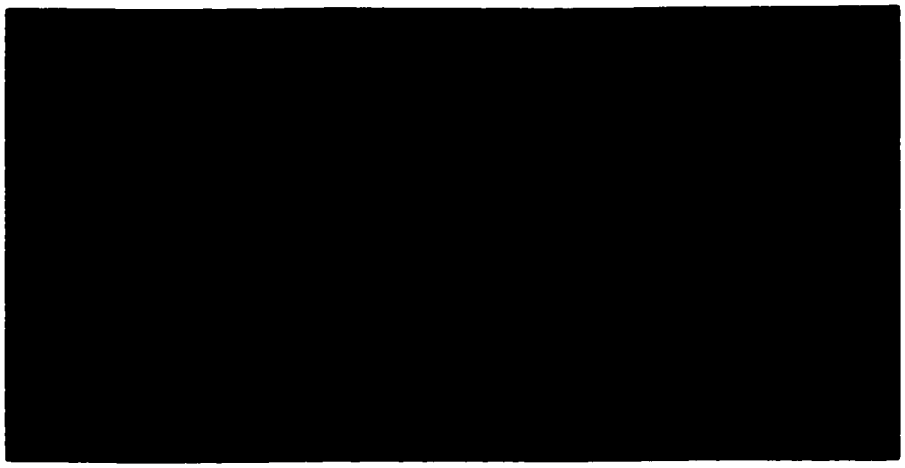

RmK298 (wild type)	RmK299 *(dctA14, pdme-maeP)*	RmH948 *(dctA14, Φpdme-maeP)*	RmK301 *(dctA14)*

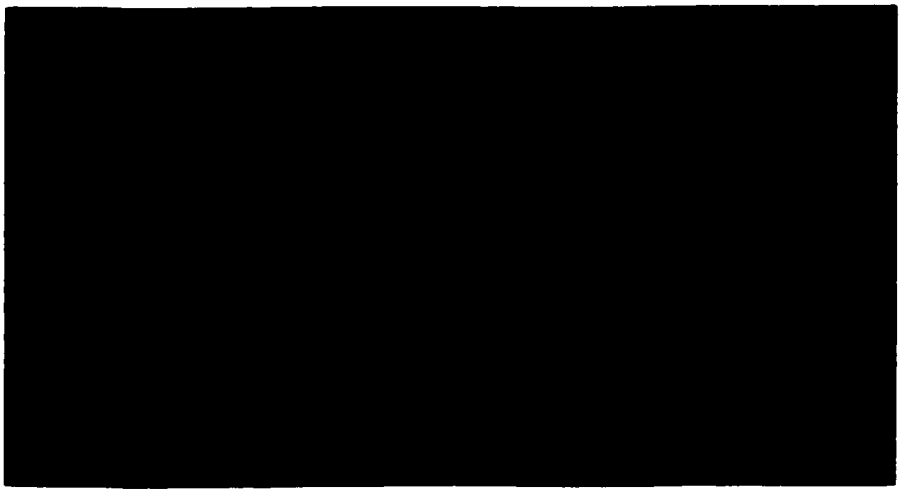

RmK298 (wild type)	RmK300 (*dctA26, pdme-maeP*)	RmH949 (*dctA26, Φpdme-maeP*)	RmK302 (*dctA26*)

out by streaking the contents of 25 random nodules of each strain on LBSm plates. The resulting colonies were replica plated onto LBGm, M9 malate and M9 succinate plates. All cells obtained from the nodules that were gentamicin resistant were only capable of growing on minimal media with malate but not succinate as the sole carbon source. This demonstrates that contamination with wild type cells was not responsible for the intermediate N_2 fixation phenotype

To further examine the effects of *maeP* gene expression, experiments were conducted with *dctA*$^-$ strains in which *maeP* was expressed from the *dctA* promoter. Plants inoculated with strains carrying the single chromosomal copy of *PdctA-maeP* were stunted and chlorotic and more closely resembled the *dctA*$^-$ negative controls and the uninoculated plants (Figure 7.8). The strains carrying the *PdctA-maeP* construct on the pBBR1MCS-5 plasmid were larger and greener than the negative control strains but not as large or as green as the plants inoculated with wild type *S. meliloti* (Figure 7.8). Plants inoculated with strains carrying the chromosomal insertions of *maeP* yielded approximately 1% the acetylene reduction activity of wild type inoculated plants while the plasmid bearing strains RmK376 and RmK377 had 49% and 31% acetylene reduction activity respectively, as compared to wild type inoculated plants (Table 7.3). The plant dry weight determinations mirrored the acetylene reduction data with the strains carrying the chromosomal insertion of *PdctA-maeP* having dry weights similar to uninoculated plants. The strains carrying the plasmid copy of *PdctA-maeP* had dry weights 27% and 30% relative to wild type for strains RmK377 and RmK376 respectively (Table 7.3). Nodule content and strain verification was carried out by streaking the contents of 25

Figure 7.7. Photograph of 38 day old alfalfa plants 38 days after inoculation with *S. meliloti dctA* mutant strains expressing the malate permease from the *S. meliloti dme* promoter.

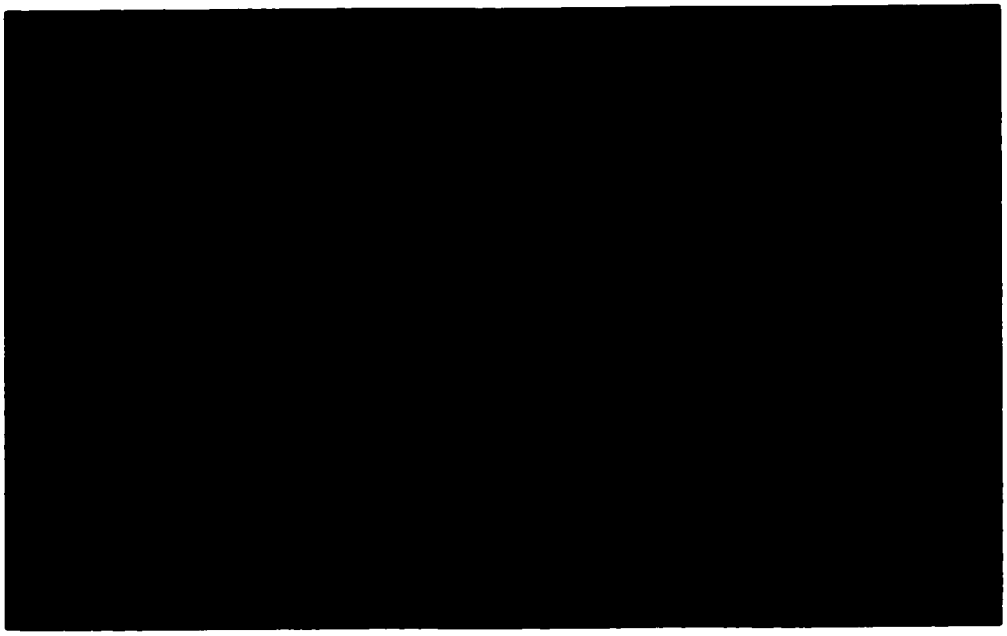

RmK298 (wild type)	RmK299 (*dctA14*, *pdme-maeP*)	RmH948 (*dctA14*, Φ*pdme-maeP*)	RmK301 (*dctA14*)	uninoculated

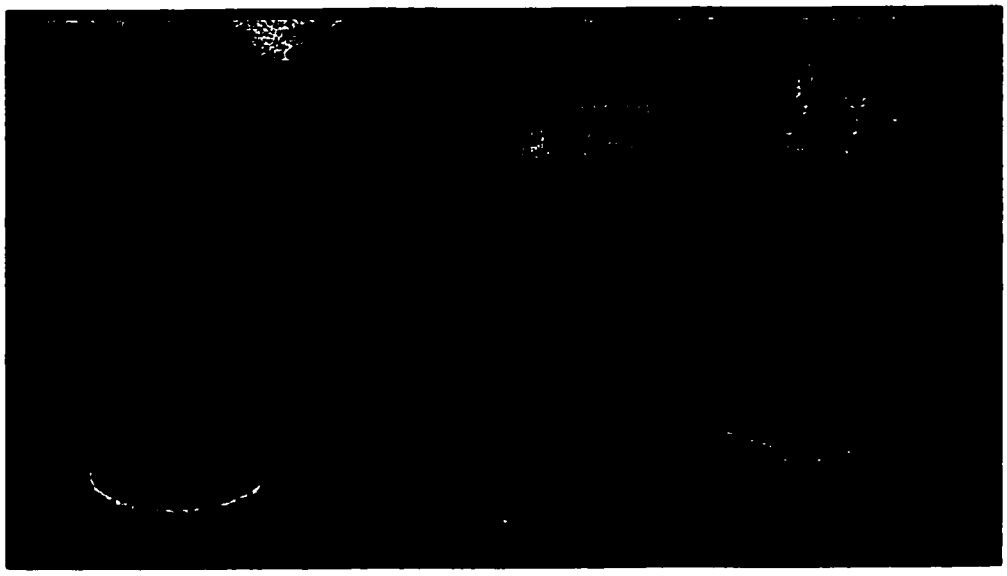

RmK298 (wild type)	RmH949 (*dctA26*, Φ*pdme-maeP*)	RmK300 (*dctA26*, *pdme-maeP*)	RmK302 (*dctA26*)	uninoculated

Table 7.2. Acetylene reduction values and plant dry weights of 38 days after inoculation with *S. meliloti dctA* mutant strains expressing the malate permease from the *S. meliloti dme* promoter.

Sample	Genotype	ARA (nmoles/min/plant)[a]	% ARA relative to wild type	Plasmid retention[b]	Plant dry weight (mgs)[c]	% Plant dry weight relative to wild type
RmK298	wild type	1089 +/- 254	100	72	131.8 +/- 9.5	100
RmH948	*dctA14*, Φ*Pdme-maeP*	8 +/- 6	0.8	100	11.1 +/- 0.6	9
RmH949	*dctA26*, Φ*Pdme-maeP*	4.3 +/- 0.4	0.4	100	12.2 +/- 1.1	9
RmK299	*dctA14* Pdme-*maeP*	416 +/- 3	38	95	33.9 +/- 4.3	26
RmK300	*dctA26 Pdme-maeP*	498 +/- 18p	46	96	30.5 +/- 5.5	23
RmK301	*dctA*14	ND	0	73	10.1 +/- 0.6	8
RmK302	*dctA*26	ND	0	58	10.3 +/- 1.0	8
uninoculated	-	-	-	-	11.0 +/- 1.0	8

[a] Acetylene reduction activity is expressed as mean +/- standard error of triplicate samples containing three root systems each.

[b] Plasmid retention based upon number of gentamicin resistant clones out of streptomycin resistant clones recovered from nodule contents.

[c] Plant dry weight is expressed as mean of +/- standard error of triplicate pots containing 7-10 plants each.

ND none detected

Figure 7.8. Photograph of alfalfa plants 43 days after inoculation with *S. meliloti dctA* mutant strains expressing the malate permease from the *S. meliloti dctA* promoter.

RmK298 (wild type)	RmK376 (*dctA14*, *pdctA-maeP*)	RmK380 (*dctA14*, Φ*pdctA-maeP*)	RmK301 (*dctA14*)	uninoculated

RmK298 (wild type)	RmK377 (*dctA26*, *pdctA-maeP*)	RmK381 (*dctA26*, Φ*pdctA-maeP*)	RmK302 (*dctA26*)	uninoculated

random nodules of each strain on LBSm plates. The resulting colonies were replica plated onto LBGm, M9 malate and M9 succinate plates. All cells obtained from the nodules that were gentamicin resistant were only capable of growing on minimal media with malate but not succinate as the sole carbon source. This demonstrates that contamination with wild type cells was not responsible for the intermediate N_2 fixation phenotype

Expression of *maeP* in the pea symbiont *R. leguminosarum*

The introduction of the *maeP* gene under control of the *S. meliloti dme* or *dctA* promoters into *R. leguminosarum dctA* mutants allowed growth on minimal media containing malate but not succinate. This indicated that both *S. meliloti* promoters were active in *R. leguminosarum* and that the *S. bovis* malate permease also functioned in this bacterium. To assess the symbiotic N_2 fixation activity of *R. leguminosarum* strains expressing the malate specific permease a series of plant tests were carried out. After 6 weeks of growth, the pea plants inoculated with the *dctA*$^-$ strains resembled the uninoculated controls being smaller and somewhat chlorotic relative to wild type inoculated plants. The plants inoculated with *R. leguminosarum* strains expressing the *maeP* gene under control of the *dme* promoter displayed an intermediate N_2 fixation phenotype being larger than the uninoculated control plants or those inoculated with the *dctA*$^-$ negative control strains but being less green than the wild type inoculated plants (Figure 7.9). Acetylene reduction assays revealed that the *dctA*$^-$ strains had little or no nitrogenase activity as expected while the strains expressing the malate permease had

Table 7.3. Acetylene reduction values and dry weights of alfalfa plants 43 days after inoculation with *S. meliloti dctA* mutant strains expressing the malate permease from the *S. meliloti dctA* promoter.

Sample	Genotype	ARA (nmoles/min/plant)[a]	% ARA relative to wild type	Plasmid retention[b]	Plant dry weight (mgs)[c]	% Plant dry weight relative to wild type
RmK298	wild type	458 +/- 67	100	70	79.2 +/- 1.8	100
RmK301	*dctA*14	1.3 +/- 0.1	0.3	95	8.7 +/- 0.3	11
RmK302	*dctA*26	2.1 +/- 0.6	0.4	100	9.7 +/- 1.2	12
RmK376	*dctA14, PdctA-maeP*	227 +/- 79	49	100	23.6 +/- 1.6	30
RmK377	*dctA26, PdctA-maeP*	143 +/- 4	31	89	21.3 +/- 1.3	27
RmK380	*dctA14, ΦPdctA-maeP*	7 +/- 1	1	100	10.9 +/- 0.1	14
RmK381	*dctA26, ΦPdctA-maeP*	5 +/- 0.2	1	100	9.8 +/- 2.0	12
uninoculated	-	-	-	-	9.3 +/- 1.8	12

[a] Acetylene reduction activity is expressed as mean +/- standard error of triplicate samples containing three root systems each.

[b] Plasmid retention based upon number of gentamicin resistant clones out of streptomycin resistant clones recovered from nodule contents.

[c] Plant dry weight is expressed as mean of +/- standard error of triplicate pots containing 7-10 plants each.

46% and 44% activity relative to wild type inoculated plants (Table 7.4). The dry weight of plants inoculated with strains RIK371 and RIK372 were 84% the dry weight of wild type inoculated plants. Plants inoculated with strains in which the malate permease was expressed from the *dctA* promoter were indistinguishable from wild type inoculated plants (Figure 7.10) and had acetylene reduction activitiy and plant dry weights that approached wild type levels (Table 7.5). When the malate permease was expressed from the *dctA* promoter in a *dctABD*$^-$ background the plants were identical to the negative controls in terms of appearance (Figure 7.10), acetylene reduction activity, and plant dry weights (Table 7.5).

Malate transport assays with *R. leguminosarum* bacteroids

To obtain an estimate of the transport rate of bacteroids carrying the *maeP* gene, malate uptake into bacteroids isolated from pea root nodules was determined. Wild type bacteroids showed levels of malate transport of 6.56 nmoles/min/mg protein (Figure 7.11, Table 7.6) while *dctA*$^-$ bacteroids in which the malate transporter was expressed from the *dme* promoter showed rates of 0.56 nmoles/min/mg protein (Figure 7.11, Table 7.6). By comparison, when the malate permease was expressed from the *S. meliloti dctA* promoter, slight increase in malate uptake, 0.75 nmoles/min/mg protein, was noted (Figure 7.11, Table 7.6). Therefore, when *maeP* was expressed from the *dctA* promoter the rate of malate uptake was increased 1.5 times relative to *maeP* being expressed from the *dme* a promoter. When *maeP* was expressed in conjunction with *dctA* the result was an increase in malate transport relative to wild type bacteroids with a transport rate of 12.44 nmoles/min/mg protein (Figure 7.11, Table 7.6). When succinate was added to a final

Figure 7.9. Photograph of pea plants 41 days after inoculation with *R. leguminosarum dctA* mutant strains expressing the malate permease from the *S. meliloti dme* promoter.

3841 (wild type)	RIK367 (wild type, pBBR1MCS-5)	RIK372 (*dctA*-, *pdme-maeP*)	RIK369 (*dctA*-)	uninoculated

3841 (wild type)	RIK367 (wild type, pBBR1MCS-5)	RIK371 (*dctABD*-, *pdme-maeP*)	RIK368 (*dctABD*-)	uninoculated

Table 7.4. Acetylene reduction values dry weights of pea plants 41 days after inoculation with *R. leguminosarum dctA* mutant strains expressing the malate permease from the *S. meliloti dme* promoter.

Sample	Genotype	ARA (nmoles/min/ plant)[a]	% ARA relative to wild type	Plasmid retention[b]	Plant dry weight (mgs)[c]	% Plant dry weight relative to wild type
RIK367	wild type	1641 +/- 465	100	40	575.8 +/- 41.3	100
RIK368	*dctABD-*	ND	0	45	319.7 +/- 12.9	56
RIK369	*dctA⁻*	6 +/- 5	0.4	40	296.8 +/- 8.6	52
RIK371	*dctABD⁻, Pdme-maeP*	752 +/- 101	46	80	483.1 +/- 31.7	84
RIK372	*dctA⁻, Pdme-maeP*	726 +/- 128	44	85	485 +/- 43.2	84
uninoculated	-	-	-	-	185 +/- 35	32

[a] Acetylene reduction activity is expressed as mean +/- standard error of triplicate samples containing three root systems each.

[b] Plasmid retention based upon number of gentamicin resistant clones out of streptomycin resistant clones recovered from nodule contents.

[c] Plant dry weight is expressed as mean of +/- standard error of triplicate pots containing 5-8 plants each.

ND none detected

Figure 7.10. Photograph of pea plants 42 days after inoculation with *R. leguminosarum dctA* mutant strains expressing the malate permease from the *S. meliloti dctA* promoter.

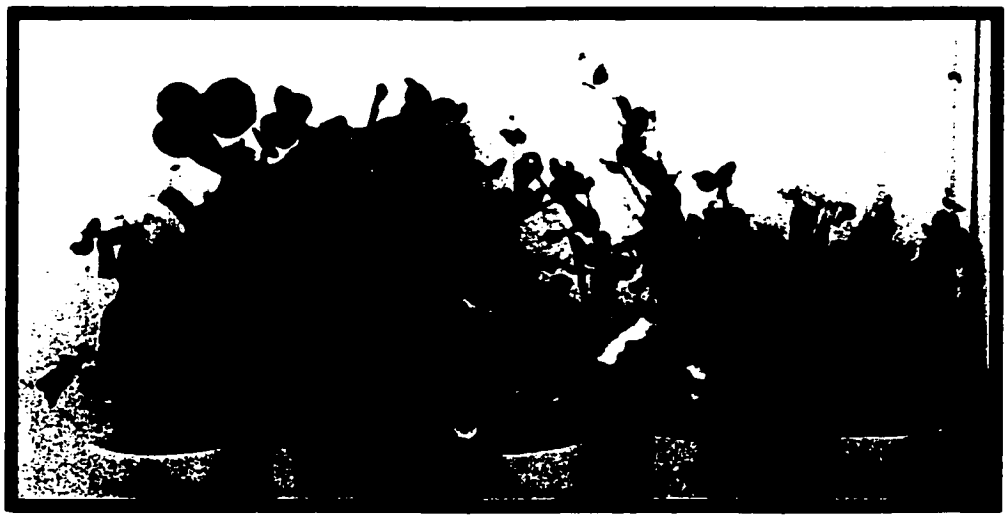

3841 (wild type)	RIK367 (wild type, pBBR1MCS-5)	RIK378 (*dctABD*-, *pdctA-maeP*)	RIK368 (*dctABD*-)	uninoculated

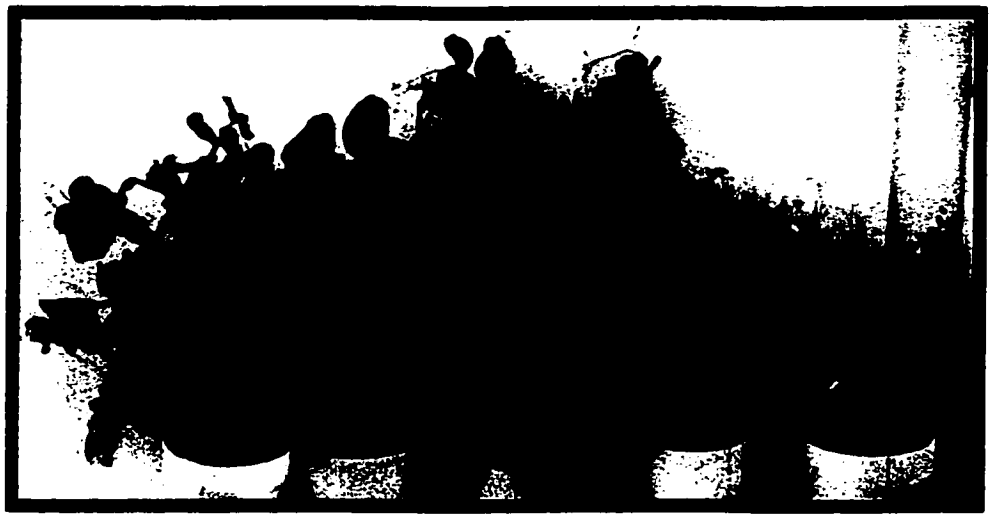

3841 (wild type)	RIK367 (wild type, pBBR1MCS-5)	RIK379 (*dctA*-, *pdctA-maeP*)	RIK369 (*dctA*-)	uninoculated

Table 7.5. Acetylene reduction values and plant dry weights of pea plants 42 days after inoculation with *R. leguminosarum* strains expressing the malate permease expressed from the *S. meliloti dctA* promoter.

Sample	Genotype	ARA (nmoles/min /plant)[a]	% ARA relative to wild type	Plasmid retention[b]	Plant dry weight (mgs)[c]	% Plant dry weight relative to wild type
RIK367	wild type	1081 +/- 707	100	35	409 +/- 71	100
RIK368	*dctABD-*	ND	-	15	243.3 +/- 17.6	59
RIK369	*dctA⁻*	ND	-	60	258.6 +/- 8.1	63
RIK378	*dctABD⁻, PdctA-maeP*	ND	-	30	267.7 +/- 40.5	65
RIK379	*dctA⁻, PdctA-maeP*	1169 +/- 273	108	90	421.8 +/- 97.5	103
uninoculated	-	-	-	-	280.3 +/- 12.3	69

[a] Acetylene reduction activity is expressed as mean +/- standard error of triplicate samples containing three root systems each.

[b] Plasmid retention based upon number of gentamicin resistant clones out of streptomycin resistant clones recovered from nodule contents.

[c] Plant dry weight is expressed as mean of +/- standard error of triplicate pots containing 5-8 plants each.

ND none detected

Figure 7.11. Transport assays for *R. leguminosarum* bacteroids with 40 μM malate. RIK367 △ (wild type), RIK368 ◇ (*dctABD*$^-$), RIK369 ● (*dctA*$^-$), RIK370 × (wild type, *Pdme-maeP*), RIK371 ◆ (*dctABD*$^-$, *Pdme-maeP*), RIK372 ■ (*dctA*$^-$, *Pdme-maeP*),). Dotted lines indicate data from a separate experiment conducted at a different time with RIK367 △ (wild type), RIK369 □ (*dctA*$^-$), and RIK379 ○ (*dctA*$^-$, *FdctA-maeP*).

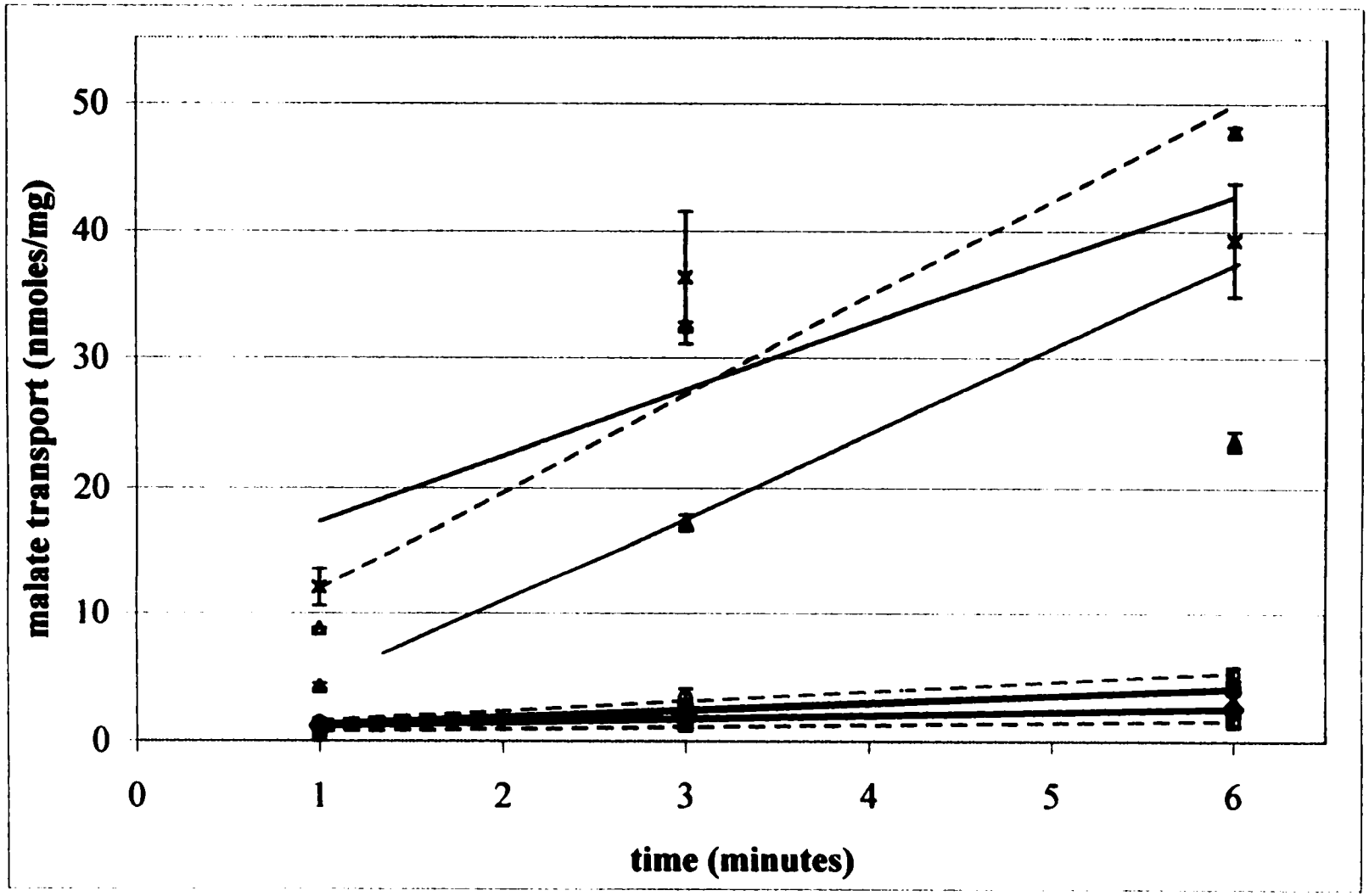
malate transport (nmoles/mg)
50
40
30
20
10
0
0
1
2
3
4
5
6
time (minutes)

Table 7.6. Transport assay results of bacteroids isolated from pea plants 40 days after inoculation with *R. leguminosarum dctA* mutant strains expressing the malate permease from the *S. meliloti dme* and *dctA* promoters.

Sample	Genotype	Malate uptake rate (nmoles/ min/mg)[a]	% activity relative to wild type	Calculated theoretical V_{max}[b]	Malate uptake rate (nmoles/ min/mg)[c]	% activity relative to wild type	Malate uptake rate with succinate (nmoles/min/mg)[d]	% activity relative to uptake rate without succinate
RIK367	wild type	6.56+/-0.39	100	-	-	-	0.39+/-0	6
RIK368	*dctABD-*	0.27+/-0.03	4	-	-	-	ND	-
RIK369	*dctA*⁻	0.27+/-0	4	-	-	-	ND	-
RIK370	wild type, *Pdme-maeP*	12.44+/-1.08	190	-	-	-	1.08+/-0.2	9
RIK371	*dctABD*⁻, *Pdme-maeP*	0.56+/-0.01	9	1.15+/-0.02	-	-	0.52+/-0.02	93
RIK372	*dctA*⁻, *Pdme-maeP*	0.56+/-0.04	9	1.14+/-0.07	-	-	0.60+/-0.08	107
RIK367*	wild type	7.61+/-1.60	100	-	8.46+/-0.1	100	0.67+/-0.28	9
RIK369*	*dctA*⁻	0.16+/-0.06	2	-	-	-	0.12+/-0.0	75
RIK379*	*dctA*⁻, *PdctA-maeP*	0.75+/-0.06	10	1.53+/-0.1	0.87+/-0.1	10	0.56+/-0.02	75

[a] Malate uptake rates are expressed as mean +/- standard error of triplicate samples measured over 6 minutes with 40 μM malate

[b] Theoretical V_{max} was determined using the malate uptake rate determined with 40 μM malate, a K_m of 41.4, and the Briggs-Haldane equation ($V_o=V_{max}[S_o]/[S_o]K_m$)

[c] Malate uptake rates are expressed as mean +/- standard error of triplicate samples measured over 6 minutes with 80 μM malate

[d] Malate uptake rates are expressed as mean +/- standard error of triplicate samples measured over 6 minutes with 40 μM malate in the presence of 800 μM succinate

concentration of 800 μM to the reaction mix containing 40 μM malate the result was a decrease in malate uptake of the DctA system with transport rates of wild type cells falling to 0.39 nmoles/min/mg protein while the malate permease expressing bacteroids showed no or slight decrease (Figure 7.12, Table 7.6). In RIK370 the malate uptake rate dropped to 1.08 nmoles/min/mg protein and this rate of uptake is presumably due to the action of the malate permease alone as the DctA system should be impaired in the presence of succinate. Experiments with aspartate as the competitor at a final concentration of 800 μM revealed the same trend as succinate with no appreciable loss of malate uptake with the malate permease expressing bacteroids (data not shown).

Determination of kinetic parameters of MaeP

In order to determine the kinetic parameters of the MaeP transporter malate concentrations ranging from 40 μM to 400 μM were used in transport assays with bacteroids of a *R. leguminosarum* RIK372, a *dctA*$^-$, *Pdme-maeP* expressing strain. The resulting Michaelis-Menten plot (Figure 7.13) showed the classical hyperbolic relationship and analysis with non-linear regression revealed a K_m of 41.4 +/- 3.345 and a V_{max} of 1.06 +/- 0.22 nmoles/min/mg protein. By using the Briggs-Haldane modification of the Michaelis- Menten formula a determination of V_{max} for strains expressing the malate permease was possible.

Discussion

Studies of the carbon sources that are present and available for metabolism by bacteroids in the root nodules have revealed that the C_4-dicarboxylic acids such as

Figure 7.12. Transport assays for *R. leguminosarum* bacteroids with 40 μM malate and 800 μM succinate. RIK367 ▲ (wild type), RIK370 ● (wild type, *Pdme-maeP*), RIK371 ■ (*dctABD*⁻, *Pdme-maeP*), RIK372 ✖ (*dctA*⁻, *Pdme-maeP*), RIK367 –△– (wild type), RIK369 –○– (*dctA*⁻), RIK379 –◇– (*dctA*⁻, *PdctA-maeP*). Dotted lines indicate data from a seperate experiment conducted at a different time.

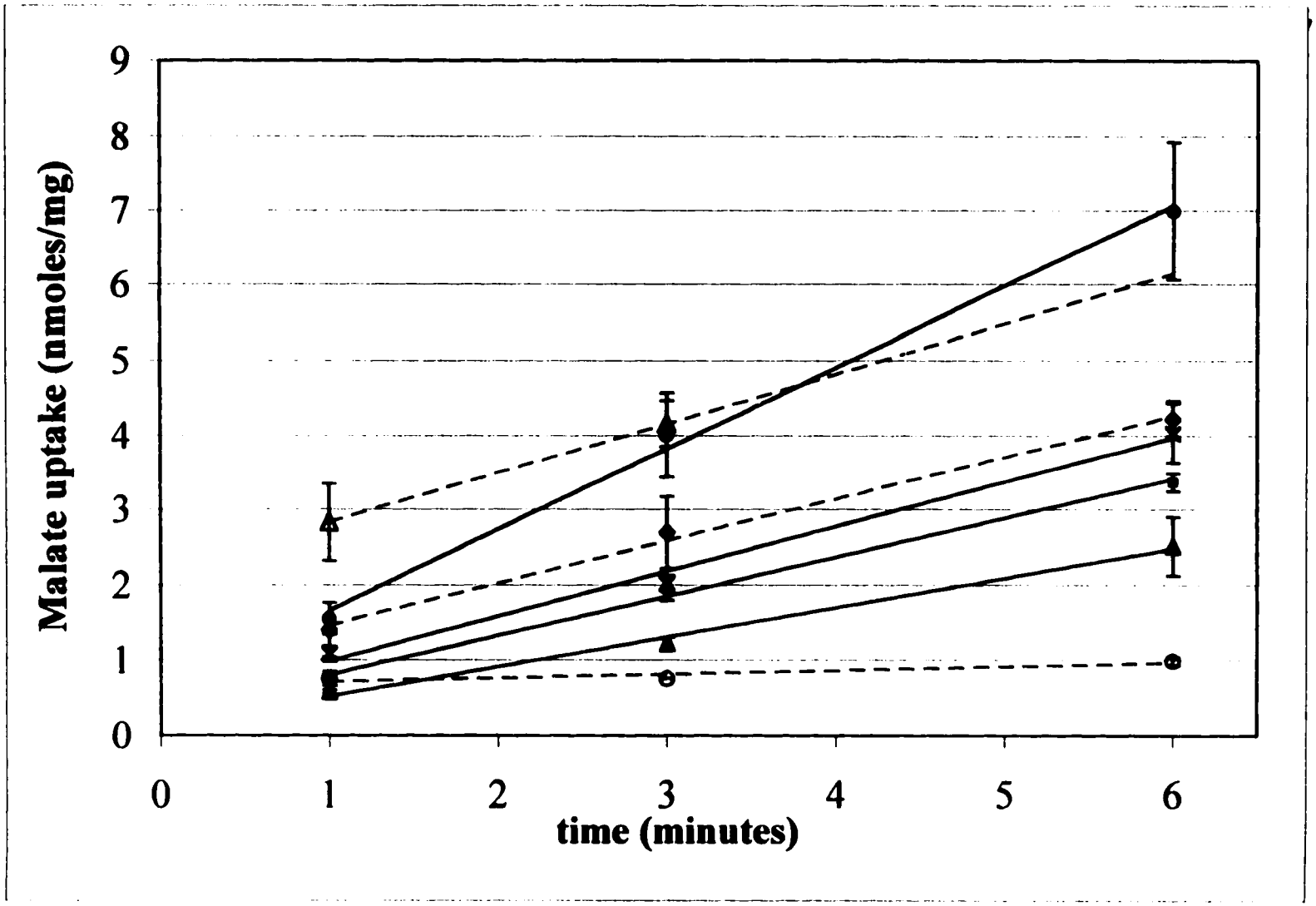
Malate uptake (nmoles/mg)
9
8
7
6
5
4
3
2
1
0
0
1
2
3
4
5
6
time (minutes)

Figure 7.13. Michaelis-Menten plot of MaeP mediated malate transport in *R. leguminosarum* strain RIK372 (*dctA*$^-$, *Pdme-maeP*). Data points represent the average of triplicate assays.

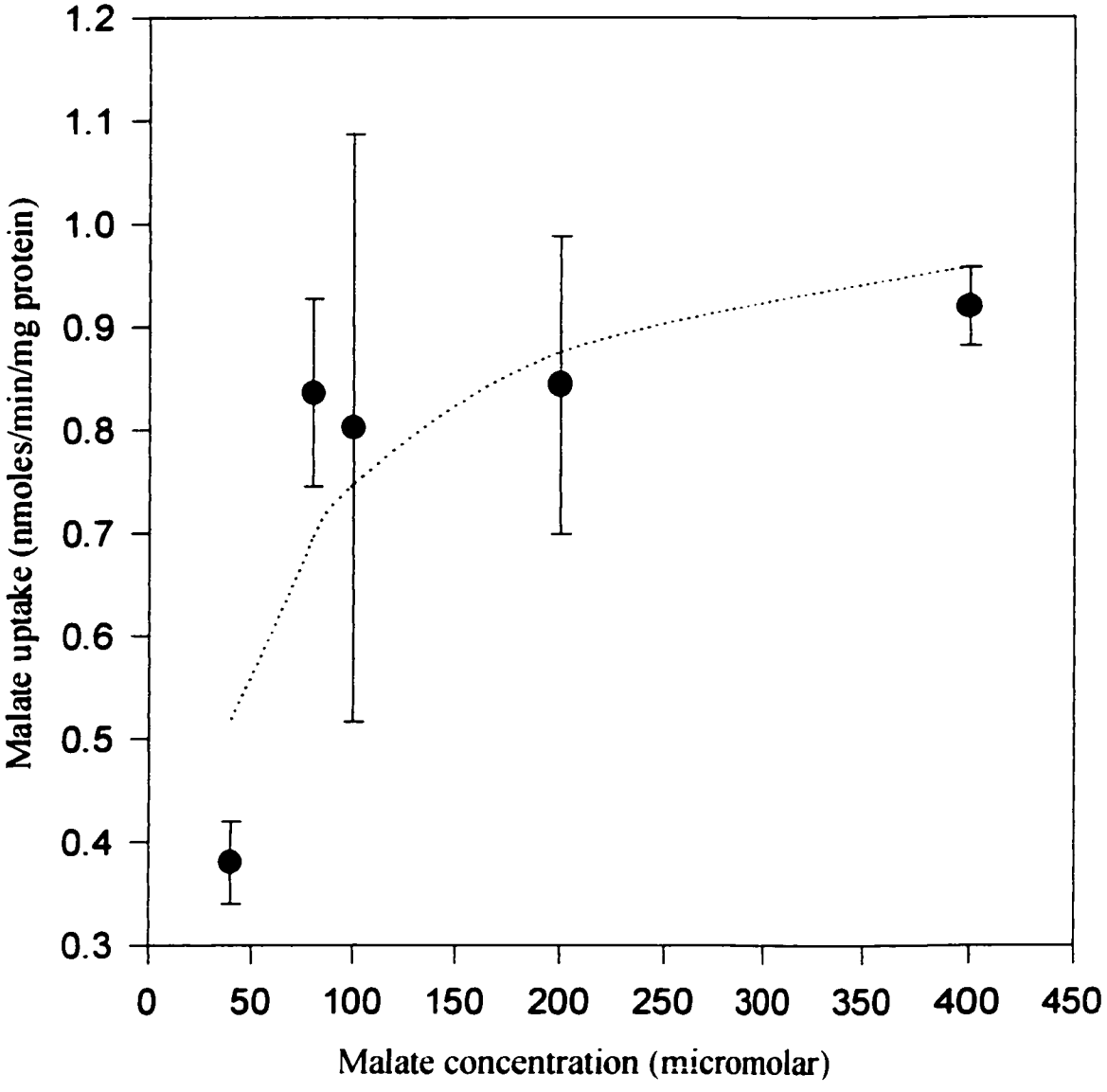
1.2
1.1
1.0
0.9
0.8
0.7
0.6
0.5
0.4
0.3
Malate uptake (nmoles/min/mg protein)
0
50
100
150
200
250
300
350
400
450
Malate concentration (micromolar)

succinate and malate are the dominant carbon compounds available. Photosynthetic sucrose is translocated to the nodule and metabolized to organic acids such as phosphoenolpyruvate (PEP) and this is believed to be converted to malate by the high levels of activity of PEP carboxylase and malate dehydrogenase in the plant tissue. Further evidence was provided by several $^{14}CO_2$ labeling studies with nodules, which have shown, that malate is the dominant carbon source produced (Vance *et al.*, 1983, Kouchi and Nakaji, 1985, Snapp and Vance, 1986). In order to be utilized by the metabolic machinery of the bacteroid, the carbon sources must traverse both the host derived peribacteroid membrane and the bacteroid membrane. The peribacteroid membrane is relatively impermeable to sugars but does contain a dicarboxylate transporter capable of rapidly transferring C_4-dicarboxylic acids to the bacteroid (Streeter, 1987, Day *et al.*, 1989). In addition to this, studies with bacteroids themselves show that they are capable of taking up C_4-dicarboxylates at rates significantly higher than sugar compounds (Salminen and Streeter, 1987, Udvardi *et al.*, 1988). Genetic studies with *Rhizobiacea* that are deficient for C_4-dicarboxylate transport revealed that they are uniformly unable to fix atmospheric nitrogen in association with their respective plant hosts (Ronson *et al.*, 1981, Finan *et al.*, 1983). Taken together, this body of evidence suggests that C_4-dicarboxylates are the dominant carbon source made available to the bacteroid as a source of energy and reductant for nitrogen fixation.

The availability of a malate specific permease, *maeP* from *S. bovis*, allowed us to investigate whether malate alone can support symbiotic N_2-fixation. MaeP, like DctA, requires an energized membrane for function and its activity can be disrupted by the

addition of the ionophores nigericin and valinomycin (Finan *et al.*, 1981, Kawai *et al.*, 1997). Unlike DctA, MaeP does not transport succinate or fumarate and shows no loss in transport activity in their presence (Kawai *et al.*, 1997). MaeP is also believed to be a proton symporter based on its high level of activity with decreasing pH (Kawai *et al.*, 1997). This matches well with the presumed symporter activity of DctA as its believed that DctA imports both H^+ and malate from the peribacteroid space driven by the pH gradient of the acidic peribacteroid space and the alkaline bacteroid (Udvardi and Day, 1997). Plant vacuoles, which share a great deal of similarity to peribacteroid membranes, are known to have internal pH values of approximately 5.5-6.0 (Roberts *et al.*, 1980) while studies with *S. meliloti* have shown that they maintain alkaline intracellular pH's when the external pH was varied from pH 5.6-7.2 (O'Hara *et al.*, 1989). *S. meliloti* growth is effected by external pH alterations and the presence of acetate and have shown that low pH and acetate are bacteriostatic in nature (Perez-Galdona and Kahn, 1994) and this may reflect the occurrence of free-living cells developing into senescent bacteroids during symbiotic nitrogen fixation. Therefore the peribacteroid space is most probably acidic in nature and this causes the slowing of growth of free-living cells and the formation of an intracellular alkaline pH condition.

In a previous report from this laboratory, the *maeP* gene was expressed from the *dme* promoter of the chromosome of *S. meliloti dctA*$^-$ mutants. The results showed that malate was transported in free-living cells but no N_2-fixing activity was observed under symbiotic conditions (Cowie, 1998). Several explanations were postulated for the lack of N_2-fixation in bacteroids including protein instability, increased proteolysis, or

insufficient protein concentrations. Subsequent experiments with free-living cells revealed that the *dctA*⁻, *Pdme-maeP* strains have very low malate uptake rates, approximately 20% that of *S. meliloti* cells expressing *dctA* (Voegele, unpublished results, Cowie, 1998). In view of the importance of the carbon source for N_2-fixation we wished to reinvestigate the apparent inability of *maeP* to restore N_2-fixation activity to *dctA*⁻ mutants of *S. meliloti*. In particular we wished to increase the *maeP* expression levels by both increasing the *maeP* copy number via cloning into a multi copy plasmid, and by cloning the *maeP* gene downstream of the strong *dctA* promoter.

When the *dme* and the *dctA* promoter were used to express the *maeP* gene in *dctA*⁻ *S. meliloti* strains, complementation studies on minimal media plates with malate as the sole carbon source showed that the malate permease was being produced and was capable of functioning in *S. meliloti*. Furthermore, the lack of growth of *dctA*⁻, *Pdme-maeP* strains on succinate as the sole carbon source verified previous observations that MaeP is a malate specific permease (Kawai *et al.*, 1997). Growth studies with malate as the sole carbon source revealed that the chromosomal insertion strains expressing *maeP* from the *dme* promoter (RmH948 and RmH949) grew at a slower rate relative to wild type *S. meliloti* cells and *S. meliloti* strains expressing the *Pdme-maeP* construct from the plasmid pBBR1MCS-5 (RmK299 and RmK300) but both reached the same terminal optical density over a period of 60 hours. A reverse situation was seen with the *PdctA-maeP* construct as the chromosomal insertions (RmK380 and RmK381) grew at a faster rate (but comparable to the *Pdme-maeP* plasmid born strains RmK380 and RmK381) than the plasmid born copy strains but both reached the same terminal optical density

over a period of 60 hours. These results would indicate that over time the malate permease can transport enough malate to support wild type levels of growth, however this does not reveal the levels of transport.

Malate uptake rates show that the chromosomal *Pdme-maeP* construct has the lowest rate of transport, 10% relative to wild type, while the plasmid born *Pdme-maeP* construct has 19% the rate of transport relative to wild type *S. meliloti*. By utilizing the Briggs-Haldane equation, the K_m for MaeP determined in this study, and the malate uptake determined at 40 μM malate we were able to determine a theoretical V_{max} for the malate permease in order to compare malate uptake rates with DctA. When the theoretical V_{max} is considered the chromosomal *Pdme-maeP* construct has 4.3 nmoles/min/mg or 17% that of wild type *S. meliloti* cells while the plasmid born *Pdme-maeP* construct has 9.9 nmoles/min/mg or 40% that of wild type *S. meliloti* cells. This data compares favorably with the growth curve data showing that the chromosomal insertion grows at a lower rate than the plasmid copy with malate as the sole carbon source. When the malate permease is expressed from the *dctA* promoter the chromosomal insertion has approximately 21% the transport rate while the plasmid born construct has 31% the transport rate of wild type *S. meliloti* respectively. When the theoretical V_{max} is considered the chromosomal *PdctA-maeP* construct has 10.6 nmoles/min/mg or 43% that of wild type *S. meliloti* cells while the plasmid born *PdctA-maeP* construct has 15 nmoles/min/mg or 61% that of wild type *S. meliloti* cells. What is unusual is that the strains expressing *PdctA-maeP* from the plasmid has a lower growth rate relative to wild type cells or strains with the *PdctA-maeP* construct inserted into the

chromosome. Since the *dctA* promoter is known to be constitutively expressed in the absence of DctA (Ronson and Astwood, 1985, Ronson *et al.*, 1987, Yarosh *et al.*, 1989), this may indicate that over production of the malate permease due to increased copy number is detrimental to the cell.

Plant assays revealed that the *Pdme-maeP* chromosomal insertion strains had less than 1% acetylene reduction capability relative to wild type levels and plant dry weights that were indistinguishable from negative controls. In contrast, the *dctA*⁻ strains carrying the malate permease in the pBBR1MCS-5 vector had acetylene reduction activity 38-46% relative to wild type nodules and plant dry weights 23-26% relative to wild type inoculated plants. Sampling of the nodule contents revealed that all cells isolated from the *dctA*⁻ strains expressing *maeP* were incapable of growth on succinate but were able to grow on malate as the sole carbon source indicating that neither contamination with wild type cells nor the generation of *dctA* revertants was responsible for the intermediate symbiotic phenotype. The high rate of plasmid retention when *maeP* was present on the pBBR1MCS-5 indicates that the gene offers a competitive advantage to the bacteroids and thus is maintained to a higher extent relative to pBBR1MCS-5 alone. Plant tests undertaken with strains expressing the malate permease from the *dctA* promoter revealed that the chromosomal insertions of the *PdctA-maeP* had 1% acetylene reduction activity and 12-14% plant dry weight relative to wild type inoculated plants. In comparison the strains carrying the *PdctA-maeP* plasmid born constructs had 31-49% acetylene reduction activity and 27-30% plant dry weight relative to wild type plants inoculated with wild type strains. Sampling of the nodule contents revealed that all cells isolated from the

dctA⁻ strains expressing *maeP* were incapable of growth on succinate but were able to grow on malate indicating that neither contamination with wild type cells nor the creation of revertants was not responsible for the intermediate phenotype. The high rate of plasmid retention when *maeP* was present on the pBBR1MCS-5 indicates that the gene offers a competitive advantage to the bacteroids and thus is maintained to a higher extent relative to pBBR1MCS-5 alone. These results show that expression of *maeP* in *S. meliloti* from a constitutive promoter or symbiotically induced promoter in a single copy situation is insufficient to yield nitrogenase activity or plants that are appreciably different from the *dctA*⁻ controls. However, if the copy number of the gene and its associated promoter is increased, nitrogenase activity and plant dry weights increase to levels that result in an intermediate symbiotic N_2 fixation phenotype. These results indicate that the level of promoter activity does not affect the level of nitrogen fixation or plant dry weight, therefore, there may be a physical constraint within the bacteroid that limits MaeP function.

To evaluate if these observations are conserved in the *Rhizobiaceae*, experiments were carried out using the pea plant symbiont *R. leguminosarum*. The *Pdme-maeP* bearing strains show 44-46% acetylene reduction activity and 84% plant dry weight relative to plants inoculated with the wild type strain. These acetylene reduction values compare favorably with the results obtained in *S. meliloti* and indicate that a comparable level of nitrogen fixation is occurring. In comparison, plants inoculated with the *dctA*⁻ strains of *R. leguminosarum* and the uninoculated control had dry weights of 32%-50% of wild type inoculated plants (Table 7.4). Therefore for both *S. meliloti* and *R.*

leguminosarum it would seem that the malate permease expressed from the *dme* promoter is only capable of a half the activity of the native DctA system. The elevated dry weights as compared to *S. meliloti* are most likely due to the large nitrogen stores in pea seeds that do not exist in alfalfa. Plant tests with the *PdctA-maeP* constructs in *R. leguminosarum* revealed that these strains were capable of increasing nitrogen fixation and plant dry weights that were indistinguishable from wild type inoculated plants. This is a different situation from that observed in *S. meliloti* where the rates of nitrogen fixation and plant dry weight did not differ between *maeP* expression from the *dme* or *dctA* promoter. It is possible that the *dctA* promoter of *S. meliloti* is more active in *R. leguminosarum* and therefore results in higher levels of malate permease production. This increase in net protein could result in more malate uptake being achieved and would result in higher levels of symbiotic nitrogen fixation.

The level of malate uptake recorded for wild type *R. leguminosarum* bacteroids was comparable to previous studies carried out on plants grown for similar periods of time (rates of 7.4 nmoles/min/mg for 31 day old plants) (Finan *et al.*, 1983). The uptake rates of our study show that strains expressing the malate permease from the *dme* promoter (RIK371 and RIK372) have approximately 9% the uptake rate of wild type cells while the strain expressing the malate permease from the *dctA* promoter (RIK379) has a malate uptake rate approximately 10% that of wild type strains. When the theoretical V_{max} is considered the *Pdme-maeP* construct has 1.14 nmoles/min/mg (1.15 nmoles/min/mg for RIK371) or 18% that of wild type *R. leguminosarum* bacteroids while the *PdctA-maeP* construct has 1.53 nmoles/min/mg or 20% that of wild type *R.*

leguminosarum bacteroids. Interestingly RIK379 bacteroids have an uptake rate 1.3 times that of RIK371 and RIK372 and based upon the observations in the plant assay this increased rate of uptake, slight though it is, is sufficient to support symbiotic nitrogen fixation and plant growth that is indistinguishable from wild type inoculated plants. When DctA and MaeP are co-expressed the result is in an increase of malate uptake of approximately 190%. This indicates that the two transport systems may work in an additive manner and increase net carbon transport however no increase in either plant dry weight or acetylene reduction activity was noted. Since bacteroids relying solely on the malate permease will no doubt be suffering from limited carbon availability this condition would result in a bacteroid impaired in function due to a limited supply of reductant. When the DctA and MaeP transporters are co-expressed this carbon limitation would no longer exist and the bacteroid would be able to function at optimal levels including the function of the malate permease. The assumption therefore is that a transport rate of 1 nmole/min/mg may be the optimum rate of activity of MaeP in bacteroids as demonstrated by RIK370. As expected (Finan *et al.*, 1981), succinate inhibited malate uptake via the DctA system in pea bacteroids (Table 7.6, strains RIK367 and RIK370), however malate uptake in *dctA*$^-$ bacteroids expressing *maeP* showed no inhibition by succinate which is consistent with the inability of MaeP to transport succinate (Kawai *et al.*, 1997). Aspartate also failed to show any inhibition of malate uptake via the MaeP system and therefore should not be transported by the malate permease. This result is particularly important given previous hypothesis suggesting that amino acids may be a carbon and nitrogen source for symbiotic N_2-fixation (Kahn *et al.*,

1985). This theory is supported by the fact that glutamine synthetase (De Bruijn *et al.*, 1989, Somerville *et al.*, 1989) and glutamate synthase activities (Lewis *et al.*, 1990, Osbourne *et al.*, 1980) are very low in *S. meliloti* bacteroids and therefore they may require a nitrogen source from the host. Thus, nitrogen exchange would ensure that the more nitrogen fixed and donated to the plant host the more substrate is made available to the bacteroid. The theory is also supported by the fact that the DctA system is capable of transporting aspartate (Watson *et al.*, 1993) and a *S. meliloti* strain deficient for aspartate aminotransferase, an enzyme that converts aspartate to oxaloacetate, is unable to support symbiotic nitrogen fixation (Rastogi *et al.*, 1991, Watson and Rastogi, 1993). The authors suggest that aspartate is an essential substrate for bacteroids and that the fact that *dctA* mutants are symbiotically impaired could be due to their inability to transport aspartate rather than C_4-dicarboxylic acids (Rastogi and Wastson, 1991). If the transport of aspartate is occurring in *S. meliloti* it could explain why MaeP is not capable of inducing a successful symbiotic N_2 fixation phenotype since the bacteroids would not have access to a nitrogen source. By comparison our results with *R. leguminosarum* show that although aspartate aminotransferase may be required for symbiotic nitrogen fixation it is not due to its ability to metabolize aspartate donated directly from the plant host to oxaloacetate to maintain the TCA cycle or as a nitrogen source. It is possible that aspartate aminotransferase, if it is required in *R. leguminosarum* for nitrogen fixation, is most likely utilized for amino acid production. Our data indicates that *R. leguminosarum* does not require aspartate as a nitrogen source to maintain symbiotic nitrogen fixation and must obtain nitrogen from a so far uncharacterized pathway.

With the acquisition of kinetic data regarding the efficiency of the malate permease we can now biochemically compare MaeP to the DctA system of the *Rhizobiaceae*. Previous succinate uptake assays with *S. meliloti* have revealed that DctA has a K_m of 5.3 μM and a V_{max} of 23.9 nmoles/min/mg (Engelke *et al.*, 1987) as determined for free-living cells while for bacteroids a K_m of 61.7 μM and a V_{max} of 18.7 nmoles/min/mg for malate was obtained (McRae *et al.*, 1989). The DctA system has also been characterized in *R. leguminosarum* and shows a K_m of 2.6 μM and V_{max} of 78 nmoles/min/mg for succinate in free-living cells (Finan *et al.*, 1981) and a K_m of 1.5 μM and a V_{max} of 22.9 nmoles/min/mg in bacteroids (Finan *et al.*, 1983). Estimates of the kinetic parameters for MaeP has revealed that it has a K_m of 41.4+/-3.35 μM and a V_{max} of 1.10+/-0.38 nmoles/min/mg. This estimate of the K_m value is reasonable as the V_o values at 80 μM are approximately double those obtained for 40 μM (Table 7.1) and estimates of the V_{max} at both concentrations are similar. Since the malate permease has an exceedingly high K_m for its substrate and a low V_{max} relative to the DctA transporter of the *Rhizobiaceae* it is possible that this system would be limited in terms of it ability to deliver enough substrate for the TCA cycle and this would result in limited symbiotic nitrogen fixation. This hypothesis is limited by the fact that the relative concentrations of substrate in the nodule would control enzyme efficiency. It is possible that there is only sufficient malate present in the nodules of alfalfa to yield approximately 40% nitrogenase activity and 25% plant dry weights when the malate permease is expressed in a DctA deficient *S. meliloti* strain. Estimates of carbon content for alfalfa nodule tissue has shown that there is approximately 137 nmoles of succinate per gram of fresh nodule

tissue (0.1 mM) while malate is present at approximately 810 nmoles per gram of fresh nodule tissue (0.6 mM) (McRae *et al.*, 1989). In *Phaseolus vulgaris*, the host for *R. leguminosarum*, malate makes up 54% of the organic acids found in the host cell cytosol (Antoni and Sprent, 1978). The relative importance or amounts of certain carbon sources provided by the plant host could influence the ability of the *Rhizobiaceae* to form a successful N_2 fixing symbiotic association. Therefore, if pea nodules contain higher levels of malate relative to alfalfa nodules, this would explain why *R. leguminosarum* strains expressing the malate permease from the *dctA* promoter are capable of sustaining wild type levels of symbiotic nitrogen fixation while *S. meliloti* strains expressing the same construct are only capable of supporting partial symbiotic nitrogen fixation. An example of this differential symbiotic response based upon host physiology was obtained through studies of bacterial mutants defective in phosphoenolpyruvate carboxykinase (PCK) enzyme which is responsible for the first step in gluconeogenesis by converting oxaloacetate to phosphoenolpyruvate. A *R. leguminosarum* strain deficient for PCK is able to form bacteroids capable of supporting symbiotic N_2 fixation (McKay *et al.*, 1985) while the symbiotic phenotype obtained with a *pck*$^-$ mutant of the broad host range *Rhizobium* NGR234 was host dependent (Osteras *et al.*, 1991). This indicates that different plant hosts make available to their bacterial symbionts different carbon sources and the ability of the bacteria to utilize these carbon sources is reflected in their success at symbiotic nitrogen fixation. It is also possible that wild type levels of nitrogen fixation can only occur if the bacteroids can exploit all C_4-dicarboxylates present in the nodule. The DctA system has been shown to take up fumarate (Bolton *et al.*, 1986) and aspartate

(McRae *et al.*, 1989, Watson *et al.*, 1993) and these carbon compounds, along with succinate and malate may be utilized to varying extents. Since the malate permease cannot transport these compounds it may limit the carbon sources available to the bacteroids. Therefore it is possible that alfalfa plants relative to pea plants produce a wider carbon source selection for the bacteroids to utilize.

Chapter 8

Cofactor switching of TME in *S. meliloti*

Abstract

Previous results in our laboratory indicated that TME is not able to functionally replace the requirement of DME for symbiotic nitrogen fixation. Possible explanations for this are that *tme* is not expressed to sufficient levels in bacteroids, that TME has different kinetic properties relative to DME, or that availability of the respective cofactors is limiting. Experiments designed to test each of these possibilities were carried out. Increased expression of *tme* in bacteroids was not sufficient to overcome the loss of *dme*. Biochemical characterization of TME revealed that it had similar K_m's for substrate and cofactor relative to DME. To investigate the possibility that a high NADPH/NADP ratio in bacteroids limits TME activity, we attempted to alter the cofactor specificity of TME from $NADP^+$ to NAD^+. Two strategies were adopted one revolving around the creation of chimeric malic enzymes with varying lengths of the N-terminal region of DME fused to the C-terminal region of TME while the second strategy involved creating point mutations within the putative cofactor binding site. In both cases no functional enzymes were obtained.

Methods and Materials

See Chapter 2 for all materials and methods. Bacterial strains and plasmids are listed in Table 2.1. Chimeric malic enzymes were produced by PCR amplification of three regions of *dme* comprising varying lengths of the N-terminal region of the open reading frame (Figure 8.1). The –48 M13 reverse primer 5'-AGC GGA TAA CAA TTT CAC ACAG GA-3' was used in conjunction with either primer 5'-CTG CCT C**G**A **G**CT CCT CGT CAC GC-3', primer 5'-ACC ATC CG**G** TCG ACC GTC GGT GCG-3', or primer 5'-TCT CCT GCG CA**T** **GC**A CGG CTT TCC ACT CG-3' (bases in bold are alterations of the *dme* sequence in order to generate restriction sites *Sst*I, *Sal*I, and *Sph*I, respectively that match with pre-existing *tme* sites). PCR conditions were denaturing at 94°C for 30 seconds, annealing at 55°C for 30 seconds, extension at 72°C for 1 minute for a total of 25 cycles. The PCR products were subcloned into pUC119 via *Hind*III/*Sst*I, *Hind*III/*Sal*I, *Hind*III/*Sph*I, and were sequenced to verify integrity of the constructs and then ligated upstream of the C-terminal region of the *tme* gene carried on pTH517 by digesting with appropriate enzymes; *Hind*III/*Sst*I, *Hind*III/*Sal*I, or *Hind*III/*Sph*I, to produce pTH601, pTH602 and pTH603 respectively. The resulting constructs were then transformed into the malic enzyme deficient *E. coli* strain EJ1321 (Hansen and Juni, 1975) to test for complementation. To express these chimeric genes in *S. meliloti*, pTH601, pTH602, and pTH603 were digested with *Hind*III and *Kpn*I and inserted into similarly digested pBBR1MCS-5 plasmids to produce constructs, pTH604, pTH605, and pTH606, respectively. The plasmids were then mobilized into RmH194 via a triparental mating. The point mutations at amino acid residues 113 and 131 of *tme* were carried out

as described in Chapter 2. The resulting point mutants of pTH607 were transferred to pTH517 by digestion with *Hind*III and *Sst*I. The resulting ligations replaced the *dme* promoter and the first 376 bp of *tme* of pTH517 with the *pdme-tme* point mutation constructs. The ligation to the *Sst*I site of the C-terminal region of *tme* resulted in a reconstituted *tme* gene with single amino acid alterations at amino acid residue 113 (pTH651) or 131 (pTH650). To express these altered proteins in *S. meliloti*, *Hind*III/*Kpn*I digests were carried out on pTH650 and pTH651 and the 3 kb fragments were ligated into pBBR1MCS-5 to produce pTH669 and pTH670 respectively. The plasmids were then mobilized into RmH194 via a triparental mating.

Figure 8.1. Production of chimeric malic enzymes with DME N-terminal regions. Boxes indicate highly conserved regions within the prokaryotic malic enzymes; **A**, putative substrate binding site, **B** and **E**, glycine rich regions/putative cofactor binding site(s), **F**, highly conserved domain of prokaryotic malic enzymes.

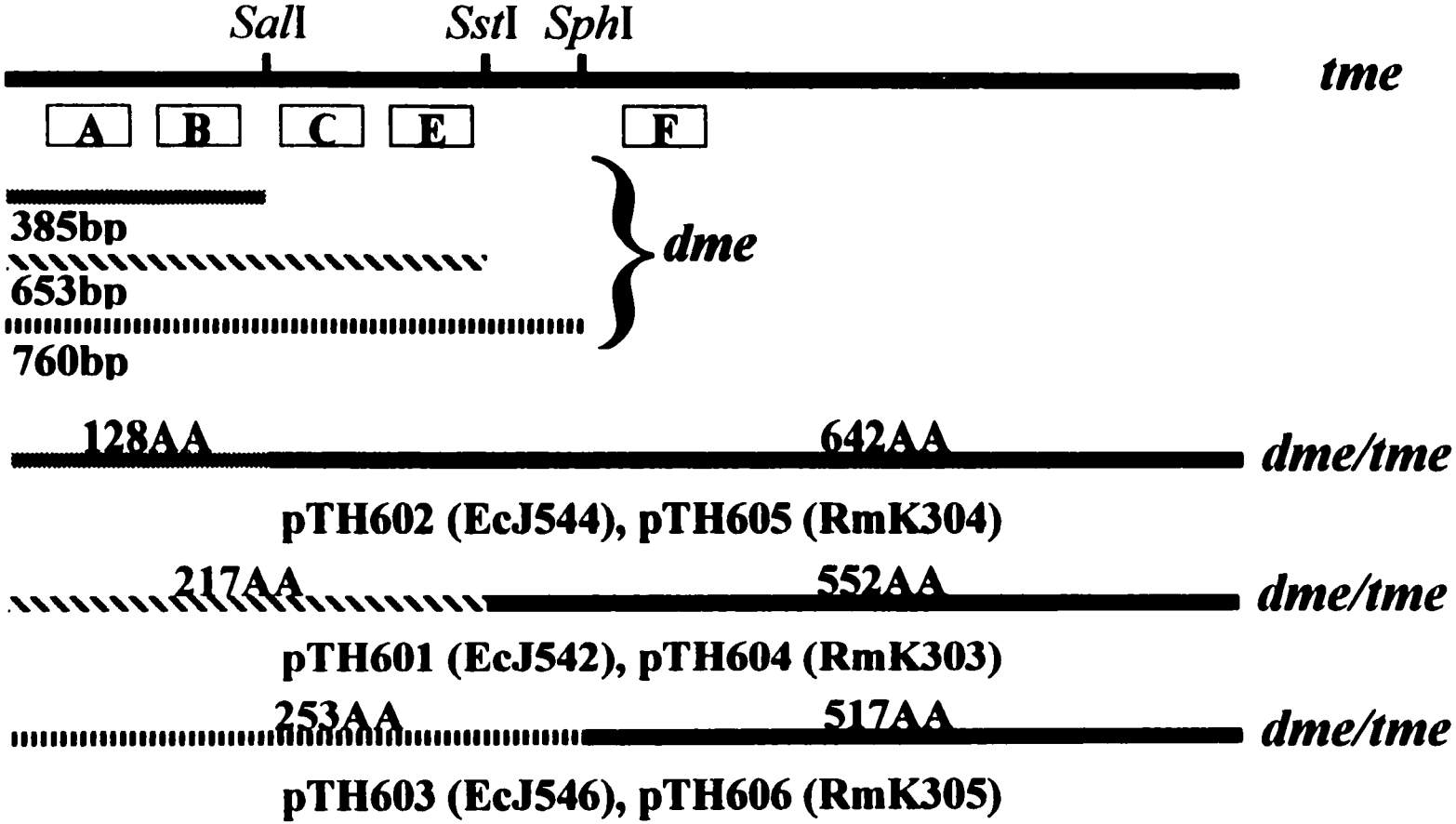
SalI
SstI
SphI
tme
A
B
C
E
F
385bp
653bp
760bp
dme
128AA
642AA
dme/tme
pTH602 (EcJ544), pTH605 (RmK304)
217AA
552AA
dme/tme
pTH601 (EcJ542), pTH604 (RmK303)
253AA
517AA
dme/tme
pTH603 (EcJ546), pTH606 (RmK305)

Results

Generation and analysis of chimeric malic enzymes

Due to limited information regarding the essential elements required for cofactor binding a strategy was adopted to replace large regions of the N-terminal region of TME with the corresponding region from DME. This strategy was adopted since the amino acid sequences indicative of $NAD(P)^+$ binding were localized to two areas designated B and E (Chapter 3) in the N-terminal region of the malic enzymes (Figure 8.1 and Chapter 3). Region A has been implicated in substrate or divalent metal ion binding due to the presence of a conserved tyrosine residue in this domain (Hsu, 1982, Viljoen *et al.*, 1994). Region B and E both contain the glycine and alanine motifs attributed to Rossman fold domains which have been implicated in cofactor binding (Scrutton *et al.*, 1990) and region B has conserved lysine residues that have been shown to play a role in $NAD(P)^+$ binding (Hsu, 1982). Region C has a conserved cysteine residue which is believed to be located at the active site and may be responsible for coordinating the binding of the substrate or the divalent metal ion (Hsu *et al.*, 1992). The plasmids carrying the chimeric genes were introduced into competent *E. coli* strain EJ1321 in order to determine if a modified gene would allow EJ1321 to grow on minimal media with succinate as a sole carbon source. No complementing clones were recovered indicating that no malic enzyme activity was present. Extracts were assayed for their ability to convert malate to pyruvate. Pyruvate formation assays were carried out (Table 8.1) and showed that the chimeric malic enzymes had no activity above that of the negative control strain EJ1321 with either NAD^+ or $NADP^+$ as cofactor. Western blots were utilized in order to

Table 8.1. Pyruvate formation assay results of chimeric malic enzymes in malic enzyme deficient *E. coli* strain.

Strain	Genotype	NAD^+-dependent activity (nmoles/min/mg)[a]	$NADP^+$-dependent activity (nmoles/min/mg)[a]	MDH activity (nmoles/min/mg)[b]
EJ1321	*dme-tme-*	73.2+/-2.0	ND	935+/-21
EcG456	EJ1321 pTH139 (*dme*)	237+/-2.0	77.3+/-1.3	1212+/-13
EcJ202	EJ1321 pTH392 (*tme*)	61.2+/-0.9	567+/-22.7	981+/-10
EcJ542	EJ1321 pTH601 (DME217/TME552)	77.9+/-11.1	ND	1177+/-32
EcJ544	EJ1321 pTH602 (DME128/TME642)	65.1+/-1.9	3.5+/-0.6	1345+/-31
EcJ546	EJ1321 pTH603 (DME253/TME517)	49.6+/-3.2	ND	1311+/-23

[a] specific activity is expressed as nmoles of pyruvate formed /minute/mg protein with the mean +/- standard error of triplicate samples.

[b] specific activity is expressed as nmoles NADH formed /minute/mg protein with the mean +/- standard error of triplicate samples

ND none detected

determine if any intact protein subunits were being produced and verify that lack of activity was not due to the insertion of a stop codon within the reading frame of the chimeric gene. Binding with the TME antibody revealed that a full-length subunit was produced and, in addition, two bands of approximately 50 kDa and 40 kDa were also detected (Figure 8.2). The 40 kDa band was more pronounced for strain EcJ542 and was less evident for strain EcJ544 while the 50 kDa fragment is most pronounced in strain EcJ544. Staining with the DME antibody showed that the 50 kDa polypeptide preferentially binds to this antibody for all strains tested with EcJ542 showing a more intense staining than EcJ544 or EcJ546 (Figure 8.3). Since no malic enzyme activity was obtained and the chimeric proteins appeared to be breaking down in *E. coli*, the chimeric genes were subcloned into the vector pBBR1MCS-5 and expressed in *S. meliloti* strain RmH194 (*dme-*, *tme-*, *pck-*, *pod*-1). No growth was observed on minimal media plates with succinate as the sole carbon source revealed no growth indicating that the chimeric malic enzymes were none functional. Pyruvate formation assays revealed activity with NAD^+ as the cofactor that was elevated relative to the negative control but these values were only 17%-25% the activity of the positive control overexpressing *dme* indicating that these enzymes were nonfunctional. When $NADP^+$ was utilized as a cofactor limited activity was seen for all constructs relative to the negative control strain with RmK304 showing approximately 43% activity relative to the positive control strain overexpressing *tme* while RmK303 and RmK305 showed 8% and 25% activity relative to the positive control strain (Table 8.2). This would indicate that RmK304 may retain some enzyme activity but in light of the complementation results and the fact that RmK304 extracts are

Figure 8.2. Western blot of EJ1321 *E. coli* cell free extracts containing chimeric malic enzymes stained with TME specific antibodys. Large arrow shows position of TME, chevron shows production of 50 kDa polypeptide while small arrow shows production of 40 kDa polypeptide. 2 μg of protein was loaded for all samples while 0.2 μg of protein was loaded for control strain EcJ202. Numbers to the right represent molecular weight markers in kDa.

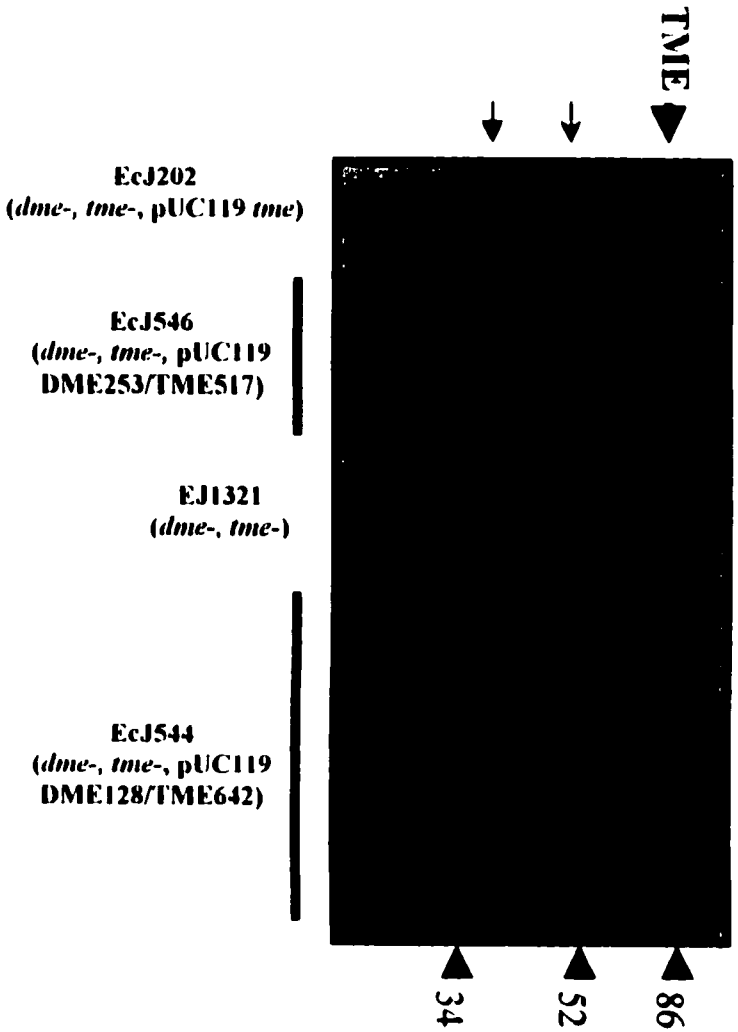
TME
EcJ202
(dme-, tme-, pUC119 tme)
EcJ546
(dme-, tme-, pUC119
DME253/TME517)
EJ1321
(dme-, tme-)
EcJ544
(dme-, tme-, pUC119
DME128/TME642)
34
52
86

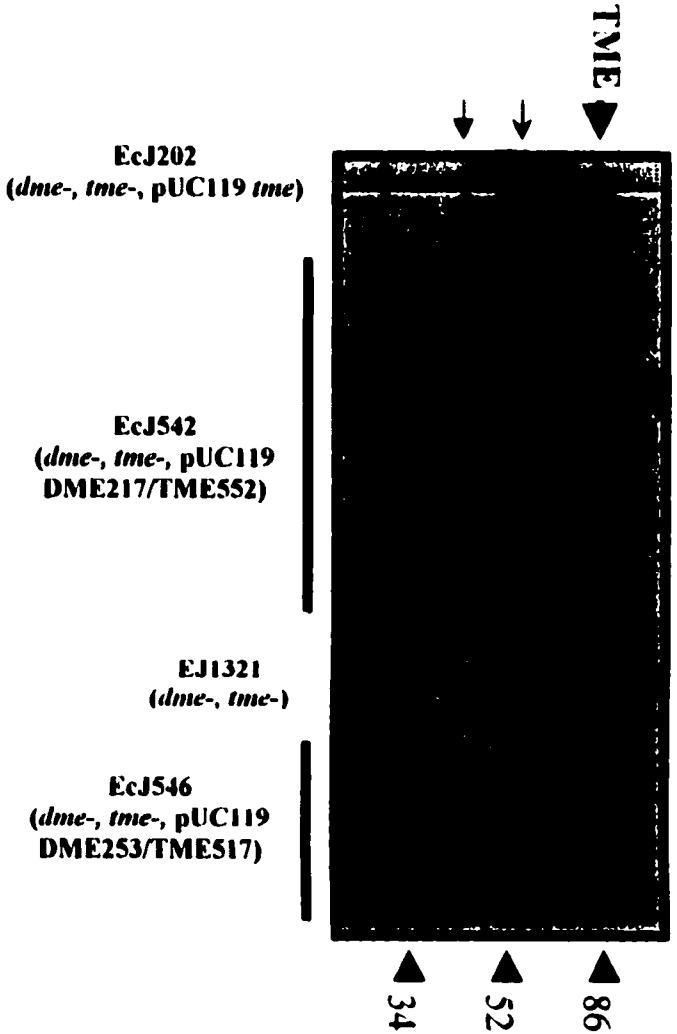
TME
EcJ202
(dme-, tme-, pUC119 tme)
EcJ542
(dme-, tme-, pUC119
DME217/TME552)
EJ1321
(dme-, tme-)
EcJ546
(dme-, tme-, pUC119
DME253/TME517)
34
52
86

Figure 8.3. Western blot of EJ1321 cell free extracts containing chimeric malic enzymes stained with DME specific antibodys. Large arrow shows position of DME while chevron shows production of 50 kDa polypeptide. 2 μg of protein was loaded for all samples while 0.2 μg of protein was loaded for control strains EcG456 and EcJ202. Numbers to the right represent molecular weight markers in kDa.

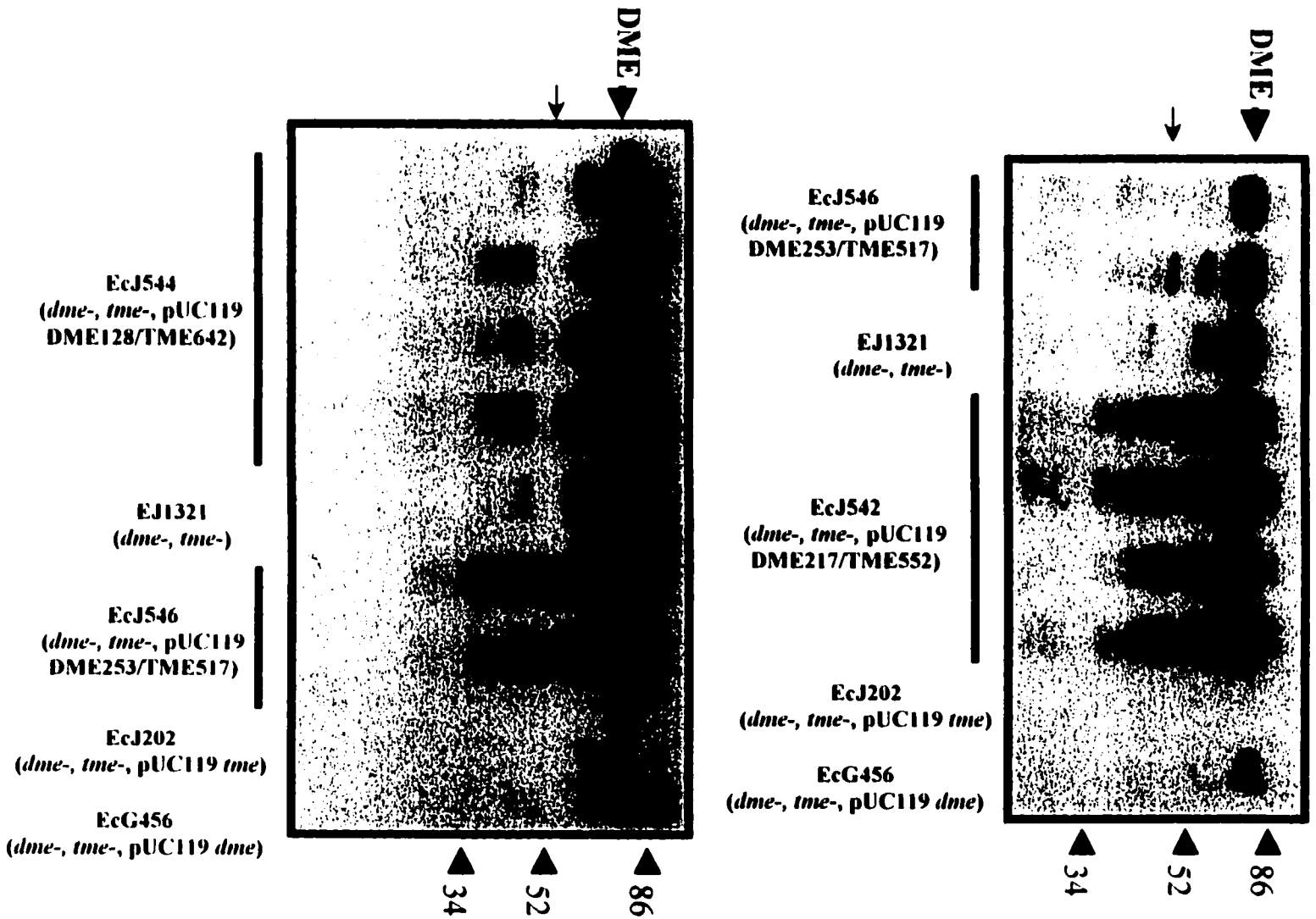
DME
EcJ544
(dme-, tme-, pUC119
DME128/TME642)
EJ1321
(dme-, tme-)
EcJ546
(dme-, tme-, pUC119
DME253/TME517)
EcJ202
(dme-, tme-, pUC119 tme)
EcG456
(dme-, tme-, pUC119 dme)
34
52
86
DME
EcJ546
(dme-, tme-, pUC119
DME253/TME517)
EJ1321
(dme-, tme-)
EcJ542
(dme-, tme-, pUC119
DME217/TME552)
EcJ202
(dme-, tme-, pUC119 tme)
EcG456
(dme-, tme-, pUC119 dme)
34
52
86

Table 8.2. Pyruvate formation assay results of chimeric malic enzymes in malic enzyme deficient *S. meliloti* strain.

Strain	Genotype	NAD^+-dependent activity (nmoles/min/mg)[a]	$NADP^+$-dependent activity (nmoles/min/mg)[a]	MDH activity (nmoles/min/mg)[b]
RmK298	Rm1021, pBBR1MCS-5	93+/-2.2	46.7+/-4.1	202+/-15
RmK303	RmH194, pTH604 (DME217/TME552)	156+/-1.2	27.3+/-2.2	213+/-4
RmK304	RmH194, pTH605 (DME128/TME642)	130+/-3.7	147+/-1.8	373+/-7
RmK305	RmH194, pTH606 (DME253/TME517)	107+/-1.3	86.1+/-1.6	182+/-1
RmK306	RmH194, pBBR1MCS-5	40.1+/-1.1	ND	150+/-1
RmK307	RmH194, pTH598 (*dme*)	632+/-3.1	253+/-2.1	465+/-13
RmK308	RmH194, pTH599 (*tme*)	31.1+/-1.1	337+/-0.9	183+/-14

[a] specific activity is expressed as nmoles of pyruvate formed /minute/mg protein with the mean +/- standard error of triplicate samples.

[b] specific activity is expressed as nmoles NADH formed /minute/mg protein with the mean +/- standard error of triplicate samples

ND none detected

Figure 8.4. Western blot of *S. meliloti* cell free extracts containing chimeric malic enzymes stained with **A**. TME specific antibodys and **B**. DME specific antibodys. Arrows shows position of TME and DME respectively. 2 μg of protein was loaded for all samples. Numbers to the right represent molecular weight markers in kDa.

A
TME
86
52
34
RmK305 (pckA1, pod-1, dme1, tme4, pBBR1MCS-5 DME253/TME517)
RmK303 (pckA1, pod-1, dme1, tme4, pBBR1MCS-5 DME217/TME552)
RmK304 (pckA1, pod-1, dme1, tme4, pBBR1MCS-5 DME128/TME642)
RmK308 (pckA1, pod-1, dme1, tme4, pBBR1MCS-5 tme)
RmK307 (pckA1, pod-1, dme1, tme4, pBBR1MCS-5 dme)
RmK306 (pckA1, pod-1, dme1, tme4 , pBBR1MCS-5)
RmK298 (wild type)
B
DME
86
52
RmK298 (wild type)
RmK306 (pckA1, pod-1, dme1, tme4 , pBBR1MCS-5)
RmK307 (pckA1, pod-1, dme1, tme4, pBBR1MCS-5 dme)
RmK308 (pckA1, pod-1, dme1, tme4, pBBR1MCS-5 tme)
RmK304 (pckA1, pod-1, dme1, tme4, pBBR1MCS-5 DME128/TME642)
RmK303 (pckA1, pod-1, dme1, tme4, pBBR1MCS-5 DME217/TME552)
RmK305 (pckA1, pod-1, dme1, tme4, pBBR1MCS-5 DME253/TME517)

unable to use NAD^+ this is unlikely and the elevated enzyme activity is probably a reflection of the insensitivity of the enzyme assay. Western blots were carried out and staining with TME antibodies revealed an 82 kDa subunit for all three chimeric proteins.The signal was more intense for RmK304 (Figure 8.4) than for strains RmK303 and RmK305. Staining with DME antibodies show that there is limited staining for all three chimeric proteins relative to the *dme* overexpressing strain RmK307 and Rm1021 (Figure 8.4).

Generation and analysis of point mutations in *tme*

In an attempt to alter the cofactor specificity of TME, two point mutations were produced within the putative cofactor binding site (region B in Figure 8.1) previously identified (Chapter 3). Alignments of the biochemically characterized prokaryotic malic enzymes revealed that the $NAD(P)^+$-dependent proteins had a conserved glycine 20 amino acids downstream from the glycine rich Rossman fold while TME had an aspartic acid residue (Figure 8.5). Since this represented an obvious difference in a region previously identified as being important for cofactor binding it was selected for substitution. In addition, DME contains an aspartic acid residue 38 amino acids down stream from the Rossman fold while TME has an asparagine residue. Since aspartic acid residues have been shown to be important for binding and interacting with the cofactor, this amino acid was selected for alteration. Site directed mutagenesis was carried out on plasmid pTH607 resulting in alterations at residue 113 (D to G) to produce pTH651 and residue 131 (N to D) to produce pTH650 which were verified by sequence analysis. Complementation studies with both plasmids in an EJ1321 background revealed that

neither construct was capable of supporting growth with succinate as the sole carbon source. $NAD(P)^+$-dependent pyruvate formation assays carried out on cell free extracts also showed that neither strain had any enzyme activity comparable to EJ1321 overexpressing *dme* or *tme* with only approximately 7%-30% residual activity (Table 8.3). Western blots carried out with cell free extracts from EcJ548 and EcJ550 showed that neither strain produced an 82 kDa subunit but instead a polypeptide of approximately 60 kDa polypeptide (Figure 8.6) was observed. Cloning of the *tme* point mutants into pBBR1MCS-5 and subsequent expression in RmH194 on minimal media with succinate as the sole carbon source revealed no growth of the *S. meliloti* strain indicating that the malic enzymes were nonfunctional. Enzyme assays supported these observations as no activity was obtained with NAD^+ with either point mutation (Table 8.4). There was limited enzyme activity with $NADP^+$ as cofactor for RmK402 (51% activity relative to the *tme* overexpressing strain) and this may indicate that this amino acid replacement, N to D at amino acid 131, is not as severe as the D to G alteration at position 113. Western blots (Figure 8.7) revealed that both RmK402 and RmK403 produced intact 82 kDa subunits indicative of wild type TME production indicating that loss of enzyme activity is not due to the insertion of a stop codon.

Figure 8.5. Putative cofactor region (region B) of biochemically characterized prokaryotic malic enzymes. Highlighted amino acid residues were targeted for site directed mutagenesis. BsME; *Bacillus stearothermophilus* malic enzyme, SbME; *Streptococcus bovis* malic enzyme, T; $NADP^+$-dependent enzyme, D/T; NAD^+-/$NADP^+$-dependent enzyme, D; NAD^+-dependent enzyme. * denotes identical amino acid residue, . denotes conserved amino acid residue.

```
TME   GLGNLGALASKPVMEGKAVLFKRFADVDSIDLEVDTENVDEFVNCVRFLGPSF T
DME   GLGNIGPLASKPVMEGKAVLFKKFAGIDVFDIEIDAPTVDRMVDVISALEPTF D/T
BsME  GLGDIGPYAAMPVMEGKAMLFKEFAGVDAFPICLDTKDTEEIIIIVKAIAPAF D
SbME  GLGNIGPEAAMPVMEGKAALFKRFAGVDSIPLVLDTQDTEEIIQTVKFLAPTF D/T
      *** **..*  *******.*** ** ** . . .*.   . ..  . . .* *
```

Table 8.3. Pyruvate formation assay results of point mutants of *tme* in malic enzyme deficient *E. coli* strain EJ1321.

Strain	Genotype	NAD^+-dependent activity (nmoles/min/mg)[a]	$NADP^+$-dependent activity (nmoles/min/mg)[a]	MDH activity (nmoles/min/mg)[b]
EJ1321	*dme-tme-*	27.2+/-1.2	4.5+/-2.9	505+/-2
EcG456	EJ1321 pTH139 (*dme*)	204+/-2.4	32.4+/-0.6	802+/-8
EcJ202	EJ1321 pTH392 (*tme*)	59.2+/-1.6	514+/-4.6	807+/-30
EcJ548	EJ1321 pTH650 (*tme*N131D)	53.3+/-1.5	118+/-2.8	738+/-7
EcJ550	EJ1321 pTH651 (*tme*D113G)	60.3+/-1.9	34.5+/-3.6	830+/-8

[a] specific activity is expressed as nmoles of pyruvate formed /minute/mg protein with the mean +/- standard error of triplicate samples.

[b] specific activity is expressed as nmoles NAD(P)H formed /minute/mg protein with the mean +/- standard error of triplicate samples

Figure 8.6. Western blot of EJ1321 *E. coli* cell free extracts containing point mutants of *tme* stained with TME specific antibodys. Arrow shows position of TME while chevron shows production of 60 kDa polypeptide. 2 μg of protein was loaded for all samples while 0.2 μg of protein was loaded for EcJ202 in the first two lanes. Numbers to the right represent molecular weight markers in kDa.

Table 8.4. Pyruvate formation assay results of point mutants of *tme* in malic enzyme deficient *S. meliloti* strain.

Strain	Genotype	NAD^+-dependent activity (nmoles/min/mg)[a]	$NADP^+$-dependent activity (nmoles/min/mg)[a]	MDH activity (nmoles/min/mg)[b]
RmK298	Rm1021, pBBR1MCS-5	93+/-2.2	46.7+/-4.1	202+/-15
RmK306	RmH194, pBBR1MCS-5	40.1+/-1.1	ND	150+/-1
RmK307	RmH194, pTH598 (*dme*)	632+/-3.1	253+/-2.1	465+/-13
RmK308	RmH194, pTH599 (*tme*)	31.1+/-1.1	339+/-1.0	183+/-14
RmK402	RmH194 pTH669 (*tme*N131D)	30.3+/-0.3	172+/-1.7	272+/-15
RmK403	RmH194 pTH670 (*tme*D113G)	33.5+/-1.6	43.5+/-2.1	268+/-2

[a] specific activity is expressed as nmoles of pyruvate formed /minute/mg protein with the mean +/- standard error of triplicate samples.

[b] specific activity is expressed as nmoles NAD(P)H formed /minute/mg protein with the mean +/- standard error of triplicate samples

ND none detected

Figure 8.7. Western blot of *S. meliloti* cell free extracts containing point mutations of *tme*. Arrow shows position of TME while chevron shows production of 60 kDa polypeptide. 4 μg of protein was loaded for all samples while 0.4 μg of protein was loaded for RmK307 and RmK308. Numbers to the right represent molecular weight markers in kDa.

Discussion

In light of the previous evidence that TME is not able to functionally replace DME in symbiosis despite the similar kinetic properties of the two enzymes (Voegele *et al.*, 1999, Cowie, 1998) we wanted to investigate the possibility that it is cofactor availability that dictates malic enzyme activity in the bacteroid. To do this we wished to alter the cofactor specificity of TME from $NADP^+$ to NAD^+. Several challenges were immediately evident; first the enzyme (and no other prokaryotic malic enzyme) has not been crystallized and therefore the exact amino acid residues important in substrate and cofactor binding are not known with certainty. Secondly, most cofactor switching experiments involve altering NAD^+-dependent enzymes to utilize $NADP^+$. This procedure usually involves removing a negatively charged amino acid, usually an aspartic acid residue, 18-21 amino acids downstream from a highly conserved GXGXXG (X represents any amino acid) motif known as the Rossman fold (Feeney *et al.*, 1990, Chen *et al.*, 1991, Fan *et al.*, 1991, Metzger and Hollenberg, 1995). Since our attempt involved the reverse situation no specific residue or region was easily identifiable. The NAD^+-dependent enzyme glutathione reductase was converted to utilize $NADP^+$ (Scrutton *et al.*, 1990, Bocanegra, *et al.*, 1993) but this protein has an unusual conserved motif which is not shared with the putative cofactor binding site of the malic enzymes, therefore limiting the possibility of using these experiments as a blueprint. To further complicate matters the malic enzymes of *S. meliloti*, like other malic enzymes, have two glycine rich motifs (one starting at position 88 and the second at position 204 of TME) characteristic of a Rossman fold (Chapter 3, Mitsch *et al.*, 1998) making it difficult to pinpoint a location to

focus upon. Finally, since malate dehydrogenase, like malic enzymes, utilizes both malate and NAD^+ in its reaction its presence in cell extracts would complicate enzymatic assays. The simple and sensitive observations of increase in absorbance at 340 nm (NAD^+ to NADH) would not be possible and instead the less sensitive pyruvate formation assay would have to be used to verify enzyme integrity.

To offset the fact that specific data on amino acid residues important for cofactor binding was lacking and the existence of two Rossman fold like domains within the protein, a more global approach was adopted. This involved producing three regions of *dme* via PCR with restriction sites designed into the downstream primer such that the engineered site would be compatible with pre-existing restriction sites in *tme* (Figure 8.1). These three fragments would encompass either the first conserved Rossman fold or both Rossman fold domains. None of the three constructs resulted in growth with malate as the sole carbon source and pyruvate formation assays using NAD^+ or $NADP^+$ showed no activity in any of the three strains. Western blots were carried out to verify if an intact protein was being produced and stains with antibodies raised against DME and TME revealed two degradation products; one of approximately 40 kDa and the other of approximately 50 kDa in addition to the intact 82 kDa subunit. The 50 kDa fragment was stained by the DME specific antibody while the 40 kDa fragment was preferentially stained by the TME specific antibody indicating that the smaller fragment is from the C-terminal region of the chimeric proteins while the larger fragment is from the N-terminus of the chimeric proteins. The production of these fragments is linked to the size of the *dme* insertion. When 128 amino acids of DME are linked to 645 amino acids of TME the

fragments are not detected by the DME antibody and only very light bands are discernable with the TME antibody. When the size of the DME region is increased to 217 and 253 amino acids the two polypeptides are easily detected by TME antibodies while the larger fragment is visible with the DME specific antibodies. Therefore, the stability of the chimeric malic enzyme subunits appears to be inversely proportional to the size of the *dme* insert present. Previous evidence with the truncated malic enzymes lacking the C-terminal domain showed that they were unstable in *E. coli* (Mitsch *et al.*, 1998, Voegele *et al.*, 1999) but retained activity in *S. meliloti* cells. We therefore reasoned that the instability and resulting loss of activity of the chimeric proteins might be overcome in an *S. meliloti* background. The chimeric genes were transferred to the pBBR1MCS-5 vector and were mobilized into the malic enzyme deficient *S. meliloti* strain RmH194. No complementation was detected on minimal media plates with succinate as the sole carbon source and pyruvate formation assays using both NAD^+ and $NADP^+$ as cofactors showed no activity. Western blots showed that an intact subunit of 82 kDa was produced and was not degraded into polypeptides as previously observed in *E. coli*. Furthermore, the amount of protein produced by each construct was variable. RmK304, which expressed the chimeric gene with the smallest *dme* insertion, produced protein at levels comparable to RmH194 strains overexpressing *tme*. In contrast, RmK303 and RmK305 had levels of protein that were greatly reduced relative to RmH194 overexpressing *tme*. These results mirror those found in *E. coli* with an inverse relationship existing between protein stability and size of the *dme* insertion. Based upon

these results it was evident that the chimeric genes were producing an intact protein subunit that lacked malic enzyme activity and was unstable in an *E. coli* background.

The second attempt to alter the specificity of TME revolved around the production of point mutants in the putative cofactor binding region located downstream from the first Rossman fold motif. Previous studies of $NAD(P)^+$ binding enzymes showed that NAD^+-dependent enzymes have a conserved aspartate residue downstream of a glycine rich region (Feeney *et al.*, 1990, Chen *et al.*, 1991, Fan *et al.*, 1991, Metzger and Hollenberg, 1995). This residue is believed to interact with the 2' hydroxyl group of NAD^+ and may act to exclude the 2' phosphate group of $NADP^+$. In comparisons of the prokaryotic malic enzymes (Mitsch *et al.*, 1998, Kawai *et al.*, 1996) an asparagine residue was noted at position 131 of TME while in DME an aspartic acid residue was present (Figure 8.5). Unfortunately, the other biochemically characterized malic enzymes did not retain an aspartic acid or glutamic acid residue in this location, however they are also not similar in structure to the *S. meliloti* malic enzymes. Since this was the only aspartic residue in DME that was not present in TME, it was selected for substitution. Twenty amino acids down stream from the GXGXXG motif at position 113, TME has an aspartic acid residue while the remaining biochemically characterized malic enzymes all have a glycine residue (Figure 8.5). There is no previous evidence that glycine residues are responsible for cofactor specificity however since this was an obvious difference in an area previously identified as being crucial for cofactor binding this substitution was also carried out.

Oligonucleotide directed mutagenesis experiments were carried out resulting in one construct with a D to G alteration at position 113 of TME while the second had an N to D alteration at position 131 of TME. The resulting mutants were analyzed in an EJ1321 *E. coli* background and no complementation was observed on minimal media plates with succinate as the sole carbon source and pyruvate formation assays on cell free extracts detected no NAD^+- or $NADP^+$-dependent activity. Western blots carried out on the extracts revealed no full-length protein subunits when stained with antibodies for TME. Instead, a polypeptide of approximately 60 kDa was detected for both point mutations. Based upon our previous data concerning protein instability in an *E. coli* background the two point mutation constructs were inserted into pBBR1MCS-5 for transfer into *S. meliloti* strain RmH194. Complementation studies on minimal media with succinate as the sole carbon source were again negative as were NAD^+- and $NADP^+$-dependent pyruvate formation assays of cell free extracts. Western blots carried out on these extracts revealed a full length protein subunit of 82 kDa was being produced by both constructs with an approximately 60 kDa degradation product visible which is believed to be a normal breakdown product of TME. Based upon these results we can conclude that the point mutants are producing a full length TME subunit that is unstable in *E. coli* but stable in *S. meliloti* but is non-functional.

The instability and lack of activity of the chimeric and point mutation malic enzymes could be due to several reasons. The altered malic enzymes may be unable to form oligomeric structures thus rendering them inactive and leaving the exposed subunits vulnerable to degradation. A model generated for the pigeon liver malic enzyme shows

that it is a holotetramer formed by two monomers in a head to tail configuration which produce a dimer and the dimers then bind in parallel to form the native enzyme (Chang *et al.*, 1994, Chou *et al.*, 1996). If this model holds true for other malic enzymes it is possible that the replacement of the N-terminal region of TME with DME would result in subunits that are no longer able to interact to form a dimer or the native oligomer and therefore may be vulnerable to proteolysis. *E. coli* has several methods to remove abnormal or overproduced proteins (reviewed in Gottesman, 1996); Lon is believed to be the primary protease degrading abnormally folded proteins, ClpAP degrades proteins with abnormal N-termini and abnormal proteins, and the essential HflB protease degrades cytoplasmic and membrane bound proteins. In both *B. japonicum* (Narberhaus *et al.*, 1998) and *S. meliloti* (Glazebrook *et al.*, 1996) a *degP* homolog has been described which is most likely responsible for protein degradation. It is likely that *S. meliloti* has several other proteases homologous to *E. coli* and any number of these could be responsible for eliminating the nonfunctional malic enzymes.

The instability of the point mutations is somewhat surprising since a single amino acid substitution should not result in protein instability. Point mutations carried out in other malic enzymes have revealed deleterious effects to enzyme activity. Alteration of glycine 444 to aspartic acid of the *Schizosaccharomyces pombe* malic enzyme results in a loss of activity (Viljoen *et al.*, 1998). Extensive studies with the well characterized pigeon liver malic enzyme have shown that deletion of the lysine residues at the N-terminal position 2 and 3 cause a decrease in enzyme activity (Chou *et al.*, 1997). In other studies, replacement of the phenylalanine residue at position 19 with glycine,

alanine, or serine result in an increase in K_m for the substrate and manganese while substitution with the structurally similar tyrosine confers wild type activity (Chou *et al.*, 1996). Replacement of aspartic acid residue 258 with asparagine, lysine, or alanine results in a loss of activity while replacement with glutamate yields residual activity (Wei *et al.*, 1995). Therefore, not surprisingly, conservative replacements have less deleterious effects relative to non-conservative replacements in the malic enzymes. What is unusual is that single amino acid replacements have such a dramatic effect on the enzyme, in some cases totally inactivating the enzyme. Our experiments involved the non-conservative replacement of aspartic acid for glycine at position 113 and the conversion of asparagine to aspartic acid at position 131, therefore the loss of activity should not be surprising. The deletion or addition of a charged residue eliminates enzyme activity presumably by interfering with the binding and interaction of the cofactor at the active site or, alternatively the gain or loss of a charged amino acid interferes with protein folding resulting in an unstable protein.

Recently, the NAD^+-dependent malic enzyme from human mitochondria has been crystallized and its three dimensional structure has been deduced (Xu *et al.*, 1999). These results have challenged traditional suppositions upon the structure of malic enzymes and the location of binding and active sites within the protein. They show that the second Rossman fold region made up of the nontraditional GXGXXA motif is responsible for binding the NAD^+ cofactor. If this characteristic is maintained in the prokaryotic malic enzymes it would suggest that our focus upon the first more traditional Rossman fold was an error. It does not explain the lack of activity of our constructs but the crystallography

results indicate that this first glycine rich region may be responsible for binding the substrate (Xu *et al.*, 1999). This hypothesis is based upon the position near the nicotinamide ring of the cofactor near the active site and since no crystals were produce in association with the substrate this is only a theory. If it is true, it would explain the lack of activity of our point mutants as any alteration in amino acid composition in this region would or may inhibit binding of malate and disrupt the active site of the enzyme.

Chapter 9

General discussion

Malic enzymes are responsible for the conversion of malate to pyruvate with the concomitant reduction of a nicotinamide cofactor. In *S. meliloti* two malic enzymes have been identified with the diphosphopyridine dependent enzyme (DME) being essential for N_2 fixation within the plant host while the triphosphopyridine dependent enzyme (TME) is not. The studies outlined in this thesis have been concerned with characterizing *tme* and its associated protein and the requirements of the malic enzymes for symbiotic N_2 fixation. Sequence analysis revealed that both *tme* and *dme* are some 320 amino acids larger than previously characterized prokaryotic malic enzymes. The protein shows a chimeric structure with the N-terminal region showing homology to malic enzymes while the C-terminal domain shows similarity to phosphotransacetylase enzymes. This unusual chimeric nature has been shown to be common to other gram-negative organisms subjected to genomic sequencing research such as *E. coli*, *H. influenzae*, and *R. prowsazekii*. A truncated *tme* gene was produced lacking the C-terminal region and this truncated protein retained malic enzyme activity, but the protein was unable to oligomerize into the native octameric state and instead formed dimers. Based upon these observations we have concluded that the C-terminal region of the protein is not involved in the conversion of malate to pyruvate and may instead be responsible for the structural integrity of the enzyme and formation of the native structure. Presumably these

observations can be extrapolated to the chimeric malic enzymes of *E. coli*, *H. influenzae*, and *R. prowsazekii*. Our research has identified a new subgroup of malic enzymes of which DME and TME are the first characterized members. It has also advanced malic enzyme research, as we have been the first group to identify the PTA-like C-terminal extension and have shown that this region is unnecessary for malic enzyme activity but its loss inhibits the formation of the native oligomer.

The expression of a NAD^+-dependent malic enzyme of *E. coli* in *S. meliloti* and its ability to offset the loss of *dme* shows that the C-terminal extension of the malic enzymes is not essential for symbiotic N_2 fixation. Therefore although the nature or function of the C-terminal region is unknown its function or presence is not required during symbiosis. The subunits of the malic enzymes of *B. japonicum* are similar in size to the malic enzymes of *S. meliloti* and therefore presumably share the chimeric structure of other gram-negative organisms. Based upon our observations we can predict that their C-terminal regions are not essential for symbiotic N_2 fixation.

Our biochemical characterization of TME has revealed that it has similar K_m's for substrate and cofactor as the symbiotically essential DME. The only major difference between the two enzymes is that unlike DME, TME is not regulated by TCA cycle intermediates. Therefore TME's inability to offset the loss of *dme* is not due to it being a less efficient enzyme relative to DME. It is possible that *tme* cannot offset the loss of *dme* due to its relatively low expression in bacteroids. Our estimates show that the relative levels of DME double during the transition from free-living to bacteroid state while TME levels drop by a factor of 5. This indicates that relative amounts of DME and

TME rise and fall in bacteroids respectively and our estimates of *tme* expression in bacteroids show that this promoter is expressed at 20-30% relative to the *dme* promoter. This level of expression maybe too low for TME to be produced at significant levels in the bacteroid. When *dme* is produced from the *tme* promoter an intermediate symbiotic phenotype was seen suggesting that this promoter is sufficiently active to partially maintain the TCA cycle. When TME was overexpressed in *dme*$^-$ bacteroids an intermediate N_2 symbiotic phenotype was obtained indicating that high levels of TME are insufficient to maintain the TCA cycle. It is of interest to note that no acetylene reduction activity is observed for *dme, tme* double mutants yet there is consistently some residual activity with *dme*$^-$ strains when *tme* is present. This leads to the speculation that TME is able to induce some symbiotic N_2 fixing activity but this ability is not governed by absolute TME amounts and instead is controlled by another physiological factor. Our current supposition is that the level of $NADP^+$ in bacteroids is extremely low and that this is the major reason that TME is not able to functionally replace DME in bacteroids. This leads to broader physiological concerns, as some enzymes of the TCA cycle require $NADP^+$ as a cofactor. $NADP^+$-dependent isocitrate dehydrogenase of *S. meliloti* is essential for a symbiotic N_2 fixation phenotype and this implies that there must be some $NADP^+$ present in bacteroids but its relative level is currently unknown. Therefore our research has enhanced our understanding of symbiotic N_2 fixation by showing the C-terminal region of the malic enzymes is not required for symbiotic N_2 fixation. We have also shown that TME is not able to offset the loss of DME in bacteroids and that this inability is not due to low levels of expression or that it is kinetically inferior to DME.

Based upon our observations we suspect that it is due to the difference in cofactor specificity. This conclusion gives insight into the biochemical make up of the bacteroid and may lead to alterations into the traditional thinking about carbon metabolism and the physiological make up of the bacteroid especially the presence or absence of the cofactors NAD^+ and $NADP^+$.

Our studies into the carbon requirements of bacteroids have led to the conclusion that malate is present in nodules of alfalfa and pea plants and can support N_2 fixation. The levels of N_2 fixation are variable between the different leguminous plant hosts and may indicate that different levels of malate are present in the nodules of these plants. Alternatively, it could also suggest that different members of the *Rhizobiaceae* have different metabolic capabilities with *R. leguminosarum* bacteroids being able to utilize malate to a higher extent than *S. meliloti* bacteroids. It would also indicate that for successful symbiotic N_2 fixation to occur, a fixed nitrogen source such as aspartate is not required for symbiosis indicating that bacteroids acquire nitrogen through a so far undescribed mechanism. Therefore our findings have enhanced our understanding of symbiotic N_2 fixation by showing that malate is present in nodules of alfalfa and pea plants and is capable of supporting symbiotic N_2 fixation to varying extents. The differential response indicates that there are fundamental physiological differences between *S. meliloti* and *R. leguminosarum* bacteroids. This could include the absolute amounts of malate present in the nodule for use by the bacteroid are different in the two plant hosts or that the bacteroids utilize different carbon sources with *S. meliloti* requiring succinate, fumarate, and potentially aspartate as a carbon source while *R. leguminosarum*

does not. These results may put to rest some of the debate as to wether bacteroids require a fixed nitrogen source from the plant host as our results demonstrate that C_4-dicarboxylates can support N_2 fixation and that a carbon and nitrogen source such as aspartate is not required as a substrate for symbiotic N_2 fixation in *R. leguminosarum*. This work also illustrates the importance of metabolic engineering as a tool for identifying certain physiological requirements for symbiotic N_2 fixation. By producing proteins that have a specific function or altered structure relative to the native *S. meliloti* proteins we have been able to broaden our understanding of bacteroid and plant physiology.

Future work regarding the malic enzymes of *S. meliloti* should be concentrated upon altering the cofactor requirements of TME so that it can utilize NAD^+. With new information regarding the structure of eukaryotic malic enzymes being generated and if these structural traits are universal in the structural makeup of malic enzymes the chances of altering the specificity of TME are greatly enhanced. If this were to be accomplished an answer to a general physiological question can be obtained with regard to bacteroid metabolism. If this alteration proved successful it would demonstrate: 1) that it is cofactor dependence that controls malic enzyme activity in bacteroids and 2) $NADP^+$ is present at reduced levels and this would indicate that the ratio of $NADP^+$/NADPH is extremely low indicating that it is utilized by the bacteroid to a high extent. This may support the hypothesis that NADPH is the source of reductant for nitrogenase activity. As more promoter regions are determined through the international effort to complete the *S. meliloti* genome more genes and promoters will be available for comparison to the

promoter regions of the malic enzymes. From these comparisons the elements responsible for *tme* regulation could be determined and this would lead to the characterization of the proteins and pathways required to down regulate genes not required for symbiotic N_2 fixation. Future metabolic engineering experiments may be used to enhance symbiotic N_2 fixation. Although increasing C_4-dicarboxylate uptake in bacteroids and increasing DME levels in bacteroids failed in increase symbiotic N_2 fixation levels in independent experiments perhaps jointly they may successfully increase plant growth. Alternatively, increasing the levels of the TCA cycle enzymes along with the transport protein and malic enzyme it may be possible to enhance symbiotic N_2 fixation. In addition, metabolic engineering could be used to determine the essential elements of DME activity. It is already known that DME is symbiotically essential but it is unknown if it is the production of malate to maintain the TCA cycle or the generation of reducing power in the form of NADH which is important during symbiosis. If an enzyme that can generate pyruvate from TCA cycle intermediates (such as pyruvate carboxylase) without generating NADH this enzyme could be produced in bacteroids. The results of theses experiments could determine the exact role of DME during symbiotic nitrogen fixation and differentiate the importance of pyruvate or NADH production.

Appendix 1

Determination of nitrogenase activity in *tme* overexpressing and Δ*dme* expressing *S. meliloti* bacteroids

Overexpression of *tme* in bacteroids

In light of the fact that DME and TME have very similar kinetic characteristics (Voegele *et al.*, 1999, Chapter 4) it was somewhat surprising that a DME deficient strain showed no residual nitrogen fixing activity (Driscoll and Finan, 1993). A possible reason for this observation was that *tme* expression is reduced in bacteroids hence TME levels may be insufficient to support nitrogen fixation (Driscoll and Finan, 1996, Driscoll and Finan, 1997). To address this issue, *tme* was expressed from the *dme* promoter (*pdme-tme*) in order to elevate the level of TME in bacteroids to that normally associated with DME (Cowie, 1998). Western blots of strains carrying the *pdme-tme* construct revealed that TME was indeed present at levels comparable to DME and enzyme assays showed that the protein from the bacteroid was functional (Cowie, 1998). Despite the presence of TME in the *dme-* bacteroids the alfalfa plants had dry weights indistinguishable from DME deficient strains (Cowie, 1998). To verify these results, acetylene reduction assays were carried out on the plant root systems since the increased sensitivity of this assay is more revealing than reliance on dry weights of plants alone. Relative to wild type inoculated plants the *dme* deficient strain RmG455 had 0.5% acetylene reduction activity while the *tme-dme-* double mutant RmG994 had no detectable activity (TableA1.1). The

Table A1.1. Acetylene reduction values and plant dry weights of alfalfa plants inoculated with *S. meliloti pdme-tme* mutant strains expressing *tme* from the *S. meliloti dme* promoter.

Sample	Genotype	ARA (nmoles/min /plant)[a]	% ARA activity relative to wild type	Plant dry weight (mg)[b]	% plant dry weight relative to wild type
Rm1021	wild type	1221+/-320	100	50.48+/-0.80	100
RmG455	*dme3*	7+/-3	0.5	10.04+/-0.61	20
RmG994	*dme3, tme4*	ND	ND	10.61+/-0.61	21
RmG995	*tme4*	1156+/-258	95	53.06+/-2.83	105
RmH897	*dme3, tme4, Φpdme-tme*	24+/-6	2	11.30+/-0.35	22
RmH899	*dme3, tme4, Φpdme-tme*	15+/-5	1	12.28+/-0.92	24
RmH900	*tme4, Φpdme-tme*	563+/-176	46	44.81+/-2.59	89
uninoculated	-	-	-	8.52+/-0.37	17

[a] Acetylene reduction activity is expressed as mean of nmoles ethylene produced per minute +/- standard error of triplicate samples containing three root systems each.

[b] Plant dry weight is expressed as mean of +/- standard error of triplicate pots containing 7-10 plants each.

TME overexpressing strains RmH897 and RmH899 had 1% and 2% activity relative to wild type inoculated plants respectively (Table A1.1). This low level of activity is by no means compelling but in light of the fact that the parental strain RmG994 had no detectable activity it is possible that the residual activity recorded could be due to TME activity. This could suggest that TME is partially functional when expressed in bacteroids and is able to carry out the conversion of malate to pyruvate albeit at a reduced level. It is also of interest to note that RmG994 displays no acetylene reduction activity while *dme* mutants show some residual nitrogenase activity (Driscoll and Finan, 1993, Chapter 5). With this evidence we can now discount that it is reduced *tme* expression that limits TME's ability to functionally replace DME in the nodule

Expression of DME lacking the C-terminal region in bacteroids

Since the C-terminal region of both TME and DME was shown to be dispensable in terms of malic enzyme activity (Mitsch *et al.*, 1998, Chapter 3) it was of interest to determine what effect the truncated protein would have in bacteroids. Previous results in our laboratory with the truncated DME protein (ΔDME) showed that it was not induced by succinate nor was it inhibited by acetyl-CoA as was the intact enzyme (Voegele, unpublished results). Also, since TME does not share DME's sensitivity to TCA cycle intermediates this had been suggested to be a possible reason why TME could not functionally replace DME in the bacteroid and this hypothesis could also be examined. Therefore, this investigation would address several important points. It would determine if the C-terminal region were required for symbiotic nitrogen fixation and would also demonstrate if DME's regulation by TCA cycle intermediates were important for its

activity in bacteroids. Previous results had shown that *S. meliloti dme-* strains producing the truncated DME protein where capable of inducing a symbiotic N_2 fixation phenotype and plants that were indistinguishable from wild type inoculated plants (Cowie, 1998). In addition, bacteroids expressing the truncated *dme* gene (Δ*dme*) had NAD^+-dependent pyruvate formation activity comparable to wild type bacteroids and western blots revealed that the truncated protein was produced at levels close to that of DME. Again a more complete picture was obtained with the acquisition of acetylene reduction data. Both RmH996 and RmH1000 showed acetylene reduction activity and in the case of RmH1000 it was appreciably higher than plants inoculated with wild type *S. meliloti* (Table A1.2). Thus the presence of the truncated DME protein is sufficient to induce nitrogenase activities and produce plants that are comparable to wild type inoculated plants.

Implications

Based upon the preceding information several conclusions can be drawn. First, the C-terminal region of DME is not essential for symbiosis and nitrogen fixation. This supports previous observations where the *E. coli* NAD^+-dependent malic enzyme that lacks a C-terminal extension was able to offset the loss of DME in the bacteroid (Chapter 6). Second, TME cannot functionally replace DME in bacteroids and the lack of complementation is not due to TME's insensitivity to TCA cycle intermediates. This conclusion is drawn from the fact that the truncated form of DME, which is insensitive to TCA cycle intermediates, is capable of inducing a symbiotic N_2 fixing phenotype in plants. Therefore, there must be an intrinsic difference between DME and TME that does

Table A1.2. Acetylene reduction values and plant dry weights of alfalfa plants inoculated with *S. meliloti dme* mutant strains expressing the truncated *dme* gene from the *S. meliloti dme* promoter.

Sample	Genotype	ARA (nmoles/min/ plant)[a]	% ARA activity relative to wild type	Plant dry weight (mg)[b]	% Plant dry weight relative to wild type
Rm1021	wild type	342+/-59	100	40.63+/-3.65	100
RmG454	*dme2*	4+/-1	1	7.44+/-0.61	18
RmG456	*dme1*	6+/-1	2	7.09+/-1.03	17
RmH996	*dme2*, ΦΔ*dme*	477+/-33	139	36.42+/-2.64	90
RmH1000	*dme1*, ΦΔ*dme*	890+/-132	260	48.31+/-0.09	119
uninoculated	-	-	-	6.32+/-0.37	16

[a] Acetylene reduction activity is expressed as mean of nmoles ethylene produced per minute +/- standard error of triplicate samples containing three root systems each.

[b] Plant dry weight is expressed as mean of +/- standard error of triplicate pots containing 7-10 plants each.

not allow them to functionally replace each other in the bacteroid. The most obvious difference is cofactor specificity. Since TME requires $NADP^+$ for function the implication would be that there is a limited amount of this cofactor available in alfalfa nodules. This would have wider implications as isocitrate dehydrogenase requires $NADP^+$ for function and as a member of the TCA cycle is essential for symbiotic nitrogen fixation as determined by McDermott and Kahn (1992). The importance of isocitrate dehydrogenase has been speculated by Kurtz and LaRue (1977) as its activity mirrors that of nitrogen fixation hinting that NADPH may be the source of reductant for the *R. leguminosarum* nitrogenase enzyme. Isocitrate dehydrogenase has been purified from *S. meliloti* and has a K_m of 15 μM for $NADP^+$ (Chandrasekharan Nambiar and Shethna, 1976) which is half that of TME (Voegele *et al.*, 1999, Chapter 4) indicating that isocitrate dehydrogenase may be capable of functioning under conditions of restricted $NADP^+$ concentrations. Estimates have been made regarding cofactor concentrations in *B. japonicum* bacteroids and have shown that $NADP^+$+NADPH levels are approximately 40 nmoles/g but the ratio of $NADP^+$ to NADPH ratio is 0.4 indicating a highly active $NADP^+$ reducing system in this symbiotic association (Tajima and Kouzai, 1989). *B. japonicum* also contains two malic enzymes differing in cofactor specificity but at present there is no genetic evidence indicating which enzyme, if any, is required for symbiotic nitrogen fixation. To complicate things further, an NAD^+-dependent isocitrate dehydrogenase has been reported for rhizobia infecting *Lotus pedunculatus* but it is not clear if this is a wide spread phenomena among prokaryotes (Moustafa and Leong, 1975).

Appendix 2

Structure of DME and TME as revealed by trypsin sensitivity

Based upon the apparent chimeric structure of TME and its counterpart DME it was of interest to analyze the structure of the respective proteins. Multi domain proteins are known to utilize characteristic amino acid segments to separate the domains required for catalysis. The multi enzyme complex of pyruvate dehydrogenase utilizes alanine and proline rich regions of dihydrolipoamide acetyltransferase to maneuver the lipoyl-lysine binding site to the three active sites of the enzyme (Miles *et al.*, 1988). These alanine-proline rich regions have substantial conformational flexibility (Radford *et al.*, 1989; Green *et al.*, 1992) and act as mobile linking regions for the enzyme. Glutamine rich regions have also been implicated as linker regions or spacers within proteins to separate structural domains (Fischer *et al.*, 1989) and these so called Q-linkers also contain large numbers of arginine and proline residues for conformational flexibility (Wootton *et al.*, 1989). In order to identify interdomain linker regions limited proteolysis experiments have been conducted with the alanine racemases from *Salmonella typhimurium* (Galaktos and Walsh, 1987) and by utilizing trypsin, chymotrypsin, and subtilisin a hinge region was identified for both DadB and Alr alanine racemases. To identify a linker or hinge region separating the malic enzyme N-terminus from the PTA-like C-terminus of both DME and TME, limited proteolysis experiments were conduced using the protease

trypsin. All DME data was obtained by Dr. R.T. Voegele while data pertaining to TME was obtained by the author.

Purified DME and TME protein was subjected to trypsin treatment as follows. 750 ng of purified protein were added to proteolysis buffer (100 mM Tris/HCl pH 7.8, 10 mM $CaCl_2$, 10 mM KCl, and 3 mM $MnCl_2$) to give a final volume of 17 µl. 2 µl of fresh trypsin samples in 100 mM Tris/HCl pH 7.8 and 10 mM $CaCl_2$ were added to give final weight ratios of 10/1, 100/1, and 1000/1 of protein to protease. Addition of water served as a negative control. Samples were incubated at room temperature for 10 min before 1 µl of PMSF was added to a final concentration of 1 mM. Samples were assayed for malic enzyme activity by following the formation of NAD(P)H at 340 nm, and by western blot following separation of the polypeptides on SDS-PAGE gels (12% T, 2.67% C) according to Laemmli (1970). Polypeptides were transferred to a PVDF membrane (Millipore Corp.) (transfer time 1 hour at 100 V) according to Towbin *et al.* (1979) using 15.6 mM Tris, 120 mM glycine, 20% methanol as electrode buffer. Membranes were probed with polyclonal antibodies raised against the purified proteins, and then visualized with peroxidase-coupled goat anti-rabbit secondary antibody (Sigma Chemical Comp.), the Amersham enhanced chemi-luminescence western blot detection kit, and Kodak XOMAT AR X-ray film. For N-terminal sequencing of the tryptic polypeptides the PVDF membrane was reversibly stained with Ponceau Red 2R. The bands were cut out and destained with H_2O. N-terminal sequencing of these samples was performed at the Alberta Peptide Institute (Edmonton) on a Hewlett Packard G1005A protein sequencer.

Trypsin treatment of DME produced two stable polypeptides of 43.4 kDa (DME-

Figure A2.1. Trypsin treatment of *S. meliloti* DME and TME proteins as revealed by SDS-PAGE and western blot. **(A)** Trypsin treatment of DME: Lane 1, DME control; lanes 2, 3, and 4 are DME to trypsin weight ratios of 1000/1, 100/1, and 10/1, respectively. **(B)** Trypsin treatment of TME: Lane 1, TME control; lanes 2, 3, and 4 are TME to trypsin weight ratios of 1000/1, 100/1, and 10/1, respectively. Products resulting from trypsin treatment of DME are indicated.

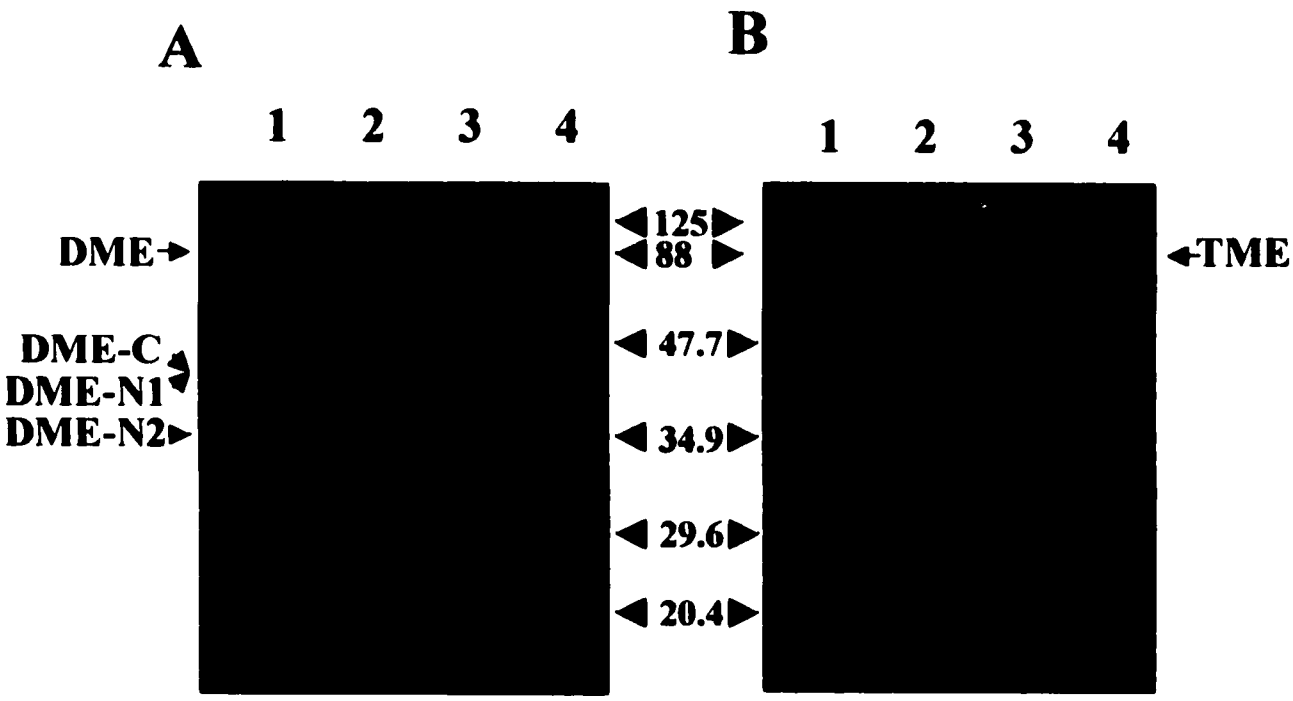
A
B
1 2 3 4
1 2 3 4
DME
DME-C
DME-N1
DME-N2
125
88
47.7
34.9
29.6
20.4
TME

C) and 41.5 kDa (DME-N1) (Figure A2.1, lane 3). A third tryptic fragment, migrating at 33 kDa (DME-N2) appeared upon treatment with higher trypsin concentrations (Figure A2.1, lane 4). The N-terminal amino acid sequence of DME-C, AYSGETPV, revealed that this polypeptide arose from trypsin cleavage after amino acid 377R of the DME protein. DME-C thus originated from the C-terminal region of DME. The N-terminal amino acid sequence of DME-N1 and DME-N2 revealed that the N-termini of these two polypeptides were identical, SQAVPAS. This sequence is consistent with a trypsin cleavage after amino acid 9K at the N-terminus of DME. Further processing of DME-N1 to DME-N2 therefore, has to occur at the C-terminus of the DME-N1 polypeptide. In contrast to DME, no stable polypeptides were observed to accumulate upon treatment of TME with identical trypsin concentrations (Figure A2.1). This would indicate that the two proteins do not share similar structural traits and that TME does not contain a trypsin sensitive linker region separating the N-terminus from the C-terminus.

The observation that both DME and TME deletion derivatives lacking the C-terminal region retain malic enzyme activity clearly suggests that these two proteins have at least two major domains. The generation of two large tryptic polypeptides upon treatment of DME with this protease represents further evidence for the proposed two domain structure. Moreover, the location of the exposed trypsin site at amino acid 377 places this site close to the interdomain region as predicted from the alignment of DME, and TME with the short form malic enzymes such as that from *S. bovis* (Chapter 3, Mitsch *et al.*, 1998). The presence of multiple exposed trypsin sites within TME is surprising given the sequence similarity of this protein to DME (44% identity, 57% similarity, Chapter 3). Unlike TME,

DME shows positive cooperativity and allosteric regulation (Voegele *et al.*, 1999), however it is not clear if these differences would lead to the observed differences in sensitivity to trypsin (Figure A2.1). The latter would appear to be particularly true as both proteins have a similar octameric native structure. With respect to the octameric structure, we found that while both DME and TME derivatives lacking the PTA-like domain retained malic enzyme activity, these proteins now appeared to be dimers. While this result suggests that the PTA-like domain may be involved in octamerization, it is also possible that the C-terminal deletion indirectly interfers with formation of the native oligomeric state. On the other hand, the formation of dimers by these deletion derivatives suggests that this may be the first step in the formation of the octamer.

References

Altschul, S.F., T.L. Madden, A.A. Schaffer, J. Zhang, Z. Zhang, W. Miller, D.J. Lipman. 1997. Gapped BLAST and PSI-BLAST: a new generation of protein database search programs. Nuc. Acids Res. 25:3389-3402

Alting-Mees, M.A. and J.M. Short. 1989. pBluescript II: gene mapping vectors. Nuc. Acids Res. 17:9494-9498

Andersson, S.G., A. Zomorodipour, J.O. Andersson, T. Sicheritz-Ponten, U.C. Alsmark, R.M. Podowski, A.K. Naslund, a.S. Eriksson, H.H. Winkler, and C.G. Kurland. 1998. The genome sequence of *Rickettsia prowazekii* and the origin of mitochondria. Nature. 396:133-140

Antoni, L.D. and J.I. Sprent. Primary metabolites of *Phaseolus vulgaris* nodules. Phytochemistry. 17:675-678.

Arwas, R., A.R. Glenn, L.A. McKay, and M.J. Dilworth. 1986. Properties of double mutants of *Rhizobium leguminosarum* which are defective in the utilization of dicarboxylic acids and sugars. J. Gen. Microbiol. 132:2743-2747

Atkins, C.A. 1991. In M.J. Dilworth and A.R. Glenn (eds) Biology and Biochemistry of nitrogen fixation, Elsevier, Amsterdam, pg 293-319

Ausubel F.M., R. Brent, R.E. Kingston, D.D. Moore, J.G. Seidman, J.A. Smith, and K. Struhl. 1989. Current protocols in molecular biology. John Wiley & Sons, Inc., New York.

Barnes, S.J., and P.D. Weitzman. 1986. Organization of citric acid cycle enzymes into a multienzyme cluster. FEBS Lett. 201:267-270

Bartolucci, S., R. Rella, A. Guagliardi, C.A. Raia, A. Gambacorta, M. De Rosa, and M. Rossi. 1987. Malic enzyme from Archaebacterium *Sulfolobus solfataricus*. J. Bacteriol. 262:7725-7731

Batut, J., M-L. Daveran-Mingot, M. David, J. Jacobs, A-M. Garnerone, and D. Kahn. 1989. *fixK*, a gene homologous with fnr and crp from *Escherichia coli*, regulates nitrogen fixation genes both positively and negatively in Rhizobium meliloti. EMBO J. 8:1279-1286

Becker, A., H. Kuster, K. Niehaus, A. Puhler. 1995. Extension of the *Rhizobium meliloti* succinoglycan biosynthesis gene cluster: identification of the *exsA* gene encoding an ABC transporter protein, and the *exsB* gene which probably codes for a regulator of succinoglycan biosynthesis. Mol. Gen. Genet. 249:487-497

Bergersen, F.J. and G.L Turner. 1990. Bacteroids from soybean root nodules: accumulation of poly-β-hydroxybutyrate during supply of malate and succinate in relation to N_2 fixation in flow-chamber reactions. Proc. R. Soc. Lond. 240:39-59

Bergmeyer, H.H, K. Gawehn, H. Klotzsch, H.A. Krebs, D.H. Williamson. 1967. Purification and properties of crystalline 3-hydroxybutyrate dehydrogenase grom *Rhodopseudomonas sphaeroides*. Biochem. J. 102:423-431

Blattner, F.R., G. Plunkett, C.A. Bloch, N.T. Perna, V. Burland, M. Riley, J. Collado-Vides, J.D. Glasner, C.K. Rode, G.F. Mayhew, J. Gregor, N.W. Davis, H.A. Kirkpatrick, M.A. Goeden, D.J. Rose, B. Mau, and Y. Shao. 1997. The complete genome sequence of *Escherichia coli* K-12. Science. 277:1453-1474

Bocanegra, J.A., N.S. Scrutton, and R.N. Pernham. 1993. Creation of an NADP-dependent pyruvate dehydrogenase multienzyme complex by protein engineering. Biochem. 32:2737-2740

Boles, E., P. de Jong-Gubbels, and J.T. Pronk. 1998. Identification and characterization of MAE1, the *Saccharomyces cerevisiae* structural gene encoding mitochondrial malic enzyme. J. Bacteriol. 180, 2875-2882

Bolton, E., B. Higgisson, A. Harrington, and F. O'Gara. 1986. Dicarboxylic acid transport in *Rhizobium meliloti*: isolation of mutants and cloning of dicarboxylic acid transport genes. Arch. Microbiol. 144:142-146

Bosworth, A.B., M.K., Williams, K.A., Albrecht, R., Kwiatkowski, J., Beynon, T.R., Hankinson, C.W., Ronson, F., Cannon, T.J., Wacek, and E.W., Triplett. 1994. Alfalfa yield response to inoculation with recombinant strains of *Rhizobium meliloti* with an extra copy of *dctABD* and/or modified *nifA* expression. Appl. Environ. Microbiol. 60:3815-3832

Bradford, M.M. 1976. A rapid and sensitive method for the quantitation of microgram quantities of protein utilizing the principle of protein-dye binding. Anal. Biochem. 72:248-254

Cai, G-Q, Driscoll, B.T., and T.C. Charles. 2000. Requirements for the enzymes acetoacetyl coenzyme A synthetase and poly-3-hydroxybutyrate (PHB) synthase for growth of *Sinorhizobium* on PHB cycle intermediates. J. Bacteriol. 182:2113-2118

Canon, F., J. Beynon, V. Buchanan-Wollaston, R. Burghoff, M. Cannon, R. Kwiatkowski, G. Lauer, and R. Rubin. 1985. Progress in understanding organization and expression of nif genes in *Klebsiella.* p 453-460. In H.J. Evans, P.J. Bottomley, and W.E. Newton (ed.), Nitrogen fixation research progress. Martinus Nijhoff Publishers, Boston, USA.

Carlson, T.A., G.B. Martin and B.K. Chelm. 1987. Differential transcription of the two glutamine synthetase genes of *Bradyrhizobium japonicum.* J. Bacteriol. 169:5861-5866

Chandrasekharan Nambiar, P.T. and Y.I. Shethna. 1976. Purification and properties of an $NADP^+$-specific isocitrate dehydrogenase from *Rhizobium meliloti.* Antonievan Leeuwenhoek. 42:471-482

Chang, G., T. Huang, S. Huang, and W. Chou. 1994. Dissociation of pigeon-liver malic enzyme in reverse micelles. Eur. J. Biochem. 225:1021-1027

Chang, G-G. and R.Y. Hsu. 1977. Mechanism of pigeon liver malic enzyme modification of histidyl residues by ethoxyformic anhydride. Biochim. Biophys. Acta. 483: 228-235

Charles, T.C., R.S. Singh, and T.M. Finan. 1990. Lactose utilization and enzymes encoded by megaplasmids in *Rhizobium meliloti* SU47: implications for population studies. J. Gen. Microbiol. 136:2497-2502

Chen, F., Y. Okabe, K. Osano, and S. Tajima. 1997. Purification and characterization of the NADP-malic enzyme from *Bradyrhizobium japonicum* A1017. Biosci. Biotechnol. Biochem. 61:384-386

Chen, F., Y. Okabe,K. Osano,S. and Tajima. 1998. Purification and characterization of an NAD-malic enzyme from *Bradyrhizobium japonicum* A1017. Appl. Environ. Microbiol. 64:4073-4075

Chen, Z., W.R. Lee, and S.H. Chang. 1991. Role of aspartic acid 38 in the cofactor specificity of *Drosophila* alcoholdehydrogenase. Eur. J. Biochem. 202:263-267

Chou, W.Y., S.M. Huang, and G.G. Chang. 1997. functional roles of the N-terminal amino acid residues in the Mn(II)-L-malate bimnding and subunit interactions of pigeon liver malic enzyme. Protein engineering. 10:1205-1211

Chou, W.Y., M.Y. Liu, S.M. Huang, and G.G. Chang. 1996. Involvement of Phe19 in the Mn(2+)-L-malate binding and the subunit interactions of pigeon liver malic enzyme. Biochemistry. 35:9873-9879

Copeland, L., R.G. Quinnell, and D.A. Day. 1989. Malic enzyme activity in bacteroids from soybean nodules. J. Gen. Microbiol. 135:2005-2011

Cowie, A. 1998. The roles of the malic enzymes of *Rhizobium* (*Sinorhizobium*) *meliloti* in symbiotic nitrogen fixation. Masters thesis, McMaster University, Hamilton Ont.

Darrow, R.A. 1980. In J. Mora and R. Palacios (eds), Glutamine synthetase, Metabolism enzymology and regulation. Academic press, pp139-166

David, M., M-L. Daveran, J. Batut, A. Dedieu, O. Domergue, J. Ghai, C. Hertrig, P. Boistard, and D. Kahn. 1988. Cascade regulation of *nif* gene expression in *Rhizobium meliloti*. Cell. 54:671-683

David, M., O. Domergue, P. Pognonec, and D. Kahn. 1987. Transcription patterns of *Rhizobium meliloti* symbiotic plasmid pSym; identification of *nifA*-independent fix genes. J. Bacteriol. 169:2239-2244

Day, D.A., and L. Copeland. 1991. Carbon metabolism and compartmentation in nitrogen-fixing legume nodules. Plant Physiol. Biochem. 29:185-201

Day, D.A., G.D. Price, G.D., and M.K. Udvardi. 1989. Membrane interface of the *Bradyrhizobium-Glycine max* symbiosis: Peribacteroid units from soybean nodules. Austral. J. Plant Physiol. 16: 69-84

De Brujin, F.J., S. Rossbach, M. Schneider, P. Ratet, S. Messmer, W.W. Szeto, F.M. Ausubel, and J. Schell. 1989. *Rhizobium meliloti* has three differentially regulated loci involved in glutamine biosynthesis, none of which is essential for symbiotic nitrogen fixation. J. Bacteriol. 171:1673-1682

Denarie, J., F. Debelle, and C. Rosenberg. 1992. Signalling and host range variation in nodulation. Ann. Rev. Microbiol. 46:497-531

Diesterhaft, M.D. and E. Freese. 1973. Role of pyruvate carboxylase, phosphoenolpyruvate carboxykinase, and malic enzyme during growth and sporulation of *Bacillus subtilis*. J. Biol. Chem. 248:6062-6070

Drincovich, M.F., C.P. Spampinato, and C.S. Andreo. 1992. Evidence for the existence of two essential and proximal cysteinyl residues in NADP-malic enzyme from maize leaves. Plant Physiol. 100: 2035-2040

Driscoll, B.T. and T.M. Finan. 1993. NAD^+ malic enzyme of *Rhizobium meliloti* is required for symbiotic nitrogen fixation. Mol. Microbiol. 7:865-873

Driscoll, B.T. and T.M. Finan. 1996. $NADP^+$ malic enzyme of *Rhizobium meliloti*. J. Bacteriol. 178:2224-2231.

Driscoll, B.T., and T.M. Finan. 1997. Properties of NAD^+- and $NADP^+$- dependent malic enzymes of *Rhizobium (Sinorhizobium) meliloti* and differential expression of their genes in nitrogen-fixing bacteroids. Microbiol. 143:489-498

Duncan, M.J. and D.G. Fraenkel. 1979. α-ketoglutarate dehydrogenase mutant of *Rhizobium meliloti*. J. Bacteriol. 37:415-419

Dunn, M.F., S. Encarnacion, G. Araiza, M.C. Vargas, A. Davalos, H. Peralta, Y. More, and J. Mora. 1996. Pyruvate carboxylase from *Rhizobium etli*: mutant characterization, nucleotide sequence, and physiological role. J. Bacteriol. 178:5960-5970

Edwards, G.E. and C. Andreo. 1992. Review article number 66: NADP-malic enzyme from plants. Phytochemistry. 31:1845-1857

Engelke, T., M.N. Jagadish, and A. Puhler. 1987. Biochemical and genetical analysis of *Rhizobium meliloti* mutants defective in C_4-dicarboxylate transport. J. Gen. Microbiol. 133:3019-3029

Engelke, T., D. Jording, D. Kapp., and A. Puhler. 1989. Identification and sequence analysis of the *Rhizobium meliloti dctA* gene encoding the C_4-dicarboxylate carrier. J. Bacteriol. 171:5551-5560

Fan, F., J.A. Lorenzen, and B.V. Plapp. 1991. An aspartate residue in Yeast alcohol dehydrogenase I determines the specificty for coenzyme. Biochemistry. 30:6397-6401

Feeney, R., A.R. Clarke, and J.J. Holbrook. 1990. A single amino acid substitution in lactate dehydrogenase improves the catalytic efficiency with an alternative coenzyme. Biochem. Biophys. Res. Comm. 166:667-672

Felsenstein, J. 1993. PYLIP (Phylogeny Inference Package), Version 3.5c. Department of genetics, University of Washington, Seattle.

Finan, T.M., J.M. Wood, and D.C. Jordan. 1981. Succinate transport in *Rhizobium leguminosarum*. J. Bacteriol. 148:193-202

Finan, T.M., J.M. Wood, and D.C. Jordan. 1983. Symbiotic properties of C_4-dicarboxylate acid transport mutants of *Rhizobium leguminosarum*. J. Bacteriol. 154:1403-1413

Finan, T.M., E. Hartwieg, K. LeMieux, K. Bergman, G.C. Walker, and E.R. Signer. 1984. General transduction in *Rhizobium meliloti*. J. Bacteriol. 159:120-124

Fischer, H-M., S. fritsche, B. Herzog, and H. Hennecke. 1989. Critical spacing between two essential cysteine residues in the interdomain linker of the *Bradyrhizobium japonicum* NifA protein. FEBS Lett. 255:167-171

Fleishman, R.D., M.D. Adams, O. White, R.A. Clayton, E.F. Kirkness, A.R. Kerlavage, C.J. Bult, J-F Tomb, B.A. Dougherty, J.M. Merrick, K. McKenney, G. Sutton, W. FitzHugh, C. Fields, J.D. Gocayne, J. Scott, R. Shirley, L-I Liu, A. Glodek, J.M. Kelley, J.F. Weidman, C.A. Phillips, T. Spriggs, E. Hedblom, M.D. Cotton, T.R. Utterback, M.C. Hanna, D.T. Nguyen, D.M. Saudek, R.C. Brandon, L.D. Fine, J.L. Fritchman, J.L. Fuhrmann, N.S.M. Geoghagen, C.L. Gnehm, L.A. McDonald, K.V. Small, C.M. Fraser, H.O. Smith and J.C. Venter. 1995. Whole-genome random sequencing and assembly of *Haemophilus influenzae* Rd. Science. 269:496-512

Galakatos, N.G. and C.T. Walsh. 1987. Specific proteolysis of native alanine racemases from *Salmonella typhimurium*: Identification of the cleavage site and characterization of the clipped two-domain proteins. Biochem. 26:8475-8480

Gardiol, A.E., G.L. Truchet, and F.B. Dazzo. 1987. Requirements of succinate dehydrogenase activity for symbiotic bacteroid differentiation of *Rhizobium meliloti* in alfalfa nodules. Appl. Environ. Microbiol. 53:1947-1950

Garrido-Pertierra, A., C. Martinez Marcos, M. Martin Fernandez and M. Ruiz-Amil. 1983. Properties and function of malate enzyme from *Pseudomonas putida*. Biochimie. 65:629-635

Glazebrook,J., A. Ichige, and G.C. Walker. 1996. Genetic analysis of *Rhizobium meliloti bacA-phoA* fusion results in identification of *degP*: two loci required for symbiosis are closely linked to *degP*. J. Bacteriol. 178:745-752

Glenn, A.R., P.S. Poole, and J.F. Hudman. 1980. Succinate uptake by free-living and bacteroid forms of *Rhizobium leguminosarum*. J. Gen. Microbiol. 119:267-271

Glenn, A.R. and M.J. Dilworth. 1981. The uptake and hydrolysis of disaccharides by fast- and slow-growing species of *Rhizobium*. Arch. Microbiol. 129:233-239

Gottesman, S. 1996. Proteases and their targets in *Escherichia coli*. Annu. Rev. Genet. 30:465-506

Guagliardi, A., M. Moracci, G. Manco, M. Rossi, and S. Bartolucci. 1988. Oxalacetate decarboxylase and pyruvate carboxylase activities, and effect of sulfydryl

reagents in malic enzyme from *Sulfolobus solfataricus*. Biochimi. Biophys. Acta. 957:301-311

Green, L.S., and D.W. Emerich. 1997a. *Bradyrhizobium japonicum* does not require α-ketoglutarate dehydrogenase for growth on succinate or malate. J. Bacteriol. 179:194-201

Green, L.S., and D.W. Emerich. 1997b. The formation of nitrogen-fixing bacteroids is delayed but not abolished in soybean infected by an α-ketoglutarate dehydrogenase deficient mutant of *Bradyrhizobium japonicum*. Plant Physiol. 114:1359-1368

Green, L.S., D.B. Karr, and D.W. Emerich. 1998. Isocitrate dehydrogenase and glyoxylate cycle enzyme activities in *Bradyrhizobium japonicum* under various growth conditions. Arch. Microbiol. 169:445-451.

Green, J.D.F., R.N. Perham, S.J. Ullirich, and E. Appella. 1992. Conformational studies of the interdomain linker peptides in the dihydrolipoyl acetyltransferase component of the pyruvate dehydrogenase multienzyme complex of *Escherichia coli*. J. Biol. Chem. 267:23484-23488

Hanahan, D. 1983. Studies on transformation of *Escherichia coli* with plasmids. J. Mol. Biol. 166:557-569

Hansen, E.J. and E. Juni. 1975. Isolation of mutants of *Escherichia coli* lacking NAD- and NADP-linked malic enzyme activities. Biochem. Biophys. Res. Comm. 59:1204-1210

Hanukoglu, I. and T. Gutfinger. 1989. cDNA sequence of adrenodoxin reductase, identification of NADP-binding sites in oxidoreductases. Eur. J. Biochem. 180:479-484

Hedrich, J.L. and A.J. Smith. 1968. Size and charge isomer separation and estimation of molecular weights of proteins by disc gel electrophoresis. Arch. Biochem. Biophys. 126:155-164

Hennecke, H. 1993. The role of respiration in symbiotic nitrogen fixation. p. 55-64. In P. Palacios, J. Mora, and W.E. Newton (ed.), New horizons in nitrogen fixation. Kluwer Academic Publishers, Dordecht, The Netherlands

Hirsch, H. M. and C.A. Smith. 1987. Effects of *Rhizobium meliloti nif* and *fix* mutants on alfalfa root nodule development. J. Bacteriol. 169:1137-1146

Hornez, J.P., M. Timinouni, C. Defives, and J.C. Derieux. 1994. Unaffected nodulation and nitrogen fixation in carbohydrate pleiotropic mutants of *Rhizobium meliloti*. Curr. Microbiol. 28:225-229

Howitt, S.M. and P.M. Gresshoff. 1985. Ammonia regulation of glutamine synthetase in *Rhizobium* sp. ANU289. J. Gen. Microbiol. 132:257-261

Howitt, S.M., M.K. Udvardi, D.A. Day and P.M. Gresshoff. 1986. Ammonia transport in free-living and symbiotic *Rhizobium* sp. ANU289. J Gen. Microbiol. 132:257-261

Hsu, R.Y. 1982. Pigeon liver malic enzyme. Mol. Cell. Biochem. 43:3-26

Hsu, R. Y., M.J. Glynias, J. Satterlee, R. Feeney, A.R. Clarke, D.C. Emery, B.A. Roe, R.K. Wilson, A.G. Goodridge, and J.J. Holbrooks. 1992. Duck liver malic enzyme. Biochem. J. 284:869-876

Irigoyen, J.J., M. Sanchez-Diaz, and D.W. Emerich. 1990. Carbon metabolism enzymes of *Rhizobium meliloti* cultures and bacteroids and their distribution within alfalfa nodules. Appl. Environ. Microbiol. 56:2587-2589

Jawali, N. and A.S. Bhagwat. 1987. Presence of essential histidine residues in NADP-malic enzyme from maize. Phytochemistry. 26:1859-1862

Jeong, H.S., and Y. Jouanneau. 2000. Enhanced nitrogenase activity in strains of *Rhodobacter capsulatus* that overexpress the *rnf* genes. J. Bacteriol. 185:1208-1214

Jiang, J., B. Gu, L.M. Albright, and B.T. Nixon. 1989. Conservation between coding and regulatory elements of *Rhizobium meliloti* and *Rhizobium leguminosarum dct* genes. J. Bacteriol. 171:5244-5253

Jimenez-Zurdo, J.I., P.V. Dillewijin, M.J. Soto, M.R. DeFelipe, J. Olivares, and N. Toro. 1995. Characterization of a *Rhizobium meliloti* proline dehydrogenase mutant altered in nodulation efficiency and competitiveness on alfalfa roots. Mol. Plant-Microbe Interact. 8:492-498.

Jonston, A.W.B. and J.E. Beringer. 1975. Identification of the *Rhizobium* strains in pea root nodules using genetic markers. J. Gen. Microbiol. 87:343-350

Johnson, G.V., H.J. Evans, and T. Ching. 1966. Enzymes of the glyoxylate cycle in *Rhizobia* and nodules of legumes. Plant Physiol. 41:1330-1336

Kahn, M.L., J. Kraus, and J.E. Somerville. 1985. A model of nutrient exchange in the *Rhizobium*-legume symbiosis. In Nitrogen fixation research progress. Evans, H.J. and P.J. Bottomley, and W.E. Newton (eds). M.J. Nijhoff, New York. pg. 193-199.

Kahn, D., M. David, O. Domergue, M-L. Daveran, J. Ghai, P.R. Hirsh, and J. Batut. 1989. *Rhizobium meliloti fixGHIS* sequence predicts involvement of a specific cation pump in symbiotic nitrogen fixation. J. Bacteriol. 171:929-997

Kaneko, T., S. Sato, H. Kotani, A. Tanaka, E. Asamizu, Y. Nakamura, N. Miyajima, M. Hirosawa, M. Sugiura, S. Sasamoto, T. Kimura, T. Hosouchi, A. Matsuno, A. Muraki, N. Nakazaki, K. Naruo, S. Okumura, S. Shimpo, C. Takeuchi, T. Wada, A. Watanbe, M. Yamada, M. Yasuda, and S. Tabata. 1996. Sequence analysis of the genome of the unicellular cyanobacterium *Syenchocystis sp.* PCC6803. Sequence determination of the entire genome and assignment of potential protein-coding regions. DNA Res. 3:109-136

Katsuki, H., K. Takeo, K. Kameda, and S. Tanaka. 1967. Existence of two malic enzymes in *Escherichia coli.* Biochem. Biophys. Res. Comm. 27:331-336

Kawai, S., H. Suzuki, K. Yamamoto, M. Inui, M. Yukawa, and H. Kumagi. 1996. Purification and characterization of a malic enzyme from the ruminal bacterium *Streptococcus bovis* ATCC 15352 and cloning and sequencing of its gene. Appl. And Environ. Microbiol. 62, 2692-2700

Kawai, S., H. Suzuki, K. Yamamoto, and H. Kumagai. 1997. Characterization of the malate permease gene (*maeP*) of *Streptoccus bovis* ATCC 15352. J. Bacteriol. 179:4056-4060

Keele, B.B., P.B. Hamilton Jr., and G.H. Elkan. 1969. Glucose catabolism in *Rhizobium japonicum.* J. Bacteriol. 97:1184-1191

Kimura, I. and S. Tajima. 1989. Presence and characteristics of NADP-malic enzyme in soybean nodules. Soil Sci. Plant Nutr. 35:271-279

Kobayashi, K., S. Doi, S. Negoro, I. Urabe, and H. Okada. 1989. Structure and properties of malic enzyme from *Bacillus stearothermophilus.* J. Biol. Chem. 264: 3200-3205

Kouchi, H. and K. Nakaji. 1985. Utilization and metabolism of photoassimilated ^{13}C in soybean roots and nodules. Soil Sci. Plant. Nutr. 31:323-334

Kovach, M.E., P.H. Elzer, D.S. Hill, G.T. Robertson, M.A. Farris, R.M. Roopa, and K.M. Peterson. 1995. Four new derivatives of the broad-host-range cloning vector pBBR1MCS, carrying different antibiotic resistance cassettes. Gene. 166:175-176

Kulkarni, G., P.F. Cook and B.G. Harris. 1993. Cloning and nucleotide sequence of a full length cDNA-encoding *Ascaris suum* malic enzyme. Arch. Biochem. Biophys. 300:231-237

Kuo, J. 1992. About non-linear regression. In Transform and curve fitting reference. Jandel Corporation, San Rafeal, CA. pg 1-7.

Kunkel, T.A., J.D. Roberts, and R.A. Zakour. 1987. Rapid and efficient site-specific mutagenesis without phenotypic selection. Meth. Enz. 154:367-382

Kurz, W.G., and T.A. LaRue. Citric acid cycle enzymes and nitrogenase in nodules of *Psium sativum.* Can. J. Microbiol. 23:1197-2000

Labes, M. and T.M. Finan. 1993. Negative regulation of σ^{54}-dependent *dctA* expression by the transcriptional activator DctD. J. Bacteriol. 175:2674-2681

Lamed, R. and J.G. Zeikus. 1981. Thermostable, ammonium-activated malic enzyme of *Clostridium thermocellum.* Biochimi. Biophys. Acta. 660:251-255

Latimer, M.T. and J.G. Ferry. 1993. Cloning, sequence analysis and hyperexpression of the genes encoding phosphotransacetylase and acetate kinase from *Methanosarcina thermophila. J. Bacteriol.* 175:6822-6829

Leonard, L.T. 1943. A simple assembly for use in testing cultures of rhizobia. J. Bacteriol. 45:523-527

Lewis, T.A., R. Gonzalez, and J.L. Botsford. 1990. *Rhizobium meliloti* glutamate synthase: cloning and initial characterization of the *glt* locus. J. Bacteriol. 172:2413-2420

Loeber, G., A.A. Infante, L. Maurer-Fogy, E. Krystek, M.B. Dworkin. 1991. Human NAD^+-dependent mitochondrial malic enzyme. J. Biol. Chem. 266:3016-3021

Lowry D, O.H., N.J. Rosebrough, Al. Farr and R.L. Randall. 1951. Protein measurement with Folin phenol reagent. J. Biol. Chem. 193:265-275

de Maagd, R.A., W.C. Yang, L. Goosen-de Roo, I.H.M. Mulders, H.P. Roest, H.P. Spaink, T. Bisseling, and B.J.J. Lugtenberg. 1994. Down regulation of expression of the *Rhizobium leguminosarum* outer membrane protein gene *rpoA* occurs abruptly in interzone II-III of pea nodules and can be uncoupled from nif gene activation. Mol. Plant. Microbe. Interact. 7:276-281

Magnuson, M.A., H. Morioka, M.F. Tecce and V.M. Nikodem. 1986. Coding nucleotide sequence of rat liver malic enzyme mRNA. J. Biol. Chem. 261:1183-1186

Mahajan, S.K., C.C. Chu, D.K. Willis, A. Templin, and A.J. Clark. 1990. Physical analysis of spontaneous and mutagen-induced mutants of *Escherichia coli* K-12 expressing DNA exonuclease VII activity. Genetics. 125:261-273

Matasuyama, A., H. Yamamoto-Otake, J. Hewitt, R.T.A. MacGillivray, and E. Nakano. 1994. Nucleotide sequence of the phosphotransacetylase gene of *Escherichia coli* strain K12. Biochima Biophys. Acta. 1219:559-562

Meade, H.M., S.R. Long, G.B. Ruvkin, S.E. Brown, and F.M. Ausubel. 1982. Physical and genetical characterization ofsymbiotic and auxotrophic mutants of *Rhizobium meliloti* induced by transposn Tn5 mutagenesis. J. Bacteriol. 149:114-122

Merrick, M.J. 1993. Organization and regulation of nitrogen fixation genes. p. 43-54. *In* Palacios, J. Mora, and W.E. Newton (ed.), New horizons in nitrogen fixation. Kluwer Academic Publishers, Dordecht, the Netherlands.

McAllister, C.F. and J.E. Lepo. 1983. Succinate transport by free-living forms of *Rhizobium japonicum*. J. Bacteriol. 153:1155-1162

McRae, D.G., R.W. Miller, W.B. Berndt, and K. Joy. 1989. Transport of C_4-dicarboxylate and amino acids by *Rhizobium meliloti* bacteroids. Mol. Plant Microbe Interact. 2:273-278

McDermott, T.R. and M.L. Kahn. 1992. Cloning and mutagenesis of the *Rhizobium meliloti* isocitrate dehydrogenase gene. J. Bacteriol. 174:4790-4797

McKay, I.A., M.J. Dilworth, and A.R. Glenn. 1988. C_4-dicarboxylic metabolism in free-living and bacteroid forms of *Rhizobium leguminosarum* MNF3841. J. Gen. Microbiol. 134:1433-1440

McKay, I.A., A.R. Glenn, and M.J. Dilworth. 1985. Gluconeogenesis in *Rhizobium leguminosarum* MNF3841. J. Gen. Microbiol. 131:2067-2073

Metzger, M.H., and C.P. Hollenberg. 1995. Amino acid substitutions in the yeast *Pichia stipitis* xylitol dehydrogenase coenzyme-binding domain affect the coenzyme specificity. Eur. J. Biochem. 228:50-54

Miles, J.S., J.R. Guest, S.E. Radford, and R.N. Perham. 1988. Investigation of the mechanism of active site coupling in the pyruvate dehydrogenase multienzyme complex of *Escherichia coli* by protein engineering. J. Mol. Biol. 202:97-106

Miller, J.H. 1972. Experiments in molecular genetics. Cold Spring Harbor Laboratory Press, Cold Spring Harbor, New York

Miller, R.W., D.G. McRae, A. Al Jobore, and W.B. Berndt. 1988. Respiration supported nitrogenase activity of isolated *Rhizobium meliloti* bacteroids. J. Cell. Biochem. 38:35-49

Mitchell, C.G., 1996. Identification of a multienzyme complex of the tricarboxylic acid cycle enzymes containing citrate synthase isoenzymes from *Pseudomonas aeruginosa.* 313:769-774

Mitsch, M.J, R.T. Voegele, A. Cowie, M. Osteras, and T.M. Finan. 1998. Chimeric structure of the $NAD(P)^+$- and $NADP^+$-dependent malic enzymes of *Rhizobium* (*Sinorhizobium*) *meliloti.* J. Biol Chem. 273:9330-9336

Morioka, H., M.A. Magnuson, T. Mitsuhashi, M.-K.H. Song, J.E. Rall, and V.M. Nikodem. 1989. Structural characterization of the rat malic enzyme gene. Proc. Natl. Acad. Sci. USA. 86:4912-4916

Mortimer, M.W., T.R. McDermott, G.M. York, G.C. Walker, and M.L. Khan. 1999. Citrate synthase mutants of *Sinorhizobium meliloti* are ineffective and have altered cell surface polysaccharides. J. Bacteriol. 181:7608-7613

Moustafa, E., and C.K. Leong. 1975. Effect of adenine nucleotides on NAD-dependent isocitrate dehydrogenase in rhizobia and bacteroids of legume root nodules. Biochim Biophys Acta. 391:9-14

Murai, T., M. Tokushige, J. Nagai, and H. Katsuki. 1971. Physiological functions of NAD- and NADP-linked malic enzymes in *Escherichia coli.* Biochem. Biophys. Res. Comm. 43:875-881

Naberhaus, F., W. Weiglhofer, H.M. Fisher, and H. Hennecke. 1998. Identification of the *Bradyrhizobium japonicum degP* gene as part of an operon containing small heat-shock protein genes. Arch. Microbiol. 169:89-97

Ochoa, S., A. Mehler, and A. Kornberg. 1947. Reversible oxidative decarboxylation of malic acid. J. Biol. Chem. 167:871-872

O'Hara, G.W., T.J. Goss, M.J. Dilworth, and A.R. Glenn. 1989. Maintenance of intracellular pH and acid tolerance in *Rhizobium meliloti.* Appl. Environ. Microbiol. 55:1870-1876

Osbourne, M.S. and E.R. Singer. 1980. Ammonium assimilation in *Rhizobium meliloti.* J. Bacteriol. 143:1234-1240

Osteras, M., T.M. Finan, and J. Stanley. 1991. Site-directed mutagenesis and DNA sequence of *pckA* of *Rhizobium* NGR234, encoding phosphoenolpyruvate carboxykinase:

gluconeogenesis and host-dependent symbiotic phenotype. Mol. Gen. Genet. 230:257-269

Perez-Galdona, R. and M.L. Kahn. 1994. Effects of organic acids and low pH on *Rhizobium meliloti* 104A14. Microbiol. 140:1231-1235

de Philip, P., J. Batut, and P. Boistard. 1990. *Rhizobium meliloti* FixL is an oxygen sensor and regulates *R. meliloti nifA* and *fixK* genes differently in *Escherichia coli.* J. Bacteriol. 172:4255-4262

Preston, G.G., C. Zeiher, J.D. Wall, and D.W. Emerich. 1989. Acetate-activating enzymes of *Bradyrhizobium japonicum* bacteroids. Appl. Environ. Microbiol. 55:165-170

Radford, S.E., E.D. Laue, R.N. Perham, S.R. Martin, and E. Appella. 1989. Conformational flexibility and folding of synthetic peptides representing an interdomain segment of polypeptide chain in pyruvate dehydrogenase multienzyme complex of *Escherichia coli.* J. Biol. Chem. 264:767-775

Rao, S.R., B.G. Kamath, and A.S. Bhagwat. 1991. Chemical modification of the functional arginine residue(s) of malic enzyme from *Zea mays.* Phytochemistry. 30: 431-435

Rastogi, V., M. Labes, T.M. Finan, and R. Watson. 1991. Overexpression of the *dctA* gene in *Rhizobium meliloti*: effect on transport of C_4 dicarboxylates and symbiotic nitrogen fixation. Can. J. Microbiol. 38:555-562

Rastogi, V.K. and R. Watson. 1991. Aspartate aminotransferase activity is required for aspartate catabolism and symbiotic nitrogen fixation in *Rhizobium meliloti.* J. Bacteriol. 173:2879-2887

Raven, P.H. R. Evert, and S. Eichorn. 1986. Biology of plants. Worth, New York. 517-541

Reibach, P.H. and J.G. Streeter. 1983. Evaluation of active versus passive uptake of metabolites by *Rhizobium japonicum* bacteroids. J. Bacteriol. 159:47-52

Reid, C.J., D.L. Walshaw, and P.S. Poole. 1996. Aspartate transport by the Dct system in *Rhizobium leguminosarum* negatively affects nitrogen-regulated operons. Microbiol. 142: 2603-2612

van Rhijn, P. and J. Vanderleyden. 1995. The *Rhizobium*-plant symbiosis. Microbiol. Revs. 59:124-142

Roberts, G.P. and W.J. Brill. 1981. Genetics and regulation of nitrogen fixation. Annu. Rev. Microbiol. 35:207-235

Roberts, J.K.M., P.M. Ray, N. Wade-Jardetsky, and O. Jardetsky. 1980. Estimation of cytoplasmic and vacuolar pH in higher plants by ^{31}P NMR. Nature. 283:870-872

Ronson, C.W. and P.M. Astwood. 1985. Genes involved in the carbon metabolism of bacteroids. In Nitrogen fixation research progress. Evans, H.J. and P.J. Bottomley (eds). Dordrecht: Martinus Nijhoff Publishers, pg. 201-207

Ronson C.W., P. Lyttleton, and J.G. Robertson. 1981. C_4-dicarboxylate transport mutants of *Rhizobium trefolii* form ineffective nodules on *Trifolium repens*. Proc. Natl. Acad. Sci. USA. 78: 4284-4288

Ronson, C.W. and S.B. Primrose. 1979. Carbohydrate metabolism in *Rhizobium trifolii*: identification and symbiotic properties of mutants. J. Gen. Microbiol. 112:77-88

Ronson, C.W., P.M. Astwood, and J.A. Downie. 1984. Molecular cloning and genetic organization of C_4-dicarboxylate transport genes from *Rhizobium leguminosarum*. J. Bacteriol. 160:903-909

Ronson, C.W., B.T. Nixon, L.M. Albright, and F.M. Ausubel. 1987. *Rhizobium meliloti ntrA* (*rpoN*) gene is required for diverse metabolic functions. J. Bacteriol. 169:2424-2431

Rosendahl, L., C.P. Vance, and W.B. Pederson. 1990. Products of dark CO_2 fixation in pea root nodules support bacteroid metabolism. Plant Physiol. 93:12-19

Sahl, H.G. and H.G. Truper. 1980. Malic enzyme of *Chromatium vinosum*. Arch. Microbiol. 127:17-24

Salminen S.O. and J.G. Streeter. 1987. Involvement of glutamate in the respiratory metabolism of *Bradyrhizobium japonicum* bacteroids. J. Bacteriol. 169: 495-499

Sambrook, J., E.F. Fritsch, and T. Maniatis. 1989. Molecular cloning: a laboratory manual, 2nd edition. Cold Spring Harbor Laboratory Press, Cold Spring Harbor, N.Y.

San Francisco, M.J.D., and G.R. Jacobson. 1985. Uptake of succinate and malate in cultured cells and bacteroids of two slow-growing species of *Rhizobium*. J. Gen. Microbiol. 131:765-773

Sanwal, B.D. 1970a. Allosteric controls of amphibolic pathways in bacteria. Bacteriol. Rev. 34:20-39

Sanwal, B.D. 1970b. Regulatory characterisitics of the diphosphopyridine nucleotide-specific malic enzyme of *Escherichia coli*. J. Biol. Chem. 245:1212-1216

Sanwal, B.D. and R. Smando. 1969a. Malic enzymes of *Escherichia coli*: diversity of the effectors controlling enzyme activity. J. Biol. Chem. 244: 1817-1823

Sanwal, B.D. and R. Smando. 1969b. Malic enzymes of *Escherichia coli*: possible mechanism for allosteric effects. J. Biol. Chem. 244: 1824-1830

Sanwal, B.D., J.A. Wright and R. Smando. 1968. Allosteric control of the activity of malic enzyme in *Escherichia coli*. Biochem. and Biophys. Res. Comm. 31: 623-627

Schweizer, H.P., T.R. Klassen, and T. Hoang. 1997. Improved methods for gene analysis and expression in *Psuedomonas*. Molecular biology of *Psuedomonads*. Nakazawa, T., Furukawa, K., Haas, D., and Silver, S. (eds). American Society for Microbiology, Washington, D.C.

Scrutton, N.S., A. Berry, and R.N. Pernham. 1990. Redesign of the coenzyme specificity of a dehydrogenase by protein engineering. Nature. 343:38-43

Shatters, R.G., J.E. Sommerville, and M.L. Kahn. 1989. Regulation of glutamine synthetase II activity in *Rhizobium meliloti* 104A14. J. Bacteriol. 171:5087-5094

Silver, W.S. and J.R. Prostgate. 1973. Evolution of asymbiotic nitrogen fixation. J. Theor. Biol. 40:1-10

Snapp S.S. and C.P. Vance. 1986. Asparagine biosynthesis in alfalfa (*Medicago sativa* L.) root nodules. Plant Physiol. 82: 390-395

Soberon, M., O. Lopez, C. Morera, M.L. Girard, and J. Miranda. 1999. Enhanced nitrogen fixation in a *Rhizobium etli ntrC* mutant that overproduces the *Bradyrhizobium japonicum* symbiotic terminal oxidase cbb_3. Appl. Environ. Microbiol. 65:2015-2019

Somerville, J.E., R.G. Shatters, and M.L. Kahn. 1989. Isolation, characterization, and complementation of *Rhizobium meliloti* 104A14 mutants that lack glutamine synthetase II activity. J. Bacteriol. 171:5079-5086

Spina, J., H.J. Bright, J. Rosenbloom. 1968. Purification and properties of L-malic enzyme from *Escherichia coli*. Biochemistry. 9:3794-3801

Streeter J.G. 1987. Carbohydrate, organic acid, and amino acid composition of bacteroids andcytosol from soybean nodules. Plant Physiol. 85, 768-773

Streeter, J.G. 1991. Transport and metabolism of carbon and nitrogen in legume nodules. Adv. Bot. Res. 18:129-187

Stols, L., and M.I. Donnelly. 1997. Production of succinic acid through overexpression of NAD^+-dependent malic enzyme in an *Escherichia coli* mutant. Appl. and Environ. Microbiol. 63:2695-2701

Summers, M.L., M.C. Denton, and T.R. McDermott. 1999. Genes coding for phosphotransacetylase and acetate kinase in *Sinorhizobium meliloti* are in an operon that is inducible by phosphate stress and controlled by PhoB. J. Bacteriol. 181:2217-2224

Suye, S.I., Y. Okada, A. Funada, M. Kawaoe and S. Inuta. 1992. Purification and properties of malic enzyme from *Pseudomonas diminuta* IFO-13182. J. Ferment. Bioeng. 73:343-347

Tajima, S., and K. Kouzai. 1989. Nucleotide pools in soybean nodule tissue, a survey of NAD(P)/NAD(P)H ratios and energy charge. Plant cell Physiol. 30:589-593

Tang, C.L., and R.Y. Hsu. 1974. Mechanism of Pigeon liver malic enzyme. Modification of sulfhydryl groups by 5,5'-dithiobis(2-nitrobenzoic acid) and N-ethylmaleimide. J. Biol. Chem. 249:3916-3922

Thompson, J.D., D.G. Higgins and T.J. Gibson. 1994. CLUSTAL W: improving the sensitivity of progressive multiple sequence alignment through sequence weighting, position-specific gap penalties and weight matrix choice. Nuc. Acids Res. 22:4673-4680.

Towbin, H., Staehelin, T., and Gordon, J. 1979. PNAS. 76:4350-4354

Tomaszewska, B., and D. Werner. 1995. Purification and properties of NAD- and NADP-dependent Malic enzymes from *Bradyrhizobium japonicum* bacteroids. J. Plant. Physiol. 146:591-595

Udvardi, M.K. and D. A. Day. 1997. Metabolite transport across symbiotic membranes of legume nodules. Annu. Rev. Plant. Physiol. Plant Mol. Biol. 48:493-523

Udvardi, M.K., G.D. Price, P.M. Gresshoff, and D.A. Day. 1988. A dicarboxylate transporter on the peribacteroid membrane of soybean nodules. FEBS lett. 231: 36-40

Vance, C.P., S. Stade, and C. A. Maxwell. 1983. Alfalfa root nodules carbon dioxide fixation. Plant Physiol. 72: 469-473

Vance, C.P. and G.H. Heichel. 1991. Carbon in N_2 fixation: limitation or exquisite adaption. Annu. Rev. Plant Physiol. Plant Mol. Biol. 42:373-392

Vasse, J., F. de Billy, S. Camut, and G. Truchet. 1990. Correlation between ultrastructural differentiation of bacteroids and nitrogen fixation in alfalfa nodules. J. Bacteriol. 172:4295-4306

Vernon, C.M. and R.Y. Hsu. 1983. Pigeon liver malic enzyme: involvement of an arginyl residue at the binding site for malate and its analogs. Arch. Biochem. Biophys. 225, 296-305

Vieira, J. and J. Messing. 1987. The pUC plasmids, an M13mp7-derived system for insertion mutagenesis and sequencing with synthetic universal primers. Gene. 19:259-268

Viljoen, M., M. van der Merwe,R.E. Subden, and H.J. van Vuuren. 1998. Mutation of Gly-444 inactivates the *Schizosaccharomyces pombe* malic enzyme. FEMS Microbiol. Lett. 167:157-162

Viljoen, M., R.E. Subden, A. Krizus, and H.J.J. Van Vuuren. 1994. Molecular analysis of the malic enzyme gene (*mae2*) of *Schizosaccharomyces pombe*. Yeast. 10, 613-624

Voegele, R.T., M.J. Mitsch, and T.M. Finan. 1999. Characterization of two members of a novel malic enzyme class. Biochim. Biophys. Acta. 1432:275-285

Waelkens, F., A. Foglia, J-B. Morel, J. Fourment, J. Batut and P. Boistard. 1992. Molecular genetic analysis of the *Rhizobium meliloti fixK* promoter: identification of sequences involved in positive and negative regulation. Mol. Microbiol. 6:1447-1456

Walter, M.H., J. Grima-Pettenati, and C. Feuillet. 1994. Characterization of a bean (*Phaseolus vulgaris* L.) malic-enzyme gene. FEBS. 227: 999-1009

Wang, Y.P., K. Birkenhead, B. Boesten, S. Manian, and F. O'Gara. 1989. Genetic analysisand regulation of the Rhizobium meliloti genes controlling C4-dicarboxylic acid transport. Gene. 85: 135-144.

Waters, J.K., B.L. Hughes, L.C. Purcell, K.O. Gerhardt, T.P. Mawhinney, and D.W. Emerich. 1998. Alanine, not ammonium, is excreted from N_2-fixing soybean nodule bacteroids. PNAS. 95:12038-12042

Watson, R.J. 1990. Analysis of the C_4-dicarboxylate transport genes of *Rhizobium meliloti*: nucleotide sequence and deduced products of *dctA*, *dctB*, and *dctD*. Mol. Plant-microbe interact. 3:174-181

Watson, R.J. and V.K. Rastogi. 1993. Cloning and nucleotide sequencing of *Rhizobium meliloti* aminotransferase genes: an aspartate amiotransferase required for symbiotic nitrogen fixation is atypical. J. Bacteriol. 175:1919-1928

Watson, R.J., V.K. Rastogi, and Y-K Chan. 1993. Aspartate transport in *Rhizobium meliloti*. J. Gen. Microbiol. 139:1315-1323

Wedding, R.T. 1989. Malic enzymes of higher plants. Plant Physiol. 90:367-371

Wei, C.H., W.Y. Chou, and G.G. Chang. 1995. Identification of Asp258 as the metal coordinate of pigeon liver malic enzyme by site-specific mutagenesis. Biochemistry. 34:7949-7954

Wierenga, R.K., P. Terpstra, and W.G.J. Hol. 1986. Prediction of the occurrence of the ADP-binding beta alpha beta-fold in proteins, using an amino acid sequence fingerprint. J. Mol. Biol. 187: 101-107

Wootton, J.C. and M. Drummond. 1989. The Q-linker: a class of interdomain sequences found in bacterial multidomain regulatory proteins. Protein Eng. 2:535-543

Xu, Y., G. Bhargava, H. Wu, G. Loeber, and L. Tong. 1999. Crystal structure of human mitochondrial NAD(P)+-dependent malic enzyme: a new class of oxidative decarboxylases. Structure. 7:877-889

Yamaguchi, M., M. Tokushige, and H. Katsuki. 1973. Studies on regulatory functions of malic enzymes, Purification and molecular properties of nicotinamide adenine dinucleotide-linked malic enzyme from *Escherichia coli*. J. Biochem. 73:169-180

Yarosh, O.K., T.C. Charles, and T.M. Finan. 1989. Analysis of C_4-dicarboxylic acid transport genes in *Rhizobium meliloti*. Mol. Microbiol. 3:813-823

Zhu, Y.X., G. Shearer, and D.H. Kohl. 1992. Proline fed to intact soybean plants influences acetylene reducing activity and content and metabolism of bacteroids. Plant Physiol. 98:1020-1028